Des lapins watanabe au syndrome hyper IgE humain : caractérisation précoce de l'athérosclérose utilisant une probe optique ciblant l'integrin aVb3

Julie Héroux

▶ **To cite this version:**

Julie Héroux. Des lapins watanabe au syndrome hyper IgE humain : caractérisation précoce de l'athérosclérose utilisant une probe optique ciblant l'integrin aVb3. Médecine humaine et pathologie. Université de Grenoble, 2012. Français. NNT : 2012GRENS041 . tel-01247017

HAL Id: tel-01247017
https://theses.hal.science/tel-01247017

Submitted on 4 Jan 2016

HAL is a multi-disciplinary open access archive for the deposit and dissemination of scientific research documents, whether they are published or not. The documents may come from teaching and research institutions in France or abroad, or from public or private research centers.

L'archive ouverte pluridisciplinaire **HAL**, est destinée au dépôt et à la diffusion de documents scientifiques de niveau recherche, publiés ou non, émanant des établissements d'enseignement et de recherche français ou étrangers, des laboratoires publics ou privés.

Year 2012

THESIS

presented for

Joseph Fourier University (Grenoble I)

for the obtention of

Doctor in Philosophy (Ph.D.) Grade

EDISCE

Doctoral School of Engineering for Health, Cognition and Environment

BIS

Biotechnology, instrumentation, signal and imaging for biology, medicine and environment

by

Julie HEROUX

From Watanabe Rabbits to Human Hyper IgE Syndrome: Characterization of Early Atherosclerosis Using a High Affinity Integrin Targeted Optical Probe

under the direction of

Dr. Roderic I. Pettigrew and Pr. Jacques Ohayon

Jury composition:

Dr. Narasimhan S. Danthi, PhD, NHLBI, NIH, Bethesda, MD, USA
Dr. Gérard Finet, Professeur/Practicien Hospitalier, Université de Lyon 1, Lyon, France
Dr. Ahmed M Gharib, MD, NIDDK, NIH, Bethesda, MD, USA
Dr. Laurent Riou, Chargé de Recherche INSERM, INSERM U 1039, Grenoble, France
Dr. Jacques Ohayon, Professeur, Université de savoie, Le Bourget du Lac, France
Dr. Roderic I Pettigrew, MD, PhD, NIDDK, NIH, Bethesda, MD, USA

Few are those who see with their own eyes and feel with their own hearts

Albert Einstein

Reading after a certain age diverts the mind too much from its creative pursuits. Any man who reads too much and uses his own brain too little falls into lazy habits of thinking

Albert Einstein

ACKNOWLEDGMENTS

First, I would like to thank my two directors, Pr. Jacques Ohayon and Dr. Roderic Pettigrew. Without their continuous support and encouragement, this thesis will not have been possible. I would like to thank Jacques, who bring the idea of this collaboration between our two laboratories and who proposed to officialized my work into the realization of a PhD. I would like to thank Dr. Pettigrew for generously agreeing to give his precious time and allowing his laboratory to host me. I also want to thank him for his humor, which helps me kept ma sanity, even in hard time.

I would like to thank Dr. Gharib for his guidance during all those years, and for the greatly appreciated help with all the problems encountered. I would also thank Dr. Gharib for the confidence and trust he gave me, and for the numerous scientific challenges that pushed me to go beyond my comfortable zone and to give my best.

I would like to thank Dr. Gerard Finet and Dr. Narasimhan Danthi for meticulously read the Thesis and to gave me their advices and comments. I would also like to thank Pr. Laurent Riou for being my biology expert and giving me his point of view and biological recommendations.

I also want to thank the director of the Doctoral school (EDISCE), Dr. Jean-Luc Schwartz, for his support and for allowing me to do this Thesis in codirection with my

laboratory in USA. I would also like to thank the director of the laboratory in Grenoble, Dr. Philippe Cinquin.

I would like to thank Dr. Narasimhan Danthi for giving us the opportunity of testing their ITOP probe on the Watanabe rabbit model, and Dr. Stanley Satz and Dr. Martin Brechbiel for later synthetized the probe for us.

A special thank you to Dr. Zu Xi Yu, from NHLBI, for his precious help with pathology and immunochemistry. His expertise was greatly appreciated. Another thank you to Saami Yazdani, who also helped with pathological interpretation.

I would also like to thank my husband, Sylvain, for all the scientific help and for being there in the good moments, as well as in the bad ones. I would also like to thank him for believing in me and for constantly reminding me that I can do this, and for putting up with my many crazy theories (sorry for the sleep deprivation!). I would like to thank my two princesses, Anouk and Alixe, for being so supportive and for understanding when mommy missed one or two school presentations! Thank you girls for reminding me that sometimes, you must unlearn in order to discover! Finally, I would also like to thank all my family and friends for being there all the way, for their precious help and for giving me all the love that make me go through the tough time. It wouldn’t have been possible without you.

CONTENTS

1.3 BIOMARKERS OF INSTABILITY

1.3.1 Angiogenesis

1.3.1.1 Integrin

1.3.1.2 αVβ3

1.3.2 Matrix Metalloproteinases (MMPs)

1.3.3 Macrophages

1.3.4 Vascular Smooth Muscle Cells Apoptosis

1.4 STATE OF THE ART: αVβ3 targeted probes

1.4.1 αVβ3 Probes Development and Historic

1.4.2 αVβ3 integrin-targeted probe synthesis

1.4.3 αVβ3 probe characterization on cancer model

1.5 ANIMAL MODEL OF ATHEROSCLEROSIS

1.5.1 Mice and Rats

1.5.2 Pigs

1.5.3 Watanabe Heritable Hyperlipidemic (WHHL) Rabbits

1.6 AD-HIES AND ATHEROSCLEROSIS

1.6.1 Aneurysm

1.7 SUMMARY

CHAPTER 1 IN VITRO ITOP LABELING ON WHHL RABBITS

2.1 INTRODUCTION

2.2 MATERIALS AND METHODS

2.2.1 Experiment design

2.2.2 Cholesterol measurement

2.2.3 Dissection

2.2.4 Histology and Immunohistology

2.2.5 Competition

2.2.6 Lipid staining

2.3 RESULTS

2.3.1 Plaque labeling

2.3.2 Adventitia labeling

2.3.3 Labeling and adventitia thickness

2.3.4 Signal correlation with an anti-αvβ3 antibody

2.3.5 Competition

2.3.6 Lipid staining

2.4 DISCUSSION

ABBREVIATION

CHD:	coronary heart diseases;
HDL:	high density lipoprotein;
LDL:	low-density lipoprotein;
NO:	nitric oxide;
VCAM:	vascular cell adhesion molecule;
ICAM:	inter-cellular adhesion molecule;
MCP:	monocyte chemotactic protein
ACS:	acute coronary syndrome;
ACE:	acute coronary event;
SMC:	smooth muscle cell;
Ox-LDL:	oxidized low-density lipoprotein;
ECM:	extracellular matrix;
PDGF:	platelet-derivated growth factor
TGF:	transforming growth factor;
FITC:	fluorescein isothiocyanate;
NZW:	New Zealand White;
WHHL:	Watanabe heritable hyperlipidemic;
PDGF:	platelet-derivated growth factor;
TNF:	Tumor necrosis factor;
IC_{50}:	inhibitory concentration;
OCT:	optimal cutting temperature;
H&E:	hematoxylin and eosin;

NI:	neointima;
M:	media;
Ad:	adventitia;
Fig:	figure;
DAPI:	4’,6-diamidino-2phenylindol.
CAD:	coronary artery diseases
AD-HIES	autosomal dominant hyper IgE Syndrome

THESIS SUMMARY

This thesis is aimed at evaluating a newly developed αvβ3 integrin targeted optical probe (ITOP) for the early detection of atherosclerotic plaque. It is equally aimed at better understand the molecular signature associated with the probe labeling and the associated mechanisms present in the context of the ITOP labeling. This thesis has been conducted under the direction of Professor Jacques Ohayon of the cellular dynamic team (DynaCell), laboratory TIMC-IMAG (techniques of medical engineering and of complexity, and of informatics, mathematics and applications of Grenoble), and Dr. Roderic I Pettigrew, of the National Institutes of Health, laboratory of integrative cardiovascular imaging science. The tools developed during this thesis have been used for the molecular and biological characterization, both *in vitro* and *in vivo* of the atherosclerotic plaque. This work has for problematic the evaluation of early atherosclerotic plaque detection with a novel αvβ3 ITOP, in different animal and human models, as WHHL (Watanabe heritable hyperlipidemic) rabbits, human with coronary arteries disease, and an AD-HIES (autosomal dominant hyper IgE syndrome) patient. Different techniques of pathological staining, immunohistofluorescence and immunohistochemistry has been used to better comprehend the link between the αvβ3 ITOP labeling and the molecular and cellular characteristic of the plaque with an emphasis on the plaque vulnerability. The ultimate goals of the study focus on the evaluation of the αvβ3 ITOP for vulnerable plaque labeling, and the better comprehension of vulnerable plaque characteristic and possible mechanism of plaque instability.

To serve this purpose, the introduction will be focusing on the description of the atherosclerotic processes and pathophysiology, the description of the clinical imaging techniques allowing the detection of those atherosclerotic plaques, and the biomarkers of plaque instability. Angiogenesis and integrin will then be discussed more extensively, with an emphasis on αvβ3 probes, which was the ITOP used in this work to target atherosclerotic plaque. The introduction will also present the different animal and human models used in the thesis with their associated pertinence.

The first chapter will be describing the results of an *in vitro* study with the αvβ3 ITOP in a WHHL rabbit model. This chapter will allow to determinate the potential of the probe for the detection of atherosclerotic plaque. In this chapter, results on molecular characterization of the probe will also be presented.

The second chapter will be focusing on the *in vivo* confirmation of the results obtained in the *in vitro* study. This chapter will also describe some pathological and morphological findings related to the ITOP probe labeling.

The third and fourth chapter will present *in vitro* results of the ITOP probe labeling on human coronary arteries, from respectively human with CAD and human with AD-HIES. Because of the importance and the difficulty to obtain human samples, there will be a more extensive pathological study in those two chapters.

The third chapter will be devoted to confirm the specificity of the αvβ3 ITOP labeling for the atherosclerotic plaque, in human coronary arteries from patients with CAD. There will be a pathological and immunological characterization of the samples, in order to associate the αvβ3 ITOP signal with plaque morphology and molecular markers.

The fourth chapter will evaluated the same αvβ3 ITOP, in coronary arteries from a patient with AD-HIES. This human model is extremely rare and possesses several characteristics that rendered it very precious for the evaluation of our αvβ3 ITOP. First, previous imaging study reported a paucity of atherosclerosis in those patients. Second, they also reported an unusual prevalence of tortuosity, ectasia and aneurysms. Since vulnerable plaques and aneurysms are both associated with αvβ3 expression, it rendered AD-HIES model very pertinent for the evaluation of our ITOP. It is like having a knockout animal model, but with the pertinence of human biology. Very often, evaluation of another pathology in the context of understanding a disease, can lead to important discoveries.

Finally, some theories will be exposed to feed further discussion, and a general conclusion and some limitations will be presented, as well as future perspectives.

INTRODUCTION

1.1 ATHEROSCLEROSIS

1.1.1 Incidence and statistics

Despite all the recent technological advances, cardiovascular disease remains the leading cause of death in the Western World. Atherosclerosis disease develops through the life course, beginning as early as adolescence, and often progresses silently before the development of its later sequelae of myocardial infarction, angina or stroke. Over the past years, cardiovascular disease has become the leading cause of death in United State adults, accounting for over 40% of deaths in both men and women[1, 2]. It is estimated that in the United States alone, more than 1 million person die annually from the complications of these conditions. According to the World Health Organization, in 2003, it was estimated that over 16 million people around the globe died of cardiovascular diseases (CVD), which represent over 29% of all deaths globally. Although CVD affects approximately 30% of both men and women at age 50, the prevalence reaches 75% by age 75. Overall, the lifetime risk for coronary heart disease (CHD) is approximately 40% in men and 30% in women. This leads to at least 20 million people surviving heart attacks and strokes every year, with many that will require continuing and costly clinical care. In the end, the cost of treating these diseases exceeds 360 billion dollars US and continues to rise importantly. These statistics reinforce the importance of developing newer methods of assessment that will allow the detection of subclinical atherosclerotic disease.

1.1.2 Pathophysiology and Inflammation

Until recently, atherosclerosis was considered as a simple lipid metabolism disorder resulting in build-up of fatty materials (cholesterol) in arteries. Mostly, atherosclerotic plaque was seen as “plumbing” issue and the treatment of choice was to try to break up these fatty build-ups to reestablish proper blood flow in the luminal area. There is now an extensive body of literature showing the complexity of atherosclerosis mechanism, and involving various key determinants. Inflammatory processes are known to play a major role in this process. There is also a consensus pointing out atherosclerosis as a multifactorial process that is largely influenced by risk factors[3] (smoking, high blood pressure, elevated blood levels of cholesterol) and resulting in a chronic inflammatory response (Fig. 1)[4]. Actually, there is a predominant theory, according to the fact that atherosclerosis is initiated by the endothelium in response to an injury (dysfunctional endothelium)[5, 6]. Effectively, endothelial cells are exposed to many stimuli: free radicals, reactive oxygen species, low-density lipoprotein (LDL) uptake and oxidation, mechanical forces (shear stress), nitric oxide (NO) diminution, etc. Then, the endothelium reacts by expressing various “adhesion molecules” at their surface, as VCAM (vascular cell adhesion molecule) and ICAM (inter-cellular adhesion molecule) and selectin, as well as cytokines like monocytes chemotactic protein (MCP)-1. These adhesion molecules trigger the recruitment of lymphocyte and monocytes, their adhesion to the arterial wall and their translocation into the vessel wall. Inside the arteries, monocytes will become activate by the ox-LDL, which lead to the expression of scavenger receptor and foam cells formation. This inflammatory state also contributes to the release of many cytokines (MMPs, interleukin-1, interleukin-6, tumor necrosis factor α, interferon, etc.) and growth

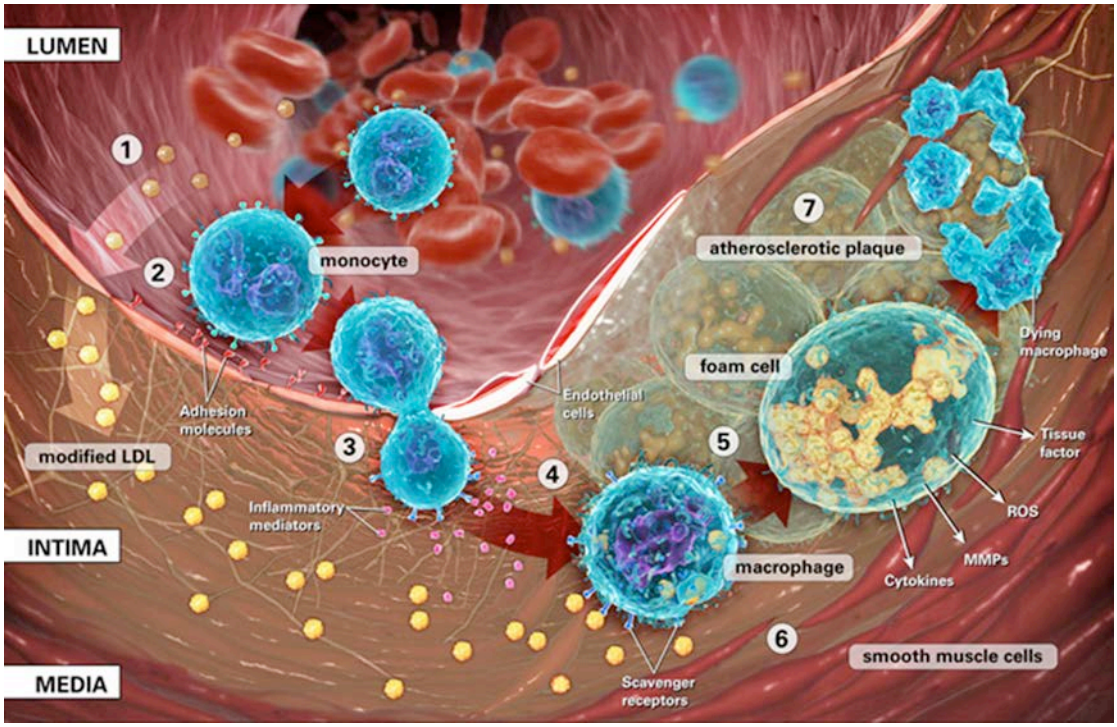

Reproduced from website: www.laddmcnamara.net

Figure 1 **Events leading to atherosclerotic plaque formation**

It is difficult to represent sequentially the events leading to atherosclerotic plaque formation, because of the complex crosstalk between plaque constituents and molecules. Nevertheless, plaque formation can be summarized as following: 1. LDL entrance and oxidation. Activated endothelium. 2. Monocytes adhesion to endothelium by VCAM, ICAM. 3. Monocytes extravagation inside vessel wall. 4. Cytokines activation. Monocytes differentiation. Scavenger receptors expression. 5. Lipid accumulation and transformation into foam cells. 6. SMCs activation and migration to form fibrous cap. Release MMPs and Tissue factor (TF). 7. Necrotic core formation and plaque growth. Note that 6 and 7 are concomitant processes and that imbalance between proteolytic activity and SMCs proliferation can lead to plaque rupture and thrombus.

factors (macrophage colony stimulating factor, colony stimulating factor) by the activated macrophages and T-cells. These growth factors will then be responsible of the recruitment and the proliferation of smooth muscle cells (SMCs), their migration from media to intima, and their proliferation into the intima. They will be a subsequent extracellular matrix (ECM) production and deposition by the activated SMCs, and the fibrous cap formation. The presence of oxidized LDL (ox-LDL), inflammatory

mediators, cytokines, foam cells, and apoptosis, contribute to plaque growth and instability. All these key molecules feed two major processes in plaque formation. The first one is intimal thickening caused principally by the constant lipid accumulation coming from the trapped intraplaque modified LDL and the absence of proper phagocytosis system that would remove extracellular debris from macrophages apoptosis and foam cells presence. The second one, caused by the presence of all the cytokines, growth factors and inflammatory mediators activated by ox-LDL that will lead to neointima formation (SMCs proliferation, migration, and ECM synthesis), and plaque healing.

1.1.3 Plaque Histology and Morphology

Normal arteries are generally composed by five different categories of tissue: endothelium, muscle cells, elastin, collagen and ECM[7]. The first layer of cells in contact with the lumen is the endothelium, and it represents a barrier between the blood and the arterial wall. It is composed by a monolayer of epithelial cells. SMCs are another type of cells present in arteries and are, in conjunction with ECM, responsible for the elastic properties of the vessel wall. Coronary arteries possess multilayers of SMCs, which are responsible for the secretion of elastin, a protein that constitutes an important part of the arteries. The elastin is present on a polymerized form inside the wall, which constitutes a fiber network that can sustain high tension and constraints. Another major protein present in the arteries and also secreted by SMCs is the collagen. Collagen fibers are bounded to each other and they are responsible for the mechanical resistance of the tissue. Finally, all these various components are hold together by a matrix called ECM. The ECM provides

structural support to the tissue, is very viscous, and principally composed by polysaccharides and proteoglycans. Structural proteins (elastins and collagen) as well as specialized proteins (fibronectin, vitronectin, laminin, etc.) also composed the ECM.

In arteries, these constituents are organized in 3 different layers: the tunica intima, the tunica media, and the tunica adventitia (Fig. 2). In textbook, the ideal representation of the intima is composed by a monolayer of endothelial cells embedded in ECM, and held together by junctional complexes. In reality, there is no ideal single monolayer of endothelium in arteries[8]. In fact, early in life, the intima differentiates into a thicker,

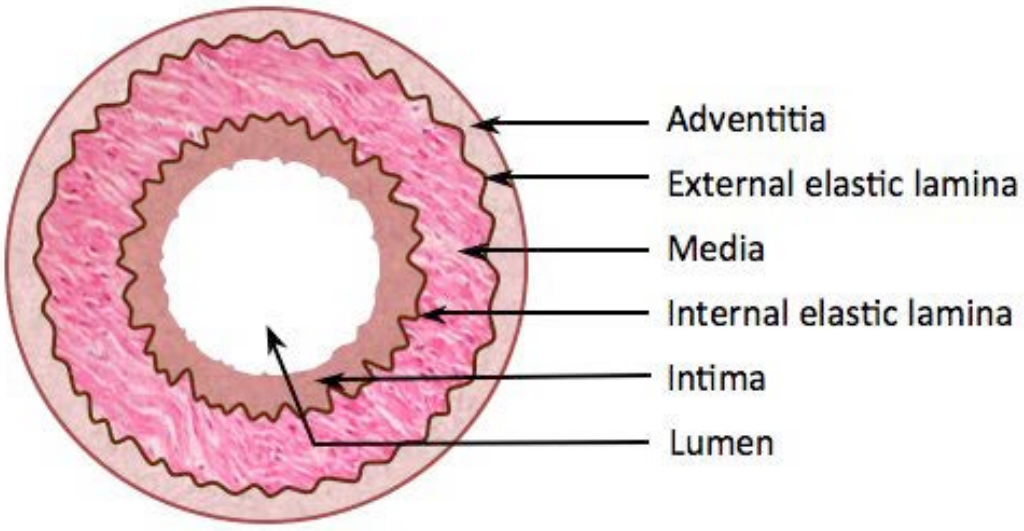

Figure 2 **Representation schematic of the constituents of the coronary wall**

In arteries, these constituents are organized in 3 different layers: the tunica intima, the tunica media, and the tunica adventitia. In textbook, the ideal representation of the intima is composed by a monolayer of endothelial cells embedded in ECM, and held together by junctional complexes. In coronary arteries, there are also two membranes separating the intima from the media and the media from the adventitia: the internal elastic lamina (IEL) and the external elastic lamina (EEL). These two membrane, as their name indicate, are constituted by elastic fibers.

better-developed intimal layer, because of the environment it is exposed to (mechanical stress, free radical, LDL). Indeed, all humans are carriers of a certain degree of hyperplasia, although this phenomenon is benign, resulting in resident SMCs into the intima. The media is principally composed by multilayers of SMCs, and bundles of collagen fibers and elastic fibrils, all embedded in the ECM. Finally, the adventitia, which is considered the most variable layer of the artery, is a relatively thin connective tissue layers. Fibroblasts are the predominant cell type, but there are also macrophages. The adventitia contains collagen, dense fibroelastic fibers (not lamellae), nutrient vessels (vasa vasorum), and nerves. In coronary arteries, there are also two membranes, constituted by elastic fibers, separating the intima from the media and the media from the adventitia: the internal elastic lamina (IEL) and the external elastic lamina (EEL). Often, the EEL will be use as a measurement of the total vessel area, because the adventitia layer is sometime difficult to delineate.

In atherosclerosis, there is an important thickening of the intima layer[9]. This is principally due to the infiltration and retention of LDL, which after being oxidized, are trapped inside the wall. These process lead to the recruitment of monocytes, differentiation into macrophages and ultimately, formation of foams cells and what is called necrotic core (lipids, foam cells, cellular debris). Cytokines and growth factors released by macrophages and T-cells will activate SMCs into the media, which will secrete more ECM, and will eventually cause the migration of SMCs into the intima, for the formation of the fibrous cap. In some circumstances, the adventitia layer will also thicken, mostly because of the neovascularization and the presence of inflammation.

1.1.4 Vulnerable Plaque and Positive Remodeling

It is very difficult to predict the rupture of an atherosclerotic plaque, and the definition of these types of plaques has been debated for decades. Most of the time, cardiovascular events are sudden and unpredictable. There are, although, some morphological, cellular, and molecular features that can be related to plaque vulnerability[10, 11]. A vulnerable or unstable plaque is an atherosclerotic plaque, which is liable to complications and is prone to thrombus. For a long time, it has been postulated that plaques that were clinically relevant was the one with an important degree of stenosis (Fig. 3). Now, it is generally accepted that plaque composition, rather than luminal stenosis is considered the major determinant of plaque vulnerability[12, 13]. Although vulnerability is difficult to define, the majority of vulnerable plaques share the same characteristics. Most importantly, it has been reported that the majority of plaque ruptures occur in a segment with low-grade stenosis, but presenting outward or positive remodeling[14-16]. Effectively, as elegantly demonstrated by Glagov[17], at early stages of plaque development, arterial vessels enlarge in relation to plaque area, and lumen stenosis is delayed until the lesion occupies approximately 40% of the potential lumen area. This phenomenon is called compensatory enlargement of the vessel wall. According to this theory, for values above 40% stenosis, the lumen diminishes markedly and in close relation to the percentage of stenosis. Glagov findings demonstrated for the first time that despite presenting an adequate or normal lumen area, coronary arteries could present advanced atherosclerosis (Fig. 4). His findings were also the premises for the discovery of positive remodeling, which is defined by an outward bulging or expansion of the arterial wall. As mentioned before, this phenomenon has been largely associated with plaque vulnerability and rupture, as

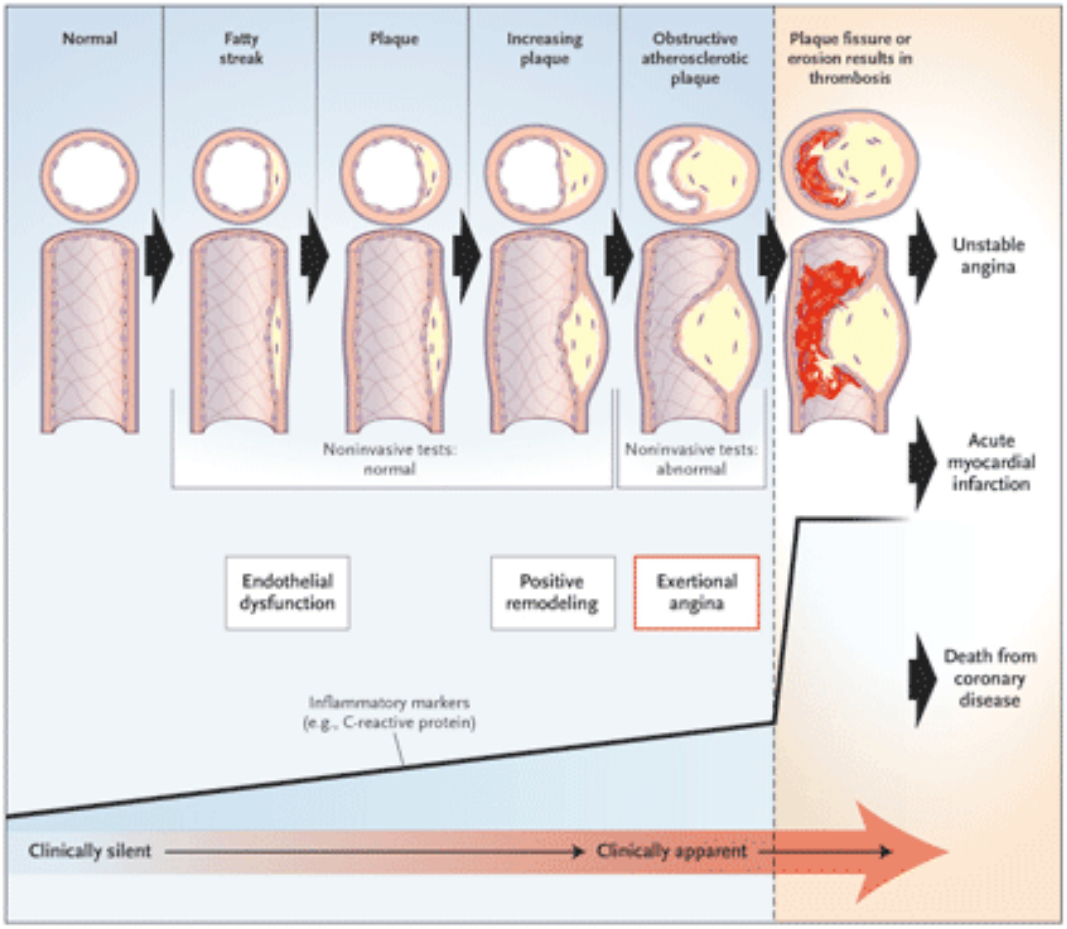

Reproduced from www.intranet.tdmu.edu.te.ua

Figure 3 **Representation schematic of plaque formation versus clinical events**

Schematic representation of atherosclerotic plaque progression, from normal coronary vessel to vessel with highly stenosed plaque. Before the plaque reaches the stenotic phase, the vessel goes into a positive remodeling phase. For a long time, it has been postulated that plaques that were clinically relevant was the one with an important degree of stenosis. It is now understand that plaque composition, rather than luminal stenosis is the major determinant of plaque vulnerability. It is becoming accepted that plaque rupture often occur in the presence of low-grade stenosis, and that stenosis is not a good predictor of ischemic events.

opposed to negative remodeling, which are associated with vessel shrinkage and higher-grade stenosis, but more stable phenotype.

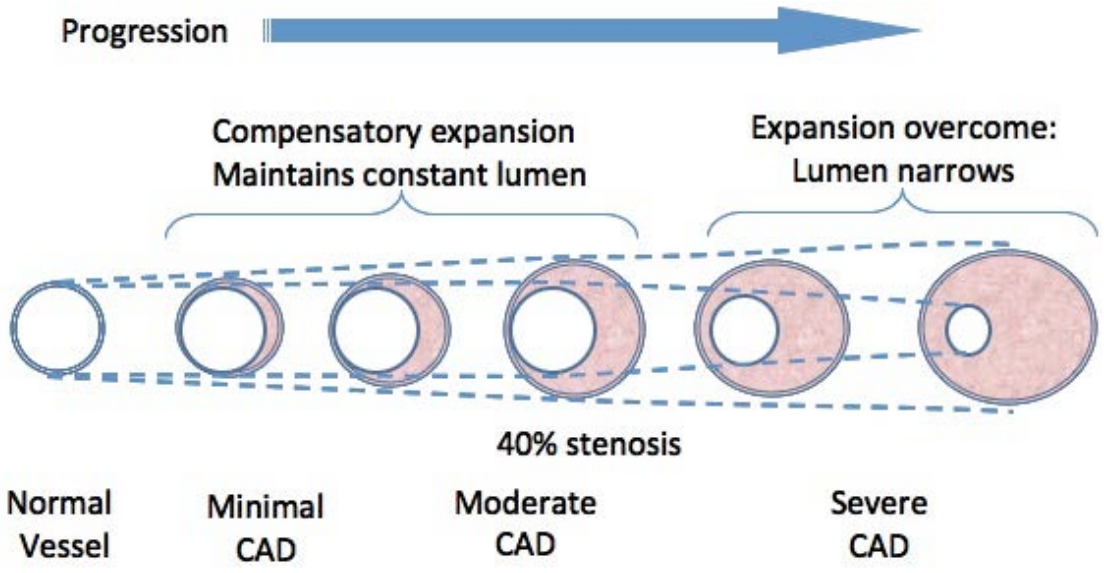

Adapted from Glagov et al. N Engl J Med 1987; 316(22):1371-1375.

Figure 4 **Compensatory enlargement of coronary artery as described by Glagov**

At early stages of plaque development, arterial vessels enlarge in relation to plaque area, and lumen stenosis is delayed until the lesion occupies approximately 40% of the potential lumen area. This phenomenon is called compensatory enlargement of the vessel wall. According to this theory, for values above 40% stenosis, the lumen diminishes markedly and in close relation to the percentage of stenosis. Glagov findings demonstrated for the first time that despite presenting an adequate or normal lumen area, many persons have advanced atherosclerosis. His findings were also the premises for the discovery of positive remodeling, which is defined by an outward bulging or expansion of the arterial wall.

Apart from being in a positive remodeling stage, vulnerable lesions also possess some common morphological features[18]. First, these plaques possess a thin fibrous cap, usually less than 65μm, with very few collagen fibers. Since the fibrous cap is a dynamic structure, its thickness depends on the collagen synthesis by VSMCs as well as on the collagen degradation by MMPs. Secondly, these plaques have a very large lipid core area, usually more than 40% of the neointima. Moreover, the lipid core contains a large

amount of cholesterol esters and is soft, which present a higher propensity to rupture than fibrotic plaques. Among the factor contributing to plaque instability and rupture, plaque inflammation, both local and systemic, is considered to be the most important one. Inflammation plays a major role in plaque formation, progression, instability and rupture, although the importance of the key players is often debated. Nevertheless, a large number of macrophages are another characteristic of unstable plaques. Indeed, the number of infiltrated macrophages in the thin fibrous cap is often greater than 25 cells per high power field (40X, field diameter 0.3mm). Macrophages are often distributed at the shoulder region of the lipid core in fibrous plaques (type V), but are distributed diffusely in vulnerable plaques[19, 20]. In the neointima of vulnerable plaques, there is generally a smaller number of VSMCs. Another important factor in plaque vulnerability is the increased plaque thrombogenecity, which is characterized by an increase in plasminogen activator inhibitor (PAI), plasma fibrinogen, tissue factor (TF), and platelet activation and aggregation. Finally, a diminution of elasticity is also an important factor for plaque instability. Effectively, as seen in aneurysm, absence of collagen and elastic fibers lead to positive remodeling and can causes rupture of the vessel wall. Microcalcifications have also been linked to plaque instability[21].

Finally, after the initial plaque formation or rupture, there are two possible fates: one is the healing and sealing of the plaque and the other one in an acute coronary event (ACE). Again, at this stage, there is a number a different biological and physical/mechanical factors that will determinate which event will take place (Fig. 5).

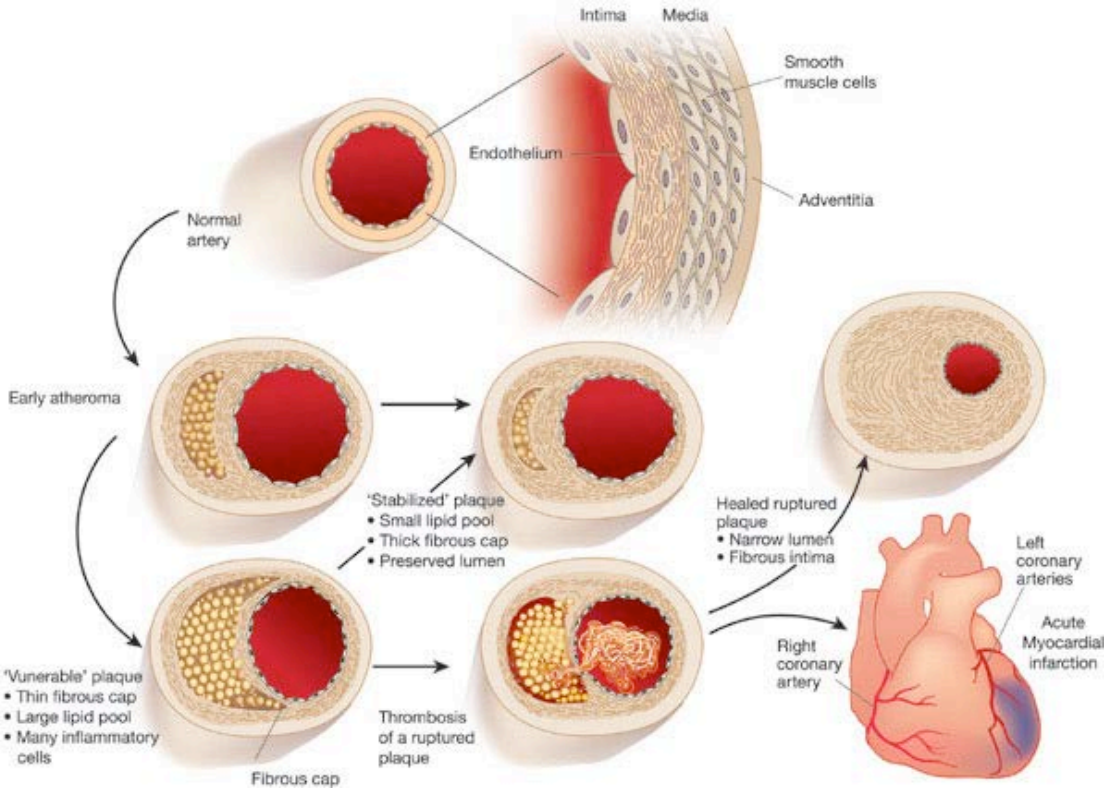

Reproduced from Libby P. Nature 2002; 420(6917):868-874.

Figure 5 Events leading to atherosclerotic plaque rupture or healing

After the initial plaque formation, there are two possible fates: the plaque can either stabilize or develop into a vulnerable plaque. In the same way, after the rupture, the plaque can either be sealed and healed, or it can produce a thrombosis and causes a coronary event.

There is an extensive body of literature and images on plaque progression and instability, and the clinical event associated with them. It is often difficult and confusing to navigate through them, because of the absence of definition or because of the conflicting representation. Plaque progression, clinical events, and coronary artery disease (CAD) severity are often associated with luminal stenosis, without taking into account plaque composition or compensatory lumen enlargement described by Glagov (Fig. 6A). Over

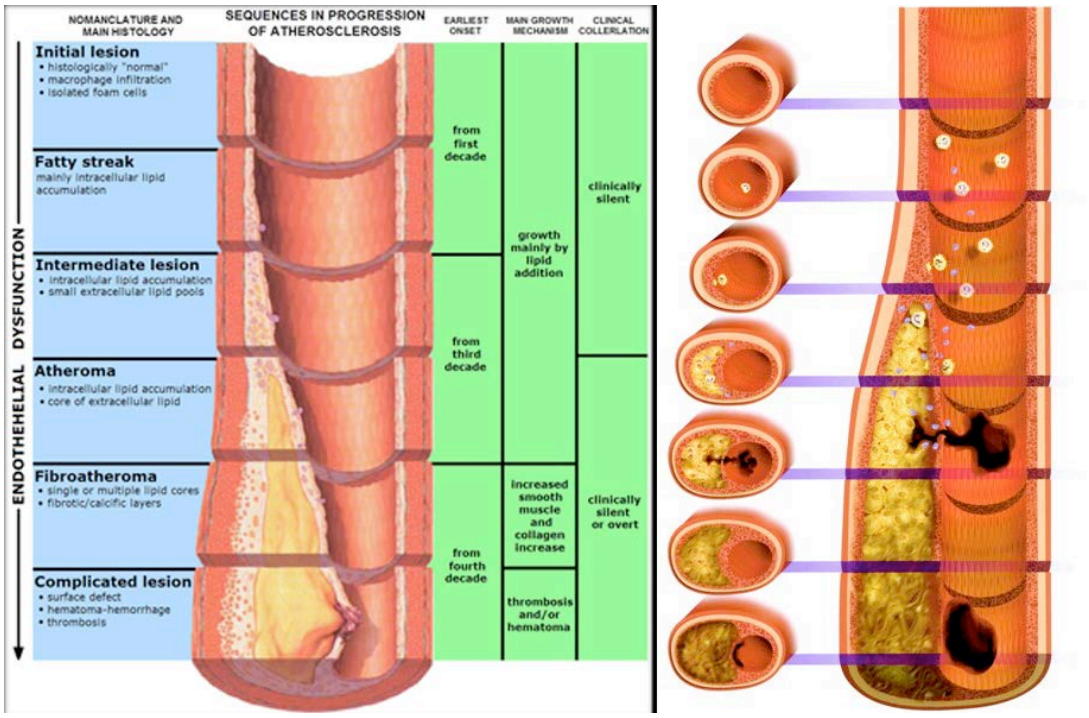

(A) Open-source image from http://en.wikipedia.org/wiki/Atherosclerosis
Adapted from Pepine CJ. Am J Cardiol. 1998; 82(Suppl.10A): 23S-27S.
(B) Libby P. Circulation 2001; 104(3):365-372.

Figure 6 **Stage of endothelial dysfunction in atherosclerotic plaque formation**

The sequence of events leading to progression of atherosclerosis, related to lumen stenosis and clinical event. **(A)** Representation schematic of plaque progression with lumen narrowing and absence of positive remodeling. **(B)** Representation schematic of plaque progression with positive remodeling and absence or minimal lumen stenosis. There is an extensive literature on plaque progression that related plaque progression, and clinical events to stenosis **(A)**. There are currently many evidences supporting that advanced atherosclerosis is present without or with minimal lumen narrowing, and that thrombosis is often associated with little lumen encroachment **(B)**.

the recent years, it has become clearer that this schematic representation of plaque progression might be bias. In fact, advanced atherosclerotic plaque and thrombosis events are often seen in vessel wall with very minimal stenosis (Fig. 6B). In the other hand, plaque's healing response often lead to increased collagen accumulation and SMCs

growth. This mechanism transform fibrofatty lesion into advanced fibrous and often calcified plaque, which may causes significant stenosis[22]. In agreement with this theory, despite being in their early stage, plaque can present advanced atherosclerosis and vulnerability to rupture, as opposed to healed plaques that can show important stenosis. In fact, as elegantly schematized by Naghavi *et al*, among the numerous types of vulnerable plaques, most of them are characterized by an absence of very little lumen narrowing (Fig. 7)[23]. Therefore, it becomes imperative to develop imaging modalities that take this important phenomenon into account.

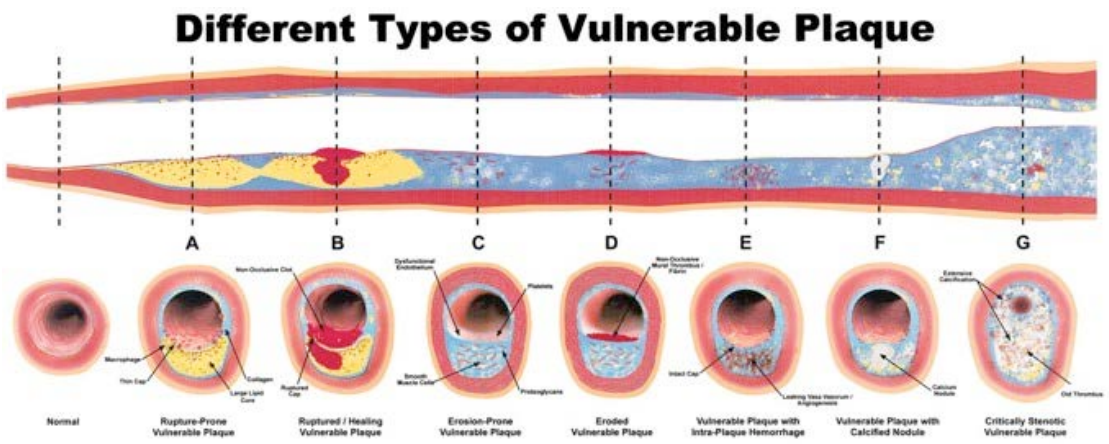

Reproduced from Naghavi M *et al*. Circulation 2003; 108(14):1664-1672.

Figure 7 **Different types of vulnerable plaque as underlying cause of acute coronary events (ACS) and sudden cardiac death (SCD)**

(A) Rupture-prone plaque with large lipid core and thin fibrous cap infiltrated by macrophages. **(B)** Ruptured plaque with subocclusive thrombus and early organization. **(C)**, Erosion-prone plaque with proteoglycan matrix in a smooth muscle cell-rich plaque. (**D)**, Eroded plaque with subocclusive thrombus. (**E)** Intraplaque haemorrhage secondary to leaking vasa vasorum. (**F)** Calcific nodule protruding into the vessel lumen. **(G)** Chronically stenotic plaque with severe calcification, old thrombus, and eccentric lumen.

1.1.5 Histological classification of atherosclerosis

As mention earlier, atherosclerotic plaque classification is not an easy task. Nevertheless, in the nineties, Stary HC and *al.* produced a series of 3 reports, published in both Circulation journal and Arteriosclerosis, Thrombosis, and Vascular Biology journal, aiming at describing and defining the characteristic components of atherosclerotic plaques by types[19, 20, 24-27]. They also try to correlate the appearance of lesions noted in clinical imaging with histological lesion types, and corresponding clinical symptoms. Those reports where the backbone of many other publications and attempt at classification. Unfortunately, in many subsequent reports and publications, there is a tendency to related stenosis with advanced atherosclerosis and clinical complications (Fig. 3, Fig 6A). In the original report, 6 principal types of plaques were described (Type I to Type VI), with type II that can be divided into type IIa and IIb, and the type V that can be divided into type Va, Vb and Vc (Table 1). The 3 first types are considered early lesions, although type I and type II are not generally precursors of more advanced atherosclerosis and can be seen in adults. Type III is the intermediate lesion forming the bridge from early to more advanced atherosclerosis. Type IV lesions are the first lesion considered as advanced atherosclerosis. It is also the first one considered to become clinically overt. Type V is generally constituted by an intima thickened by substantial reparative fibrous tissue (mainly collagen). The presence of fibrous connective tissue and lipid core(s) characterized type Va (fibroatheroma), and the predominant presence of calcification into a fibrolipid lesion characterized type Vb (calcific). Type Vc (fibrotic) only has minimal lipid and no calcification. Type VI lesions are lesions with thrombus, hematoma, and surface defect.

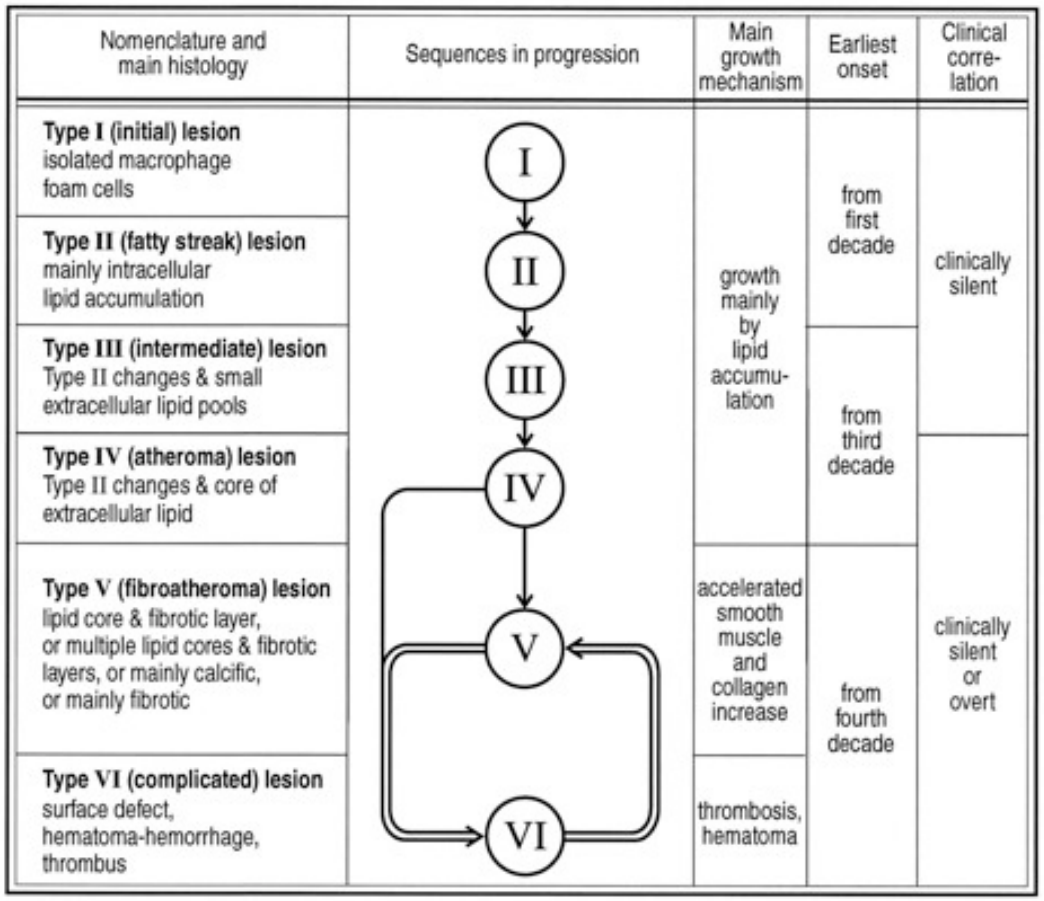

Reproduced from Arterioscler Thromb Vasc Biol 1995; 15(9):1512-1531.

Table 1 **Evolution and progression of human atherosclerotic lesions**

Flow diagram in center column indicates pathways in evolution and progression of human atherosclerotic lesions. Roman numerals indicate histologically characteristic types of lesions. From type I to type IV, changes in lesion morphology occur primarily because of increasing accumulation of lipid. The loop between types V and VI illustrates how lesions increase in thickness when thrombotic deposits form on their surfaces.

According to this classification, type IV lesions can be seen as the vulnerable plaques that are extensively described in the literature. Therefore, as illustrated in the diagram of Table 1, type IV lesion can either rupture to produce a clinical event, or healed and

become a more stable type V lesion. Type IV lesions, and sometime type V lesions, can rupture, healed and become a type VI lesion. It can also be noted that type VI lesion can also healed and evolve into type V lesion. In summary, a vulnerable plaque can rupture and produce symptoms, or it can heal and become stable. The plaque rupture can also be sealed and become more stable.

Lesion from type I to III are not considered to thicken the arterial wall and do not produce lumen narrowing. Type IV lesions are considered minimally obstructive and do not produce significant lumen narrowing. Type V lesions produced different degrees of lumen narrowing, while type VI lesions are often very obstructive. Inasmuch, it is not unreasonable to think that lumen narrowing and stenosis is a result of a process of plaque healing. Therefore, when representing plaque progression, the phenomenon of compensatory enlargement previously described by Glagov[17], one of the author of those reports, has to be taken into account. Also, it has to be noted that the type of plaques described into those publications does not necessary represent a linear progression of atherosclerosis evolution. For example, type I and II lesions are not necessary the precursor of more advanced lesions. In the same way, type IV lesions can either rupture and create a coronary event, healed and become a more stable plaque (type V), or rupture and healed creating a type VI lesion. Moreover, type VI lesion can regressed into a more stable type (type V).

It is consequently imperative to pursue the challenge of characterizing atherosclerotic lesions in the context of clinical situations. This clinical classification will allow depicting the plaque histology as closely as possible, and specifically targeting the problematic lesions with appropriate treatments.

1.2 IMAGING THE PLAQUE[28]

1.2.1 Current diagnostic medicine

Angiography has been used for decade to evaluate patients with atherosclerosis and is seen as the conventional method for imaging the plaque. Nevertheless, with the recent insight regarding plaque composition and the better understanding of plaque biology, it has become imperative to find new imaging techniques that rely on plaque constituents, rather than degree of stenosis (Fig. 8). Effectively, there is growing evidences that the

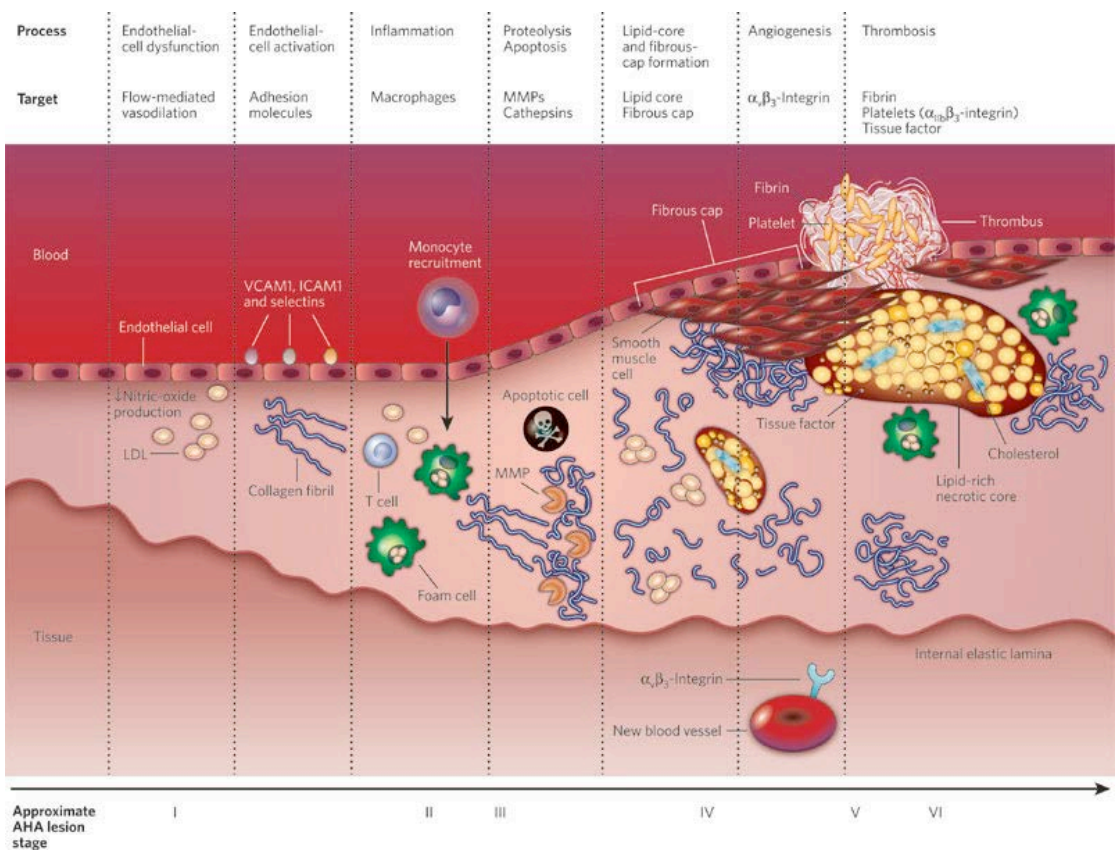

Reproduce from Sanz J and Fayad ZA. Nature 2008. 451(7181):953-957.

Figure 8 **Molecular imaging of the atherosclerotic plaque**

With the recent advances in plaque composition and the better understanding of inflammation processes in plaque formation, there is a broad development of targeted probes for the detection of vulnerable plaques.

events leading to coronary disease and sequelae appeared at an earlier stage of atherosclerosis, and that it is poorly correlated with the degree of stenosis. Thus, a number of new biomarkers and imaging techniques has been developed to detect atherosclerosis at an earlier stage and better predict plaque rupture.

1.2.2 Angiography

Despite its numerous limitations, X-ray angiography is considered as the current "golden standard" regarding the detection of advanced atherosclerotic lesions and measurement of degree of stenosis (Fig. 9). The major limitation of angiography is the fact that it is

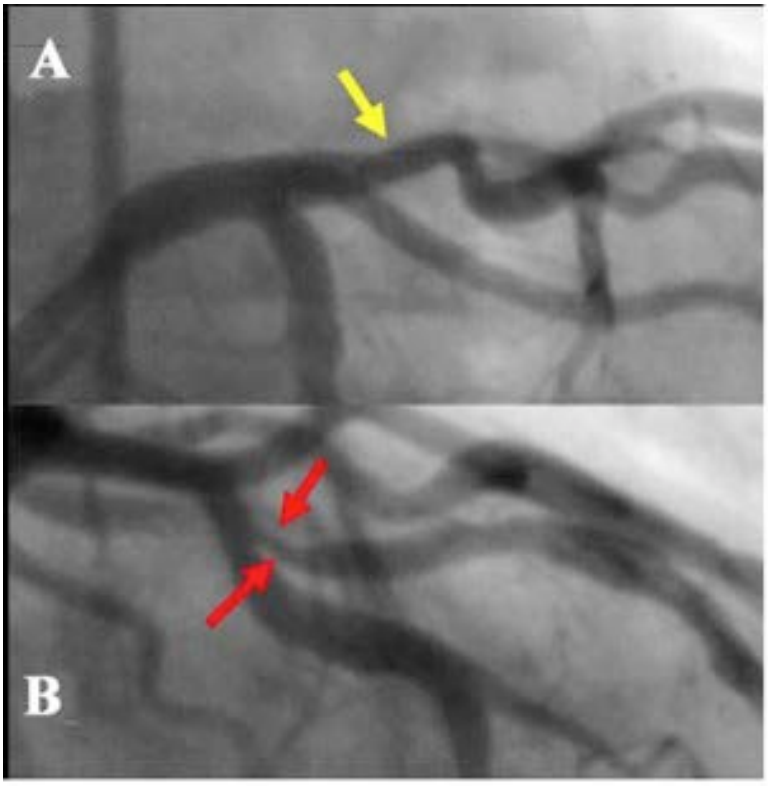

Figure 9 **Conventional angiogram of LAD in left anterior oblique views**

76-year-old male with none-significant stenosis (A) in the proximal LAD (yellow arrow) and significant stenosis (B) in mid LAD (red arrows) seen by conventional angiogram

simply based on imaging the vessel's lumen, thus it fails to detect atherosclerotic lesion that does not protrude into the lumen, or the one with positive remodeling, which are considered important in term of vulnerability. This imaging method also provides very little information about plaque composition. These important limitations prevent angiography to differentiate between stable and unstable plaque, therefore rending it unable to assess or predict the risk of plaque rupture. Consequently, the main value of angiography will be to delineate the causative lesions in a symptomatic patient, making it a mostly "symptom driven" imaging technique.

1.2.3 IVUS

Intravascular ultrasound (IVUS) is an invasive imaging modality in which a small ultrasound probe mounted on a catheter is passed through the blood vessels. It allows direct imaging of the vessel area and atheroma, as well as a cross-sectional image of the complete plaque and vessel wall (Fig. 10). Thus, unlike angiography, IVUS can detect non-stenotic atheromatous plaques. It also allows plaques to be categorized as soft, fibrous or calcified. In spite of its utility for the detection of plaques otherwise missed by angiography, IVUS has major drawbacks: it is invasive, expensive, and demand more level of expertise than the other imaging modalities to be performed. In USA, it is mostly confined to research and determining the success of interventions, but in European countries, it is practice more often for the exploration of patients already considered at risk. Despite all these drawbacks, IVUS can be useful to detect plaque that are in a positive remodeling stage and considered as vulnerable.

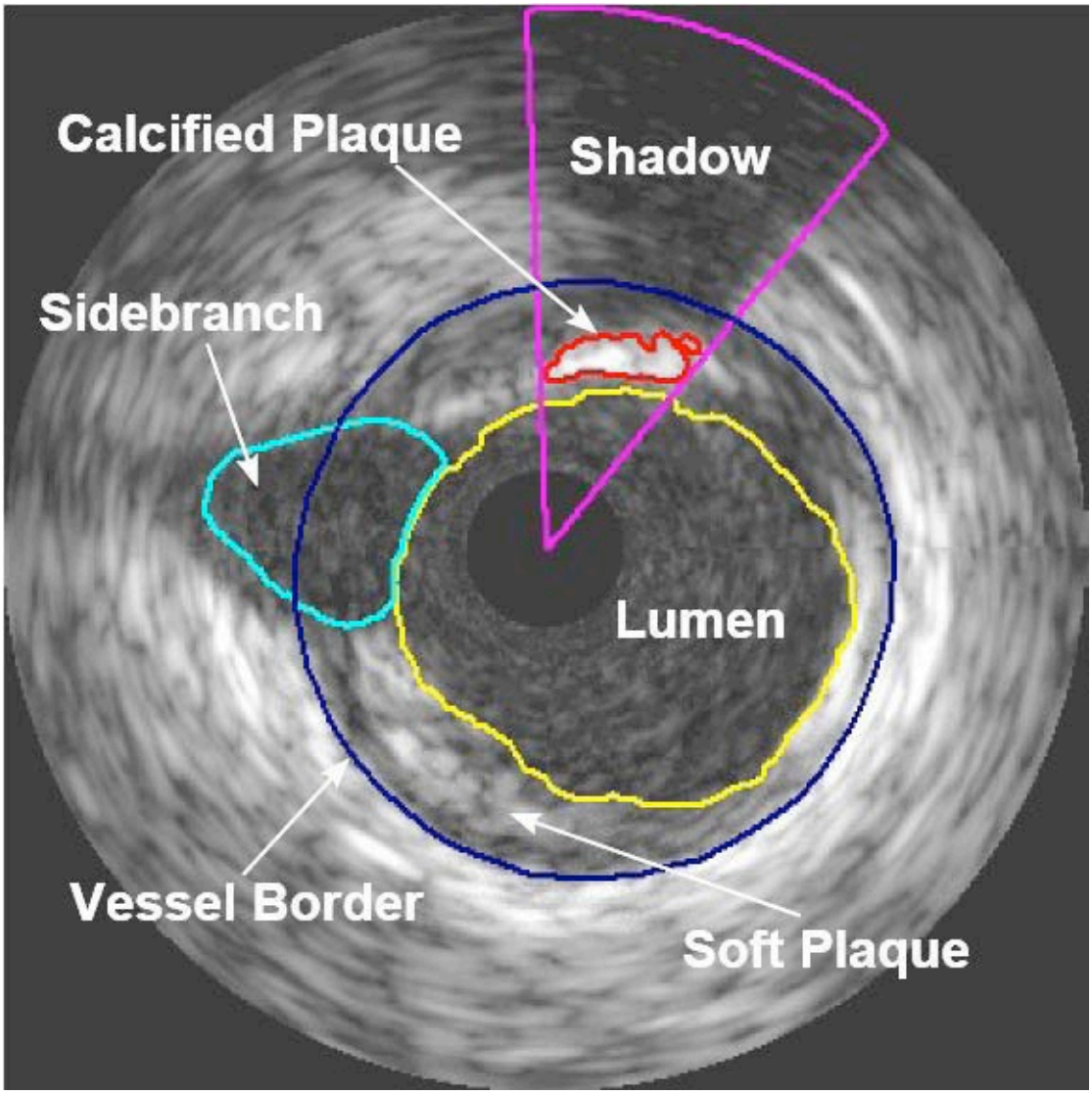

Reproduced from www.natcomp.liacs.nl

Figure 10 **Cross-section of a coronary artery seen by IVUS**

In vivo imaging of a coronary artery by IVUS, showing the different constituent of the atherosclerotic plaque: calcification, necrotic core, and lumen. Unlike angiography, IVUS can detect atherosclerotic plaques that are not stenotic.

1.2.4 PET

Position emission tomography (PET) is the use of a radioactive tracer, administered intravenously, to detect its accumulation at a site of interest (Fig. 11). After a certain amount of time (depending of the radiotracer used), the tracer's level became sufficiently low in the blood, and high in the target site, allowing a favorable target to background signal. PET is an imaging technique currently functional at the molecular level. The sensitivity of the modality is several orders higher than MRI, however, the resolution achieved is significantly less. Another drawback of the PET is that it requires the use of ionizing radiation.

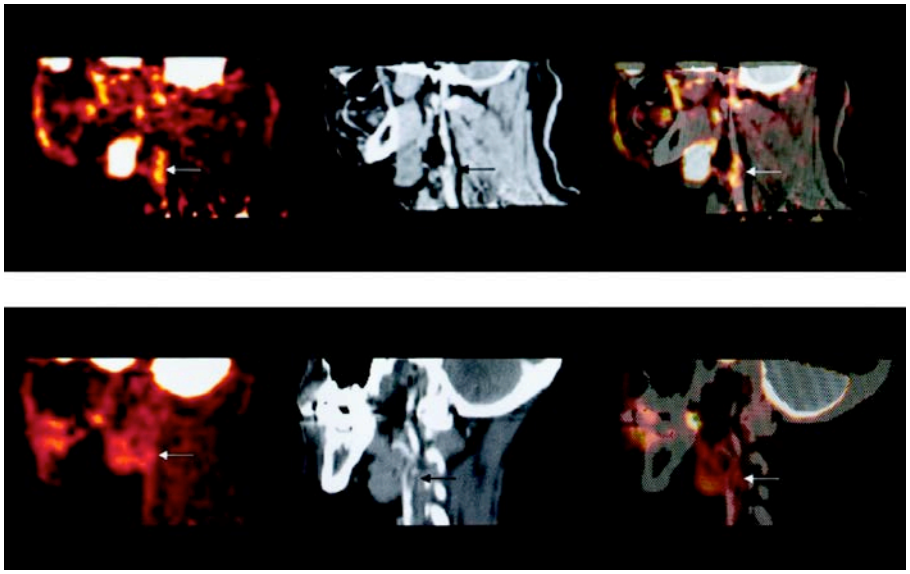

Reproduced from Rudd JH *et al.* Circ 2002; 105(23):2708-2711.

Figure 11 **Imaging by PET scan with 18FDG**

The upper row (left to right) shows PET, contrast CT, and co-registered PET/CT images in the sagittal plane, from a 63-year-old man who had experienced 2 episodes of left-sided hemiparesis. Angiography demonstrated stenosis of the proximal right internal carotid artery; this was confirmed on the CT image (black arrow). The white arrows show 18FDG uptake at the level of the plaque in the carotid artery. As expected, there was high 18FDG uptake in the brain, jaw muscles, and facial soft tissues. The lower row (left to right) demonstrates a low level of 18FDG uptake in an asymptomatic carotid stenosis. The black arrow highlights the stenosis on the CT angiogram, and the white arrows demonstrate minimal 18FDG accumulation at this site on the 18FDGPET and co-registered PET/CT images.

1.2.5 CT

Computed tomography (CT) is an imaging modality that uses X-ray beam to image a patient in thin sections. The computer generates an image based on different densities with multiple detectors, after the beam has traversed the patient. CT is an excellent imaging technique for soft tissue contrast and discrimination, so it allows to determinate plaque composition. It also allows imaging deep structures like coronary arteries, with a relatively high degree of resolution (Fig. 12), but it is not a functional technique for molecular imaging or plaque vulnerability assessment. Although CT is useful to image small vessels, it is a very expensive imaging technique and it involves the use of radiations and contrast agents that introduce risks of nephrotoxicity and anaphylaxis.

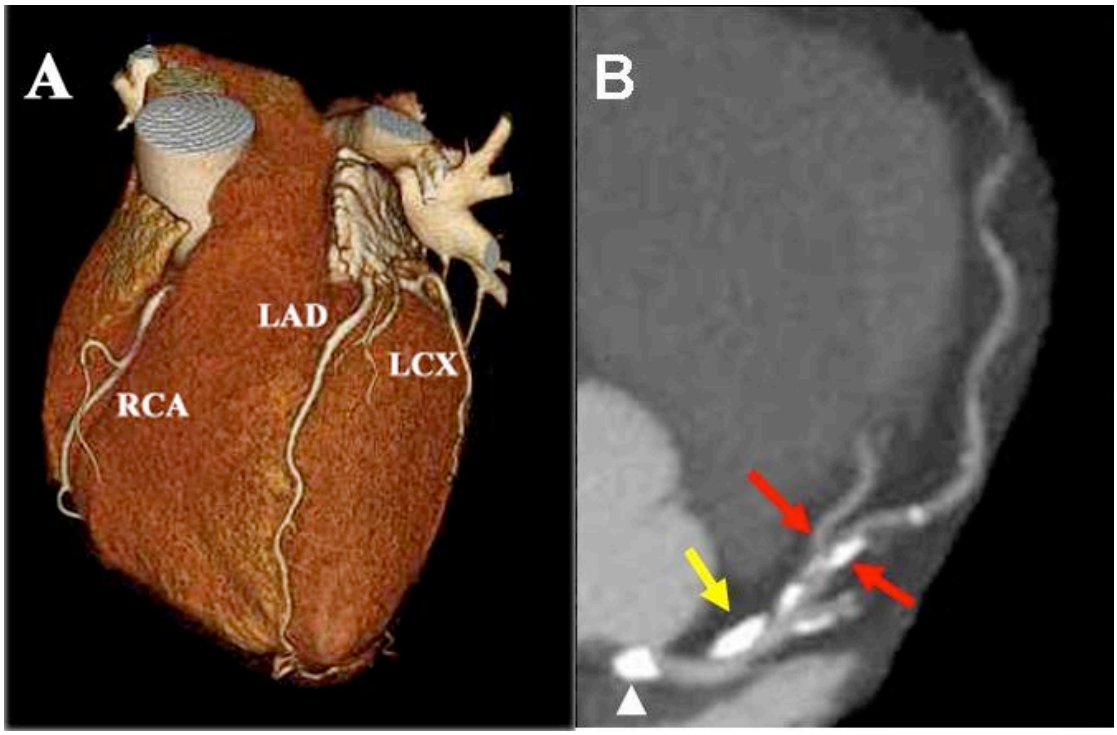

Figure 12 **320-detectors CT scan of coronary arteries**

(A) 3D reconstruction of a CT scan, showing RCA, LAD, and LCX. (B) 76 year old male with none-significant stenosis in the proximal LAD (yellow arrow) and significant stenosis in mid LAD (red arrows) seen by maximum intensity projection (MIP) in left anterior view of the LM/LAD.

1.2.6 MRI

Magnetic resonance imaging (MRI) is a method of choice for the first screening of atherosclerosis: it is non-invasive, does not involve ionizing radiation, and provides high-resolution images of multiple vascular territories. Unlike CT, MRI contrast agents are well tolerated and less likely to alter kidney function or to cause an allergic reaction. The major technical advantage of MRI is the capacity of characterizing and discriminating among tissues using their physical and biochemical properties (Fig. 13). Thus, it allows

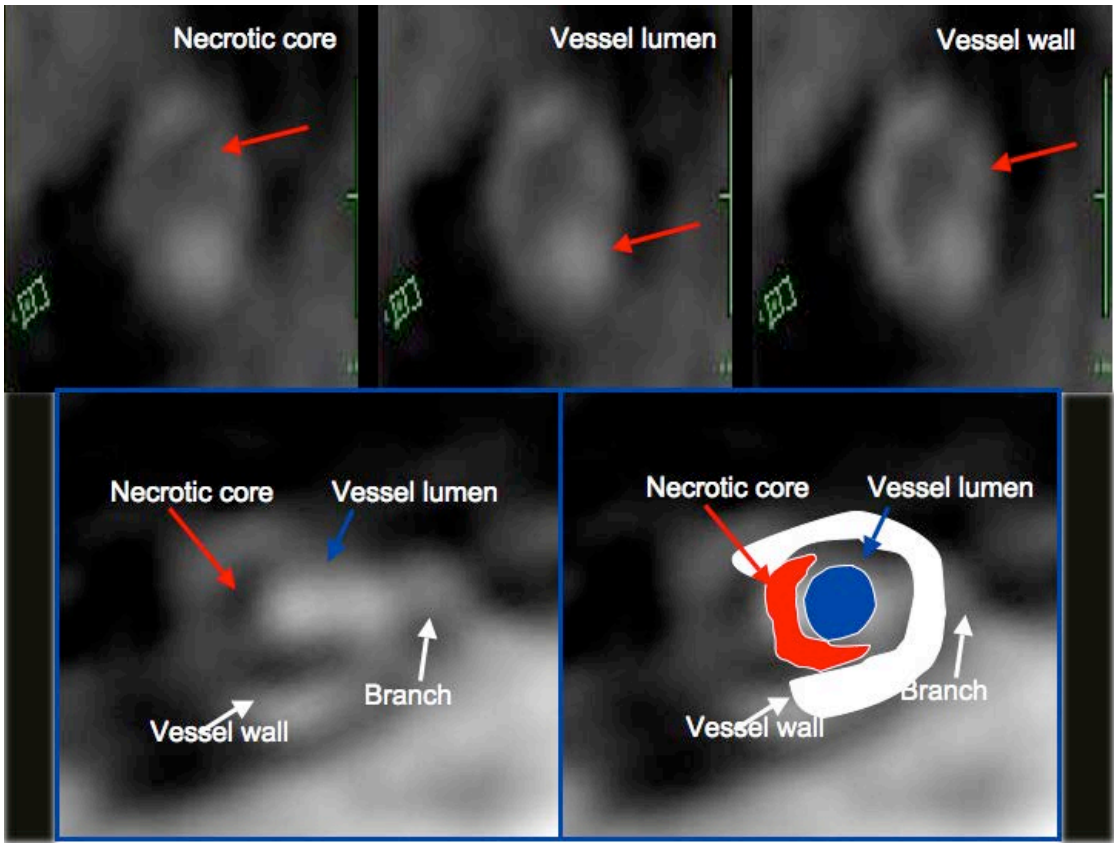

Figure 13 **Comparison between MRI and CT of a cross-section of a coronary artery**

CT scan **(upper panel)** compare to MRI **(lower panel)** of coronary artery wall. MRI showed some of the constituents of the coronary artery wall at a plaque area. The lumen, vessel wall, coronary branch, and a necrotic core can be visualized.

differentiating between different constituents of the plaque (lipids, calcium, fibrous tissue, hemorrhage, necrotic core…). In the other hand, one of the most important challenges of MRI is the motion of the heart, rending the scan more difficult and time-consuming. It is also a relatively expensive imaging modality and is probably the imaging modality the most technically challenging. Also, due to the resolution, it is difficult to detect plaques at the stage of positive remodeling.

1.2.7 Optical Imaging

The perfect imaging modality for atherosclerosis would be easy to use, has a limited cost, and could be integrated with traditional laboratory techniques. Optical imaging (bioluminescence, fluorescence molecular tomography…) can fulfill these requirements and is an attractive imaging method for scientists without extensive knowledge (Fig. 14). Indeed, optical imaging apparatus are less expensive to purchase, easier to maintain, and does not require radiation permits or shielding. Moreover, optical imaging agents are usually harmless and nontoxic, plus they do not decay, so they can be stored on the shelf. Optical imaging also integrate very well with other laboratory techniques, as imaging agents can be use *ex vivo* for FACS or immunofluorescent histology, after *in vivo* imaging. Unfortunately, one of the major drawbacks of optical imaging is the low penetration of imaging agents, making it difficult to use for deep tissue like heart, or necessitating invasive procedures as catheterization.

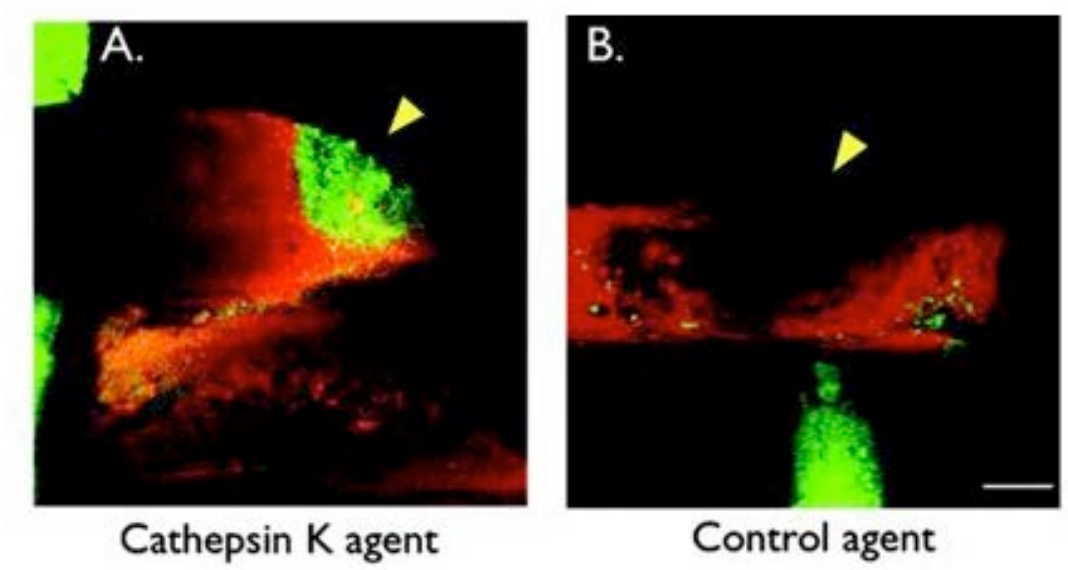

Adapted from Farouc AJ *et al*. Circ 2007; 115(17):2292-2298.

Figure 14 **In vivo optical imaging of cathepsin K in carotid atherosclerotic plaques of ApoE-/- mice**

(A) Fusion *in vivo* image of a carotid vessel (5X magnification; 13X13 μm in-plane resolution; 10 μm slice thickness) demonstrating focal cathepsin K signal (green) in an atherosclerotic lesion (arrowhead). **(B)** Fusion image of a carotid plaque (arrowhead) in the control group demonstrating minimal NIRF signal in the cathepsin channel.

1.2.8 Multimodality Imaging

It is becoming clear that there is no such thing as the perfect imaging modality for the detection of early or vulnerable atherosclerosis. Indeed, all the imaging modality are complementary, in a way that one modality can compensate for the lack of the others. By combining the different imaging modalities, which can overcome the limitations of some of them by using their respective strengths (Fig. 15). Heart is probably the most challenging structure to image, as it is deep inside the body, in constant movement, and contains arteries that are relatively small and difficult to visualize. By combining high-

resolution imaging and good soft tissue contrast that give us information about anatomic structures, with high sensitivity technique that provide us with molecular information, we can probably achieve the challenge of detecting atherosclerotic plaque, before the apparition of the clinical symptoms, rupture and heart attack or stroke.

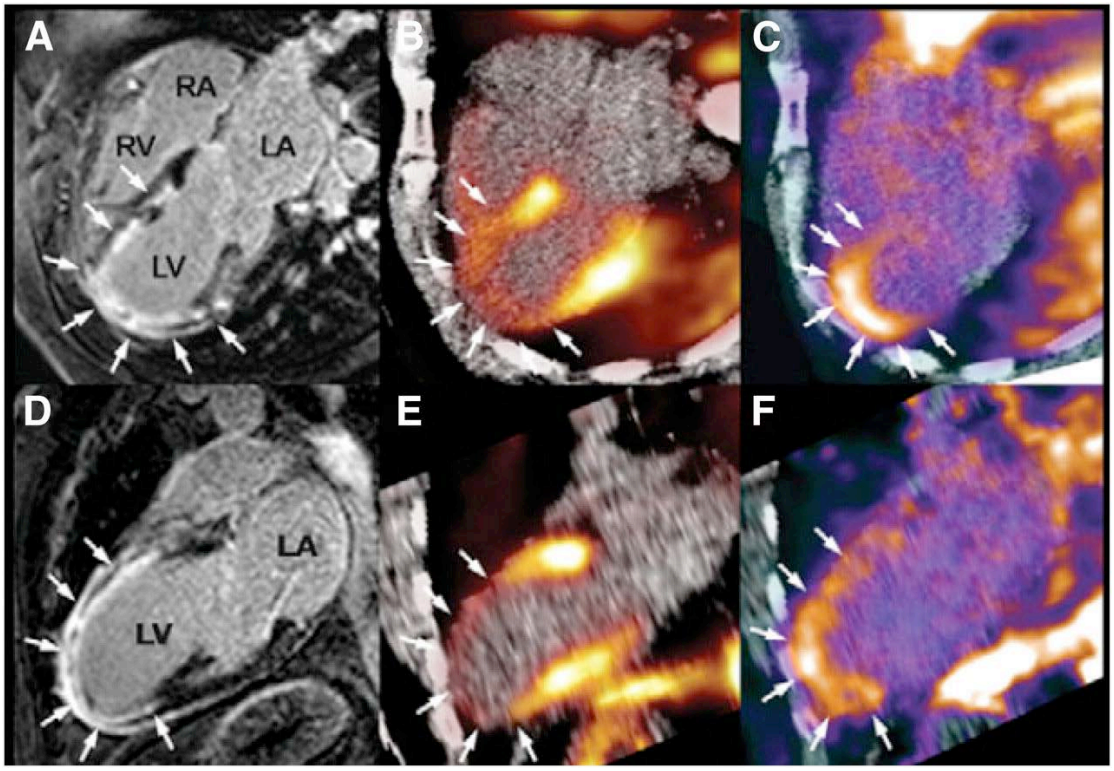

Adapted from Makowski MR *et al*. Eur Heart J 2008; 29(18):2201.

Figure 15 **Multimodality imaging of angiogenesis**

Cardiac MRI with delayed enhancement (arrows) extending from anterior wall to apical region in 4-chamber (A) and 2-chamber (D) views. Identically reproduced location and geometry with severely reduced myocardial blood flow obtained with 13N-ammonia, corresponding to regions of delayed enhancement on cardiac MRI (arrows) (B and E). Focal 18F-RGD signal colocalized to infarcted area. This signal may reflect angiogenesis within healing area (arrows) (C and F). LA = left atrium; LV = left ventricle; RA = right atrium; RV = right ventricle.

1.3 BIOMARKERS OF INSTABILITY

1.3.1 Angiogenesis

1.3.1.1 Integrin

Integrin are glycoproteins belonging to a family of heterodimeric transmembrane receptors, each consisting of an α (alpha) and a β (beta) polypeptidic chain[29-31]. The role of integrin is to mediate cell-to-cell and cell-to-extracellular matrix (ECM) interactions and communication, so they are involved in many mechanisms like cell grow, cell division, cell survival, cell differentiation and apoptosis. Thus, the two main functions of integrin are: attachment of the cell to the ECM and signal transduction from the ECM to the cell. To date, there are 19 alpha and 8 beta mammalian subunits that have been identified. The pairing of these different subunits provides a combination of 25 unique integrins. Electron microscopy studies about the basic structure of integrins revealed that these proteins consist of a very large extracellular N-termini domain with a membrane–spanning region and a very small cytoplasmic tail (about 40-70 amino acids). Both α and β subunit contain separate cytoplasmic tails penetrating the plasma membrane. The molecular mass of the subunits can vary from 90 kDa to 160 kDa. Both α and β subunits contain binding sites for several divalent cations. The β subunit also contains four cysteine-rich repeated sequences. In a non-activated environment, integrins exist in bent "closed" conformations, which have low affinity for the ligand. When the environment become favorable (triggers by cellular event), the integrin become activated and the structure can be unfolded to facilitate visualization of the domain leading to better receptor affinity for the ligand. When activated, integrin can also form clusters of hetero-

oligomers. Integrin activation is a complex multi-steps process that require the participation of many factors and that is controlled by different mechanisms (Fig. 16). This activation is achieved by reversible changes in the conformation of the extracellular domain of the integrin heterodimer, which leads to an increased affinity for the ligand.

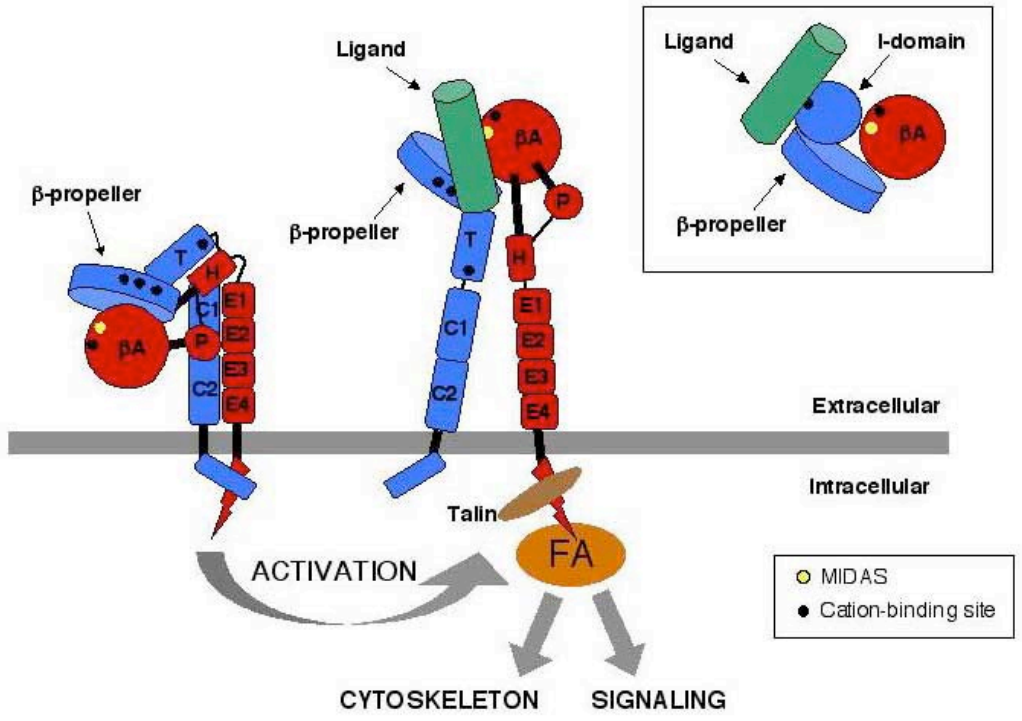

Reproduced from www2.unil.ch/cepo_research/introduction.html

Figure 16 **Proposed model of integrin activation**

In a non-activated environment, integrins exist in bent "closed" conformations, which have low affinity for the ligand. When the environment becomes favorable, integrins become activated and the structure can be unfolded to facilitate the binding of the ligand. When activated, integrin can also form clusters of hetero-oligomers. This activation is achieved by reversible changes in the conformation of the extracellular domain of the integrin heterodimer, which leads to an increased affinity for the ligand. The association with another protein called Talin also regulates it activation by separating the two intracellular subunits of the integrin and by opening the binding site.

The association with another protein called Talin also regulates it activation, by separating the two intracellular subunits of the integrin and opening the binding site. The tight regulation of integrin activation is highly important, as these molecules are involved in many key mechanisms like tumor metastasis and embryonic development. In atherosclerosis only, they play many different roles, being involve in leukocyte trafficking[32], cell migration[33], angiogenesis[34], and thrombus formation[35].

1.3.1.2 αvβ3

The αvβ3 integrin is composed of two subunits: one αv (CD51 protein) subunit and one β3 subunit (CD61 protein). αvβ3 integrin is also called vitronectin receptor. Even though the high-resolution structure of integrin proved to be challenging to discover, the complete extracellular domain of the αvβ3 integrin structure was obtained in 2001 by X-ray crystallography[36]. A more recent study by the same team elucidated the entire ectodomain by crystallography[37]. Unlike all the postulated molecular models, the X-ray structure showed the molecule folded into an inverted V-shape (Fig. 17), which was a surprise compare to the predicted structure. This inverted V-shape brings the ligand-binding site very close to the cell membrane. This structure poses many challenges in regard of the ligand binding and signal transduction. Effectively, the ligand-binding site, which is directed toward the C-terminal of the integrin will be obstructed, especially considering that integrin ligands are large and massive molecules, also cross-linked to the ECM. Although the crystal structure remains surprisingly the same after the ligand binding (in this case cilengitide), the current hypothesis is that integrin function involves conformational changes, which moves the binding site away from the cell surface, into a

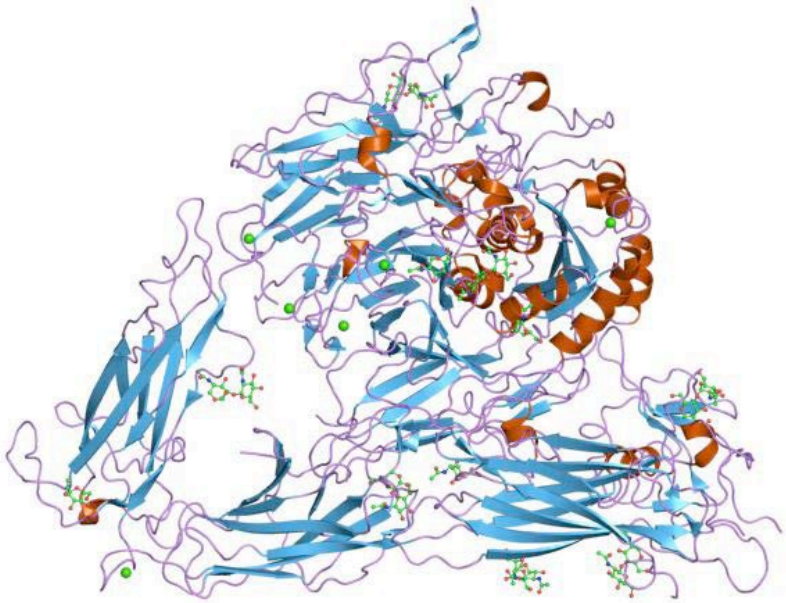

Reproduced from Xiong JP *et al*. Science 2001. 294(5541):339-45.

Figure 17 **Crystallography structure of the ectodomain of the integrin αvβ3**

Unlike all the postulated molecular models, the X-ray structure showed the molecule folded into an inverted V-shape, which was very different from the predicted structure. Because this structure is hiding the catalytic domain close to the cell membrane, it has later been postulated that an activation step is necessary for the binding of the ligand.

more accessible site. Thus, integrin activation is a necessary process for ligand binding. It is postulated to be accomplished by a protein named Talin, which bind the β tale of the molecule and triggers a change in the integrin shape[38]. The most convincing evidence supporting this theory is that some antibodies only recognize integrin in their activated form, when they bonded with their ligands[39]. The mechanism of integrin activation and their inside-out/outside-in signaling is very sophisticated and complex. Inasmuch, it is

beyond the scope of this study to explain those mechanisms. Vitronectin, fibronectin, fibrinogen, osteopontin and Cyr61 are some of αvβ3 ligands[36, 40]. The variety of ligands explains its large distribution among melanoma, glioblastoma, activated endothelial cells, smooth muscle cells and macrophages. In the context of atherosclerosis alone, αvβ3 integrin is involved in many processes. Effectively, the vitronectin receptor mediates several biological events that are critical to the formation of the neointima[41, 42]. First, αvβ3 promotes SMCs migration[43]. Effectively, it as been previously shown that, by outside-in signaling, the occupied αvβ3 receptor enables the platelet-derivated growth factor (PDGF) to activate a series of event that will ultimately lead to cell migration[44]. Secondly, αvβ3 increases transforming growth factor-β (TGF-β) activation, by a mechanism still unknown[45]. In fact, in normal condition, TGF-β is expressed as an inactive complex that necessitate activation for binding to its receptor and be effective. *In vitro*, αvβ3 integrin has been shown to bind latent TGF-β and liberate an active form of the cytokine. Interestingly, αvβ3 expression can also be upregulated by TGF-β, suggesting a possible feed-forward loop that might drive further TGF-β activation. Another implication of αvβ3 in neointima formation involves its effect on apoptosis. In recent studies, it has been shown that the presence of αvβ3 receptor inhibits foam cell formation and apoptosis, and promotes cell survival[46]. For example, ligation of αvβ3 integrin in macrophages down-regulates the expression of scavenger receptor CD36 and SRA, which in turn decreases lipid accumulation and foam cell formation. In a different manner, expression of αvβ3 integrin in VSMC prevents the down-regulation of PINCH-1, a survival protein linked with integrin and the cytoskeleton[47]. This stabilization of PINCH-1 prevents the disruption of the cytoskeleton and ultimately leads to cell survival.

Finally, another role of αvβ3 in neointima formation is the enhancement of neovascularization[48-50]. Effectively, vasa vasorum angiogenesis and medial infiltration provides nutrients to the developing and expanding neointima, which contribute to plaque growth in early lesions[51]. Also, in more advanced lesions, the constant infiltration of inflammatory cells and the concomitant production of numerous pro-angiogenic and pro-inflammatory cytokines could lead to an unstable rupture-prone environment.

1.3.2 Matrix Metalloproteinases (MMPs)

MMPs proteins are belonging to a family of proteases known as metzincin superfamily[52]. There are numerous forms of MMPs with various substrate specificities, even though there is overlapping substrate specificity in many of them. MMPs are zinc-dependent endopeptidases involve in the degradation of different kinds of extracellular matrix proteins as well as the process of bioactive molecules. They are involved in many cellular processes as in the activation and inactivation of chemokines and cytokines, the cleavage of cell surface receptors, as well as the release of apoptotic ligands such as FAS ligand. MMPs are also known to play a major role in cell behaviors such as proliferation, migration, differentiation, angiogenesis, apoptosis and host defense. Dysregulation of MMPs has been linked to abnormal arterial remodeling, plaque instability and aneurysm formation[53]. MMPs can either be synthetized and secreted, or membrane-associated[54], and can be found in macrophages[55], SMCs[56] and epithelial cells[57]. All the MMPs share a common three domains structure: the pro-peptide, the catalytic domain, and the haemopecxin-like C-terminal domain. The structure is also composed of a hinge region that links the catalytic domain and the haemopecxin-like C-terminal domain together.

MMPs are always synthetized in a latent form called Zymogen that will require a further extracellular activation to become fully functional. This activation can be accomplished by different proteases, like serin proteases (plasmin) as well as other MMPs (mutual activation). These proteases are allowing the cleavage of the pro-peptide domain, which contains a conserved cysteine residue interacting with the zinc in the active site and keeping the enzyme in an inactive form (cysteine switch). After cleavage, the zinc dependent catalytic domain can exercise his function on the substrate. MMPs substrate can be classified into two different categories: matrix substrates and bioactive substrates. Bioactive molecules comprise other MMPs and pro-cytokines as pro-TNF-α, whereas matrix substrates include collagen, elastin, fibronectin and vitronectin.

Inside the atherosclerotic plaque, MMPs presence and inhibition by TIMPs (Tissue inhibitor of matrix metalloproteinases) are representing a very critical balance. In one hand, MMPs expression allow tissue repair and even seem to be beneficial in certain circumstances. Effectively, in a study on apolipoprotein E knockout (apoE0), they demonstrate that transgenic mice expressing MMP-1 surprisingly shown a decreased in lesion size compare to their littermates that didn't express MMP-1[58]. They also notice less extensive and immature lesions, fewer cellular layers and a diminished content of fibrillar collagen and no evidence of plaque rupture. This all point out to a beneficial role of MMP-1 expression in the progression of lesions by the remodeling of the neointimal extracellular matrix. In the other hand, MMPs can lead to extensive tissue damage and plaque instability. Convincing evidences have demonstrated that MMPs contribute to the extracellular matrix loss in the fibrous cap and have been implicated in promoting the plaque rupture, which lead to the related vascular events[53, 59, 60]. In summary, inside the

atherosclerotic plaque, the delicate balance between MMPs and TIMPs is compromised and the extensive damage that can be induce by this unbalance will eventually destabilize the plaque and promote plaque instability and rupture, as well as clinical acute vascular events.

1.3.3 Macrophages

Inflammation and macrophages and well know biomarkers of plaque instability[18]. Effectively, one of the first events to occur following damage to the endothelium is the recruitment of macrophages at the site of injury[4, 61, 62]. Because endothelial cells are the primary barrier between blood and tissue, there are a large number of events that can initiate endothelial cells injury and ultimately lead to the biological cascade that constitute the pathological response. Among the myriad of factors affecting vascular integrity, there is direct tissue injury, genetic defect, infection, disturbed hemodynamic flow, dyslipidemia, ischemia, hypoxia, and oxidative stress. As mentioned earlier, those factors will activate endothelial cells that will in turn express adhesion molecules like VCAM and ICAM. Blood monocytes will then be rolling and retained at the surface of the epithelium and be extravagated into the arterial wall. Although macrophages infiltration is a necessary phenomenon and essential for the removal of ox-LDL, as lipids accumulate, they will eventually transform into foam cells and be responsible for the formation of the necrotic core. Macrophages also release numerous proinflammatory cytokines that are believed to further exacerbate the inflammatory response, like TNF-α and IL-1β. They are also responsible of the secretion of more ROS, which will contribute to feed the oxidative stress/inflammatory state. Moreover, macrophages will release

MMPs, another major key player in the atherosclerotic process. Most importantly, MMP-9 will play an important role in plaque instability and vulnerability, by stimulating monocytes infiltration as well as matrix degradation. In the other hand, as mention before, ECM degradation by macrophages will clear the path for the SMCs migration, and formation of the fibrous cap, which will stabilized the plaque (type V). Also, macrophages and lymphocytes T cross-talk can lead to neointima formation, stenosis and plaque healing (type VI). Nevertheless, because of the numerous roles of macrophages in plaque vulnerability, macrophages infiltration is considered to be a histological marker of unstable plaque. Indeed, plaques with thin fibrous cap and macrophages count (CD68 positive) > 25 cells per high power field (40X, field diameter 0.3mm) are considered vulnerable to rupture[3]. Macrophages localization in plaques is often at the shoulder area of the necrotic core, although in vulnerable plaques, they are believed to have a more diffuse distribution[19, 20].

1.3.4 Vascular Smooth Muscle Cells Apoptosis

Vascular smooth muscle cells (VSMCs) are another very important component of atherosclerotic plaques, as they are responsible for the promotion of plaque stability in advanced lesions[63]. Effectively, VSMCs apoptosis has numerous deleterious effects on the atherosclerotic process, like inflammation, calcification, vessel remodeling, and ultimately plaque rupture. Indeed, as the plaque grow, VSMCs will migrate from the media into the neointima to form the fibrous cap, which prevent blood molecules from being in contact with the thrombogenic material of the necrotic core. However, as the necrotic core enlarge or in the presence or certain conditions, the balance between

VSMCs proliferation and apoptosis is compromised. Because VSMCs are also responsible for the formation of collagen into the fibrous cap, VSMCs apoptosis is associated with the thinning of the fibrous cap in the neointima, by both diminution of the muscle cells content and diminution of the ECM and collagen content. The consequence of that will be the formation of thin fibrous cap atheromas (TFCAs), which are the prevalent type of plaques causing most fatal heart attacks. Also, it is worth to mention that microcalcifications, a product of VSMCs apoptosis and cellular death, although still debated, have been described as a major contributor to plaque instability and vulnerability to rupture[64]. Interestingly, calcium crystals themselves have been link to the induction of VSMCs death and atherosclerotic plaque destabilization[65]. Moreover, VSMCs apoptosis has also been linked to vascular remodeling[66, 67], and aneurysm formation[52, 64, 68]. Thus, VSMCs are playing a very important role in maintaining the integrity of the endothelium as well as a physical barrier between blood and thrombogenic material of the necrotic core. As a consequence, VSMCs apoptosis is related to plaque instability and a marker of plaque vulnerability to rupture.

1.4 STATE OF THE ART: αvβ3 TARGETED PROBES

1.4.1 αVβ3 Probes Development and Historic

αVβ3 targeted probes has been largely used for imaging different pathologies. Since αVβ3 receptor is upregulated in many pathological conditions including osteoporosis[69], rheumatoid arthritis[48], cancer angiogenesis[34], and atherosclerosis[41], it represents a target of choice for imaging these diseases. Many research groups have developed αVβ3

targeted nanomaterials for imaging[70] and even dual system that allows detection of the disease as well as delivery of therapeutic drugs[71]. In the case of atherosclerosis, previous studies has shown the great potential of targeting αVβ3 for the development of contrast agents enhancing the detection of the plaque[49] and for therapeutic use[72]. Effectively, human atherosclerotic lesions, albeit very different in plaque composition, show expression of αvβ3[41], which plays a role in thrombus formation[73], cell migration[32], neovascularization[34, 74] as well as many other processes. They have been some studies correlating the vulnerability of the plaque with neovascularization[11]. Some other studies have controversially linked plaque vascularization with ischemic repair, negative remodeling and plaque stabilization[75]. Although αvβ3 is expressed on a variety of cells, its expression seems to be predominant in smooth muscle cells[41], endothelial cells[76], and macrophages during foam cells formation[46]. Most interesting is the fact that αvβ3 expression seems to be an early event in plaque formation[77, 78] and is also correlated with plaque instability[11, 79]. For all of those reasons, αvβ3 has been the target of growing interests for the molecular imaging of atherosclerosis.

In 2003, Winter *et al* published a paper in Circulation were they fed New Zealand White rabbits with an atherogenic diet and they imaged them with αvβ3-Integrin-targeted paramagnetic nanoparticles injected intravenously[77]. They reported the specific detection of neovasculature within 2 hours, at a clinically relevant field strength (1.5T), by MRI. The same team published another paper in Atherosclerosis, Thrombosis, and Vascular Biology, in 2006, where they combined molecular imaging and drug therapy[49]. In this study, they imaged cholesterol-fed rabbit at 1.5 T using integrin-targeted paramagnetic nanoparticles that incorporated fumagillin and demonstrated a decreased in

MRI enhancement among fumagillin-treated rabbits with a single dose (30μg/kg) of integrin-targeted paramagnetic nanoparticles, when readministrated after 7 days. Although there is many studies using MRI based probe, there is also other examples of probe based on imaging modalities like fluorescence, PET, and SPECT. For example, in 2008, Wadeck *et al* published a paper in the Journal of Nuclear Medicine, with a αvβ3-targeted Arg-Gly-Asp (RGD) peptide labeled with cyanine 5.5 (Cy 5.5) dye[80]. They reported the imaging of atherosclerotic plaques in apolipoprotein E-deficient mice after 24 hours injection of the probe by fluorescence reflectance imaging. A more recent study in the Journal of Nuclear Medicine, in February 2012, reported the imaging of Winstar rats that underwent coronary ligation, with a ^{18}F-galacto-RGD probe[81]. ^{18}F-galacto-RGD is a PET tracer binding to αvβ3 integrin receptors that are upregulated after myocardial infarction (MI) as part of the healing process. They showed that one week after MI, ^{18}F-RGD uptake was increased in the defect area as compared with the remote myocardium of MI rats or sham-operated controls. Finally, as mentioned before, since there is no perfect single modality that is sufficient to obtain all necessary information, there is a growing interest into the development of multimodality imaging of αvβ3. For that matter, a very interesting review has been published in 2011 in Theranostics journal, which focused on dual modalities imaging (PET and optical, SPECT and fluorescence, PET and MRI, SPECT and MRI, and lastly, MRI and fluorescence) and their synergetic advantages over any modality alone[82]. Those multimodality probes can build on the strength of one imaging modality and compensate the lack of the other, which open up new avenues in the field of research. For example, MRI can compensate for the low resolution of PET imaging, and inversely, PET can compensate for the low sensitivity of

MRI, which might translate some day into better detection, treatment or follow up of the beneficial effect of therapy of vulnerable plaques.

Apart from the numerous imaging studies on animal model of atherosclerosis with αVβ3 directed probes, there is an even more extensive literature on αVβ3 probe with animal models of cancer. In fact, αVβ3 targeting for cancer imaging has been reported with virtually every imaging modality possible (optical[83], PET[84, 85], PET/CT[86], SPECT[87], MRI[88], fluorescence[89]). Moreover, the probe that we used in this study has already been tested on nude mice bearing receptor-positive M21 human melanoma xenografts using a micro-SPECT single photon emission computed tomography system (A-SPECT, Gamma Medica Instruments, Northridge, CA) with a 2 mm pin-hole collimator for high resolution animal imaging[90]. More interestingly, this same molecule, labeled with ^{68}Ga and linked with NODAGA[91], has been recently used to efficiently detect cancer in human (unpublished results). In this first human study in a breast cancer patient, they reported 25 integrin αvβ3 positive lesions detected by the probe (THERANOST cRGD™), versus 12 by ^{18}F FDG. They also pointed out many advantages over ^{18}F and ^{64}Cu labeled RGD peptides, like the availability of ^{68}Ga, the convenient radiolabelling, the high stability and the good imaging properties.

1.4.2 αVβ3 integrin-targeted probe synthesis

The αvβ3 integrin targeted optical probe (ITOP) 4-[2-(3,4,5,6-Tetrahydropyrimidin-2ylamino)ethyl-oxy]benzoyl-2-(S)-[N-(3-amino-neopenta-1-carbamyl)]-aminoethylsulfonylamino-β-alanine fluorescein thiourea was synthesized as previously described[92]. Briefly, ITOP was developed from a potent fibrinogen receptor antagonist

(3-amino-2(*S*)-arylsulfonylaminopropionic acid derivative)[93] and further structural modifications and optimization followed by conjugation to fluorescein isothiocyanate (FITC) led to the targeted probe (Fig. 18). This conjugation of the fluorophore to the integrin antagonist did not alter the binding affinity or selectivity to integrin αvβ3. This compound represents the first example of a non-peptidic integrin αvβ3 targeted optical probe. For in vivo studies, the probe was labeled with ^{111}In. For that purpose, the amino terminus of IA or IAC (10-20 mM) was reacted with 2-(p-isothiocyanatobenzyl)-DOTA (Macrocyclics, Inc., Dallas, TX; SCN-Bz-DOTA; 1-2 mM) in 40 µl of 0.1 M sodium bicarbonate at pH 8.4 for 2 days at room temperature. The product formation was monitored by reverse-phase HPLC. In the binding assays as well as in the cell adhesion inhibition assays, this compound showed very high binding affinity (3nM) and selectivity to αvβ3 compared to αIIbβIIIa, αvβ5 and αvβ6.

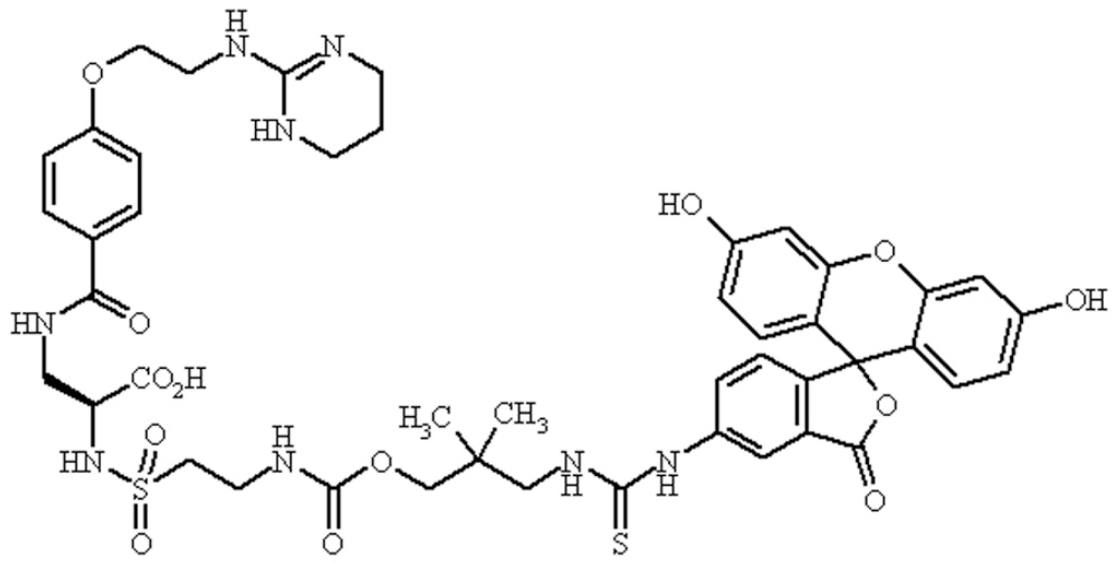

Figure 18 **Representation schematic of the ITOP**

Structure of integrin αvβ3 targeted optical probe: 4-[2-(3,4,5,6-Tetrahydropyrimidin-2ylamino)ethyl-oxy]benzoyl-2-(S)-[N-(3-amino-neopenta-1-carbamyl)]-aminoethylsulfonylamino-β-alanine fluorescein thiourea.

1.4.3 αVβ3 probe characterization on cancer model

Recently, an ITOP was synthesized and has been shown to efficiently target the αvβ3 receptor with high affinity in an *in vivo* mouse model of cancer[92]. The probe is a small non-peptidic carbamate integrin antagonist (RGD mimic), which is fluorescently labeled and targets the αvβ3 integrin. Compare to nanoparticles ranging in sizes of hundreds of nanometers (nm), this probe is much smaller (<1nm), which should translate into better clearance from blood and better diffusion into the targeted tissue. *In vitro*, this labeled compound has very high affinity for αvβ3 (IC_{50} of 3nM) and greater selectivity towards αvβ3 compared to αIIbβIIIa, αvβ5 and αvβ6 (IC50 > 100μM). When incubated with commercially available αvβ3, the same compound labeled with ^{111}In produce a shift in HPLC peak to a higher molecular weight, with a retention time identical to that of integrin $\alpha_V\beta_3$ in a concentration-dependent manner. The percent bound was 6%, 40% and 72%, respectively, when incubated with 0.08, 0.4 and 0.8 μM $\alpha_V\beta_3$. The receptor binding was completely blocked by a 25 times molar excess of cold IA to integrin $\alpha_V\beta_3$. This synthetic probe has at least 20 times higher binding affinity for αvβ3 compared to the commercially available cyclic peptide c[RGDfv]. *In vivo*, the αvβ3 probe has been labeled with ^{111}In and injected intravenously in tumor bearing mice and detected by micro-SPECT single photon emission computed tomography system (A-SPECT, Gamma Medica Instruments, Northridge, CA) with a 2 mm pin-hole collimator[90]. The ITOP persisted in the tumor for more than four hours, while disappeared from most of the other tissues within an hour, demonstrating that its biodistribution is conducive for use in imaging. The tumor uptake (5.3±0.6 %ID/g) of the ^{111}In-labeled probe was significantly inhibited (1.4±0.3 %ID/g) after 1 h co-injection with the cold probe, whereas there was

no inhibition by the control lysine co-injection, indicating that the tumor uptake was receptor mediated. Another preliminary study with the same compound showed *in vitro* promising results for the development of a dual imaging probe/drug delivery systems targeting αvβ3[50]. As neovascularization is also an important mechanism in plaque formation, in this study, we have explored the utility of this ITOP to probe the molecular processes involved in atherosclerosis, in a Watanabe rabbit model.

1.5 ANIMAL MODEL OF ATHEROSCLEROSIS[94]

1.5.1 Mice and Rats

There are a variety of different animal models allowing us to mimic human atherosclerosis plaque development and study different target molecules. Currently, there is no single golden standard animal model of vulnerable plaque. The most common animal model known and used in laboratory for atherosclerosis study is probably the apolipoprotein E (apoE) knockout mouse. In fact, since mice do not develop atherosclerosis without genetic modifications, genetically engineered mice with disorders of lipid metabolism has been developed, such as apoE knockout mice. These mice have been genetically modified, so they do not express the glycoprotein apoE that mediates the binding of very low-density lipoprotein (vLDL) to the LDL receptor. The result is a blockade of the vLDL particles uptake in the liver and the accumulation of cholesterol rich particles in the plasma. These mice develop normally, but exhibit five times normal serum plasma cholesterol and spontaneous atherosclerotic lesions. There are also a large

number of other knockout mice (LDL receptor knockout, type A scavenger receptor knockout…) and even double knockout mice developed and useful for investigating atherosclerosis and plaque rupture. Unfortunately, mouse model does present some limitations, beside the fact that they do not develop atherosclerosis without genetic manipulation. First, lipid physiology in mouse is radically different from the one in human, as most of their cholesterol transport is accomplished by high-density lipoprotein (HDL)-like particles. In second hand, mice weight (25g) is some 3000 times less than the average human, which can lead to very different biological responses. Furthermore, mice transport cholesterol mostly in the form of HDL, unlike human that also transport it in LDL form, which constitute the problematic lipid in atherosclerosis.

Some other models include dogs and rats, but these animals are very resistant to atherosclerosis and will only develop it following extensive diet modifications.

1.5.2 Pigs

Another very useful animal model is the pig. Pig can develop atherosclerosis even on a normal porcine diet and when fed cholesterol diet, they develop plasma cholesterol levels and atherosclerotic lesions very similar to humans. Some varieties of pig have also exhibit sudden coronary death as a response to stress. However, pigs are difficult to house and the cost of the maintenance is often too high for most laboratories. They require special facilities and more extensive knowledge beyond the capability of our laboratory. We therefore choose the most appropriate animal model for our goal, which appears to be the Watanabe heritable hyperlipidemic rabbit.

1.5.3 Watanabe Heritable Hyperlipidemic Rabbits (WHHL)

Watanabe rabbit has been discovered in 1973, when Dr. Yoshio Watanabe noticed that a white rabbit was showing hyperlipidemia despite the fact that he was feed a normal standard diet[95]. Dr Watanabe later confirmed that the hyperlipidemia was inherited recessively from its parent. In 1980, the first mutant strain of this rabbit was established and called WHHL. Later on, in 1985, some other modifications have been added to the strain, to make it more susceptible to coronary atherosclerosis. Finally in 1992, Dr Watanabe developed a colony of coronary atherosclerosis-prone WHHL rabbits. The major characteristic of the WHHL rabbit are an in-frame deletion of 12 nucleotides that eliminates four amino acids from the cystein-rich ligand binding domain of the LDL receptor. This mutation delays the LDL receptor protein maturation and affects the transportation rate of the receptor to the cell surface. Ultimately, this defect will reduce the LDL receptor function in a manner similar to the human Familial Hypercholesterolemia (FH). In WHHL rabbits, average plasma cholesterol levels are about 1100 mg/dl at 6 months old, about 900 mg/dl at 12 months old and about 800 mg/dl at 18 months old. A normal rabbit will have an average plasma triglyceride level between 150 and 300 mg/dl. Compared to mouse models (apoE-KO or LDLR-KO) fed standard chow, WHHL rabbits resemble human in lipoprotein metabolism (Table 2). Another important difference in the WHHL rabbit compare to the normal rabbit is the enzyme activity of the cholesterylester transfer protein (CETP), which is about 2 to 3 fold higher in WHHL rabbit. This plasma protein facilitates the transport of cholesteryl esters and triglycerides between lipoproteins, and mutations leading to its increased function have been link to accelerated atherosclerosis.

Table 2 Difference in lipid metabolism and atherosclerosis between WHHL rabbits, human with FH and apoE-KO and LDLR-KO mice

	WHHL Rabbits	**Human FH**	**ApoE-KO mice**	**LDLR-KO mice**
Plasma cholesterol levels	Extremely high	Extremely high	Mildly high	Moderate
Main lipoprotein in plasma	LDL	LDL	VLDL	LDL and HDL
LDL levels	Extremely high	Extremely high	Moderate	Moderate
HDL levels	Low	Low	Low	High
ApoB of VLDL	B-100	B-100	B-48	B-48 and B100
Expression of apoB-editing enzyme in liver	No	No	Yes	Yes
Cholesteryl ester transfer activity in plasma	Yes	Yes	No	No
Features of aortic atherosclerosis	Complicated lesions	Complicated lesions	Foamy lesions	(Not developed)
Myocardial infarction	Spontaneous	Spontaneous	Resistant	Resistant

Table 2 **Comparison of lipid metabolism and atherosclerotic features between humans, rabbits and mice**

When compare to human FH, WHHL rabbit model has more similar features related to lipid and plaque metabolism than the mice models have. The pattern of lipid metabolism is relatively identical and the types of atherosclerotic lesion are also very similar, which made them a better animal model than mouse for the study of atherosclerotic processes

In WHHL rabbit, aortic lesions begin to appear around 2 months old despite feeding them on a normal rabbit chow diet. The lesions are first noticed at the orifices of the branches and expand to about 40% of the aortic surface around 6 months old, 70% around 12 months old, and covering almost the entire surface around 18 months old. In early lesions, intima is composed mostly of macrophages and a few SMCs, with some macrophages penetrating the arterial media. Transitional lesions are, alternatively, composed of large foam cells derived from macrophages and located in the deeper area of the intima. These transitional lesions presented also a fibromuscular cap covering the surface of the intima. Above 18 months old, these transitional lesions become more advance and complex, with decreased cellular content, but increased collagen fibers, extracellular lipid accumulation and cholesterol cleft. Calcium accumulation can also be observed in some of these advanced lesions. Another important fact about WHHL rabbits is that a previous study has showed that they can develop plaque with outward remodeling[96], a feature related to plaque instability in human.

After considering all of the above information, we decide that WHHL rabbit was the most appropriate and suitable animal model for our need.

1.6 AD-HIES AND ATHEROSCLEROSIS

AD-HIES disease or autosomal dominant hyper-IgE syndrome (AD-HIES) is a rare primary immunodeficiency caused by a dominant negative mutation in STAT3[97, 98]. It is characterized by various clinical manifestations such as high serum level of IgE,

recurrent infections, eczematous dermatitis, and connective tissue abnormalities[99]. Because AD-HIES is categorized as an immunodeficiency disease[99], and because it is characterized by less advanced stenotic plaques[100], as seen by imaging study, it is an extremely interesting model for the study of the atherosclerotic process. Effectively, AD-HIES patients have an abnormal immunity system that prevents them to efficiently fight infections, and as a result, they develop lot of secondary infection problems[99]. On the other hand, they also develop abnormal exacerbated allergic response, which is observed by their elevated IgE blood level. One manifestation of their immunodeficiency is their improper T cells maturation process. It is translated into an absence of Th17 T cells subtype. It is well known that atherosclerosis is an inflammatory disease and T cells subtypes are important in plaque characterization. Indeed, while Treg subtype of T cells have been linked to more stable plaque, Th17 subtype have been link to more vulnerable type of plaque. Also, since there is an important crosstalk between inflammatory cells, especially macrophages and T cells, AD-HIES would be an interesting model to study plaque formation, inflammatory processes and stenosis. It could lead to important understanding on inflammatory cells crosstalk mechanism and what happens in case of defect.

Recent studies in AD-HIES also described the presence of coronary aneurysm and ectasia, despite the uncommon presence of atherosclerosis, evaluated by luminal stenosis[100, 101]. Moreover, those features were also often accompanied by a general dilatation of the vessel wall[100]. Aneurysms can be caused by many different mechanisms, as vasculitis, trauma, connective tissue disorders, and most interestingly, atherosclerosis[68]. It is still debated if atherosclerosis is causing the aneurysms or if

aneurysms come before the development of atherosclerosis. The most accepted theory is that those two mechanisms are probably developing in parallel, because of the presence of inflammatory conditions, cytokines or altered blood flow[102]. In AD-HIES population, there is a high prevalence of coronary abnormalities, such as dilation of the coronary wall and aneurysm[100], but a paucity of severe atherosclerosis[100, 101]. For all these reasons, AD-HIES patient could be a very interesting model for the study of atherosclerosis.

1.6.1 Aneurysm

Aneurysm, by medical definition, is a sac formed by the dilatation of the wall of an artery, a vein or the heart, and filled with fluid or clotted blood (thrombus). An atherosclerotic aneurysm is defined by the weakening of the vessel wall in the case of severe atherosclerosis, and is usually seen in large arteries like abdominal aorta (Fig. 19). According to Stary HC *et al*, atherosclerotic lesions from type IV, V, and VI can be associated to, and appeared to be the cause of localized dilatations of the vascular wall they occupy[19, 20]. It is also mentioned that thrombotic deposits in atherosclerotic aneurysms can form large masses that fill the aneurysm, but usually preserving the lumen area of the original vessel.

In general, for aneurysms to occur, specific conditions need to be present: degraded matrix fibers[103], proteolytic enzyme activity increased (wall destruction and remodeling)[102], and increased collagenases and elastase activity[104]. Destruction of the media by experimental mechanical injury has also been linked to aneurysm formation, especially in the presence of hyperlipidemia[105, 106]. Inasmuch, hystological features of aneurysms include medial necrosis, inflammatory infiltration, and elastic fibers

degradation (Fig. 20)[102]. It remains controversial if atherosclerosis is the direct cause of aneurysms, if aneurysms predispose to atherosclerosis, or if they are parallel phenomenon. In a recent ultrasound study by Johnsen *et al*, they postulated that atherosclerosis and aneurysm are likely to be developing in parallel, rather than atherosclerosis directly leading to aneurysm[107]. Unfortunately, findings from this study were not able to convincingly refute a role for atherosclerosis in aneurysm.

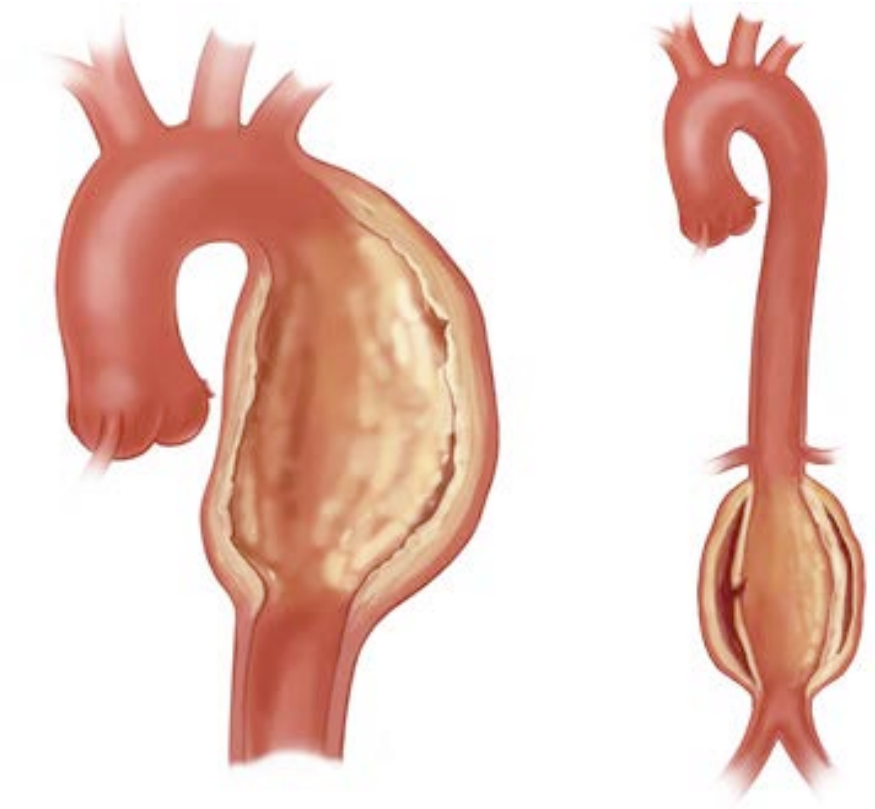

Reproduced from www.mountsinai.org

Figure 19 **Representation schematic of an atherosclerotic aneurysm**

An aortic aneurysm is a dilatation, bulging or ballooning of a weakened part of the aortic artery wall. An aneurysm is most often the result of degeneration and weakening of the wall of the aorta. In addition to atherosclerosis, the risk of an aortic aneurysm can be increased by factors such as high blood pressure and smoking. In rare cases an aortic aneurysm can be caused by an infection or inflammation. All three tunica layers are involved in true aneurysms (fusiform and saccular). In false aneurysms, blood escapes between tunica layers and they separate. If the separation continues, a clot may form, resulting in a dissecting aneurysm.

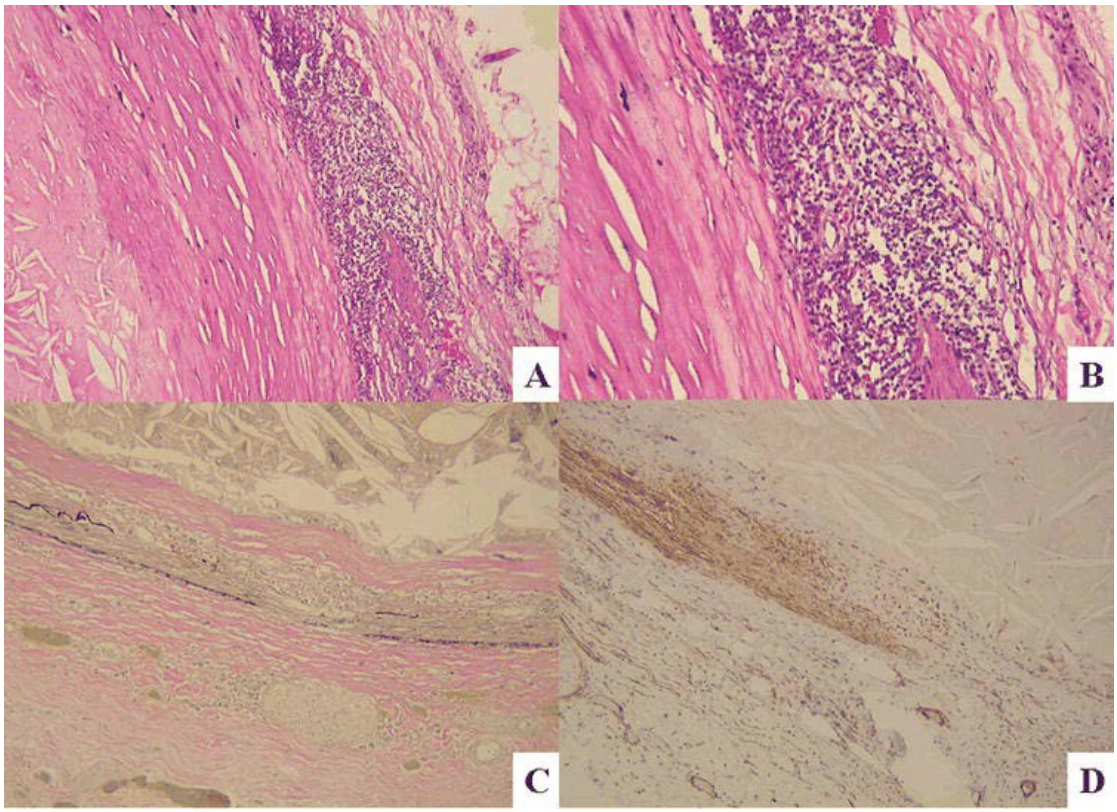

Reproduced from Nichols et al, Arch Pathol Lab Med 2008; 132(5):823-828.

Figure 20 **Histology of a left circumflex coronary artery aneurysm**

(A) Tunica intima expanded by atherosclerosis (left) and tunica media attenuated and densely infiltrated by inflammatory cells (right) (H&E, 10X magnification). **(B)** Higher power showing the inflammatory cells to be predominantly lymphocytes, with a few residual smooth muscle cells (bottom center) (H&E, 20X magnification). **(C)** Verhoeff van Gieson stain showing only wisps of black elastin in the attenuated tunica media (10X magnification). **(D)** Immunostain for smooth muscle actin showing markedly decreased staining transitioning to totally absent staining (center, left to right), representing the loss of SMCs in the tunica media (10X magnification).

1.7 SUMMARY

In previous sections, the biological processes leading to atherosclerosis have been explained. A particular emphasis has been put on the vulnerability of atherosclerotic plaques. Those plaques are generally in the positive remodeling phase and present an absence or low-grade stenosis. They also possess a large necrotic core with lipid crystals, a thin fibrous cap, heavy macrophages infiltration, important enzyme activity (MMP-9), and can also feature intraplaque hemorrhage and microcalcifications. It is very important to develop imaging techniques that will allow to detect vulnerable plaques, as they are often the key determinant leading to plaque rupture, and can cause coronary events and strokes. Because the degree of stenosis has a poor predictability for coronary events, it becomes essential to study the molecular mechanisms of plaque vulnerability. The integrin αvβ3 seems to be an important target for atherosclerotic plaque imaging, since αvβ3 is involved in numerous processes controlling the balance between plaque stability and instability (neovascularization, intraplaque hemorrhage, cell migrations, apoptosis, etc…). This study is aimed at evaluating the efficiency of a new synthetic αvβ3 ITOP for the imaging of early atherosclerotic plaque. For this purpose, a WHHL rabbit model has been used, considering that this model shares many common characteristics with the human disease. The results have also been confirmed *in vitro* in human. Finally, the probe has been tested on an AD-HIES human model. Because of the rarity of this model, and the important features interconnecting this disease and atherosclerosis (paucity of stenotic atherosclerosis, prevalence of aneurysms, connective tissues abnormalities, immunodeficiency), it becomes a very useful tool for the study of atherosclerosis. With

the help of those models and immunohistopathological studies, it becomes possible to better understand the mechanisms involved in plaque vulnerability and maybe develop imaging techniques that will allow plaque detection before the apparition of its sequelae, and prevent heart attacks and stroke.

CHAPTER 1

IN VITRO ITOP LABELING ON WHHL RABBITS

2.1 INTRODUCTION

The detection of early atherosclerosis, before the development of its later sequelae of myocardial infarction, angina or stroke, constitutes an important challenge in current diagnostic medicine. Despite all the recent technological advances, cardiovascular disease remains the leading cause of death in the Western World and needs to be detected at an earlier stage to allow for more timely therapeutic intervention[1]. Therefore, one potential promising molecular target for the detection of atherosclerotic plaque is αvβ3, a widely recognized target and the basis for the development of molecular probes and the detection of pathological conditions like rheumatoid arthritis[48] and cancer[34]. In addition, human atherosclerosis lesions show extensive expression of αvβ3[41]. This integrin plays a role in thrombus formation[73], cell migration[32], neovascularization[34, 74] as well as many other processes involved in atherosclerotic plaque formation. The αvβ3 receptor has been found on the surface of a wide variety of cells inside atherosclerotic plaques, but expression seems to be predominant in smooth muscle cells and endothelial cells[41, 76]. Macrophages also express αvβ3 during the formation of foam cells[46]. Moreover, most interesting is the fact that αvβ3 expression seems to be an early event in plaque formation[77, 78] and is also correlated with plaque instability[11, 79]. Additionally, previous studies had shown the great potential of targeting αvβ3 integrin for the

development of contrast agents that enhance the detection of plaque[49] and for the delivery of therapeutic drugs[72]. Consequently, these characteristics make αvβ3 a very attractive target for molecular imaging of early atherosclerosis.

Recently, a fluorescein labeled integrin analog was synthesized and had been shown to efficiently target the αvβ3 receptor with high affinity in an *in vivo* mouse model of cancer[92]. The probe is a small non-peptidic carbamate integrin antagonist (RGD mimic), which is fluorescently labeled using a neopentyl linker and targets the αvβ3 integrin. *In vitro*, this compound with the fluorescein label had very high affinity for αvβ3 (IC_{50} of 3nM) and greater selectivity towards αvβ3 compared to αIIbβIIIa, αvβ5 and αvβ6 (IC50 > 100μM)[92]. This synthetic probe demonstrated at least 20 times higher binding affinity for αvβ3 compared to the commercially available cyclic peptide c[RGDfv][92]. When intravenously injected in tumor bearing mice, the probe persisted in the tumor for more than four hours, while disappeared from most of the other tissues within an hour, demonstrating that its biodistribution is conducive for use in imaging[90]. In this study, we explored the utility of this labeled molecule to probe the molecular processes involved in atherosclerotic plaque formation, particularly the overexpression of the integrin αvβ3. The purpose of this initial study was to investigate the potential of this new synthetic αvβ3 targeted optical probe to identify early atherosclerosis in a Watanabe rabbit model.

2.2 MATERIALS AND METHODS

2.2.1 Experiment design

All experiments were performed on specimens taken from 3 month to 12 month old Watanabe Heritable Hyperlipidemic (WHHL) rabbits, 2 females and 3 males (n=5), fed a standard rabbit chow diet. The animals were purchased from Brown Family Enterprises (Gemini Research of Alabama, Odenville, Alabama, USA). Control aortic tissues without atherosclerosis were taken from New Zealand White (NZW) rabbits (n=2) and purchased from Zyagen (San Diego, CA, USA). Prior to any experiment, rabbits were anesthetized with a ketamine (30mg/kg) and xylazine (5mg/kg) cocktail administered subcutaneously, and then euthanized by intravenous pentobarbital (100mg/kg) injection while still under anesthesia. All experiments were performed in accordance with protocols approved by the Animal Care and Use Committee of the National Heart Lung and Blood Institute.

2.2.2 Cholesterol measurement

Blood was collected before euthanasia and centrifuged at 1400*g* for 10 minutes, and the serum was frozen at -20°C, until it was assayed within 2 months after collection. Total cholesterol levels were measured by the Brown Family Enterprises Laboratory, at the Gemini Research of Alabama facility, using a cholesterol esterase/cholesterol oxidase colorimetric assay procedure. Total cholesterol values were expressed as mg/dL (mean6SEM).

2.2.3 Dissection

The rabbit abdomen was open, and the aortic arch was excised and cut into different sections (ascending, descending thoracic, and descending abdominal). 2-3mm thick samples were taken from each segment, and 1 segment was put in a formalin solution, while the other segments were put in Optimal Cutting Temperature (OCT) media and quick frozen in methylbutane containing dry ice. Samples were kept at –80°C for further histological and immunohistological experiments.

2.2.4 Histology and Immunohistology

OCT blocks from frozen aortic tissues were cut into 7-8 μm sections with a cryostat and mounted onto slides. Routine hematoxylin and eosin (H&E) straining was performed on frozen sections of the rabbit aortas. Expression of αvβ3 integrin in the aortic wall was assessed by immunohistofluorescence with the new ITOP. Briefly, sections were thawed for 15 minutes at room temperature, fixed 10 minutes with cold acetone, washed in phosphate buffer solution and then incubated with the targeted fluorescent probe for 1 hour. After the incubation period, the slides were washed again in phosphate buffer solution, mounted with VECTASHIELD mounting medium containing DAPI (Vector Laboratories, Inc., Burlingame, CA). An antibody against human αvβ3, anti-human integrin αvβ3, clone LM609 (Chemicon International, Inc, Temecula, CA, USA), was used to confirm the presence of the integrin and as a reference for the localization of any experimental fluorescence signal. This antibody was used in conjunction with an anti-mouse horseradish peroxidase detection kit, according to the specifications of the company (Chemicon International, Inc, Temecula, CA, USA). Images of staining or

fluorescence signal were acquired under a microscope (Nikon E1000 with a Nikon DXM-1200 color camera or Leica DM5500B with a Leica DFC500 camera) using a visible or ultraviolet light source, respectively. For the ITOP (FITC labeling), the emission wavelength was set up at 495nm, while absorption wavelength at 521nm.

2.2.5 Competition

Slides were transferred from -80°C to -20°C for 15min, and then allowed to air dry for another 15min. The slides were then fixed for 10min in cold acetone (-20°C), washed with 3 changes of PBS (5min) and incubated with the ITOP (1,4mg/100µl) diluted 1/200 for 2hrs. The slides were then washed with 3 changes of PBS, and incubated with the non-labeled ITOP diluted 1/20 for 1hr. After the incubation period, the slides were washed again in phosphate buffer solution, excess liquid was wipe off, and the slides were mounted with VECTASHIELD mounting medium containing DAPI (Vector Laboratories, Inc., Burlingame, CA).

2.2.6 Lipid staining

OCT blocks from frozen aortic tissues were cut into 7-8 µm sections with a cryostat and mounted onto slides. Slides were stored at -80°C and allowed to air dry for 30 minutes at room temperature (RT) prior to staining. Slides were then fixed with 10% ice cold Formalin for 5 minutes, rinse in water and incubate 5 minutes with Propylene Glycol to avoid carrying water into Oil Red O. Sections were stained 10 minutes with Oil Red O solution at 60°C and subsequently rinsed 5 minutes with 85% Propylene Glycol followed by water. Slides were then counterstained for 30 seconds in Gill's Hematoxylin solution,

washed thoroughly for 3 minutes in running water and rinsed two times with water. Finally, sections were mounted with aqueous mounting medium (Supermount Permanent Aqueous Mounting Medium, Biogenex, San Ramon, CA).

2.3 RESULTS

2.3.1 Plaque Labeling

Histological staining (H&E) of WHHL rabbit aortic tissues in transverse slices demonstrated intimal thickening of the aortic wall in some areas of the aorta, which was not observed in the control animals. Other WHHL rabbits did not showed any plaque in the intima. Examination of the aortic tissues with plaque incubated for 1 hour with the ITOP showed a strong fluorescent signal (Fig. 21A) in some cases, and a weaker signal in other parts of the aorta with plaque. Signal enhancement was predominately localized in the adventitia and the neointima of the vessel wall, although there was also some fluorescence in the media. The medial signal was associated with strong adventitial and neointimal labeling. As opposed to that, there was no medial labeling when the adventitial or neointimal labeling was weaker. In contrast, the specific fluorescent signal of the ITOP was absent in images from aortas of the control NZW rabbits (Fig. 21B). There was some autofluorescence in the aortic tissues, but it was negligible compared to the specific signal enhancement from the ITOP. Images from control rabbit aortas (Fig. 21B) were taken at a higher magnification (10X), in order to see the background fluorescence, which was undetectable at a lower magnification (4X).

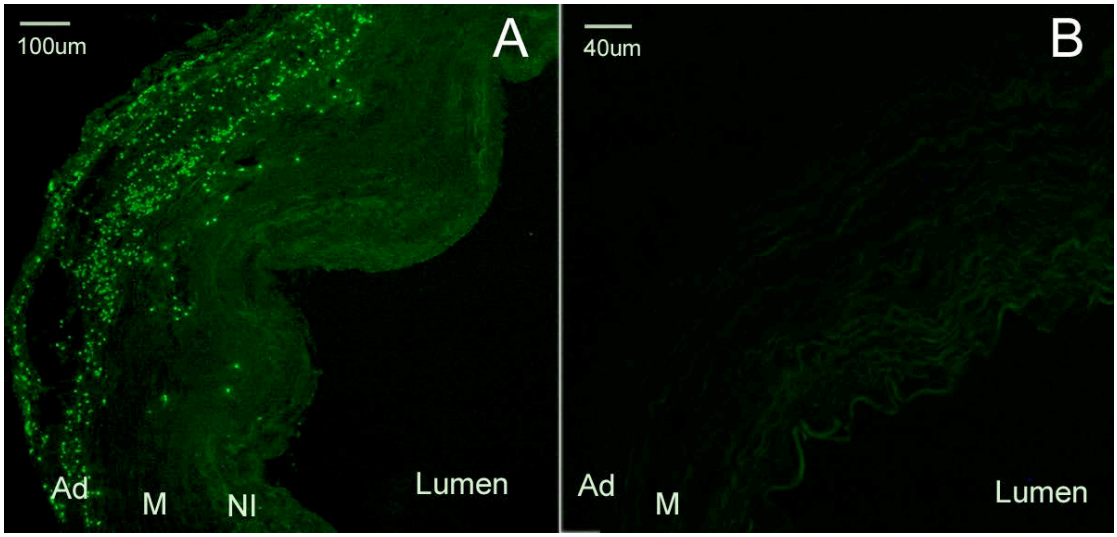

Figure 21 **Fluorescence microscopy of descending Watanabe rabbit aorta sections (transverse cut) from tissue incubated with FITC-αvβ3 antagonist**

(A) Image (4X magnification) of slide exposed to FITC-αvβ3 antagonist (2.8μM) for 1 hour. **(B)** Background fluorescence of the same region in slide from control NZW rabbit exposed to the fluorescent particle with the same conditions (10X magnification). Results indicated specific plaque labeling with the fluorescent antagonist with a very small amount of autofluorescence background from tissues. FITC, fluorescein isothiocyanate; Ad, adventitia; M, media; NI, neointima.

2.3.2 Signal Correlation with an Anti-αvβ3 Antibody

A transverse image of the ascending aorta of the WHHL rabbit showed that the intimal thickening (neointima) of the tissue was a component of the atherosclerotic plaque (Fig. 22). Upon comparison, the immunohistological labeling of αvβ3 (Fig. 22, right panels) and the fluorescence signal of the ITOP (Fig. 22, left panels) appeared co-localized to the same regions. Higher magnification (10X) of the neointimal region (Fig. 22C, D) demonstrated corresponding strong fluorescence and immunohistological signals near the interface of the lumen and intima. The fluorescent and immunohistological labeling were

mostly localized in the adventitia and proximal intima of the ascending aorta. A similar distribution was showed in the descending aorta sections (Fig. 22).

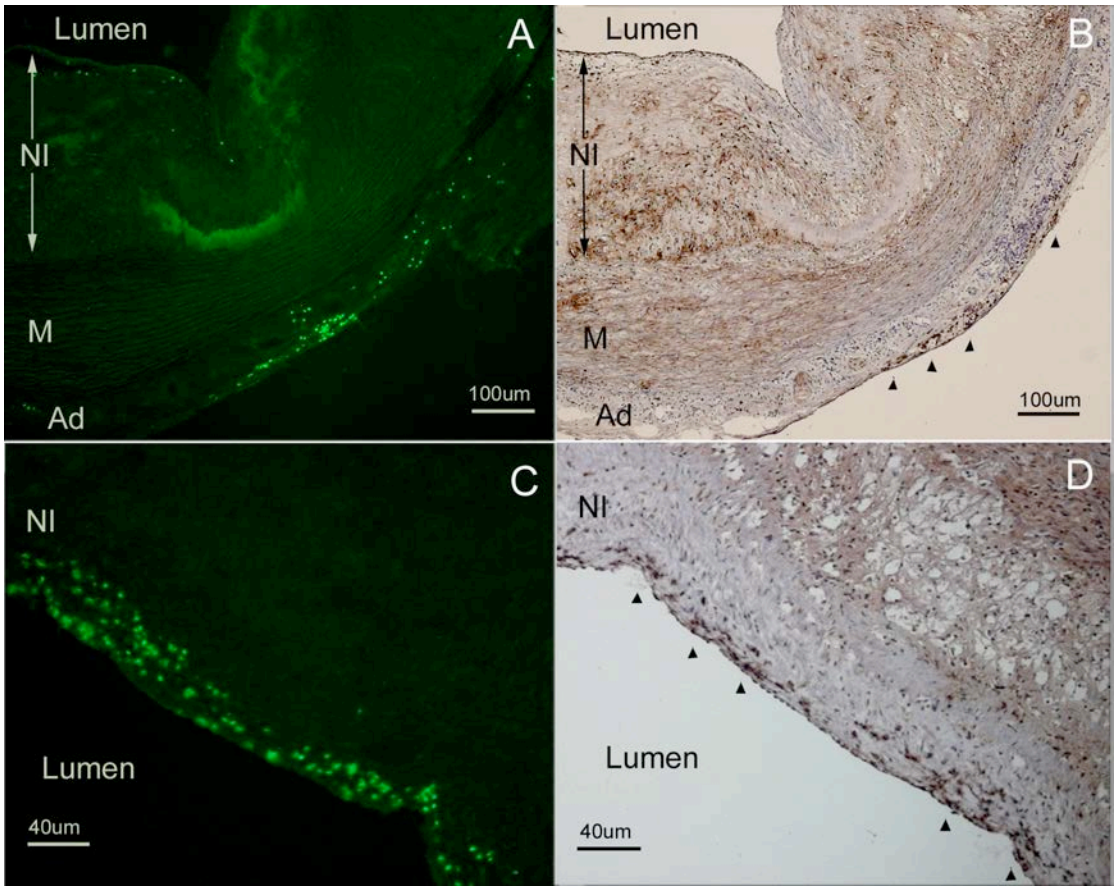

Figure 22 **Co-localization study of αvβ3 expression on Watanabe rabbit ascending aorta sections labeled with fluorescence**

Immunofluorescence **(A, C)** or immunohistochemistry **(B, D)**. The upper panels displayed the whole aortic wall (4X magnification) while the bottom panels were focused on the neointimal region (10X magnification). Both the fluorescence signal **(A, C)** and the immunohistological labeling **(B, D)** were co-localized predominantly in the adventitia and proximal neointima. Arrowheads illustrate immunohistological staining. Ad, adventitia; M, media; NI, neointima.

2.3.3 Competition

In order to verify the specificity of the ITOP signal, the descending aorta of the rabbit had been incubated with the FITC labeled ITOP, following by incubation with the non-labeled ITOP. After incubation with the labeled ITOP (Fig. 23A, C), the non-labeled ITOP displaced part of the signal produce by the αvβ3 probe (Fig. 23B, D). Although there was still some signal after the incubation with the non-labeled probe, the diminution of signal is clearly demonstrating the specificity of the αvβ3 ITOP. The displacement of the ITOP signal can be observed on the three different layers of the vessel wall (intima, media, adventitia), as shown in the lower panel (Figure 23C, D).

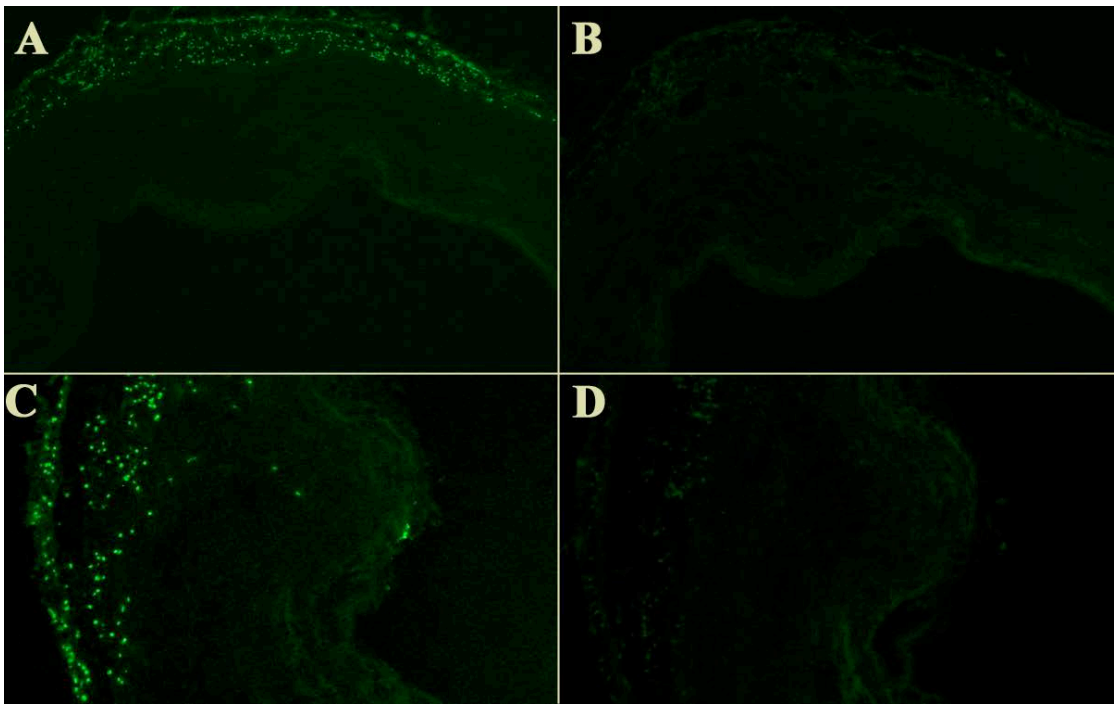

Figure 23 **Competition with non-labeled ITOP**

Left panel (**A, B**) represents results of fluorescence microscopy for two different parts of the descending aorta of the Watanabe rabbit labeled with the ITOP (2.8μM, 1hr). **Right panel** (**B, D**) represents the two same parts after a post-incubation with non-labeled ITOP (28μM, 1hr). Results indicate a loss of signal after the competition with the non-labeled ITOP (**B, D**).

2.3.4 Adventitia Labeling

Higher magnification images of the adventitial sections demonstrated co-localization between the ITOP signal and the DAPI (4',6-diamidino-2phenylindole) labeling of cell nuclei, suggesting that the signal from the fluorescent particle is found close to the nucleus of the cell (Fig. 24). Adventitial co-localization results also showed neovessel-like structures, located around regions delineated by cells labeled with fluorescent ITOP. Under microscopic examination, this was also correlated with an expansion of the aortic vasa vasorum in atherosclerotic rabbits compared to controls.

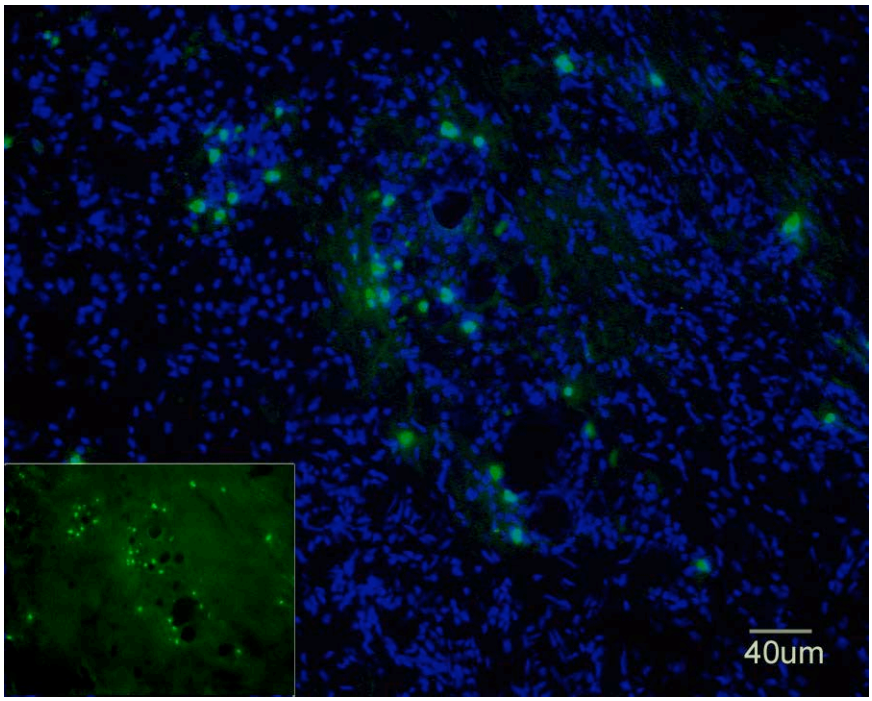

Figure 24 **Fluorescence microscopy of localization of the αvβ3 antagonist labeling inside the adventitia.**

Merged image showing FITC-integrin antagonist labeling and DAPI staining (nuclei of cells) of the same aortic region. Smaller inset image represents the antagonist labeling alone. The antagonist signal appeared to be localized on the surface of the cells, near to the nucleus. There was presence of some structures similar to early neovessels that were labeled with fluorescence. FITC, fluorescein isothiocyanate; DAPI, 4',6-diamidino-2phenylindole.

2.3.5 Labeling and Adventitia Thickness

Comparison between fluorescent labeling with the αvβ3 targeted probe (Fig. 25, upper panel) and histological staining (Fig. 25, bottom panel) of the corresponding descending aorta sections demonstrated a qualitative correlation between fluorescent signal intensity and adventitial thickness. Indeed, histological staining (H&E) showed a range of adventitial thickening that was as much as 3 times greater in the thickest plaques as in non-atherosclerotic controls. In these plaques, the relative intensity of the optical probe

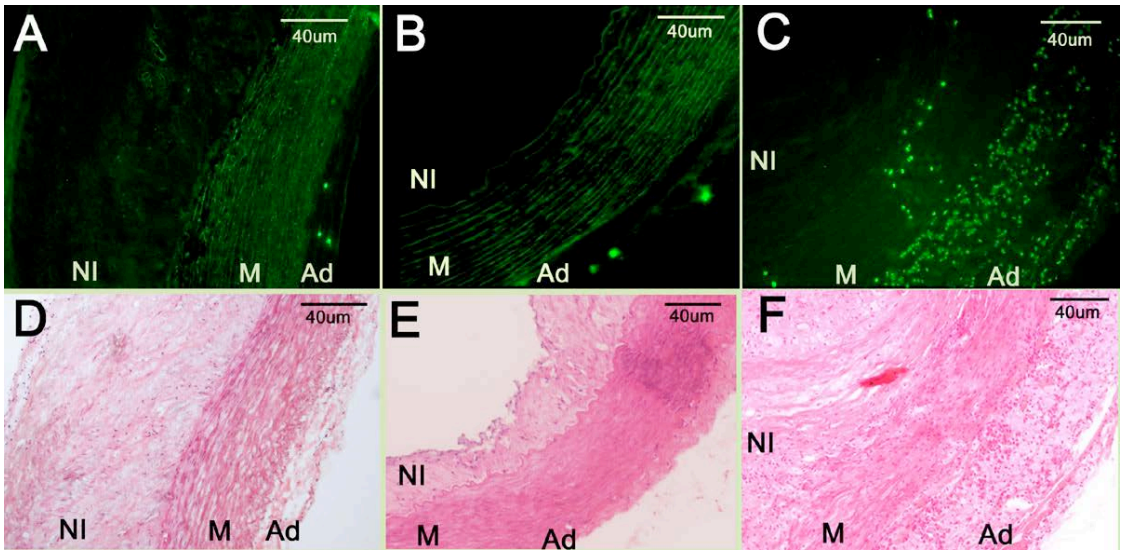

Figure 25 **Correlation between intensity of ITOP labeling and adventitia thickening**

Intensity of fluorescence staining in Watanabe rabbit descending aorta sections **(A, B, C)** correlated with adventitia thickness and plaque histology **(D, E, F)**. In images (10X magnification) of aorta sections with smaller adventitia **(D, E)**, the level of labeling with the αvβ3-targeted probe was weaker **(A, B)**. Inversely, in the aorta sections with a larger adventitia **(F)**, the signal from the αvβ3-targeted probe was very intense **(C)**. There were also some correlation between the intensity of labeling and the organization level into the plaque: labeling was very intense when the media looked digested **(C)** and less intense when the media was well delineated **(A, B)**. Ad, adventitia; M, media; NI, neointima.

qualitatively corresponded to the relative degree of adventitial thickening. Thus, a mild signal was present in plaques with a small adventitia thickness (Fig. 25A, B, D, E), while a strong signal appeared on plaques with marked adventitia thickness (Fig. 25C, F). There was also an inverse correlation between the intensity of fluorescence labeling and the organization level of the plaque. Staining was very intense (Fig. 25C) when the media was disorganized (Fig. 25F) and less intense (Fig, 25A, B) when the media was well delineated (Fig. 23D, E). In the plaque with very intense ITOP labeling (Fig. 25C), there was a structure resembling intraplaque hemorrhage in the intima of the corresponding H&E (Fig. 25F). Moreover, the H&E labeling of the same section also showed important inflammatory infiltrate, visualized by the typical red dot, into the adventitia, media, and neointima.

2.3.6 Lipid Staining

In order to characterize the lesions in the Watanabe rabbit model, a lipid staining was performed on the descending and ascending aortas of the rabbits. Results showed lipid accumulation localized throughout the entire circumference of the neointima (Fig. 26). Indeed, there was no real formation of a delimitated necrotic core, as seen in human plaques, but instead a general distribution of the lipids inside the entire neointima layer. Note that there was absence of lipids in the media layer. In both ascending (Fig. 26A, B) and descending (Fig. 26C, D) aortas, there was a region were it seemed that the media had completely disappeared. In the descending aorta (Fig. 26C), there was a portion of the vessel wall, inside the neointima, presenting signs of calcification (arrow).

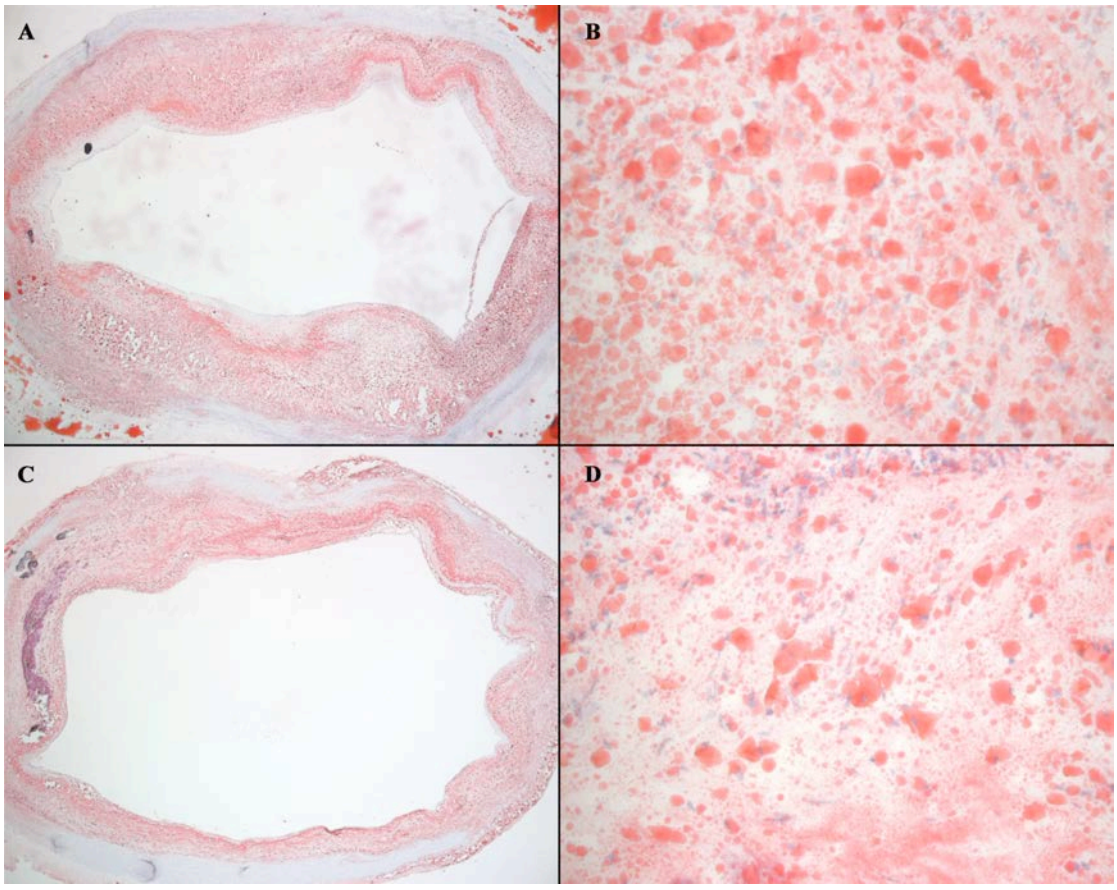

Figure 26 **Oil Red O staining of ascending and descending aorta of Watanabe Rabbits**

Oil red O staining showing lipid accumulation in Watanabe rabbit descending aorta sections **(A, B)** compared to ascending aorta **(C, D)**. Diffuse accumulation of lipids was clearly seen around the entire neointimal area, instead of a more define lipid area forming a necrotic core. Images on **right panel** are higher magnifications (20X) of images in **left panel** (4X).

2.4 DISCUSSION

Integrin expression, particularly αvβ3, in atherosclerotic plaques is a component of the inflammatory process that can drive the plaque toward a more unstable state[9, 108] leading to plaque rupture[10, 109, 110], and its clinical complications such as stroke and myocardial infarction. In the other hand, it is also related to plaque stenosis and healing[42]. Many processes taking place during the initiation and progression of inflammatory vascular lesions require αvβ3 expression, including foam cell formation[46], smooth muscle cell migration[111] and thrombus formation[73]. These observations point towards the use of αvβ3 as a molecular target for imaging and early detection of atherosclerotic disease.

In this study, we described the use of a novel synthetic high affinity and high specificity αvβ3 integrin targeted optical probe and confirmed the *in vitro* labeling of rabbit atherosclerotic plaques (Fig. 21 and 22). We also show that the ITOP signal was localized near the nucleus of the cells (Fig. 23), which indicates that fluorescence was correlated to cells (αvβ3 receptors are membrane-bound) instead of unspecific ECM labeling. One interesting observation in the present work was that the fluorescent signal of the integrin targeted optical probe seemed to extend from the adventitia toward the media of the aortic wall (Fig. 21A). The presence of fluorescent signal in the media was correlated with strong labeling and expansion of the adventitial layer (Fig. 21A and 24). This finding was probably associated with the development of angiogenic processes that first begin within the adventitia (vasa vasorum expansion) and then extends to the media of the vessel wall[112]. Most importantly, there was a strong correlation between the labeling with the integrin targeted probe and the thickness of the adventitia (Fig. 25). Thus,

adventitial thickening was characterized by a strong and widely distributed signal enhancement from the probe, which may signal a more advanced inflammatory state. Moreover, stronger αvβ3 labeling was located where the media was less organized, which is another sign of the presence of inflammation. Further evaluation of other biomarkers of inflammation inside the plaque can confirm this hypothesis and help to better understand the chronology of plaque development.

In agreement with other studies[41, 49, 77], we also found that the most significant accumulation of αvβ3 receptors were in the adventitia of the aortic wall, a privileged site for the formation of neovessels. We also observed a characteristic expansion of the adventitia, a process that had been extensively described by others studies [49, 77, 113, 114]. This expansion allows angiogenesis to take place and will further attract more inflammatory cells and lipids into the plaque, contributing to plaque growth, instability and rupture, but also stenosis and healing.

In addition to the adventitial localization of the signal, we also observed fluorescence within the neointima of plaques, close to the lumen. Previous studies had shown that activated or proliferative endothelial cells express high levels of αvβ3[34, 74]. This integrin is critical for the survival signal of these cells and is also recognized to influence adhesion and migration pathways[76]. Hence it is not surprising to observe evidence of αvβ3 within the intima.

Relative to peptide-based molecules, this synthetic probe provides easier production and purification[92]. Moreover, its affinity as a labeled probe for the αvβ3 receptor is higher than the commercially available labeled cyclic peptide c[RGDfv][90, 92]. This should

translate into a smaller injected dose for the plaque detection and also a better sensitivity. In addition, our ITOP is specific to αvβ3, whereas linear and cyclic RGD peptide specificity is broader (αvβ3, αIIbβ3a, αvβ5)[92].

The physiochemical characteristics of this probe are also important. As opposed to antibodies, this small synthetic molecule (<1nm) has less potential to induce an immune response and has important advantages related to the blood clearance and its diffusion into the targeted atherosclerotic tissue. Moreover, unlike antibodies, the probe is very suitable for further derivatives or structure modifications. However, future *in vivo* studies will be necessary to evaluate the labeling efficiency and kinetic uptake properties of this new optical probe.

With the broad development of nanoparticles in disease detection[115, 116], we can extrapolate the use of this new αvβ3 integrin targeted probe for imaging atherosclerosis in combination with a variety of high-resolution molecular imaging techniques. The synthetic nature of this molecule makes it attractive for the development of various nanoparticle structures incorporating this molecule to target the plaque. For example, as demonstrated in other studies, this integrin targeted probe can be coupled with iron or gadolinium for magnetic resonance imaging[77], or even with fluorescent and magnetic particles for dual imaging techniques[117, 118]. As previously suggested, this αvβ3 targeted probe could also be used in systems that may carry drugs into the site of inflammation for simultaneous molecular imaging and drug treatment[49]. For example, this probe was efficiently used in a novel integrin targeted nanoparticle system for targeted drug delivery and imaging of cancer angiogenesis[50].

CHAPTER 2

IN VIVO ITOP INJECTION ON WATANABE RABBITS

3.1 INTRODUCTION

In the previous chapter, *in vitro* labeling studies on Watanabe rabbits showed labeling of atherosclerosis plaques on aortic tissue samples, as opposed as an absence of labeling on aortic tissues from normal control New Zealand White rabbits[119]. There was also an absence of labeling in disease rabbits where aortic tissues do not show sign of plaque. Moreover, the ITOP signal seemed to correlate with the thickness of the adventitia layer, more than the thickness of the neointima. It also seemed that there was a correlation between the degree of inflammation and the presence of the ITOP in the aortic tissue.

These *in vitro* results were promising, but isolated vessel wall tissue samples present a limited array of possible competing binding sites. Ideally a probe for plaque formation has to specifically bind and target atherosclerotic plaques, and nothing else in the entire body. *In vitro* tests for specificity can only reveal the affinity to competing or non-binding entities chosen for such test, but they can give no guarantee for the absence of competing binding sites in the whole body. We therefore used the Watanabe Heritable Hyperlipidemic rabbit model to test our ITOP *in vivo*.

From previous *in vivo* study on a mouse model[92], we evaluated the dose of ITOP to be injected at approximately 1mg/kg. Since we lack dose-response data for the previous mouse studies, we decided to inject 5mg of ITOP to each rabbit, independently of the

weight, to allow evaluation of the appropriate dose. Rabbits were chosen according to their age. Although some of them showed signs of plaques as early as 3 month old, they usually showed more extensive sign of atherosclerosis around 6 months age. Rabbits ranged in age from 3 month old to 4 year old, and from 1.5 kg to 5 kg, with an average weight of 4 kg. Although plaques in coronary tissue are clinically more important, we chose aortic vessel wall tissues as a model for plaque formation, because Watanabe rabbits rarely develop myocardial infarction and have a low incidence of coronary atherosclerosis[95]. Moreover, it is easier to manipulate aortic tissue than coronary tissue, and it is also easier to visualize plaque areas before dissection. We euthanized the rabbits 2 hours after injection, to allow proper blood diffusion and retention of the ITOP into plaques. The 2 hour incubation time has been evaluated from a previous mouse study[92]. We dissected the aortic tissues and used histological staining to compare and characterize the ITOP labeling with histological features in the vessel walls of the Watanabe rabbits.

3.2 MATERIALS AND METHODS

3.2.1 Experimental Design (In vivo Injection)

WHHL rabbits and NZW rabbits were fed a normal diet by the vendor company. Prior to any experiments, Watanabe rabbits (n=7) and New Zealand White rabbit (n=1) were anesthetized with a ketamine HCl (30mg/kg) and xylazine (5mg/kg) cocktail administered subcutaneously with a 23G butterfly needle in their hindlegs. After the rabbits were completely anesthetized, a catheter was put in place. Briefly, each rabbit ear

was cleaned, hairs from a small part of the ear were removed by gently poking the area, and a 21G butterfly needle was inserted through the vein. A heparin solution (10unit/ml) was pushed through the needle to ensure the right placement, and the catheter was attached. A cotton cloth was placed in the ear and the catheter was taped with it to secure it to the ear and prevent accidental removal. The heparin solution was then pushed again to verify positioning. The ITOP was then injected (5mg in 50mM Tris pH 8.0) through the catheter for 2hrs. During this time, rabbits received isoflurane gas through a nose cone to keep them anesthetized, and their heartbeats were monitored. After 2 hrs, the heparin solution was pushed again through the catheter to ensure it hasn't been displaced, and rabbits were euthanized by intravenous injection with a solution of Sodium Pentobarbital (150mg/Kg) (EUTHANASIA III). All experiments were performed in accordance with protocols approved by the Animal Care and Use Committee of the National Heart Lung and Blood Institute or the National Institute of Diabetes, Digestive and Kidney Diseases.

3.2.2 Cholesterol Measurement

Blood was collected and centrifuged at 1400*g* for 10 minutes, and the serum was frozen at −20°C, until it was assayed within 2 months after collection. Total cholesterol levels were measured by the Brown Family Enterprises Laboratory, at the Gemini Research of Alabama facility, using a cholesterol esterase/cholesterol oxidase colorimetric assay procedure. Total cholesterol values were expressed as mg/dL (mean6SEM). Cholesterol measurements were made between a week to a month of the euthanasia.

3.2.3 Dissection

The rabbit abdomen was open, and the aortic arch was excised and cut into different sections (ascending, descending thoracic, and descending abdominal). 2-3mm thick samples were taken from each segment, and 1 segment was put in a formalin solution, while the other segments were put in Optimal Cutting Temperature (OCT) media and quick frozen in methylbutane containing dry ice. Samples were kept at –80°C for further histological and immunohistological experiments.

3.2.4 Histology and Immunohistology

For probe's visualization, slides were removed from –80°C and transferred to –20°C for 15min. The slides were then air dry for another 15min before to be fixed in cold acetone (–20°C) for 10min, and washed with 3 changes of PBS (5 min each). Finally, the slides were carefully wiped off the excess of liquid, and mounted with VECTASHIELD mounting medium containing DAPI (Vector Laboratories, Inc., Burlingame, CA).

3.3 RESULTS

3.3.1 Plaque Labeling

Histological staining (H&E) of WHHL rabbit aortic tissues in transverse slices demonstrated intimal thickening of the aortic wall and plaque accumulation in some of

the Watanabe rabbits, whereas others Watanabe rabbits showed no intimal thickening and no lipid accumulation. In the rabbits without apparent plaque formation, some samples presented an adventitial thickening, even in the absence of neointima. Those same samples did not show ITOP labeling, which seemed to indicate that the αvβ3 probe was related to the adventitial thickening, but only when there was a corresponding neointimal formation. In some of the Watanabe rabbits with plaque accumulation, examination of the aortic tissues incubated for 1 hour with the ITOP showed a fluorescent signal in both descending and ascending aorta (Fig. 27A). Signal enhancement was predominately localized in the adventitia and the neointima of the vessel wall, though there was also some fluorescence in the media. The fluorescent signal of the ITOP was absent from the aorta of Watanabe rabbits without plaque (Figure 27B).

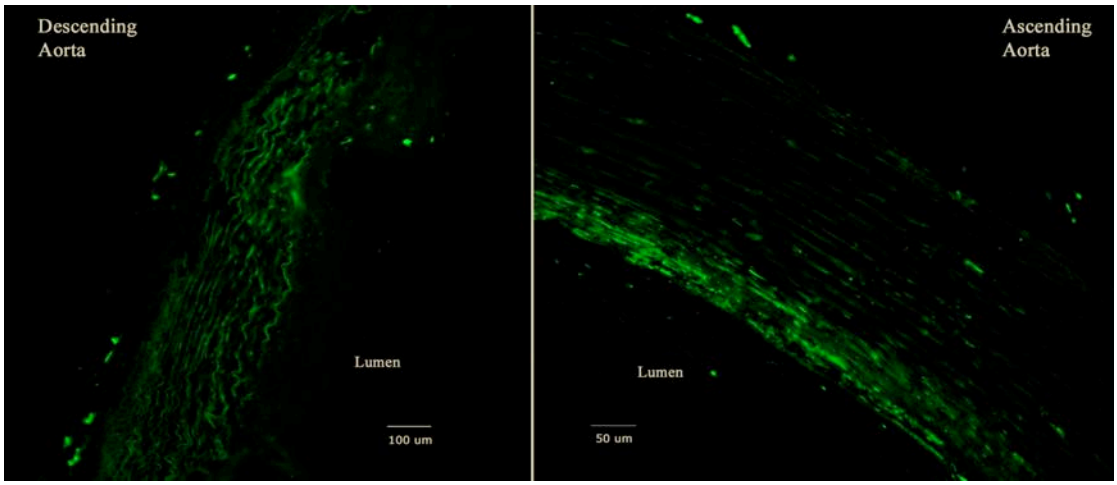

Figure 27 ***In vivo*** **plaque labeling on Watanabe aorta with ITOP**

Left panel (**A**) represents results of fluorescence microscopy for the descending aorta of the Watanabe rabbit injected with the ITOP (5mg, 2hrs), while **right panel** (**B**) represents results of fluorescence microscopy for the ascending aorta. The αvβ3 signal appeared stronger in the adventitia of both descending and ascending aorta, and in both parts, there was a weak associated αvβ3 signal in the neointimal layer. There was also an important background signal from the aortic tissues, probably caused by the collagen. The background signal was more important than the one in the *in vitro* experiments.

For the *in vivo* injection, a specific plaque signal enhancement could be observed from the probe, as in the *in vitro* experiment. However, the *in vivo* labeling produced a more important autofluorescence and background signal in the aortic tissues than in the *in vitro* labeling experiments. Moreover, in some of the rabbits, there was a very weak ITOP signal, despite the formation of a neointima (Fig. 28). The absence of signal seemed to be correlated with an adventitia less developed and without important inflammation, as seen with *in vitro* results.

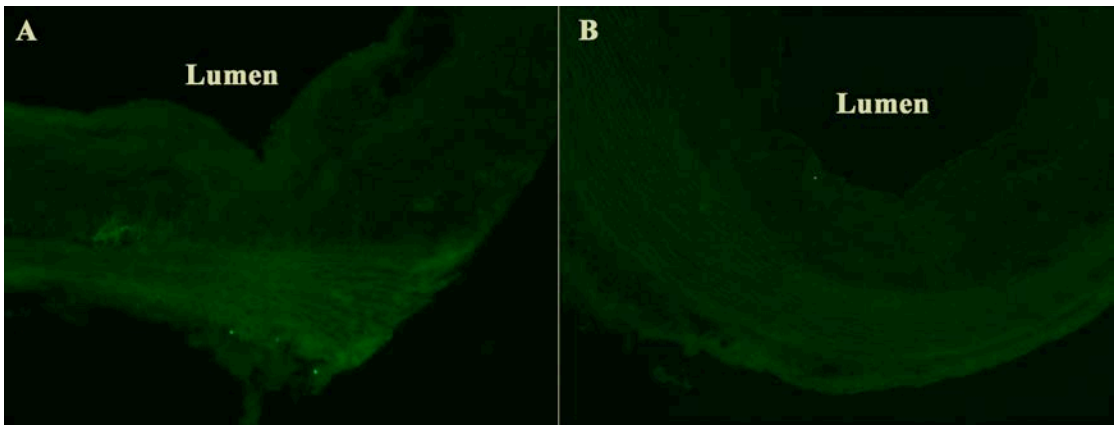

Figure 28 **In vivo plaque labeling on Watanabe aorta with ITOP**

Left panel (**A**) represents results of fluorescence microscopy for the descending aorta of the Watanabe rabbit injected with the ITOP (5mg, 2hrs), while **right panel** (**B**) represents results of fluorescence microscopy for the ascending aorta. In this rabbit, there was a very weak αvβ3 signal in the adventitia of the descending aorta and absence of signal in the ascending aorta. 10X magnification.

3.3.2 Neointima Labeling

In some Watanabe rabbits injected with the αvβ3 probe, the presence of αvβ3 signal was more important in the neointimal area rather than in the adventitia (Fig. 29A). Interestingly, this signal was also visually correlated with a thinning of the SMCs layer, and has observed before, with a beginning of adventitial thickening (Fig 29B). In the *in*

vivo experiments, αvβ3 labeling seemed to be related to the complexity of the plaques. Effectively, the neointimal αvβ3 labeling (Fig. 29A) was also characterized by important calcification areas (Fig. 29C), as well as intraplaque hemorrhages (Fig. 29D). There was also presence of lipid crystals in the neointima, which is often seen in plaques with late cores. Those characteristics were also present in the *in vitro* experiments, in the rabbit with important αvβ3 signal. The neointimal labeling and thinning of the SMCs layer seemed to be correlated with an important acellular region in the neointima (Fig. 29D).

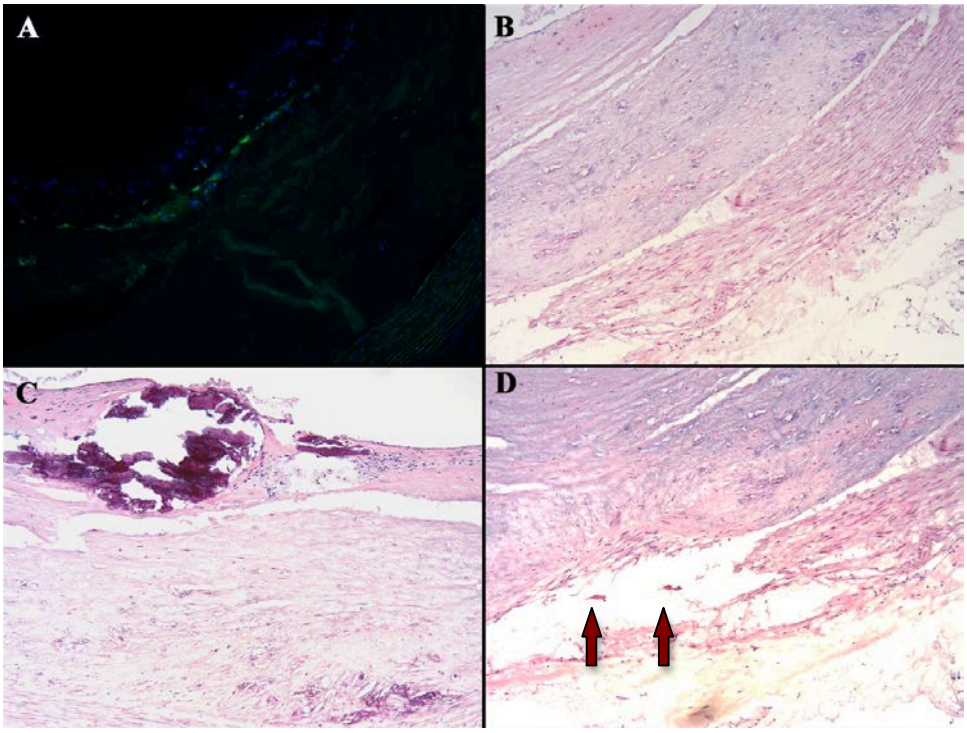

Figure 29 **In vivo plaque labeling on Watanabe aorta showing neointima labeling and plaque complexity**

(**A**) Results of fluorescence microscopy for the descending aorta of the Watanabe rabbit injected with the ITOP (5mg, 2hrs). (**B**) H&E staining of the same region, demonstrating the thinning of the SMCs layer and the beginning of adventitial thickening. On the same section of the rabbit's descending aorta (thoracic part), there was an important zone of calcification **(C)** and some intraplaque hemorrhages **(D)**. Red arrows: intraplaque hemorrhages. 10X magnification.

3.3.3 Adventitia Labeling

In the *in vivo* experiments, as seen also *in vitro*, there was presence of αvβ3 probe labeling in the adventitia, when there was presence of adventitial thickening (Fig. 30A). In those samples, elastic fibers from the SMC layer seemed to be disorganized and even disrupted in some areas, and the neointima of the vessel was characterized by the presence of foam cells (Fig. 30B). Although no specific blood vessel staining was done, the signal seemed to be localized in zones of vessels-like structures and inflammation, as observed with the H&E staining. This result was also observed previously during the *in vitro* experimentation. There seemed to be an absence of medial labeling in the samples, although the strong background staining of the elastic fibers in the media rendered the specific αvβ3 ITOP signal difficult to differentiate. In some of the samples (Fig. 30B), an αvβ3 signal in the media cannot be excluded. There seemed to be some weak neointimal ITOP signal in the samples, but it is far less intense than the adventitial signal (Fig. 30A).

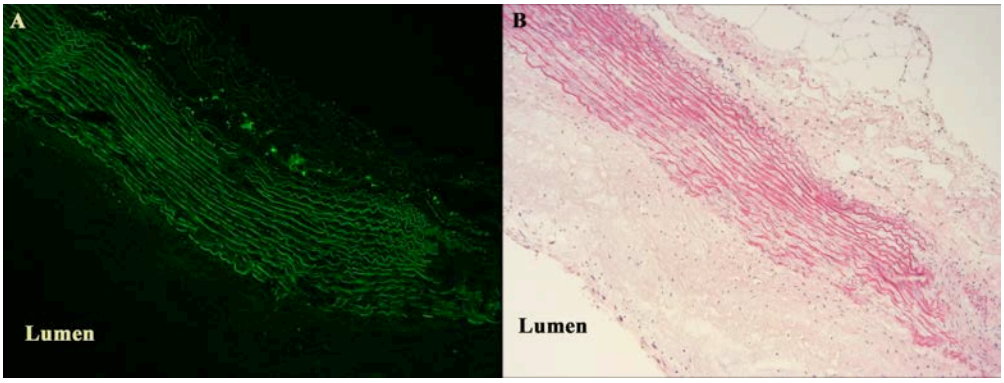

Figure 30 ***In vivo*** **ITOP labeling on Watanabe aorta showing adventitia labeling**

Left panel (**A**) show results of fluorescence microscopy for the descending aorta of the Watanabe rabbit injected with the ITOP (5mg, 2hrs), while **right panel** (**B**) represents the H&E staining of the same region, demonstrating adventitial thickening and disrupted collagen content into the SMC layer. In the H&E staining (B), the adventitia with an αvβ3 ITOP signal presented vessel-like structures that can be characterized as blood vessels. 10X magnification.

3.3.4 Labeling and Adventitia Thickness

As seen with the *in vitro* samples, comparison between fluorescent staining with the αvβ3 targeted probe (Fig. 31, upper panel) and histological staining (Fig. 31, bottom panel) of the corresponding descending aorta sections demonstrated a qualitative correlation between fluorescent signal intensity and adventitial thickness. Accordingly, there was presence of mild signal in plaques with a small adventitia thickening (Fig. 31A, D), while a stronger signal appeared on plaques with marked adventitia thickening (Fig. 31C, F).

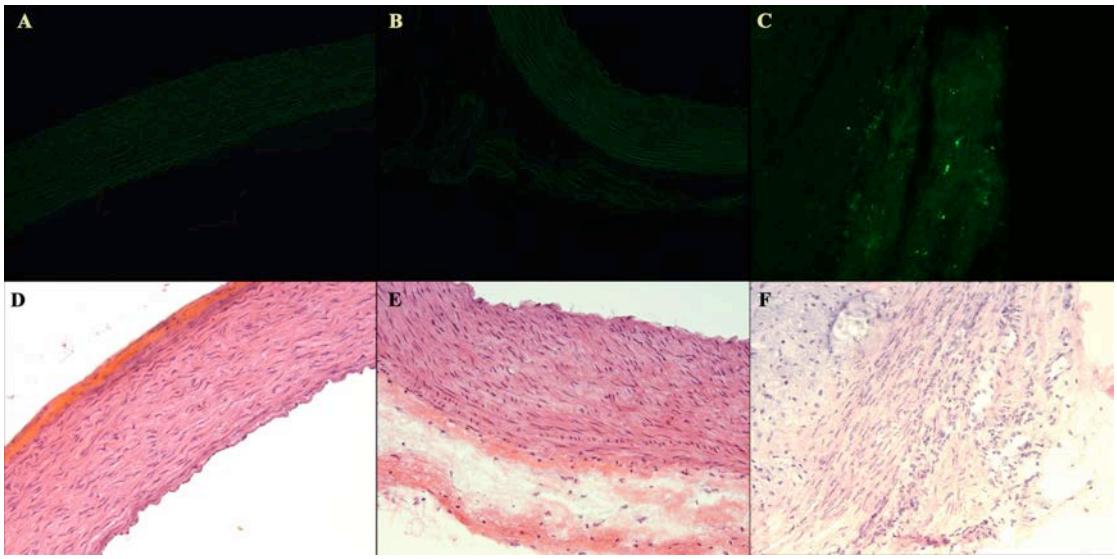

Figure 31 **Correlation between intensity of ITOP labeling and adventitia thickening**

Intensity of fluorescence labeling in Watanabe rabbit aorta sections **(A, B, C)** correlated with adventitia thickening and plaque histology **(D, E, F)**. In the section with smaller adventitia **(D)**, the level of staining with the αvβ3 targeted probe was weaker **(A)**. Inversely, in the aorta sections with a larger adventitia **(F)**, the signal from the αvβ3 targeted probe was more intense **(C)**. Interestingly, when the adventitia was larger, but there was no plaque formation **(E)**, there was also absence of signal. There was also some correlation between the intensity of labeling and the organization level into the plaque: staining is very intense when the media seems digested **(C)** and less intense when the media is well delineated **(A, B)**. 20X magnification.

The histological staining (H&E) showed an adventitial development as much as 10 times greater in some plaques (Fig. 31F) than in Watanabe rabbit without plaque (Fig. 31D). In these plaques, the relative intensity of the optical probe qualitatively corresponded to the relative degree of adventitial thickening. Notably, when there was presence of adventitial thickening without associated plaque (Fig. 31E), there was absence of staining. Again, as seen *in vitro*, an inverse relationship between the intensity of fluorescence labeling and the organization level of the plaque appeared to exist. Staining was more intense (Fig. 31C) when the media was disorganized (Fig. 31F), and less intense (Fig. 31A, B) when the media was well delineated (Fig. 31D, E). As opposed to the *in vitro* results, there was no plaque with very intense αvβ3 labeling.

3.3.5 Labeling and Markers of Plaque Vulnerability

The Watanabe rabbit aortas that produced an αvβ3 signal were characterized by some important cytological features. First, there was adventitial thickening and extensive inflammatory cell infiltration in either neointima, adventitia, or both in some cases (Fig. 32A, C, D). Interestingly, most of the rabbits producing an αvβ3 signal also presented heavy calcification (Fig. 32B) and intraplaque hemorrhages (Fig. 32C). The calcified areas also corresponded to areas of thinning of the medial layer or complete absence of media (Fig. 32A, B). There were also some important discontinuities in the collagen fibers of the media (Fig. 32E, F). In some instances, it seemed to be a localized discontinuity, probably due to macrophage infiltration (Fig. 32E). In other cases, there was an important discontinuity along the length of the media, correlated with what seemed to be another small upper layer of elastic fibers (Fig. 32F).

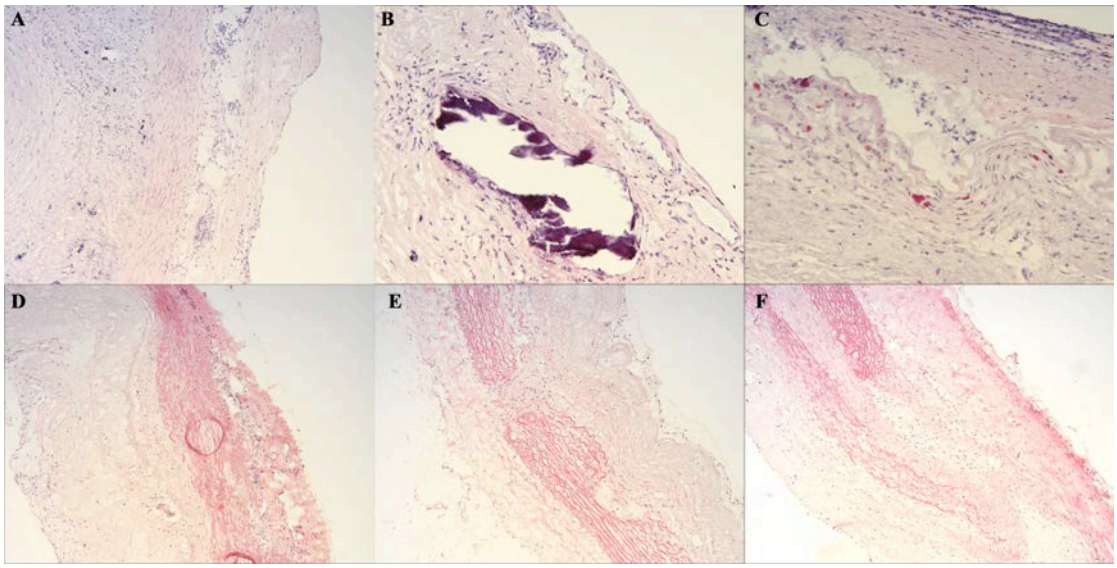

Figure 32 **Characteristics of the Watanabe atherosclerotic plaques that produce an αvβ3 ITOP signal**

Watanabe rabbit aorta sections that showed some of characteristics of the plaques that has produced an αvβ3 signal. The αvβ3 ITOP signal correlated with important cytological characteristics: adventitial thickening and inflammatory cells infiltration **(A, D)**, heavy calcification **(B)**, intraplaque hemorrhage **(C)**, and collagen discontinuities **(E, F)**. There was also some areas without apparent media layer, usually correlated with calcifications **(A, B)**. **(A, D, E, F)** 10X magnification. **(B, D)** 20X Magnification.

3.4 DISCUSSION

We previously reported the use of a novel synthetic high affinity and high specificity αvβ3 integrin targeted optical probe, *in vitro* on rabbit atherosclerotic plaques[119]. In this previous study, we showed that the majority of the ITOP signal was founded in the neointima and adventitia, although there was some associated medial labeling when the signal was important. We also reported the qualitative correlation between the intensity of αvβ3 labeling and the thickening of the adventitial layer. In the present study, we seek to correlate the *in vitro* results with *in vivo* injection to evaluate the labeling efficiency and kinetic uptake properties of this new optical probe.

In this study, we showed that *in vivo* injection of the αvβ3 ITOP produced a specific signal in the adventitia and in the neointima of the Watanabe rabbits. It was in concordance with our previous *in vitro* study and also with other studies showing angiogenesis in atherosclerotic plaques[120]. As opposed to the *in vitro* results, we did not see intense ITOP labeling in the rabbit's atherosclerotic plaques. This could be explained by the difficulty to differentiate between background fluorescence and specific signal or the greater accessibility of the receptor on tissue samples, as opposed to *in vivo* accessibility. Further *in vivo* studies on blood clearance and dose optimization would be necessary. Moreover, as opposed to the *in vitro* study, αvβ3 labeling with an antibody was not possible, since the ITOP was injected, an the probe is designed as an antagonist of the αvβ3 receptor. Consequently, ITOP binding will further prevent the binding of the αvβ3 antibody.

In this study we also showed that in some cases, beside the adventitial and neointimal labeling, there was an associated αvβ3 signal in the media. The aortic segments that produced a medial αvβ3 signal seemed to be the ones that presented early plaques. In those segments, there were no heavy calcification, no intraplaque hemorrhage, and no medial discontinuity. This can be explained by the fact that in plaques with calcification or hemorrhages, there were often medial necrosis and thinning, with associated discontinuities in collagen synthesis due to SMC death[64]. Together with the overexpression of MMPs, this caused digestion of ECM proteins and a diminution in ECM synthesis. Since αvβ3 is an integrin that play a role in cell-to-cell and cell-to-ECM contact and communication, it is expected that extensive medial necrosis and ECM degradation will lead to an absence of expression in the media. In that case, adventitial angiogenesis and neointima hemorrhages will be the principal site of αvβ3 expression. Inversely, in the event of plaque healing, there will be SMC migration and ECM synthesis, mechanisms that will involve the expression of αvβ3[43].

Another observation of the *in vivo* study was the absence of αvβ3 signal in the case of adventitial thickening without corresponding neointimal formation. Moreover, *in vivo* results also confirmed the correlation between adventitial thickening and αvβ3 signal intensity, as previously seen *in vitro*. Indeed, αvβ3 labeling seemed to be positively related to the degree of adventitial thickening and also with the degree of plaque inflammation. This observation was in agreement with other studies reporting that plaque neovascularization is related to both degree of inflammation and neointima formation[112]. Finally, *in vivo* results also demonstrated that there was often concomitant presence of vulnerability markers or stenosis markers in plaque demonstrating an αvβ3 ITOP signal.

Effectively, some of the Watanabe rabbits presented calcification, intraplaque hemorrhages, heavy inflammatory cell infiltration in both neointima and adventitia, as well as collagen/elastic fibers rupture and discontinuities, in some cases associated with a thinning or absence of the SMC layer. Interestingly, all those characteristics had been previously reported in the *in vitro* results. Indeed, the rabbit that produced the most extensive αvβ3 ITOP signal presented all these features, but medial thinning. While numerous studies have link inflammation, plaque hemorrhage, angiogenesis, and medial necrosis to plaque vulnerability[11, 121], the relation between calcium and vulnerability remain controversial. While microcalcifications had emerged as a new biomarker of vulnerability[21], heavy calcification is usually seen in advanced stenotic plaques, and has been link to more stable type of atherosclerosis[122]. In the case of Watanabe rabbits, there was extensive plaque calcification in the aortas that produced an αvβ3 signal. This could be due to discrepancy between the animal models and human atherosclerosis. Effectively, while rabbits have a similar lipid mechanism to human, they are less prone to plaque rupture[123]. In the other end, link between plaque calcification in rabbits and more advanced atherosclerosis have been previously reported[124]. The mechanism by which microcalcifications and calcifications processes may differ in rabbits and humans remained to be elucidated.

In this chapter, we correlated the *in vitro* data of the new αvβ3 ITOP probe with *in vivo* injection on a WHHL rabbit model. We showed that the probe efficiently labeled the plaques when intravenously injected to rabbits. The *in vivo* results confirmed the *in vitro* findings that ITOP labeling seemed to qualitatively correlate with the degree of adventitial thickening and inflammation. We also showed that when there was labeling of

the media, it seemed to be related to plaque healing, as opposed as when the signal was only located in the adventitia and neointima. More pathological and histological studies will be necessary to better understand the link between the ITOP signal and the plaque composition, but these results indicated that ITOP labeling could be a valuable tool for the detection of atherosclerotic plaques, if combined with method that detect stenosis.

CHAPTER 3

IN VITRO ITOP LABELING ON HUMAN ATHEROSCLEROTIC SAMPLES AND HISTOLOGICAL CHARACTERISATION

4.1 INTRODUCTION

Our new αvβ3 ITOP has been tested *in vitro* and showed specific labeling of atherosclerotic plaques in a WHHL rabbit model[119]. Labeling was found on adventitia and neointima layers, with associated media labeling in some cases. The *in vitro* study also suggested an association between adventitial thickening, inflammatory cell infiltration, and the intensity of labeling. After the *in vitro* study, the ITOP had been injected intravenously to WHHL rabbits for *in vivo* evaluation. The αvβ3 ITOP showed specific *in vivo* labeling of atherosclerostic plaques in WHHL rabbits, although the background signal was more important than in the *in vitro* study. Labeling of the adventitia and neointima was confirmed, as well as media labeling, as seen in the previous *in vitro* study. Correlation between adventitial thickening, presence of inflammation, and intensity of labeling was also observed. Moreover, the *in vivo* study showed that adventitial thickening without neointima formation resulted in an absence of αvβ3 ITOP labeling. In this part of the study, the labeling efficiency of our αvβ3 ITOP signal in atherosclerotic plaques will be evaluated in human coronary artery samples, and correlated with pathological examination.

4.2 MATERIALS AND METHODS

4.2.1 Experimental Design

Studies were performed on autopsy specimens from the left anterior descending (LAD) region of the coronary arteries from multiple cases of sudden deaths (7 atherosclerotic cases, 1 case with adaptive intimal thickening, and 1 case with pathological intimal thickening). Specimens were purchased from CVPath Institute (Gaithersburg, MD). Immunohistology staining, immunohistofluorescence and immunohistochemistry on frozen tissue sections from those specimens were then carried out.

4.2.2 Histology and Immunohistology

OCT blocks from snap frozen coronary arteries (left anterior descending) were cut into 7-8 μm sections with a cryostat and mounted onto slides. Routine hematoxylin and eosin (H&E) straining was performed on the frozen sections. For immunohistochemistry, an antibody against human α-actin (ab7817, Abcam, USA), and an antibody against CD-68 (ab955, Abcam, USA), were used, at a dilution 1/200 (PBS), to confirm the presence of α-actin and macrophages respectively. These antibodies were used in conjunction with an anti-mouse horseradish peroxidase detection kit, according to the specifications of the company (Chemicon International, Inc, Temecula, CA, USA). For immunohistofluorescence, an antibody against human MMP-9 (ab58803, Abcam, USA), and an antibody against CD-40 (ab61401, Abcam, USA), were used, at a dilution 1/100 (PBS). These antibodies were used in conjunction with an anti-mouse secondary antibody conjugated to FITC, at a dilution of 1/500 (ab6785, Abcam, USA). Expression

of αvβ3 integrin in the aortic wall was assessed by immunohistofluorescence with our new αvb3 integrin targeted optical probe (ITOP). Briefly, sections were thawed for 15 minutes at room temperature, fixed 10 minutes with cold acetone, washed in phosphate buffer solution and then incubated with the targeted fluorescent probe for 1 hour. After the incubation period, the slides were washed again in phosphate buffer solution, and mounted with VECTASHIELD mounting medium containing DAPI (Vector Laboratories, Inc., Burlingame, CA). An antibody against human αvβ3, anti-human integrin αvβ3, clone LM609 (Chemicon International, Inc, Temecula, CA, USA), was used to confirm the presence of the integrin and as a reference for the localization of any experimental fluorescence signal. This antibody was used in conjunction with an anti-mouse horseradish peroxidase detection kit, according to the specifications of the company (Chemicon International, Inc, Temecula, CA, USA). Images of staining or fluorescence signal were acquired under a microscope (Leica DM5500B with a Leica DFC-500 color camera) using a visible or ultraviolet light source, respectively. For the ITOP (FITC labeling), the emission wavelength was set up at 495nm, while absorption wavelength at 521nm.

4.3 RESULTS

4.3.1 Histological Characterization of the Coronary Wall

Since atherosclerotic plaques present many different characteristics, it was very difficult to choose a specimen representing a typical plaque. Indeed, every atherosclerotic plaque is characterized by its own features, and it is difficult to draw any conclusion without

extensive pathological studies. For this reason, in other to test our probe *in vitro* on human samples, we chose plaques that demonstrated signs of complexity. First, all of the human plaque specimens were taken from left anterior descending (LAD) coronary arteries. The coronary wall on those samples appeared very thick (Fig. 33A) due to the formation of an important neointima (Fig. 33B, D). In most cases, there were associated adventitial thickening (Fig. 33A, C, E). Most of the plaques that were tested also presented some inflammatory cell infiltration (Fig. 33A, C, E). Typically, the necrotic

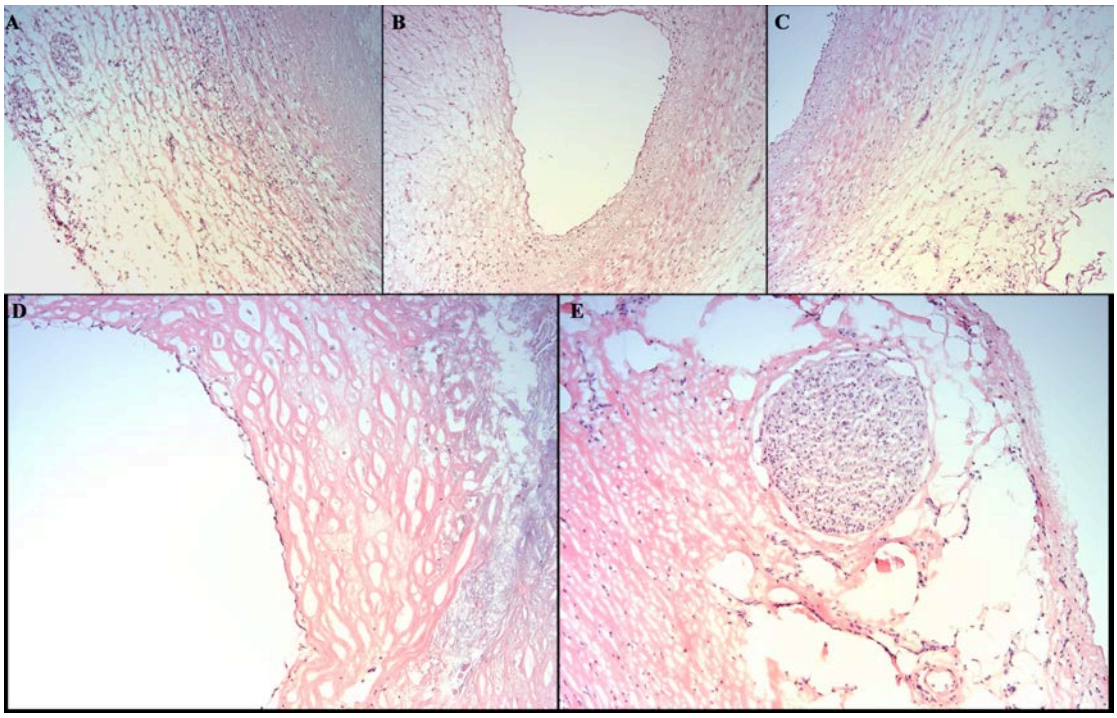

Figure 33 **Characteristics of the coronary artery walls of human atherosclerotic plaque specimens**

Human sections that showed some of the characteristics of the plaques that had produced an αvβ3 signal. Features of the tested plaques included adventitial thickening **(A, C, E)**, important neointimal formation **(B, D)**, stenosis **(B)**, fibrous cap and necrotic core formation **(D)**, and inflammatory cell infiltration **(A, C, D)**. Typically, plaque did not present intraplaque hemorrhages or microcalcification. 10X Magnification.

core thicknesses (Fig. 33D) were more than 65μm, which was not considered thin fibrous caps or markers of plaque vulnerability[3]. Two of the plaques tested presented signs of complexity, as superimposed necrotic cores (Fig. 34B, C). The human samples tested were also characterized by an absence of intraplaque hemorrhage or microcalcification.

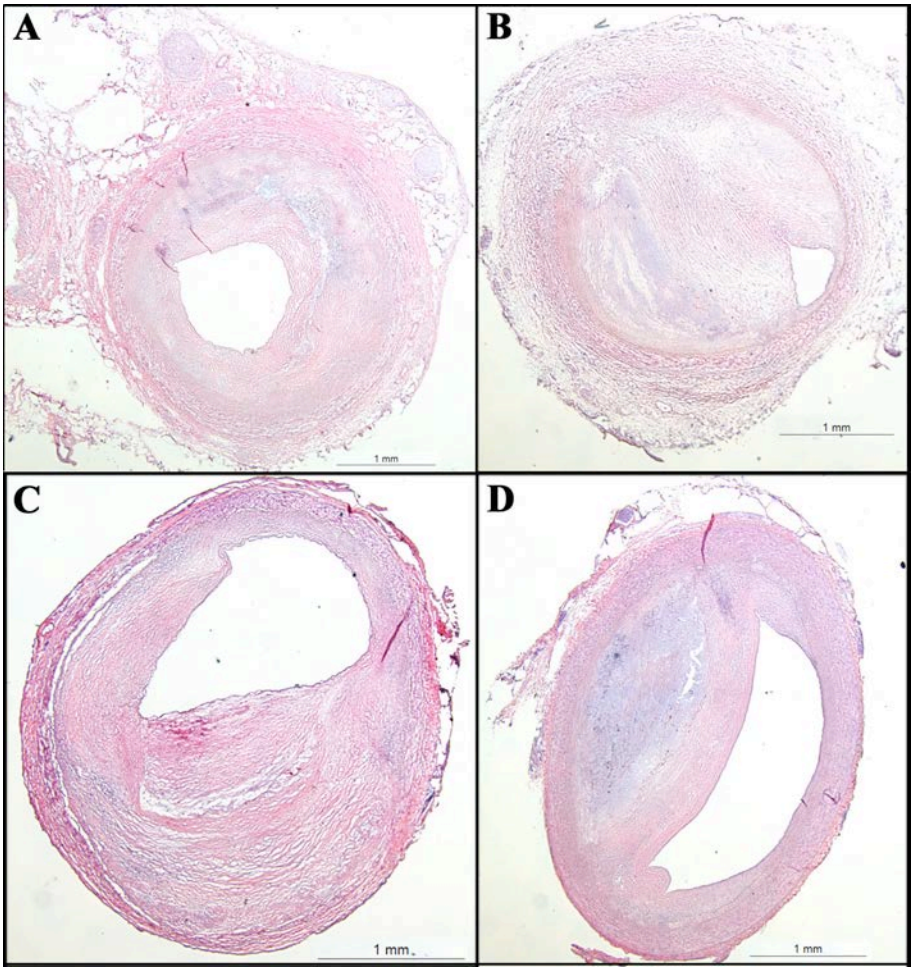

Figure 34 **Cross-sectional view of human atherosclerotic plaque specimens**

Cross-sectional image of human atherosclerotic plaques showing mostly plaques with luminal stenosis **(A, B, C)**, evaluated by the small lumen area. The plaque in **D** seemed to be in positive remodeling phase, although it is not possible to confirm without the associated adjacent segment presenting no stenosis. 1,25X Magnification.

Most of the plaque samples obtained seemed to be presenting stenosis, observed by the overall small cross-sectional areas, and the small size of the lumen areas (Fig. 34A, B, C). One plaque seemed in positive remodeling, although the overall morphology made it difficult to evaluate (Fig. 34D). The fact that the vessel area and lumen size were larger than the other specimens of plaque, and the oval morphology with asymmetrical plaque formation point out toward positive remodeling. Unfortunately, because the lumen was not pressurized or the vessel conformation and morphology not preserved by the method of fixation, it was difficult to draw any conclusion. Some plaques appeared to be fibrous (type V; Fig. 34A), two more complex (type VI; Fig. 34B, C), and one between fibrous and vulnerable (between type V and type IV; Fig. 34D).

4.3.2 αvβ3 Labeling

All of the human atherosclerotic plaque samples tested produced a certain level of αvβ3 ITOP signal. The signal was found in the neointima (Fig. 35B, D), media (Fig. 35A), as well as in the adventitia (Fig. 35A, C, E). As previously found *in vitro* on Watanabe rabbits, most of the signal was localized in the adventitia and near lumen area. Medial labeling seemed to be sparser and was associated with intense adventitia and neointima labeling (Fig. 35A, B, C). The background signal on the human samples was very weak. As seen with the Watanabe animal model, the background appeared more intense in the zone where the collagen localized. One of the plaques tested was presenting a very intense αvβ3 signal, with ITOP labeling in the adventitia, media and near lumen areas (Fig. 35A, B, C). This plaque was characterized by two necrotic cores: a healed necrotic core with another one in development (Fig. 36B), which is characteristic of type VI

plaques. Moreover, there was presence of adventitial thickening on the whole length of the cross-sectional area. Also, this plaque was extremely stenotic. Finally, on the segment of the developing necrotic core, there was intense staining around structures inside the adventitia that look like neovascularization (Fig. 36), as well as near elongated structures that resemble muscle sprouts (Fig. 36A, C). The specificity of the αvβ3 binding was confirmed with an αvβ3 antibody. The signal was co-localized, although less intense with the antibody (Fig. 37).

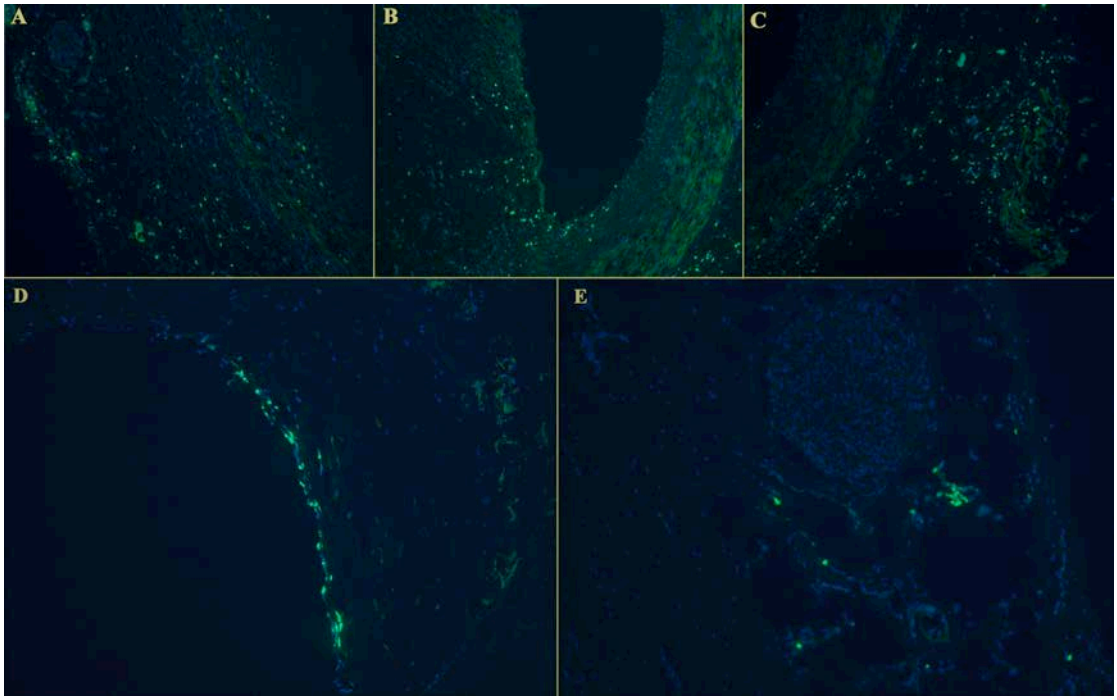

Figure 35 **Fluorescence microscopy of human coronary artery sections from tissues incubated with FITC-αvβ3 antagonist**

Image of slide exposed to FITC-αvβ3 antagonist (2.8μM) for 1 hour. All of the coronary arteries tested produced an αvβ3 signal. In the samples producing an important intensity of signal, the adventitia **(A, C)**, media **(A, C)** and neointima **(B)** were all labeled. In the samples with a weaker signal, near lumen neointima **(D)** and adventitia **(E)** both produced an αvβ3 signal. Results indicated specific plaque labeling with the fluorescent ITOP with a very small amount of autofluorescence background from tissues. 10X Magnification.

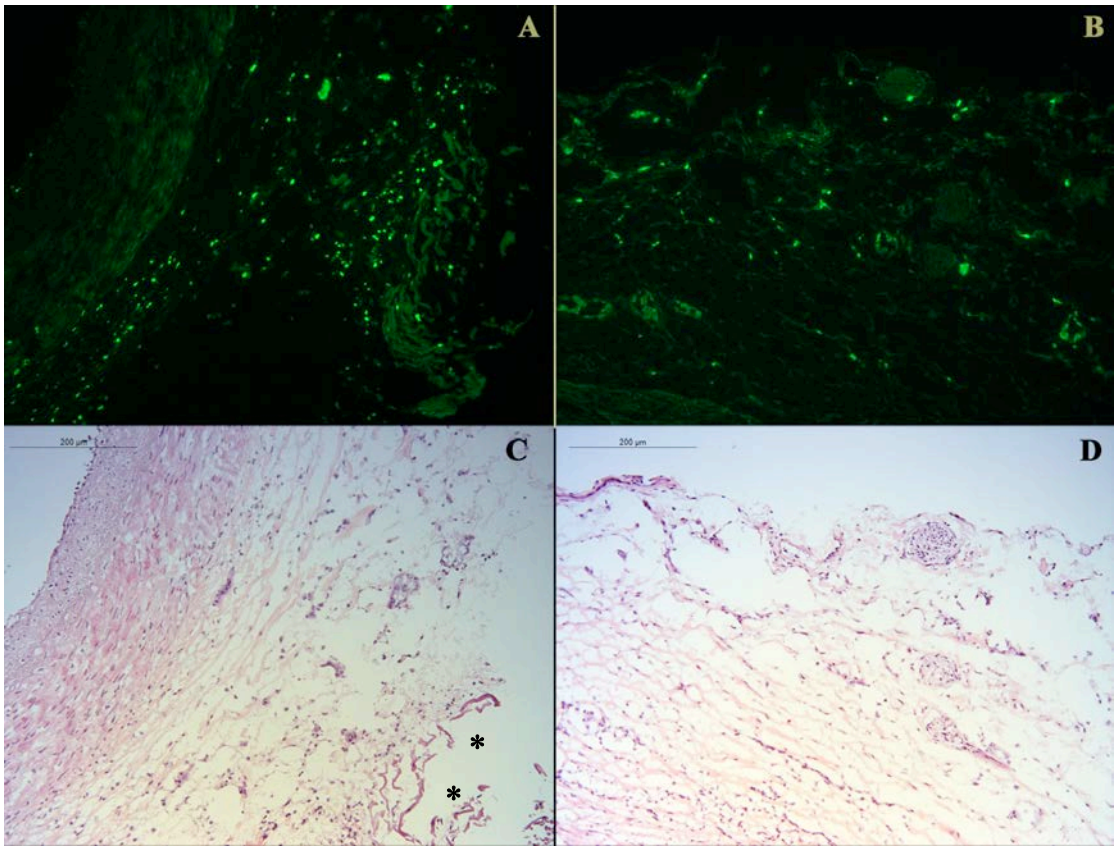

Figure 36 **Characteristics of human coronary artery section producing the most intense αvβ3 ITOP labeling**

Image of slide exposed to FITC-αvβ3 antagonist (2.8μM) for 1 hour **(upper panel)**, with correspondent H&E staining **(lower panel)**. Adventitia labeling **(A, B)** seemed to be corresponding to neovessel-like structures in H&E staining **(C, D)**. In the adventitia of the segment with developing necrotic core, there was some elongated structures **(∗)** that resemble muscle sprouts **(C)**. 10X Magnification.

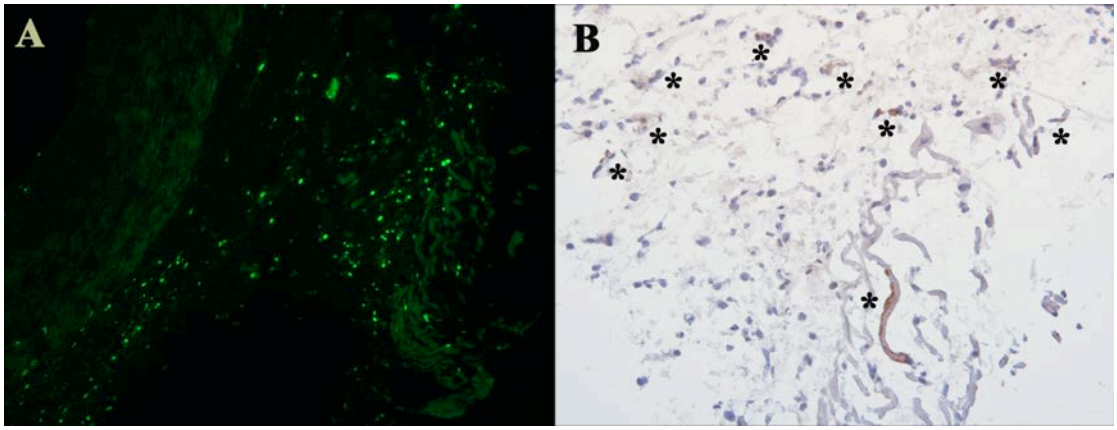

Figure 37 **Co-localization study of αvβ3 expression on human coronary artery sections labeled with αvβ3 ITOP or an αvβ3 antibody.**

(A) αvβ3 immunofluorescence and **(B)** immunohistochemistry of a human coronary artery labeled with the ITOP **(A)** and with an αvβ3 antibody **(B)**, respectively. The panel (**A)** displayed a portion of the aortic wall producing a fluorescent ITOP signal. The panel **(B)** displayed a higher magnification of the same area incubated with an αvβ3 antibody, which was necessary in order to better visualize the signal. Both the fluorescence signal **(A)** and the immunohistological labeling **(B)** were co-localized predominantly in the adventitia and proximal neointima. The ITOP signal was stronger than the antibody signal, which can be explained by the better avidity of the ITOP toward the receptor. **(A)** 10X Magnification. **(B)** 40X Magnification. The asterix (*) signs displayed the zone were there was a αvβ3 signal.

4.3.3 α-Actin Labeling

As mentioned previously, human atherosclerotic plaques are very heterogeneous. The α-actin staining for the presence of SMCs in the coronary wall was a good illustration of this complexity. All of the plaques showed α-actin staining in the media and neointima area, but with different intensity. For example, some plaque demonstrated an important α-

actin staining in the medial layers, but a weak and sparse staining in the neointima layers (Fig. 38A, B), which typically characterized fibrous plaques (type V) or vulnerable plaques (type IV). As opposed to that, other plaques showed less staining in the medial layers with some discontinuities, associated with a more important neointima staining (Fig. 38C, D), which is often present in healed plaques (type VI).

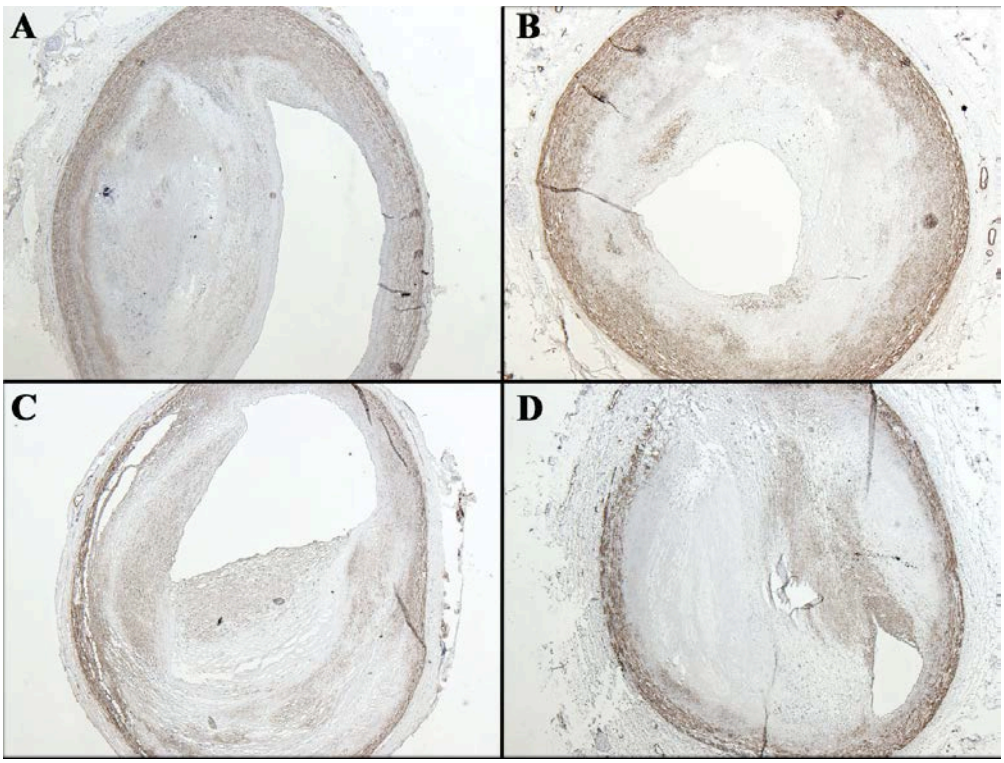

Figure 38 **α-actin labeling on human coronary artery sections demonstrating the presence of SMCs**

α-actin labeling showing SMCs presence in the media and neointima of the coronary wall. Some samples showed strong medial labeling of SMCs, associated with weak and sparse neointima labeling **(A, B)**, while other samples showed weak and discontinuous medial labeling, associated with strong neointimal labeling **(C, D)**. Strong medial α-actin labeling could be associated with young **(A)** or healed **(B)** plaques, while strong neointimal labeling could represent healed plaques or more complex type of plaques **(C, D)**. 2,5X Magnification.

4.3.4 MMP-9 Labeling

MMP-9 expression on the coronary wall of the human samples was dispersed throughout the entire cross-sectional areas (Fig. 39). Indeed, the MMP-9 signal appeared in the neointima, media, and adventitia of the plaques. Despite some variability among the samples, MMP-9 expression seemed relatively comparable in all the samples. Since the antibody used to label MMP-9 recognized both active and inactive forms, MMP-9 presence did not necessary predicted MMP-9 activity in the samples. The background signal seemed to be more important in the neointima layer than in other parts, maybe because of the presence of collagen and elastic fibers inside the neointima.

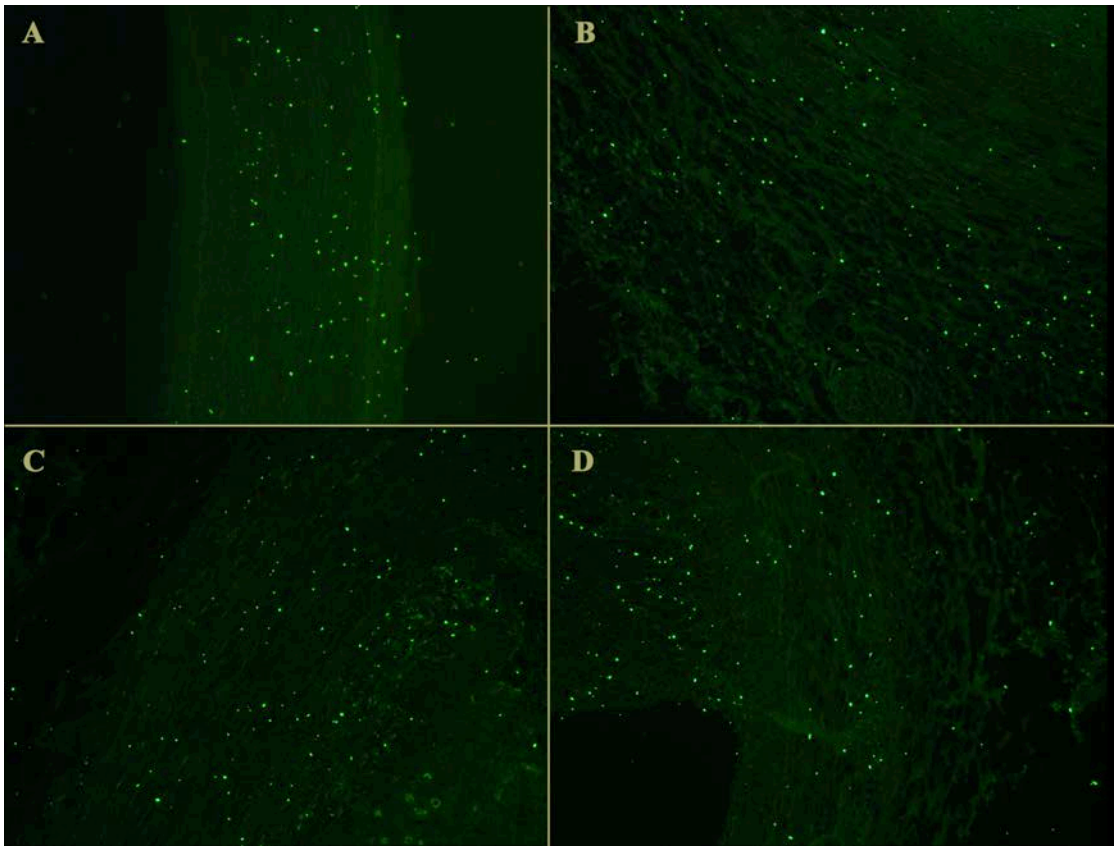

Figure 39 **MMP-9 expression on human coronary arteries**

Sections of left anterior descending coronary arteries showing MMP-9 expression. In the atherosclerotic plaques tested, MMP-9 expression was dispersed throughout the neointima, media and adventitia layer. Magnification 10X.

4.3.5 Macrophages Labeling (CD68)

In atherosclerosis, macrophages are often localized in the neointima, at the shoulder areas of the plaques. Surprisingly, even if the human plaque tested were complexes, CD68 labeling revealed very few positive cells (Fig. 40). Most of CD68+ cells were found in the neointima of the plaques, around the necrotic core areas and shoulders (Fig. 40A, B), although that in the plaque with the most important αvβ3 labeling, there was also presence of CD68 labeling in the adventitia layer (Fig. 40C, D).

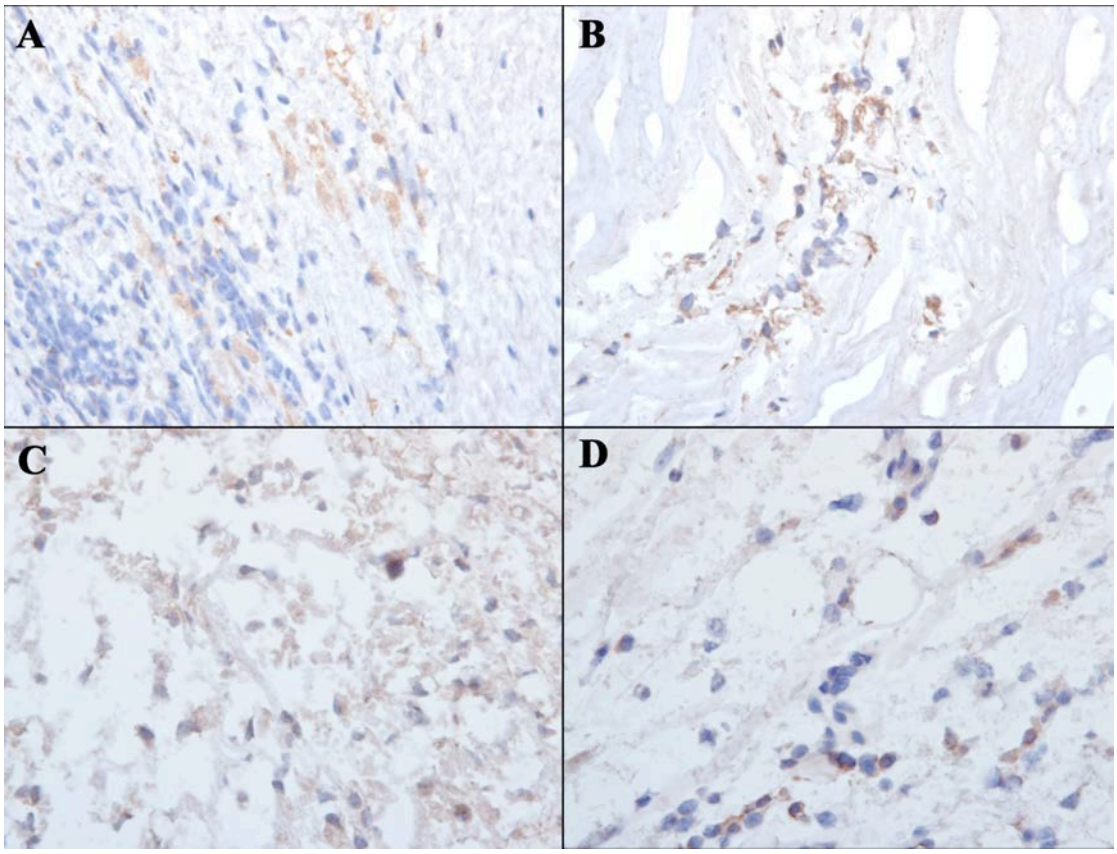

Figure 40 **CD68 expression on human coronary artery sections demonstrating the presence of macrophages in the plaques**

CD68 labeling showing the presence of macrophages in the neointima **(A, B)** and adventitia **(C, D)** of the plaques. In the human plaques tested, most of the labeling was found in the neointima, although the plaque with important αvβ3 labeling showed presence of CD68+ cells in the adventitia. 40X Magnification.

4.3.6 T-Cell/B-Cells Labeling (CD40)

In atherosclerotic plaque formation, there is a very sophisticated mechanism of cross-talking between inflammatory cells like macrophages and T-cells. Immunofluorescence labeling of CD40, a receptor present at the surface of T-cells and B-cells, revealed the presence of inflammatory infiltration in all of the plaques tested (Fig. 41). CD40 expression was relatively important, especially in the neointima of the plaques (Fig. 41A, B, C). As seen previously with macrophage expression, the plaque with an important αvβ3 labeling also presented CD40 expression in the adventitia layer.

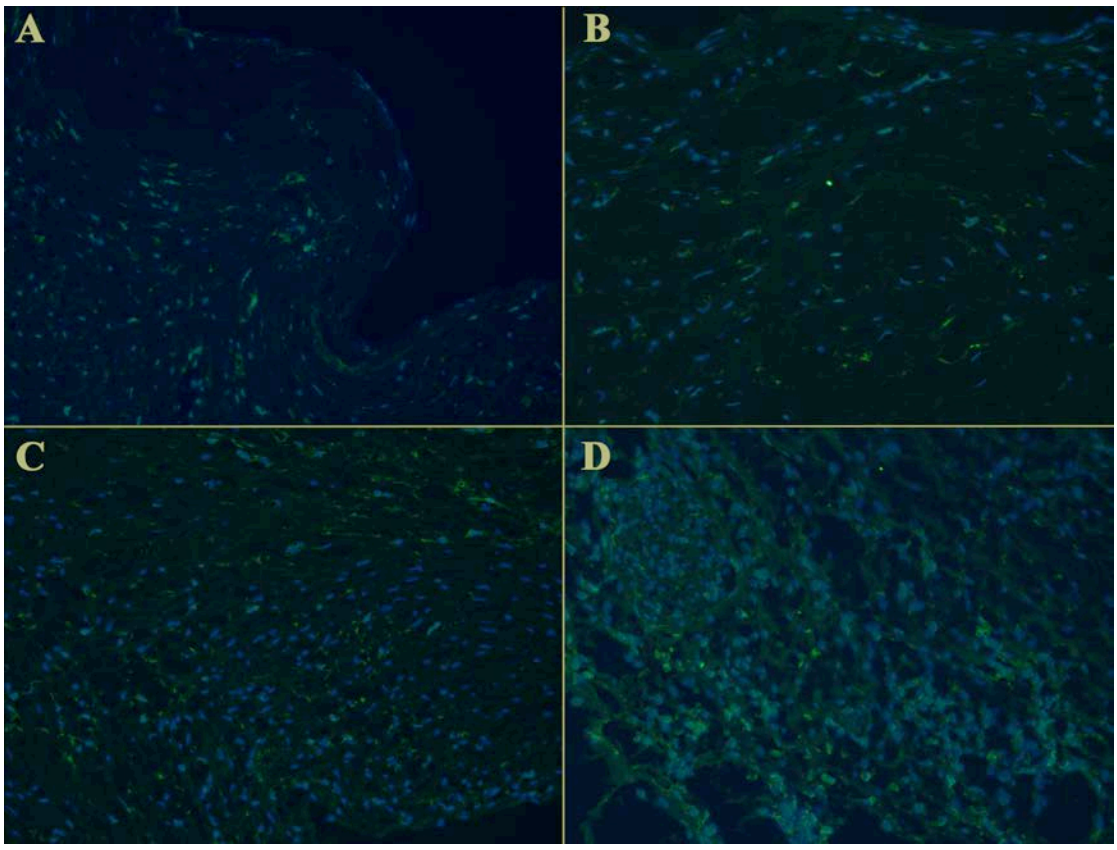

Figure 41 **CD40 expression on human coronary artery sections demonstrating the presence of lymphocyte T**

CD40 labeling in the coronary wall demonstrated the presence of T-cells or B cells mostly in the neointima of the plaques **(A, B, C)**, with associated adventitial expression **(D)** for the plaque with the most important αvβ3 signal. 20X Magnification.

4.3.7 Elastic Fibers - Verhoeff's Van Gieson (EVG) Staining

In coronary arteries, there are two important elastic fiber membranes that confer arteries their elastic properties: the internal elastic lamina (IEL) and the external elastic lamina (EEL). EVG staining of the coronary plaques revealed that on the plaques with a thicker adventitia, the IELs were almost disappearing (Fig. 42A, C, D), while in the plaques with smaller adventitia, it were still present, but contained numerous discontinuities (Fig. 42B). On the other hand, the EELs seemed intact in samples where the adventitia appeared to have a high density of collagen and fibers (Fig. 42A, B), while almost absent from the samples where the adventitia layers had less collagen and fibers (Fig. 42C, D).

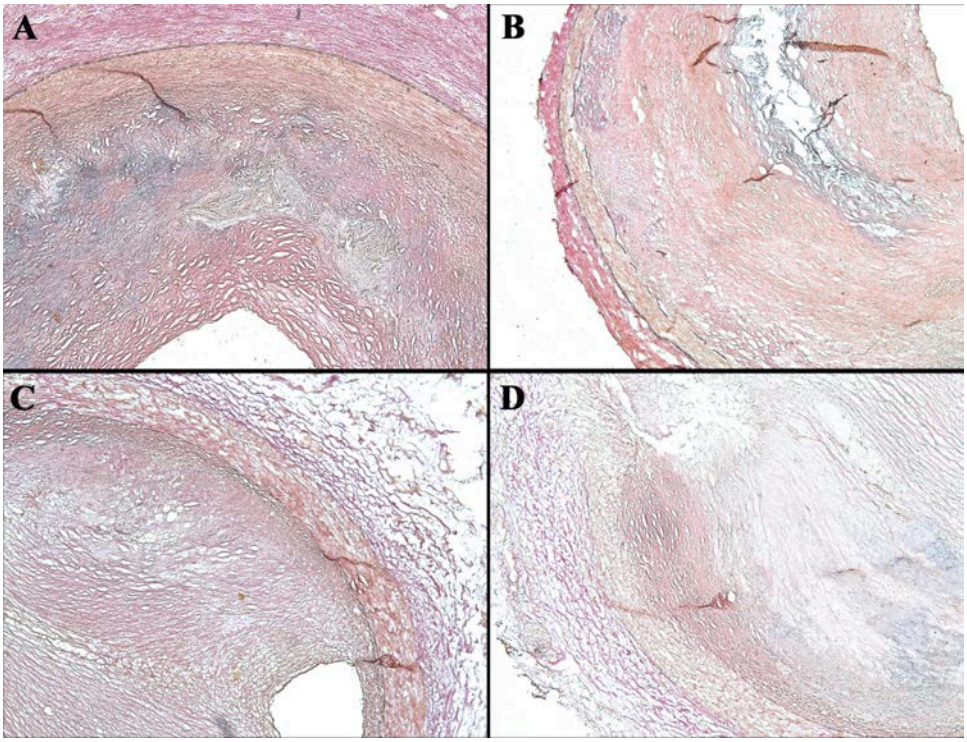

Figure 42 **Elastic tissue fibers staining of the human coronary artery plaques with elastic Van Gieson (EVG) stain**

The IELs were almost absent from samples with thick adventitia **(A, C, D)**, while it was present, but contained discontinuities, in samples with smaller adventitia **(B)**. The EELs were intact in samples with dense content of adventitial fibers and collagen **(A, B)**, while it were absent from the samples with sparse content of adventitial fibers and collagen **(C, D)**. Black: elastic fibers. Magnification 5X.

4.3.8 Masson Trichrome Staining

The collagen content in atherosclerotic plaques is another feature that confer the physicoproperties to the wall and can give information on plaque stability. Some of the tested plaques presented absence of staining in the necrotic core area, demonstrating loss of collagen into the neointimal regions (Fig. 43A, B). This is typical of late cores, with numerous cholesterol clefts, cellular debris and an absence of ECM, particularly collagen, as opposed as early cores, which show collagen interspersed with intact foamy macrophages. One plaque tested seemed to have the characteristics of an early core (Fig. 43C, D), but surprisingly showed the most cross-sectional degree of stenosis. This could be explained by the fact that this plaque possessed two different necrotic cores: one that had been healed, and another one superimposed. Plaques with late cores seemed to have higher collagen content in the neointima (Fig. 43A, B) than the plaque with and early core (Fig. 43C, D), and also possessed a denser collagen content in the adventitia layers. In the late cores, the media layers were intact, as opposed as the early core, where the media layer seemed to be disorganized with an absence of SMCs in some parts (Fig. 43D) of the wall. In the plaque that produced the most αvβ3 signal, there were SMC labeling in the adventitial layer, where we found most of the αvβ3 signal (Fig. 43C, asterisk). The SMCs were arranged in elongated structures that resembled muscle sprouts. In this plaque, the collagen content appeared much more sparser than in the other plaques, with a density much more smaller in all the different layers (neointima, media, and adventitia). The late cores possessed fibrous caps that showed an important accumulation of dense collagen. As opposed to that, the plaque with the early core

showed an important formation of SMC layer in the fibrous cap, but associated with a smaller density of collagen.

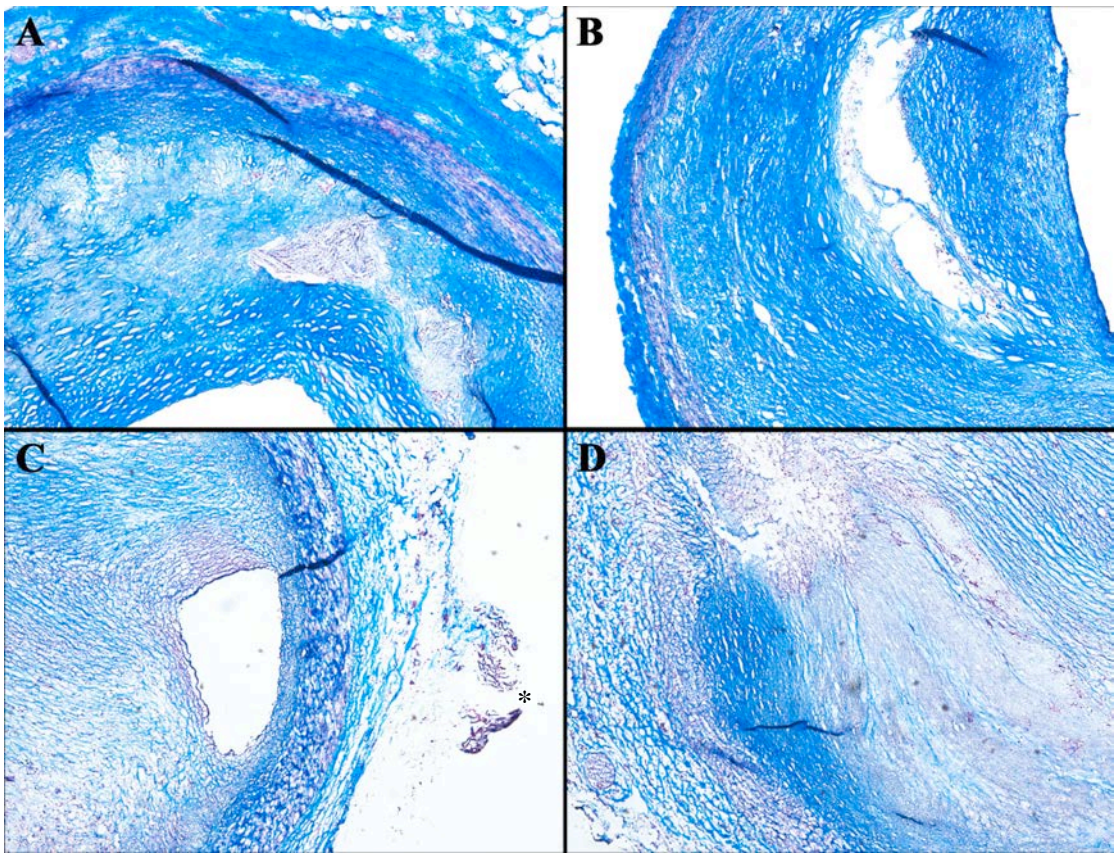

Figure 43 **Masson Trichrome staining of the human coronary arteries with plaques**

Upper panel showed typical late cores with absence of staining, with and associated high density of collagen in the vessel wall. **Lower panel** showed an example of plaque with healed core **(C)**, and another superimposed core **(D)**, with a lower density of collagen content in the vessel wall. The late core showed intact medial layer, while the other core presented some areas with absence of SMCs in the media. * SMC staining in the adventitia, resembling muscle sprouts. Blue: collagen. Red: muscle, red blood cells. Pink: cytoplasm. Black: Nuclei. 5X Magnification.

4.3.9 Labeling and Adventitia Thickness

Because of the small number of plaque tested, it was difficult to draw any conclusion on the correlation between the thickness of the adventitia and the intensity of αvβ3 labeling. Nevertheless and albeit the small sampling, the human plaques showed the same tendency than the previously published results on Watanabe rabbits. Effectively, it appeared that the area with smaller adventitia showed less intense αvβ3 ITOP labeling (Fig. 44A, B, D, E), as opposed to the area with thicker adventitia that showed more intense labeling (Fig. 44C, F). Therefore, comparison between fluorescent αvβ3 probe

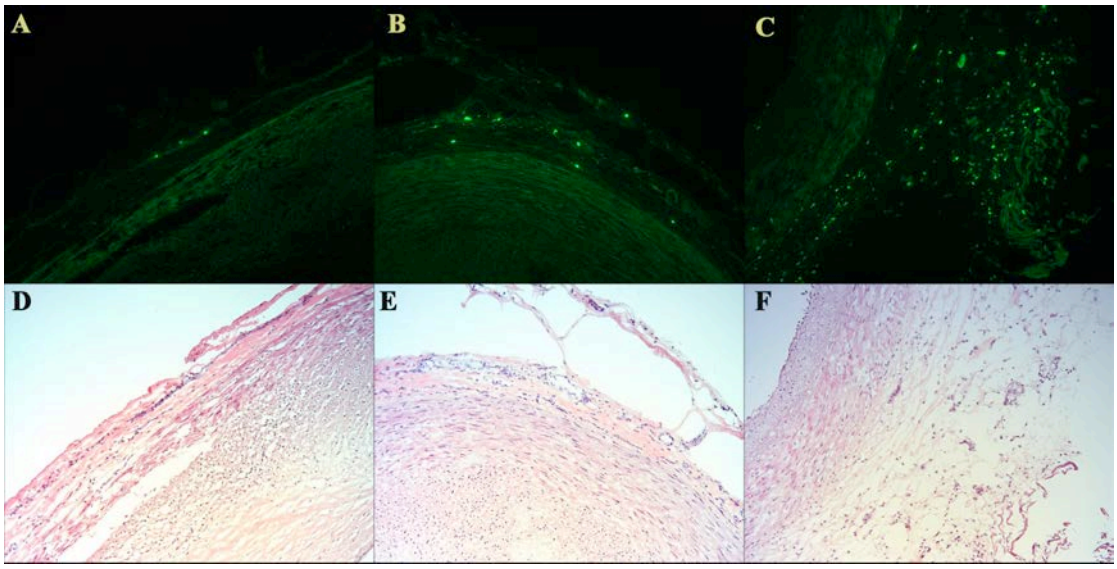

Figure 44 **Relationship between intensity of ITOP labeling and adventitia thickening**

Intensity of fluorescence staining in human coronary sections **(A, B, C)** correlated with adventitia thickness and plaque histology **(D, E, F)**. In sections with smaller adventitia **(D, E)**, the level of staining with the αvβ3 targeted probe was weaker **(A, B)**. Inversely, in sections with a larger adventitia **(F)**, the αvβ3 signal was more intense **(C)**. There was also some correlation between the intensity of labeling and the organization level into the plaque: staining was more intense in plaque with disrupted media **(C)** and less intense when the media was well delineated **(A, B)**. 10X Magnification.

signal (Fig. 44, upper panel) and H&E staining of the corresponding coronary artery (Fig. 44, lower panel) showed the same qualitative correlation between the intensity of signal and the adventitial thickening. Moreover, as also seen previously in the Watanabe rabbit model, there were an association between the intensity of labeling and the plaque morphology. Indeed, plaques with intact medial layers showed less intense labeling (Fig. 44A, B, D, E) than plaques with discontinuous and disorganized medial layers (Fig. 44C, F).

4.4 DISCUSSION

In the previous chapters, we tested a new αvβ3 ITOP on a Watanabe rabbit model, both *in vitro* and *in vivo*. We showed that it efficiently labeled atherosclerotic plaques with high affinity, although there was some background signal from the *in vivo* injection. We also showed that the signal was mostly found in the adventitia and neointima layers, although there was also signal from the media in samples with intense signal. We also found that the intensity of αvβ3 ITOP signal seemed to correlate with the degree of adventitial thickening, as well as the level of organization of the media and collagen content in the media[119].

The goal of this chapter was mostly to show that our αvβ3 ITOP could also labeled efficiently human atherosclerotic plaques *in vitro*. Since we had a very limited amount of samples, we do not had the ambition to elucidate the mechanism of ITOP labeling in regard to the type of plaque. In this regard, our conclusions will be draw only for

discussion purpose, and the markers used in conjunction with the ITOP probe, only served to better characterized the samples tested. We kept in mind that a more extensive sampling will be needed to collaborate any conclusions.

Most of the plaque samples obtained seemed to be in negative remodeling phase or stenosed, observed by the overall small cross-sectional areas, and the small size of the lumen areas (Fig. 34). Unfortunately, because the lumen was not pressurized or the vessel conformation and morphology not preserved by the method of fixation, it was difficult to draw any conclusion. In the other hand, the negative remodeling/stenotic stage could explain the fact that none of the tested human atherosclerotic plaques had ruptured, since vulnerable plaques are most likely characterized by positive remodeling[14, 16], and the degree of stenosis appears to be a poor predictor of cardiovascular event[22, 125]. Only one of the plaque tested appeared to be in positive remodeling phase, with minimal cross-sectional stenosis. This plaque showed minimal αvβ3 ITOP labeling, with signal localized in neointima and adventitia. This observation seemed to correlate with the expression of vasa vasorum (vv) in plaque with low-grade stenosis and positive remodeling[126, 127]. As opposed to this plaque, the plaque with the most intense signal (neointima, media and adventitia) appeared severely stenosed, and possessed two different necrotic core areas: one healed and one superimposed. This intense labeling can be linked to the fact that in this particular plaque, there were two mechanisms responsible for the apparition of neovascularization: ischemia and hypoxia. Indeed, lumen stenosis produce by the healed necrotic core contributes to tissue ischemia[128, 129], in the same way inflammatory processes produced hypoxia[75, 130]. As mentioned before, those two

mechanisms are associated with neovascularization[131, 132], which might explain the intensity of the αvβ3 ITOP labeling in this plaque.

Another characteristic of the plaque with the most important αvβ3 signal was the presence of adventitial elongated structures resembling muscle sprouts. Those structures were localized in the same adventitial region where an intense αvβ3 ITOP signal was found. Previous reports have shown that before the formation of neovessels, activated SMCs will sprout and form elongated structure, a phenomenon preceding the formation and organization of new vessels into a circular lumen[44, 133]. We could postulate that the intense αvβ3 labeling on the adventitia, among the elongated structures, represented activated SMCs that will further become neovessels.

All of the plaques tested showed MMP-9 expression in the entire coronary wall, macrophage infiltration, and CD40 expression at some level of intensity. Those inflammatory features point out toward the presence of hypoxia[134, 135], an important stimulus for the formation of neovascularization[121, 136, 137], but also stenosis. Unfortunately, because of the small sampling, it was difficult to draw some conclusion. Nevertheless, it could be mentioned that the plaque with the most αvβ3 labeling, also demonstrated the most T-cells labeling. T-cells are important in plaque formation, because of their crosstalk with macrophages and other immune cells in the plaque[138-140] and are also involved in remodeling[141, 142] and neovascularization[143, 144], which can lead to stenosis and plaque healing.

Finally, as demonstrated previously with the Watanabe rabbit model, preliminary results on the human plaques also seemed to point out toward a relationship between the intensity of labeling and the thickness of the adventitial layer. Effectively, some other

studies reported that angiogenesis[145] and inflammatory mechanisms involved the development of the adventitia into a thicker layer[146]. Although we had a very limited amount of samples, we did see a qualitative correlation between the intensity of the signal and the adventitial thickening. Results showed a tendency to have more important level of signal in areas of adventitial thickening, as seen in the Watanabe rabbit model. This also seemed to be correlated with the degree of organization into the plaques. In the Watanabe rabbit model, the media of the samples presenting important staining was often discontinuous or disorganized. In the human samples, the plaque showing the most important αvβ3 labeling also showed and absence of medial layer in some areas, and a collagen content less important than in plaques with weaker αvβ3 labeling, but also an important fibrous cap formation (thick layer of neointimal SMCs). This could be explained by the fact that plaque formation involves the migration of SMCs and remodeling of the vessel wall[147]. That phenomenon can be associated with a disorganization of the medial layer and a smaller density of collagen fiber to allow migration and matrix remodeling. In conjunction with the Watanabe rabbit results, it also seemed to point out toward the fact that healed plaques (where necrotic core has been replaced by fibrous tissues and the SMCs layer is disorganized) seemed to be characterized by an intense αvβ3 labeling. This is in contradiction with previous studies correlating neovascularization with plaque instability.

The principal limitation of this study was the small number of samples. Although it has been possible to form some hypothesis, a larger sampling will be needed for the confirmation of our finding. It would also been interesting to verify the labeling efficiency of our probe on other models of diseases. Effectively, to understand the

mechanism of plaque formation or neovascularization, it is crucial to use other pathological models that behave differently. For example, AD-HIES patient has been reported to have a paucity of atherosclerosis[100, 101], as opposed to HIV patients that seem to develop accelerated atherosclerosis[148, 149]. It would be interesting to investigate the comportment of our probe on those patients and compare it with our previous results.

CHAPTER 4

IN VITRO ITOP LABELING ON AD-HIES SAMPLES WITH MOLECULAR CHARACTERIZATON

5.1 INTRODUCTION

Because of the rarity of this disease, it is extremely fortunate that we had access to autopsy samples from an AD-HIES patient. Consequently, because of the novelty and scientific importance of any discovery, this chapter will be more developed and discussed.

AD-HIES disease or autosomal dominant hyper-IgE syndrome (AD-HIES) is a rare primary immunodeficiency caused by a dominant negative mutation in STAT3[97, 98]. It is characterized by various clinical manifestations such as high serum level of IgE, recurrent infections, eczematous dermatitis, and connective tissue abnormalities[99]. Most of the extracellular bacterial infections in hyper IgE patient are caused by Staphylococcus Aureus bacteria and are characterized by milder inflammation than in normal population. Another important clinical aspect of this disease is the presence of connective tissue abnormalities and hyperextensibility. Recent studies had described an unset of vascular abnormalities in hyper-IgE patients, characterized by the presence of tortuosity, arterial aneurysms, and ectasia, despite the uncommon presence of atherosclerosis, indicated by luminal stenosis[100, 101]. These interesting characteristics make AD-HIES an extremely attractive model for the study of atherosclerotic processes. Therefore, we used

histological, immunohistological and immunofluorescence studies to identify coronary physiological features and molecular markers in an AD-HIES case.

5.2 MATERIALS AND METHODS

5.2.1 Experimental Design

We took autopsy specimens of different segments of the coronary arteries (right n=2, left anterior descending n=2, left circumflex n=2, left main at bifurcation point n=2) from an AD-HIES case. Coronary artery specimens were obtained less than 24 hours after death and the samples were immediately processed. Briefly, 1 sample from each of the right, left anterior descending, left circumflex, and left main at the bifurcation point were dissected from the heart and keep on ice. 2 segments of each coronary artery (about 0.5mm) were taken out, embedded in Optimal Cutting Temperature (OCT) medium and stored at -80°C. The remaining tissues were put in a bag and stored at -80°C. We carried out immunohistology staining, immunohistofluorescence and immunohistochemistry on frozen tissue sections from the biopsy tissues.

5.2.2 Histology and Immunohistology

OCT blocks from snap frozen coronary arteries (right, left anterior descending, left circumflex, left main at bifurcation point) were cut into 7-8 μm sections with a cryostat and mounted onto slides. Routine hematoxylin and eosin (H&E) straining was performed on the frozen sections. Routine elastic fiber staining was performed with elastic tissue fibers – Verhoeff's Van Gieson (EVG) staining. Briefly, samples were fixed with 4%

paraformaldehyde, and then incubated with Verhoeff's hematoxylin for 30 minutes. After being washed with water, samples were differentiated with 2% ferric chloride solution, rinsed in water again, and then incubated 1 minute with 5% Hypo to remove iodine. Finally, samples were washed in water, counterstained in Van Gieson's for 5 minutes, dehydrated, cleared in xylene and coverslip. For collagen staining, we used Masson Trichrome. Briefly, frozen samples were fixed with Bouin's solution, washed, and incubated with Weigert's iron hematoxylin for 10 minutes. After being rinse in tap water and washed in distilled water, samples were stained with Biebrich scarlet-acid fuchsine for 10-15 minutes, and washed again. Samples were then differentiated in phosphomolybdic-phosphotungstic acid solution for 10-15 minutes, transferred directly to aniline blue solution for 5-10 minutes, rinse briefly, and differentiated in 1% acetic acid solution for 2-5 minutes. Finally, sections were washed in distilled water, quickly dehydrated through 95% ethyl alcohol, absolute ethyl alcohol, clear in xylene and mount using resinous mounting medium. Special Movat staining was also used. Briefly, frozen samples were fixed in Bouin's, rinsed in cold running water for 10 minutes, incubated in Sodium Thiosulfate for 5 minutes, and washed again under cold running water. Samples were then stained in 1% Alcian Blue for 20 minutes, and rinsed under cold running water again. Samples were then placed in preheated Alkaline Alcohol for 10 minutes in the oven, and rinsed in cold running water. Then, samples were placed in Movat's Weigerts for 1 hour, washed in cold running water and rinsed with distilled water, and placed in Crocein Scarlet/Acid Fuchsine for 1 minute. After a rinse in distilled water, samples were placed 5% Phosphotungstic Acid for 5 minutes, transferred to 1% Acetic Acid for 5 minutes, and rinsed again in distilled water. Finally, samples were dehydrated in 1 change

95% ETOH, 2 changes of 100% ETOH, put in Alcoholic Saffron for 20 minutes, rinsed with 2 changes of 100% ETOH, cleared with xylene, and mount. For immunohistochemistry, an antibody against human α-actin (ab7817, Abcam, USA), and an antibody against CD-68 (ab955, Abcam, USA), were used, at a dilution 1/200 (PBS), to confirm the presence of α-actin and macrophages respectively. Those antibodies were used in conjunction with an anti-mouse horseradish peroxidase detection kit, according to the specifications of the company (Chemicon International, Inc, Temecula, CA, USA). For immunohistofluorescence, an antibody against human MMP-9 (ab58803, Abcam, USA), and an antibody against CD-40 (ab61401, Abcam, USA), were used, at a dilution 1/100 (PBS). Those antibodies were used in conjunction with an anti-mouse secondary antibody conjugated to FITC, at a dilution of 1/500 (ab6785, Abcam, USA). Expression of αvβ3 integrin in the aortic wall was assessed by immunohistofluorescence with our new αvb3 integrin targeted optical probe (ITOP). Sections were thawed for 15 minutes at room temperature, fixed 10 minutes with cold acetone, washed in phosphate buffer solution and then incubated with the targeted fluorescent probe for 1 hour. After the incubation period, the slides were washed again in phosphate buffer solution, and mounted with VECTASHIELD mounting medium containing DAPI (Vector Laboratories, Inc., Burlingame, CA). An antibody against human αvβ3, anti-human integrin αvβ3, clone LM609 (Chemicon International, Inc, Temecula, CA, USA), was used to confirm the presence of the integrin and as a reference for the localization of any experimental fluorescent signal. This antibody was used in conjunction with an anti-mouse horseradish peroxidase detection kit, according to the specifications of the company (Chemicon International, Inc, Temecula, CA, USA). Images of staining or

fluorescence signal were acquired under a microscope (Leica DM5500B with a Leica DFC-500 color camera) using a visible or ultraviolet light source, respectively. For the ITOP (FITC labeling), the emission wavelength was set up at 495nm, while absorption wavelength at 521nm.

5.2.3 Measurements and Definitions

Quantification of each cross-sectional section was made under non-pressurized condition. Measurements were made of lumen area (Lu_{area}, mm^2), neointimal area or plaque area (Pla_{area}, mm^2 = IELarea - Lu_{area}), medial area (Me_{area}, mm^2 = EEL_{area}- IEL_{area}), adventitial area (Ad_{area}, mm^2), internal elastic lamina area (IEL_{area} = Lu_{area} + Pla_{area}, mm^2), external elastic lamina (EEL_{area} = Me_{area} + Pla_{area} + Lu_{area}, mm^2), necrotic core area (NC_{area}, mm^2), cap thickness (Cap_{thick}: measured at the location of thin cap, μm). Cross-sectional degree of stenosis, according to Glagov, was calculated as 100 X Pla_{area} / IEL_{area}. Luminal percentage of stenosis was calculated as 100 X [(Lu_{area} at reference site – minimum Lu_{area}) / (Lu_{area} at reference site)], where lumen area at reference site is an adjacent segment of the same coronary artery judged to be free of plaque. Plaque burden was calculated as 100 X (Pla_{area} + Me_{area})/ EEL_{area}. Eccentricity index is calculated as 360° X (plaque free arc angle / total vessel circumference). Remodeling index (RI) was calculated as vessel area (EEL_{area}) at minimum lumen area / reference vessel area.

5.3 RESULTS

5.3.1 Histological Characterization of the Coronary Wall

Apart from the left main artery at the bifurcation point, the AD-HIES case revealed intimal thickening in all the region of the coronary artery (right, left anterior descending, left circumflex) without apparent lipid pool or necrotic core presence (Fig. 45). The

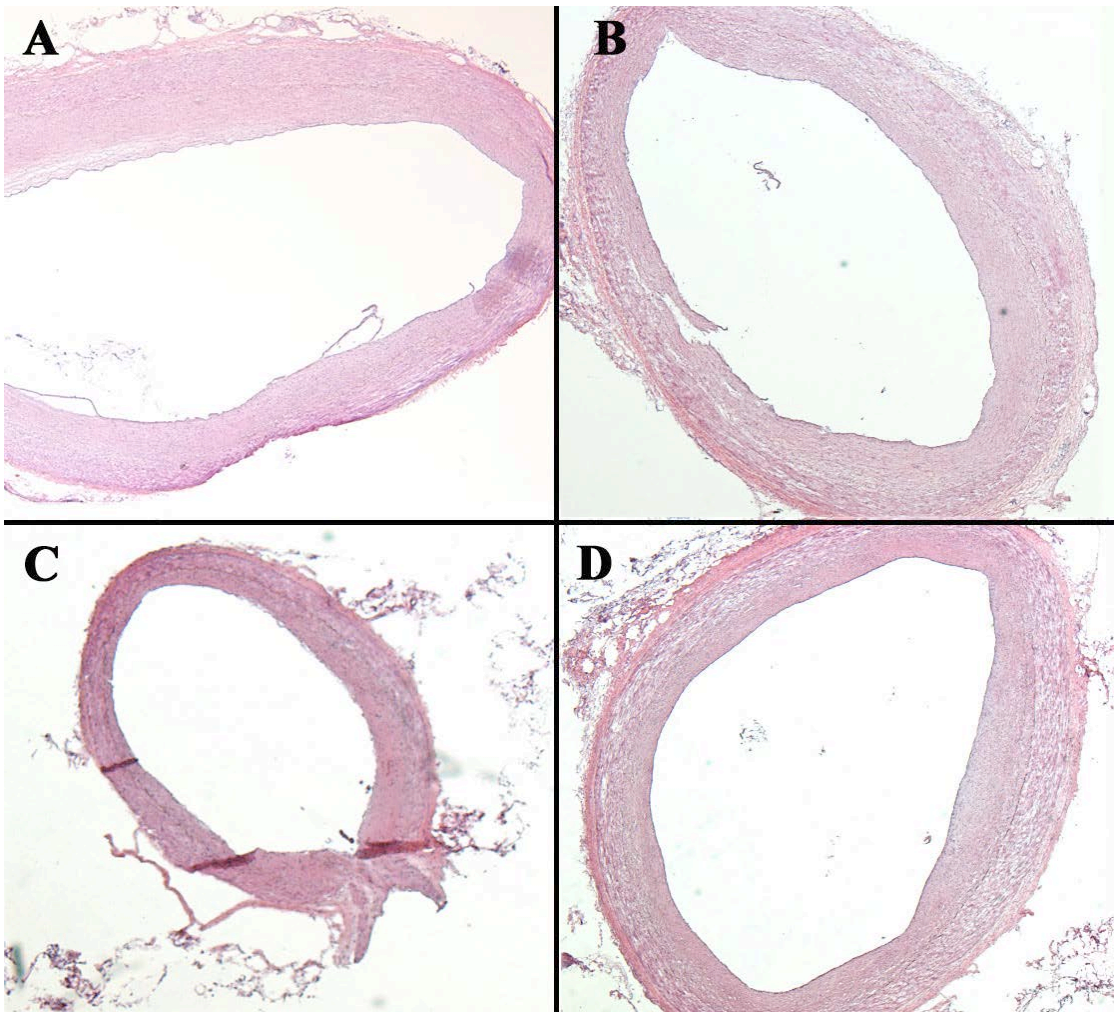

Figure 45 **H&E staining of the AD-HIES coronary arteries**

Section of the left anterior descending **(A),** right **(B)**, left circumflex (**C)**, and left main at the bifurcation point **(D),** coronary artery. 2,5X magnification. The vessels appeared to be generally dilated, as they show a mean vessel size of approximately 12 mm^2, even at pressure zero.

intimal thickening of the vessel mainly consisted of smooth muscle cells (SMCs) in a matrix of proteoglycan, similar to adaptive intimal thickening appearing with age. The AD-HIES case presented a generalized dilation of the vessels' wall without plaque, as shown by the large vessel area even at no pressure (mean 12mm^2, Fig. 45). Pathological examination of the AD-HIES coronary tissues showed an atherosclerotic plaque at the bifurcation point of the left main coronary artery, which was very unusual, and presented all the features of an advanced lesion, but without associated luminal narrowing or very mild stenosis (Fig. 46A, B). It was characterized by compensatory enlargement of the vessel size, or positive remodeling (Fig. 46), compared to the atherosclerotic samples presenting late CAD and stenosis. Interestingly, using Glagov calculation, the cross-sectional degree of stenosis was evaluated to 60%, stage at which the vessel is known to be passed the compensatory luminal enlargement phenomenon, and should be presenting important stenosis. On the other hand, the luminal stenosis, calculated with an adjacent reference segment free of plaque, is evaluated to be around 3% (Table 3), which is considered to be very mild. Effectively, at the plaque site, the lumen appeared similar in size to the reference site, with only minimal stenosis. Notably, morphological evaluation of the plaque seemed to correlate strongly with vulnerability. First, the vessel's localized dilation exceeded 1.3 times the diameter of the adjacent normal segment (Fig. 46A, B), with a remodeling index of 1.63 (Table 3), which correspond to positive remodeling (RI>1.05), and a plaque burden of 68%. There was a large necrotic core area representing 66% of the plaque area (Table 3 and Fig. 46B, C, D), and presenting an important thickness (~650μm). The necrotic core was composed by lipids and small cholesterol clefts (Fig. 46D), microcalcifications (Fig. 46E), and small

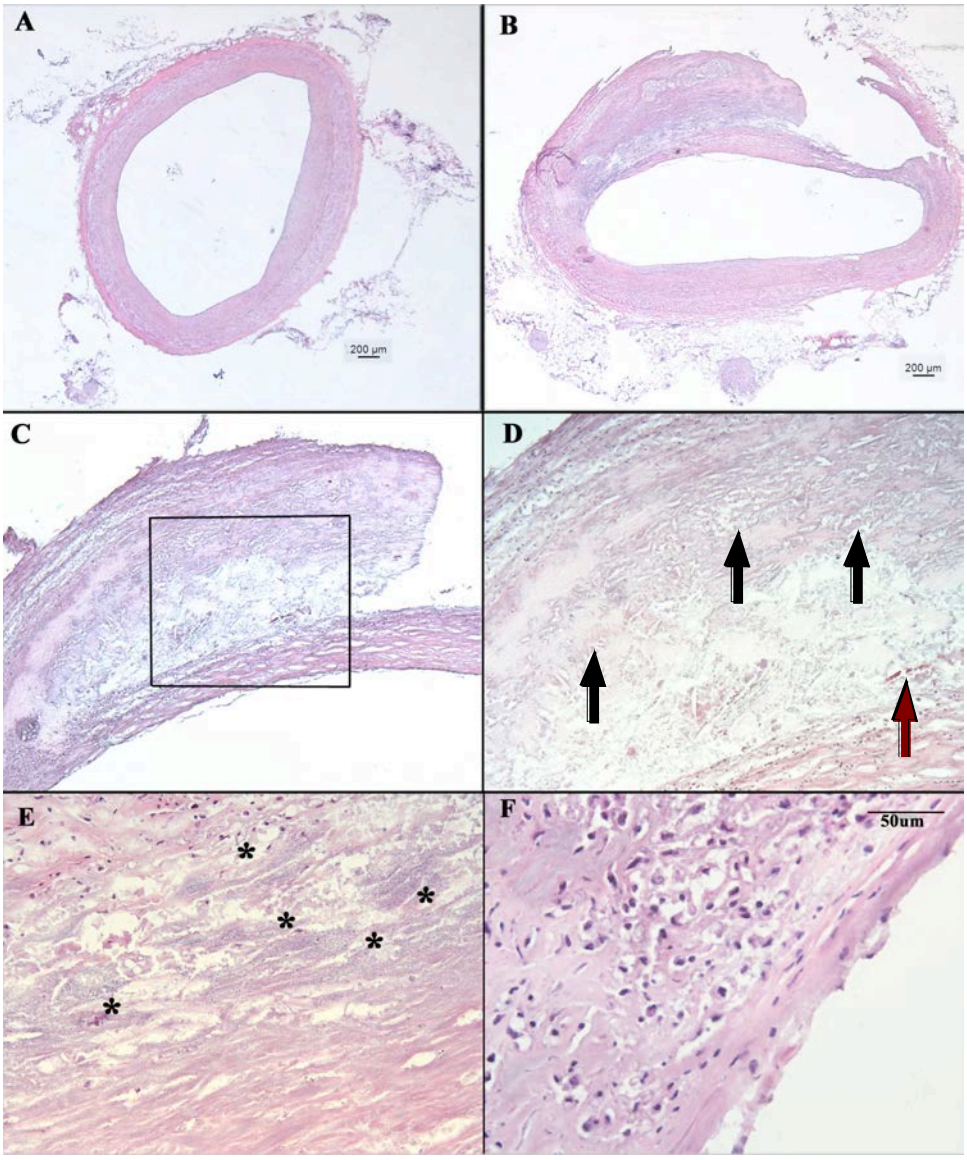

Figure 46 **H&E staining of the AD-HIES left main coronary artery at the bifurcation point**

Section of the left main coronary artery representing the reference site **(A)** and another adjacent section showing characteristic outward plaque accumulation **(B)**, taken at 1.25X magnification. (**C), (D), (E), and (F)** are higher magnifications of the left main coronary artery with plaque shown in (**B)**: 5X, 10X, 20X, and 40X respectively. Boxed area in **(C)**: region that is magnified 2X in (**D)**. **(C)** Region with plaque showing an important necrotic core area, lipid pool, and cholesterol clefts. **(D)** Image showing 10X magnification of the plaque area, with cholesterol clefts (black arrow) and also intraplaque hemorrhage (red arrow). **(E)** 20X magnification showing extensive microcalcifications in the plaque. **(F)** 40X magnification of the shoulder region showing the thin fibrous cap, which appears to be smaller than 45µm. Red Arrow: red blood cells. Black arrow: cholesterol clefts. *: Region of microcalcifications.

hemorrhages (Fig. 46D), with an absence of collagen, a characteristic of late core. The cap thickness at the shoulder area was very thin, estimated to be less than 45μm (Table 3 and Fig. 46C, boxed area, D), and heavily infiltrated by macrophages (Table 3). The media and adventitia layers appeared thinned below the atherosclerotic plaque, as opposed to the adventitia layer opposite the plaque, that showed a beginning of thickening (Fig. 46B).

TABLE 3 Left Main Coronary Artery Measurements at the plaque site

Morphological Indexes	Value
LS (%)	**2.7%**
Cross-sectional DS (%)	**60%**
PB (%)	**68%**
NC (%)	**66%**
NCT (μm)	**~650μm**
CT (μm)	**<45μm**
RI	**1,63**
EI (°)	**176º**
Macrophages count by High Power Field	**~40**

Table 3 **Morphological indexes of the AD-HIES left main coronary artery at the bifurcation point**

LS: luminal stenosis. DS: degree of stenosis. PL: plaque burden. NC: necrotic core area. NCT: necrotic core thickness. CT: cap thickness. RI: Remodeling Index. EI: eccentricity index

5.3.2 αvβ3 Labeling

Neovascularization has been reported to play a role in plaque instability and vulnerability[11, 79] as well as in the aneurysm formation[150]. Expression of αvb3 was evaluated with an integrin targeted optical probe, which we previously published[119], and confirmed with an antibody against αvb3. The AD-HIES case presented a paucity of αvb3 expression in the asymptomatic vessel wall (samples without plaque) (Fig. 47 B, C), associated with a low level of expression when there is a beginning of adventitial

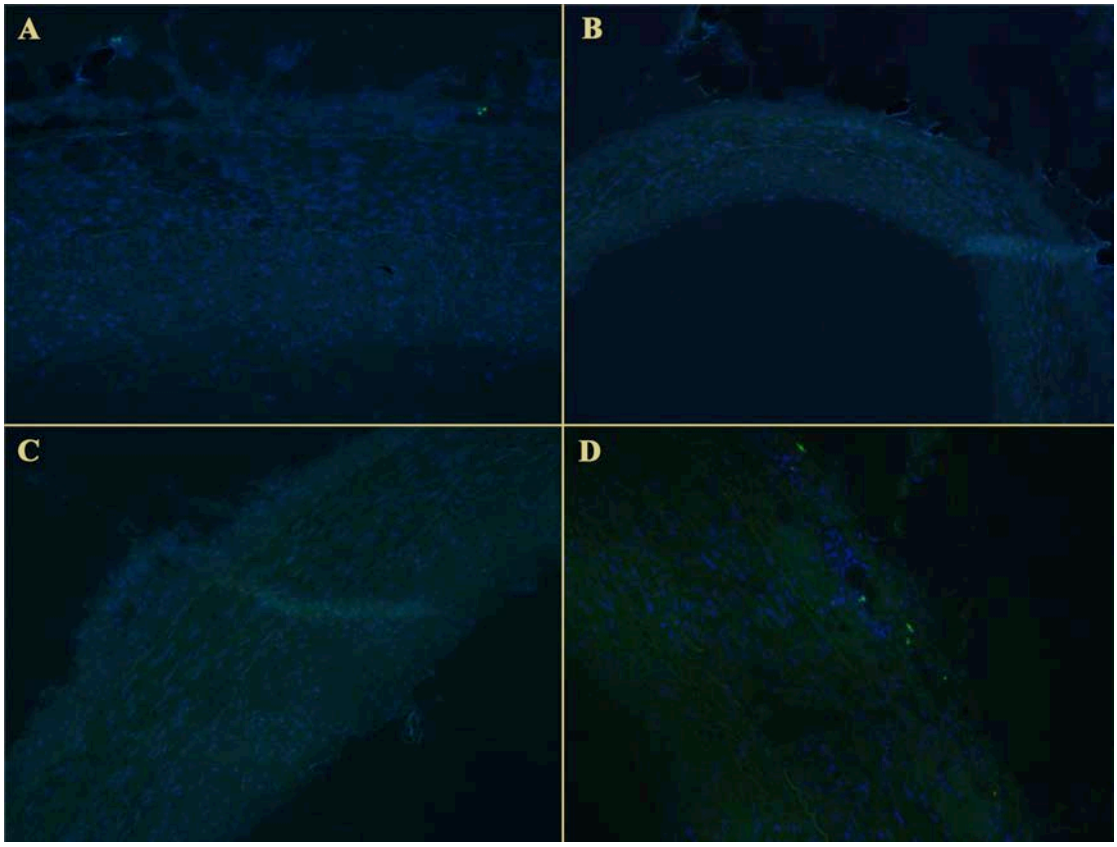

Figure 47 αvβ3 labeling of the AD-HIES coronary arteries

Section of the left anterior descending **(A)**, left circumflex (**B)**, and right **(C, D)** coronary arteries labeled with an anti-αvβ3 probe. Apart from few + cells, there was a paucity of αvβ3 labeling in the coronary sections of the AD-HIES case without the plaque. The right coronary artery seemed to present more + cells and a relative thickening of the adventitia. 10X magnification.

thickening (Fig. 47A, D). At the plaque site, there were few αvb3+ cells on the neointima, in the near lumen area (Fig. 48B), and inside the adventitia below the plaque (Fig. 48A).

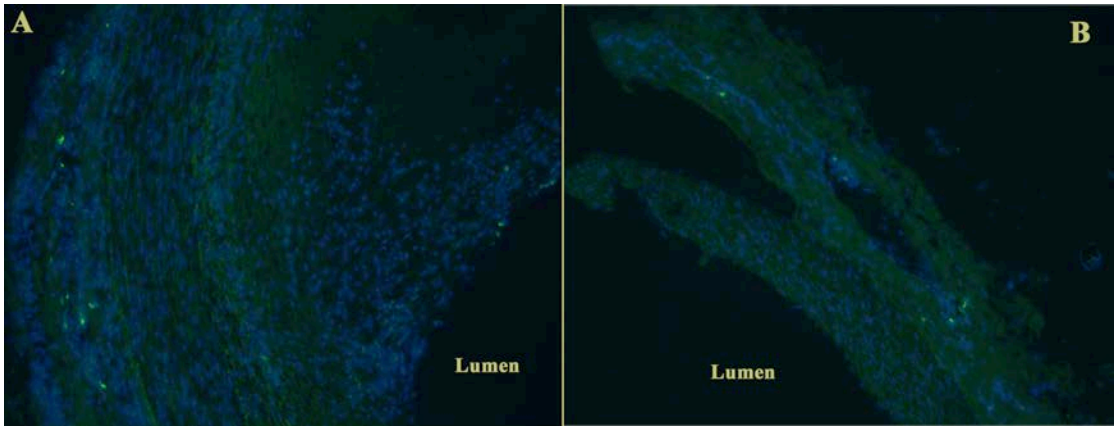

Figure 48 **αvβ3 labeling of the AD-HIES left main coronary artery at the plaque site**

Section of the left main coronary artery showing characteristic outward plaque accumulation labeled with an anti-αvβ3 probe. **(A)** A section of the plaque showing shoulder area is characterized by anti-αvβ3 positive cells in the adventitia layer below the plaque, and at the surface of the lumen. (**B)** The same section showing part of the adventitia below the plaque with few αvβ3 positive cells. 10X magnification.

5.3.3 α-Actin Labeling

SMCs are largely involved in numerous aspect of the vessel wall integrity, playing a role in matrix remodeling, vessel repair, atherosclerosis and aneurysm[102, 151, 152]. Immunohistochemical analysis of biopsy specimens from AD-HIES showed the presence of α-actin inside the media of the coronary artery wall, with associated neointimal α-actin expression (Fig. 49). This is characteristic of normal arterial thicknening caused by aging, which is principally characterized by proliferation of SMCs and

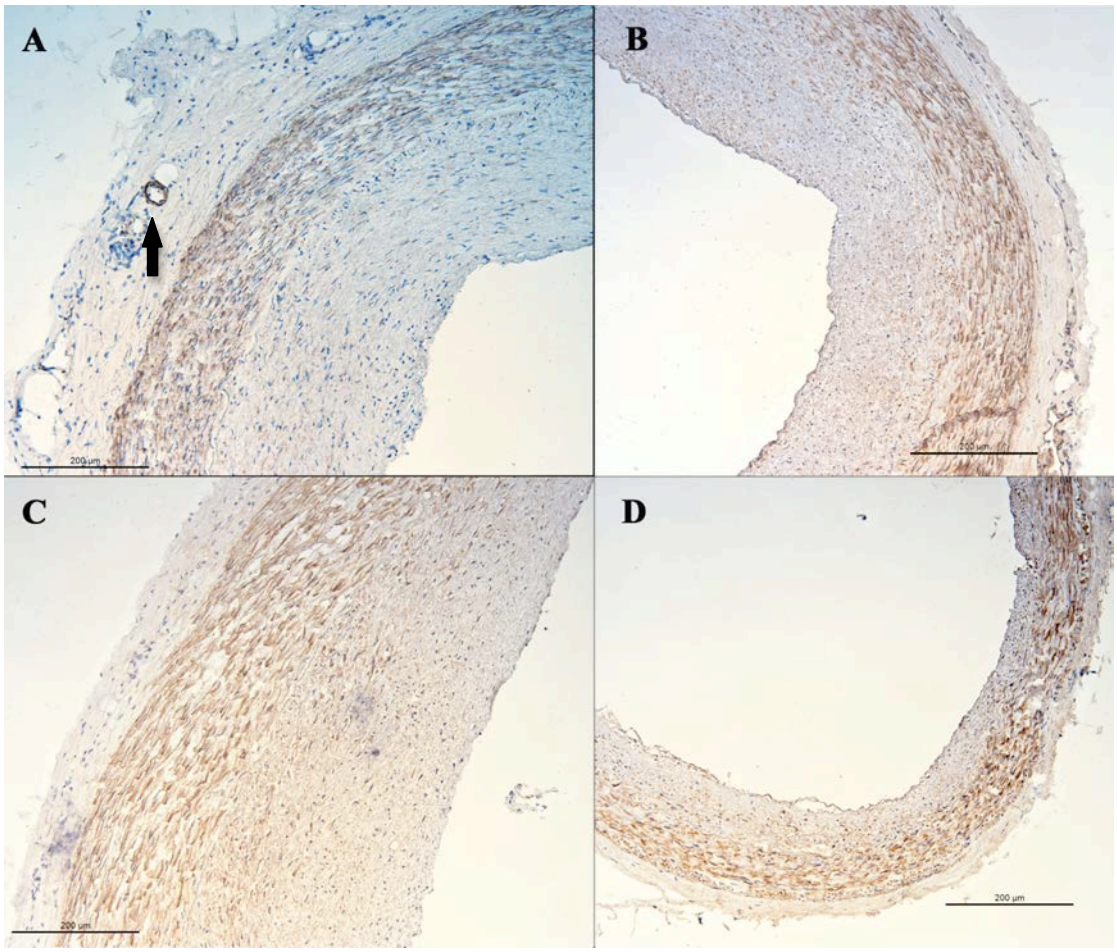

Figure 49 **SMCs labeling of coronary arteries in the AD-HIES patient**

Section of the right **(A)**, left anterior descending **(B)**, left main at the bifurcation point **(C)**, and left circumflex **(D)** coronary artery labeled with an antibody against α-actin. We can clearly see the smooth muscle cells labeling in the media layer, as well as a few sparse smooth muscle cells labeled in the neointima. **Arrow** in panel **(A)** represents smooth muscle cells surrounding a blood vessel. Magnification 10X.

proteoglycans/collagen deposit. AD-HIES coronary samples were characterized by a strong smooth muscle cell staining in the media, associated with sparse and weak neointimal labeling (Fig. 49). The AD-HIES coronary artery at the plaque site showed very few neointimal SMCs labeling, suggesting an absence of SMCs migration and cap formation (Fig. 50A, B, C). In atherosclerosis, we typically see a migration of the SMCs

into the near lumen area during the formation of the fibrous cap. Also, the SMC layer was almost absent on the arterial wall below the plaque, which point out toward medial necrosis (Fig. 50A, B, D).

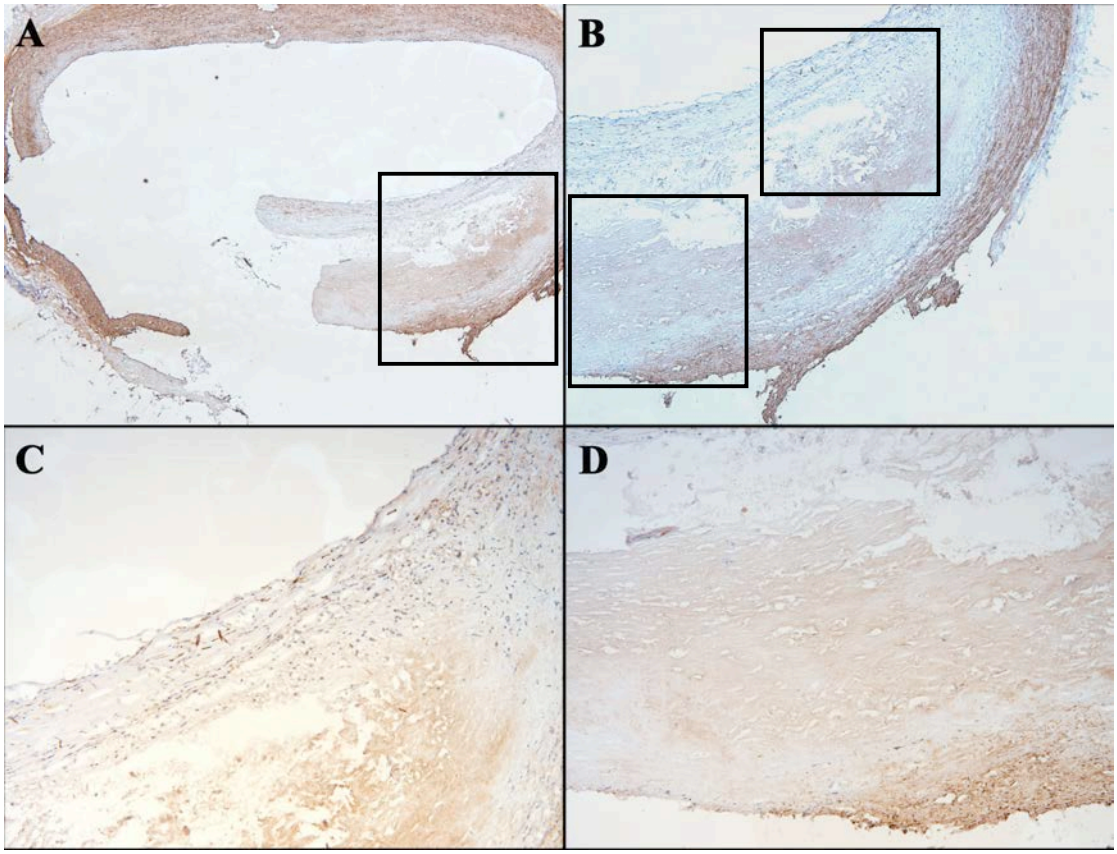

Figure 50 **SMCs labeling of the atherosclerotic plaque in the AD-HIES patient**

Section of the left main coronary artery at the bifurcation point labeled with an antibody against α-actin. The plaque area seemed to label very weakly for SMCs **(A)**. Few α-actin+ cells were seen in the neointima layer **(B, C)**, as well as in the adventitia below the plaque **(B, D)**. Usually, important necrotic core are characterized by the formation of a fibrous cap. Also, adventitial necrosis is a feature of aneurysms. **(A)** 2,5X Magnification. **(B)** 5X Magnification. **(C, D)** 10X Magnification. Boxed area in **(A)** represents magnified area in **(B)**. Boxed areas in **(B)** represents magnified areas in **(C)** and **(D)**. SMCs: smooth muscle cells.

5.3.4 MMP-9 Labeling

Matrix metalloproteinase 9 (MMP-9) is involved in matrix remodeling and cell migration[153, 154]. Immunohistofluorescence study of the expression of MMP-9 showed important findings in the AD-HIES case. While the expression of MMP-9 was usually widely distributed into the adventitia, media, and neointima in atherosclerosis, it was mostly confined to the adventitia region for the AD-HIES samples (Fig. 51). Despite

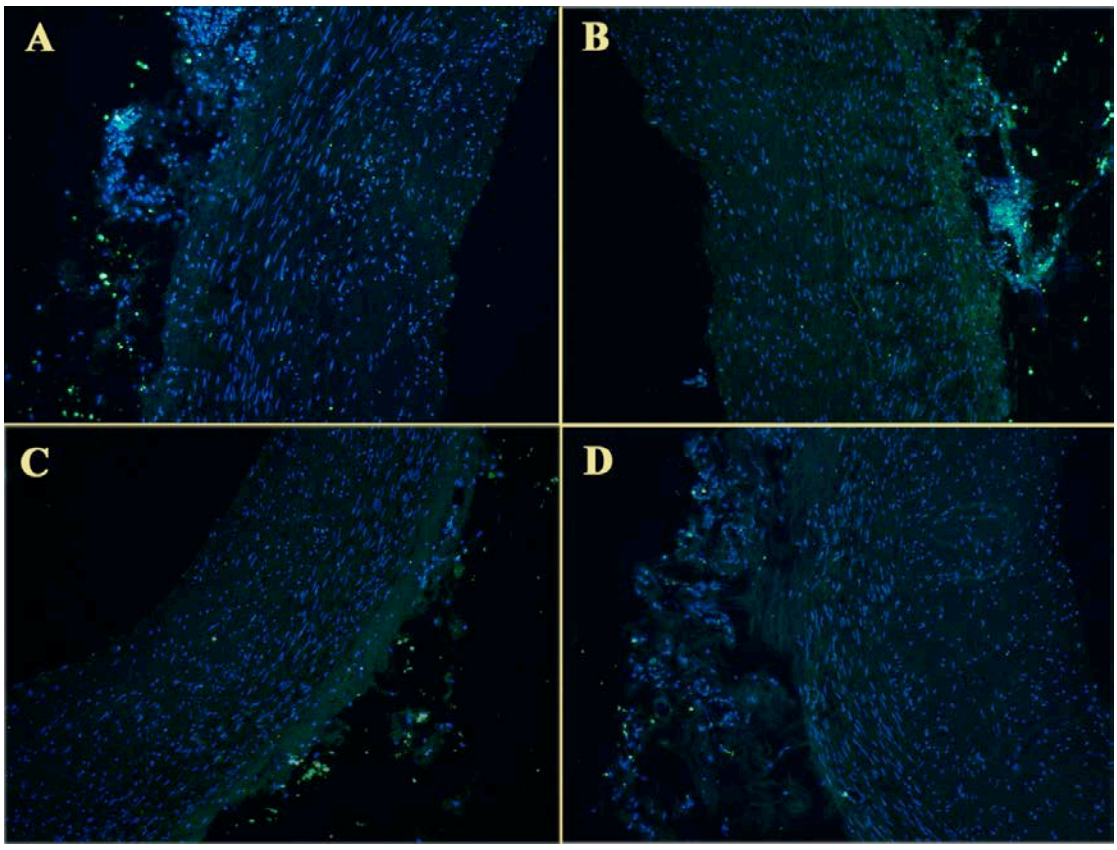

Figure 51 **MMP-9 labeling of the AD-HIES coronary arteries**

Section of the left anterior descending coronary artery **(A, B)** and right coronary artery **(C, D)** showing MMP-9 expression. In the AD-HIES patient, plaque free coronary arteries expressed MMP-9 at a low density, and mostly confined to the adventitia layer. Magnification 10X.

some variability among the samples, MMP-9 signal was stronger where there was a more important inflammatory cell infiltration in the adventitia. Generally, it also appeared that the MMP-9 expression was more important when there was a neointimal bump or protuberance. The left main artery at the bifurcation point (LMbp), presenting the symptom of an advanced atherosclerotic plaque, showed an important MMP-9 overexpression inside the proximal neointimal region, in the near lumen of the plaque area (Fig. 52A). In the segment opposite to the plaque, MMP-9 expression was not confined to the adventitial area, but was instead widely distributed along the adventitia, media and neointima (Fig. 52B), which could be related to a remodeling process inside the coronary segment with plaque. Despite some variability among the different regions of the arteries, and apart from the plaque site, MMP-9 density was clearly lower in the AD-HIES coronary walls than in atherosclerosis. MMP-9 expression in the coronary walls was co-localized with macrophages expression.

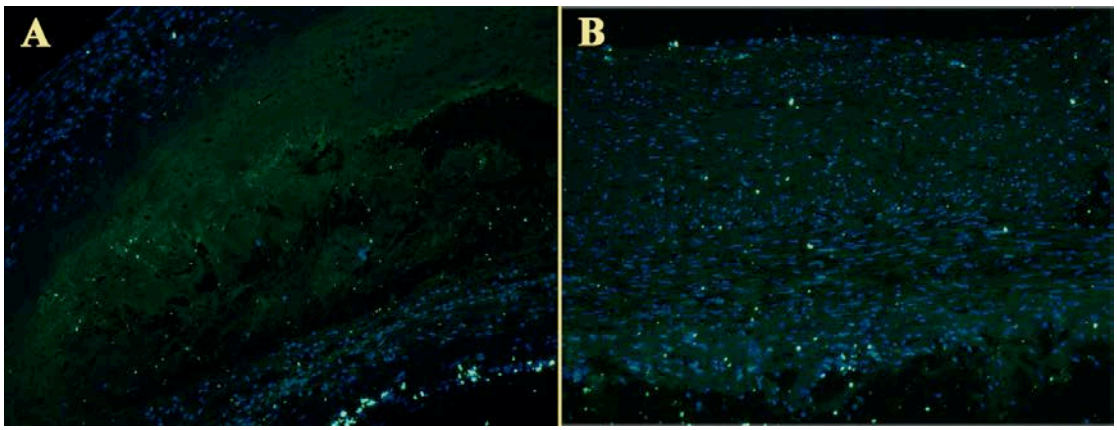

Figure 52 **MMP-9 labeling of the AD-HIES left main coronary artery at the plaque site**

Section of the left main coronary artery at the bifurcation point **(A, B)** showing MMP-9 expression. In the AD-HIES plaque, MMP-9 was strongly overexpressed on the near lumen neointima layer **(A)**, a characteristic often seen in aneurysm. Interestingly, the plaque free segment on the same cross-section, showed MMP-9 expression in the three vessel wall layers (adventitia, media, and neointima) **(B)**. Magnification 10X.

5.3.5 Macrophages Labeling (CD68)

Monocytes and macrophages play a central role in immunity and the process of atherosclerosis[62, 155]. Immunohistochemical study of the expression of CD-68, a cell surface receptor present on monocytes/macrophages, confirmed de presence of macrophages almost exclusively into the adventitia of de AD-HIES patient coronary

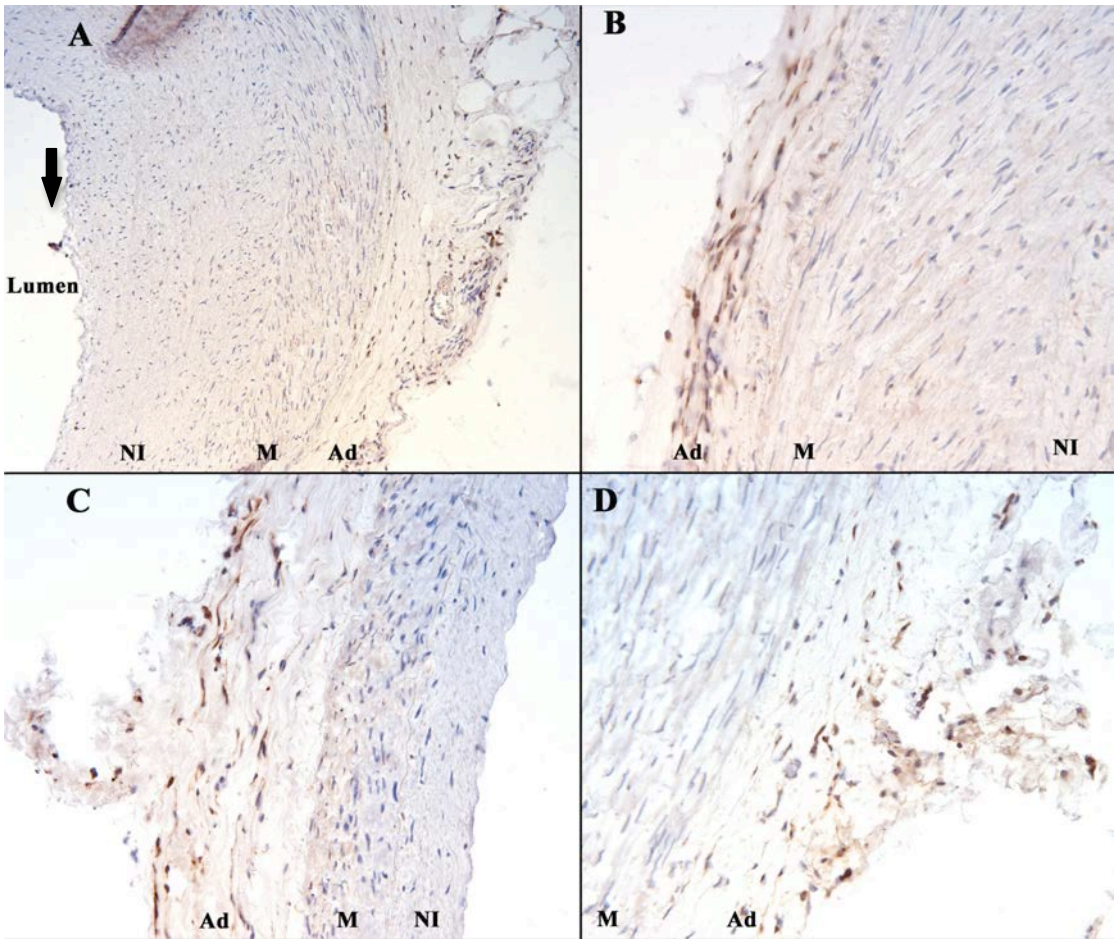

Figure 53 **Macrophages localization in the AD-HIES coronary arteries**

Macrophages labeling with an anti-CD68 antibody in the left anterior descending **(A),** right **(B),** left circumflex **(C),** and left main at the bifurcation point **(D)** coronary arteries**.** We can clearly see that CD68+ cells are almost exclusively express in the adventitia layer of the coronary wall. **Arrow** in panel (**A)** shows a group of CD68+ cells that seems to be on the neointimal section of the coronary artery. Panel (**A)** was taken at 10X magnification to be able to visualize the entire wall. Panel **(B**, **C)**, and **(D)** has been taken at 20X magnification.

arteries presenting no sign of plaque accumulation within the wall (Fig. 53).

As opposed to the coronary arteries without plaque, the left main artery with the plaque showed an important and heavy infiltration of macrophages into the neointimal area (Fig. 54). The macrophages count at high power field (40X) was around 40 CD68+ cells (Fig. 54A and Table 3), which is considered as histological marker of plaque vulnerability (≥25 macrophages per high power field)[3]. Another interesting fact was the localization of the macrophages along the whole length of the plaque in the cross-sectional section (Fig. 54B). Effectively the CD68+ cells did not seem to be concentrated on the shoulder region of the plaque, but instead they were widely distributed along the near lumen area in front of the plaque. The adventitial layer showed only few CD68+ cells. CD-68 expression generally co-localized with MMP-9 expression.

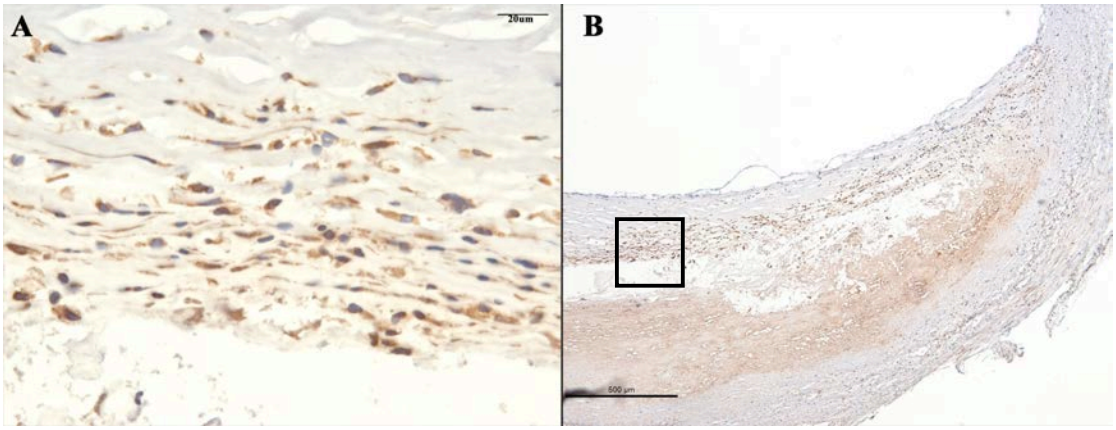

Figure 54 **Macrophages labeling of the AD-HIES left main coronary artery at the plaque site**

In the coronary artery segment of the left main coronary artery showing plaque accumulation, there was a heavy infiltration of macrophages in the neointimal area near the lumen. Panel **(A)** is showing a 40X magnification of the plaque, with a macrophages count of ~40 CD68+ cells. Panel **(B)** is showing a 5X magnification of the same region. Macrophages are mostly localized into the near lumen neointima, and diffusely distributed over the whole length of the plaque cross-sectional area. Boxed area in **(B)** represents the magnified area in **(A)**.

5.3.6 T-Cell Labeling (CD40)

CD-40 is a receptor mainly expressed on the surface of antigen presenting cells (APCs) responsible for the induction of a variety of downstream effects, as the induction of anti-microbial substance from macrophages, as well as vascular remodeling and neointimal formation[156, 157]. The presence of CD-40 was assessed by immunohistofluorescence. All AD-HIES samples showed a similar pattern of CD-40 expression, mostly in the adventitia and neointima of the vessel wall, but the signal found was very weak (Fig. 55). Effectively, there were very few CD-40+ cells in the AD-HIES cases. When

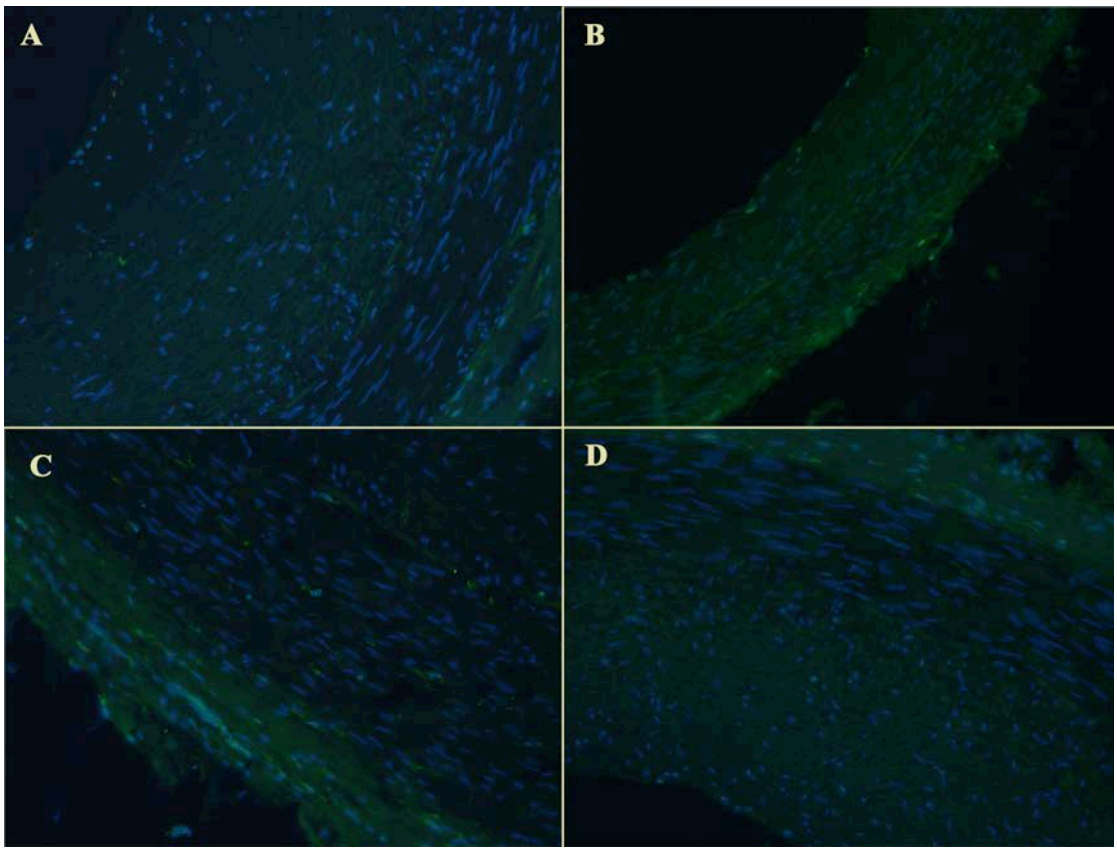

Figure 55 **CD40 labeling of the AD-HIES coronary arteries**

Left anterior descending **(A),** left circumflex **(B)**, right **(C)**, and left main at the bifurcation point **(D)** coronary arteries labeled with an anti-CD40 antibody. Although there were some small differences in the density of CD-40+ cells, there was very few CD40 labeling in the coronary arteries of the AD-HIES case. 20X Magnification.

atherosclerotic lesions are associated with adventitial inflammation and stenosis, there is usually a high level of CD-40 expression. Similar to the other molecular markers, the LMbp artery presented a different pattern of expression at the plaque site, showing a greater density of CD-40 expression in the neointima (Fig. 56).

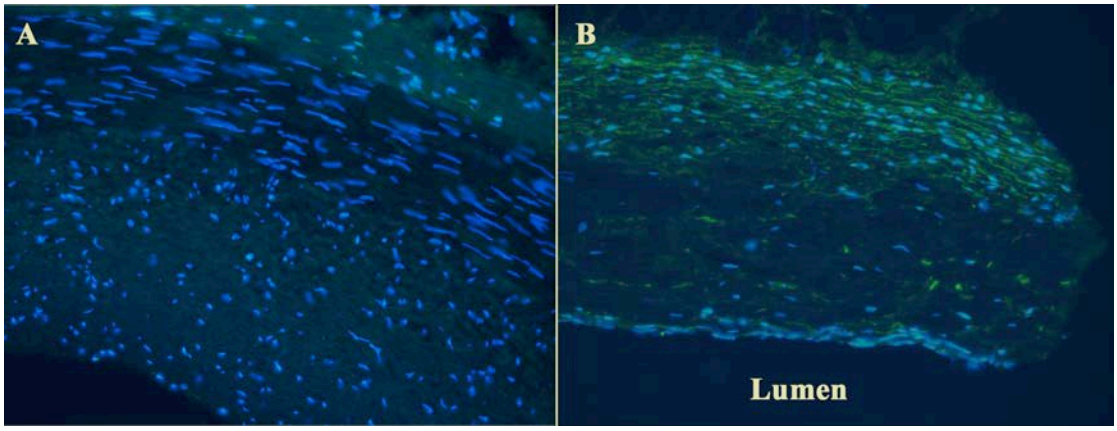

Figure 56 **CD40 labeling of the AD-HIES left main coronary artery at the bifurcation point in the reference segment and in the segment with plaque**

Left main coronary artery labeled with an anti CD-40 antibody showed more important density of CD40+ cells in the segment presenting the plaque **(B)** than in the segment before the plaque **(A)**. Although there was a difference of density between the segment without plaque **(A)** and the segment with plaque **(B)**, the density of labeling in AD-HIES was weaker than CAD samples presenting stenosis. 20X Magnification.

5.3.7 Elastic fibers - Verhoeff's Van Gieson (EVG) Staining

The internal elastic lamina and external elastic lamina are two different layers of elastic fibers delimitating, respectively, the media from the intima, and the adventitia from the media, in the coronary arteries. Those two layers of elastic fibers are very important for the arteries' biophysical properties and they have been involved in positive remodeling[12, 158], ectasia[158], and aneurysm[159]. We used elastic Verhoeff's Van Gieson (EVG)

staining to evaluate the integrity of the internal and external elastic lamina. In the AD-HIES coronary arteries, there was a general thinning of the external elastic lamina, which was very difficult to localize (Fig. 57). The internal elastic lamina also appeared thinned, with some discontinuities in the elastic network. The left anterior descending coronary artery's internal elastic lamina seemed to have completely disappeared in some region of

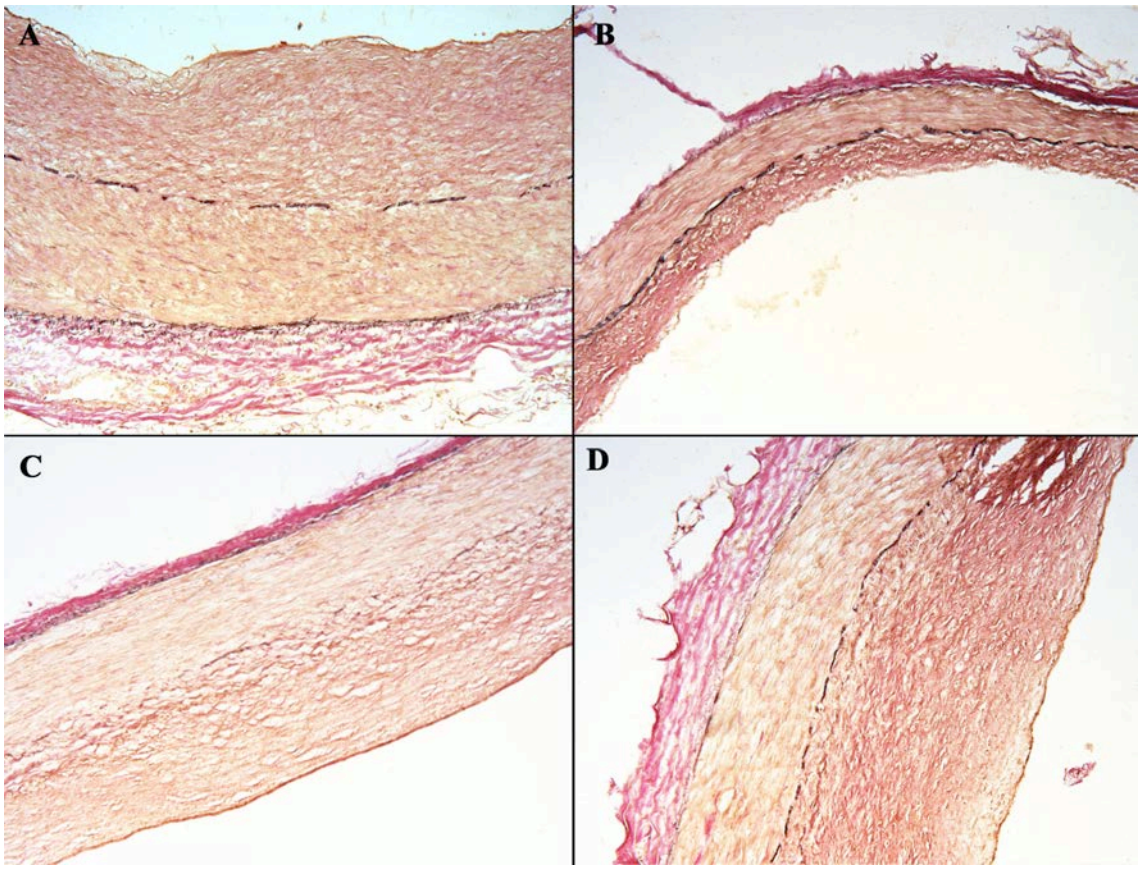

Figure 57 **Elastic tissue fibers staining of the AD-HIES coronary arteries with elastic Van Gieson (EVG) stain**

Right **(A),** left circumflex **(B)**, left anterior descending **(C)**, and left main at the bifurcation point **(D)** coronary arteries stained with an elastic Van Gieson stain. The right **(A)**, left circumflex **(B)**, and left main **(D)** coronary arteries seemed to have few elastic fiber breaks into the internal elastic lamina. Interestingly, the left anterior descending coronary artery **(C)** internal elastic lamina seemed to have completely disappeared. In all samples, the external elastic lamina separating the media from the adventitia was very difficult to differentiate. Black: elastic fibers. 10X Magnification.

the cross-sectional section, which could be link to the fact that this artery presented the highest degree of dilatation. In the cross-sections with the plaque, there was a high number of internal elastic lamina discontinuities in the segment below the plaque (Fig. 58B, C), and a complete absence of this layer on the wall opposite to the plaque (Fig. 58D). This could suggest a vessel's remodeling process in the wall opposite the plaque.

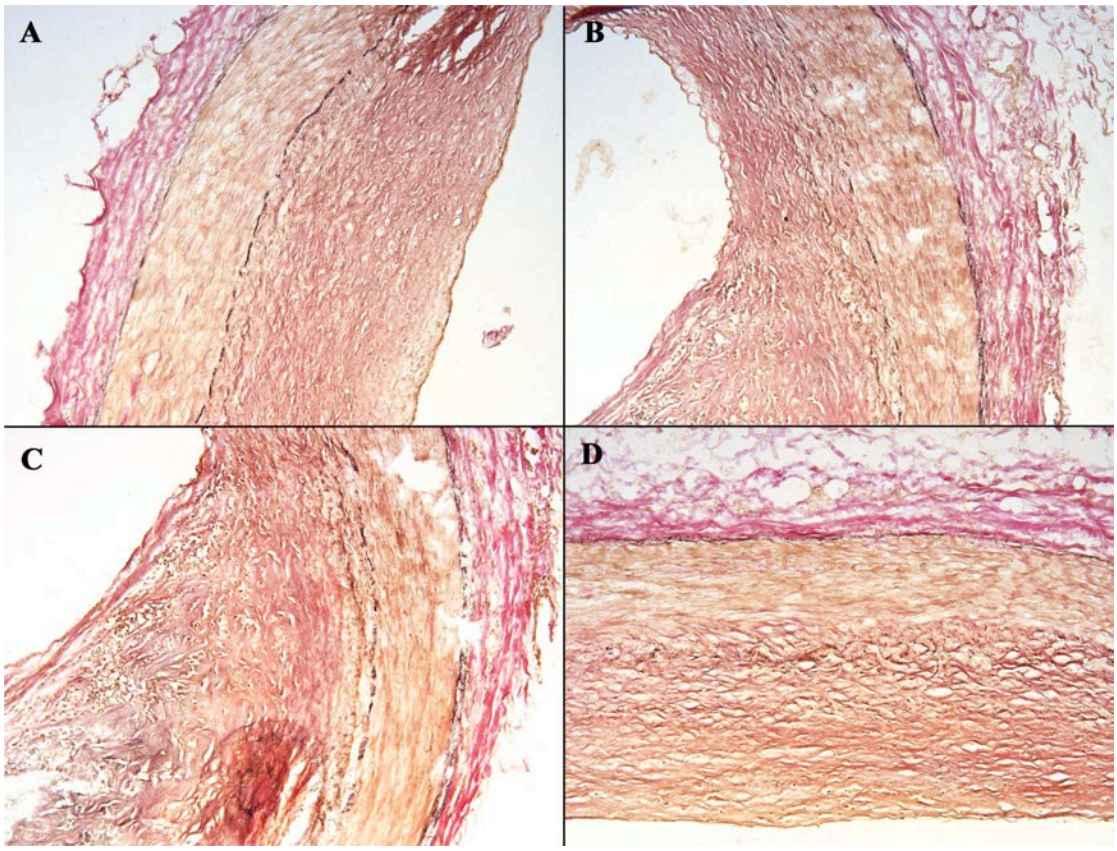

Figure 58 **Elastic tissue fibers staining of the AD-HIES left main coronary artery at the reference site and plaque site with elastic Van Gieson (EVG) stain**

Elastic fibers staining in the reference segment in the left main coronary artery at the bifurcation point **(A)** and in the same coronary artery at the plaque site **(B, C, D)**. On the wall below the plaque, there were numerous discontinuities in the internal elastic lamina **(B, C)**. The segment opposite to the plaque showed a complete absence of the internal elastic lamina **(D)**. Black: elastic fibers. 10X Magnification.

5.3.8 Masson's Trichrome Staining

SMCs and the collagen content deposed by them is also an important feature for the biomechanics properties of the coronary arteries[160]. Masson staining of the AD-HIES coronary arteries showed that intimal thickening was principally due to SMCs proliferation and collagen deposition (Fig. 59). The same phenomenon has been

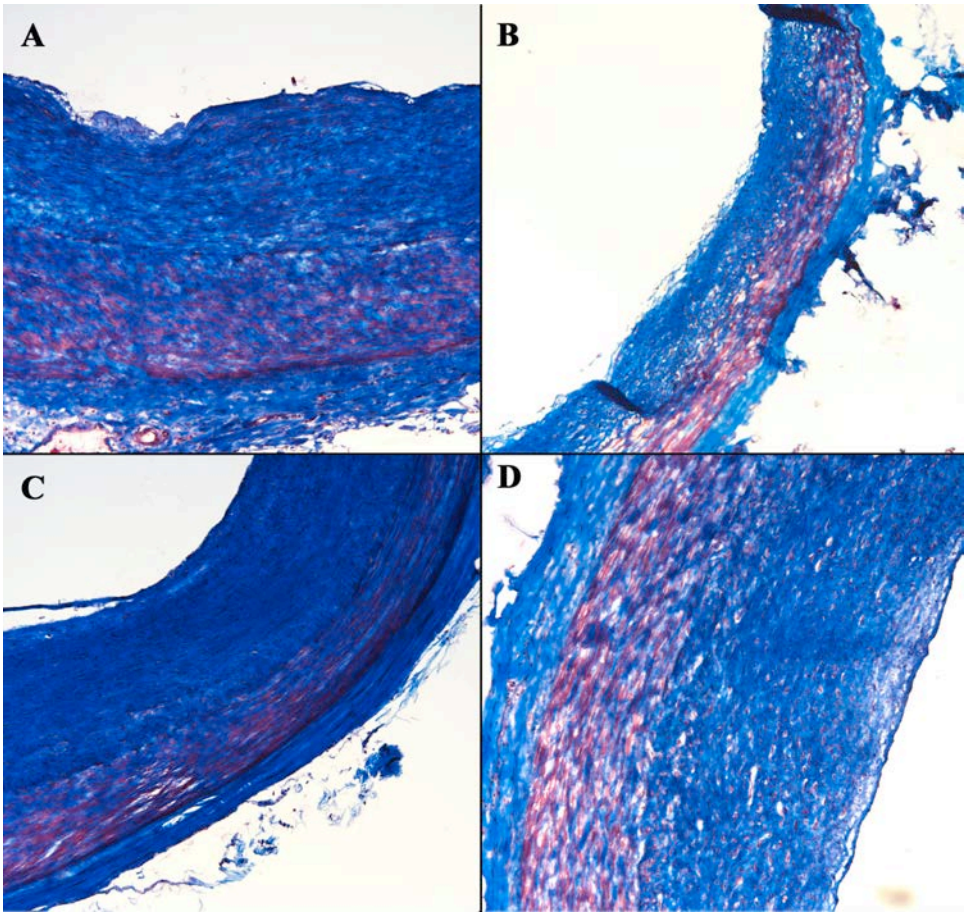

Figure 59 **Masson Trichrome staining of the AD-HIES coronary arteries**

Right **(A),** left circumflex **(B)**, left anterior descending **(C)**, and left main at the bifurcation point **(D)** coronary arteries stained with a Masson Trichrome stain. The right **(A)**, left circumflex **(B)**, and left main **(D)** coronary artery presented similar density of collagen. The left anterior descending coronary artery **(C)** collagen content appeared denser. In the near intima of the LMbp **(D)**, there was a region with loser collagen content, which corresponds to the region with the plaque in the adjacent coronary artery segment. Blue: collagen. Red: muscle, red blood cells. Pink: cytoplasm. Black: Nuclei. 10X Magnification.

described in adaptive intimal thickening, phenomenon associated with aging. We can clearly identify the coronary arteries' media layer staining red for SMCs, and the high collagen content in blue in the neointima, media, and adventitia layers. Notably, the left anterior descending presented a much more denser pattern of collagen fibers, as seen in relatively normal artery (Fig. 59C). As opposed to that, the left main coronary artery at the bifurcation point demonstrated looser collagen content in all the layers, plus a beginning of collagen loss into the near lumen neointima (Fig. 59D), which could be related to the beginning of the plaque formation seen in the adjacent segment of the same artery (Fig. 60). In the segment of the left main coronary artery with plaque (Fig. 60), there was an important loss of collagen into the neointimal region (Fig. 60A, B). This is typical of a late core, with numerous cholesterol clefts, cellular debris and an absence of ECM, particularly collagen, as opposed as an early core, which shows collagen interspersed with intact foamy macrophages. The SMC layer of the adventitia below the plaque seemed to have almost completely disappeared, and the collagen staining appeared weaker (Fig. 60C). The segment opposite the plaque also presented a looser pattern of collagen fibers in all layers, with a thinned media layer and a more disorganized collagen content (Fig. 60D). The thin fibrous cap (TFC) almost disappeared at the shoulder region, with a thickness of less than 45μm (Fig. 60B). There was an absence or very few SMCs labeling in the neointimal region above the plaque (Fig. 60B). This is uncharacteristic of a plaque with a large necrotic core, which should present SMC labeling in the near lumen area, usually forming the fibrous cap.

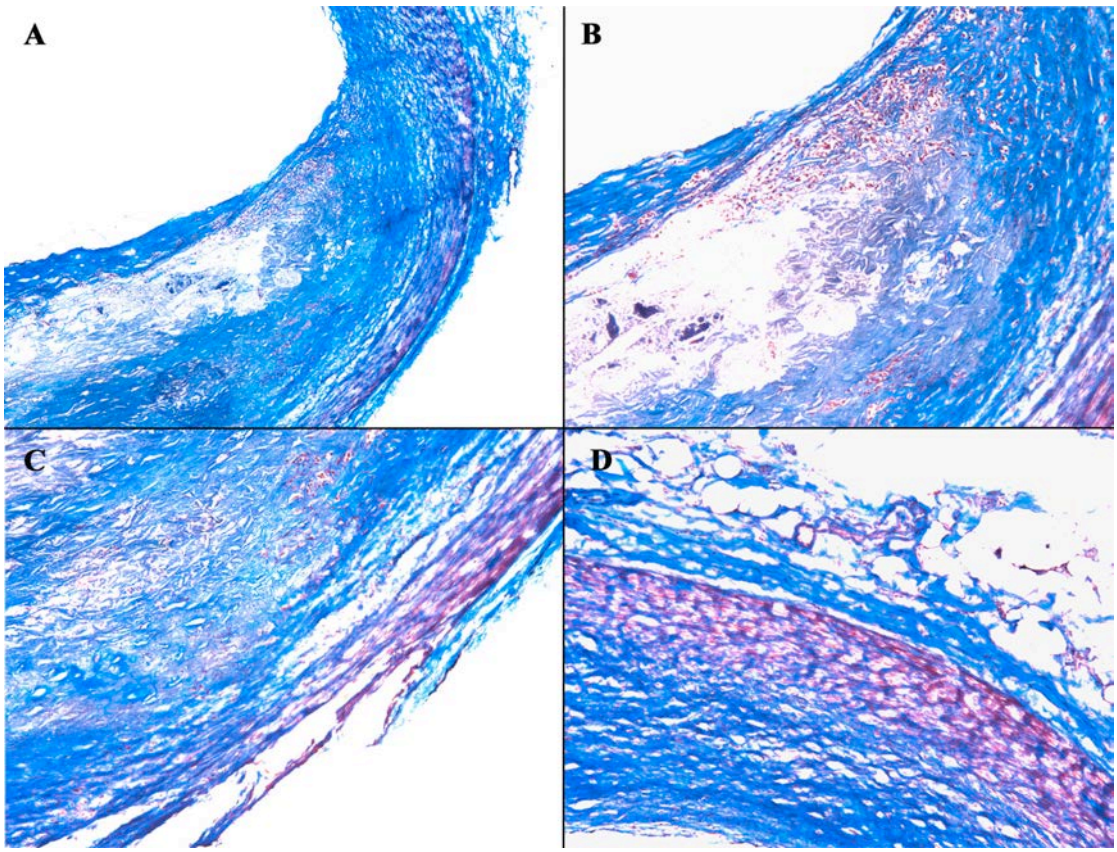

Figure 60 **Masson Trichrome staining of the AD-HIES left main coronary artery at the plaque site**

Masson Trichrome staining in the left main coronary artery at the plaque site. In the necrotic core, there was absence of staining, which is characteristic of a late core **(A, B, C),** and the collagen content in the fibrous cap was extremely thinned on the shoulder region **(B)**. Interestingly, the segment opposite to the plaque showed collagen staining, but with fibers demonstrating a looser pattern **(D)**. The wall below the plaque showed thinning of the medial layer, which almost entirely disappeared, and an absence of the adventitial layer (**C).** Blue: collagen. Red: muscle, red blood cells. Pink: cytoplasm. Black: Nuclei. **(A)** 5X Magnification. **(B, C, D)** 10X Magnification.

5.3.9 Movat Staining

For evaluating the biomechanical properties of the coronary wall, SMCs, collagen, elastic fiber content, and ground substance are important[160]. Movat staining is a very useful type of stain, as it allows the differentiation between all those different components. The elastic fiber content of the external elastic lamina in the AD-HIES coronary walls without plaque appeared again very low and very difficult to see (Fig. 61). In the other hand, the internal elastic lamina looked relatively easy to visualize, although it contained many discontinuities along the length of the cross-sections in almost all of the samples. Those results are consistent with the EVG staining, which showed the same pattern of discontinuities in the internal elastic lamina and very weak staining in the external elastic lamina of the AD-HIES samples without plaque. In the segment of the AD-HIES with plaque, were we saw a weak staining of the internal elastic lamina and no external elastic lamina with EVG, there seemed to be a total absence of both internal and external elastic lamina (Fig. 62). This could be due to less specific staining of the Movat stain for elastic fibers, or the fact that the cross-section used in the Movat staining, even if adjacent to the one used in EVG staining, has loss all of the elastic fibers. Interestingly, the collagen staining, although similar to the one with Masson, showed a slightly different pattern of staining. Effectively, unlike Masson stain, Movat stain allows to differentiate between collagen content (yellow) and ground substance and mucin (blue). Accordingly, the segments without plaque in the AD-HIES coronary walls stained with Movat showed different pattern of collagen staining than the Masson's stain previously showed. First, in the left circumflex and left anterior descending (Fig. 61B, C) coronary arteries, there was a denser collagen content in both adventitia and neointima. In the other hand, the right

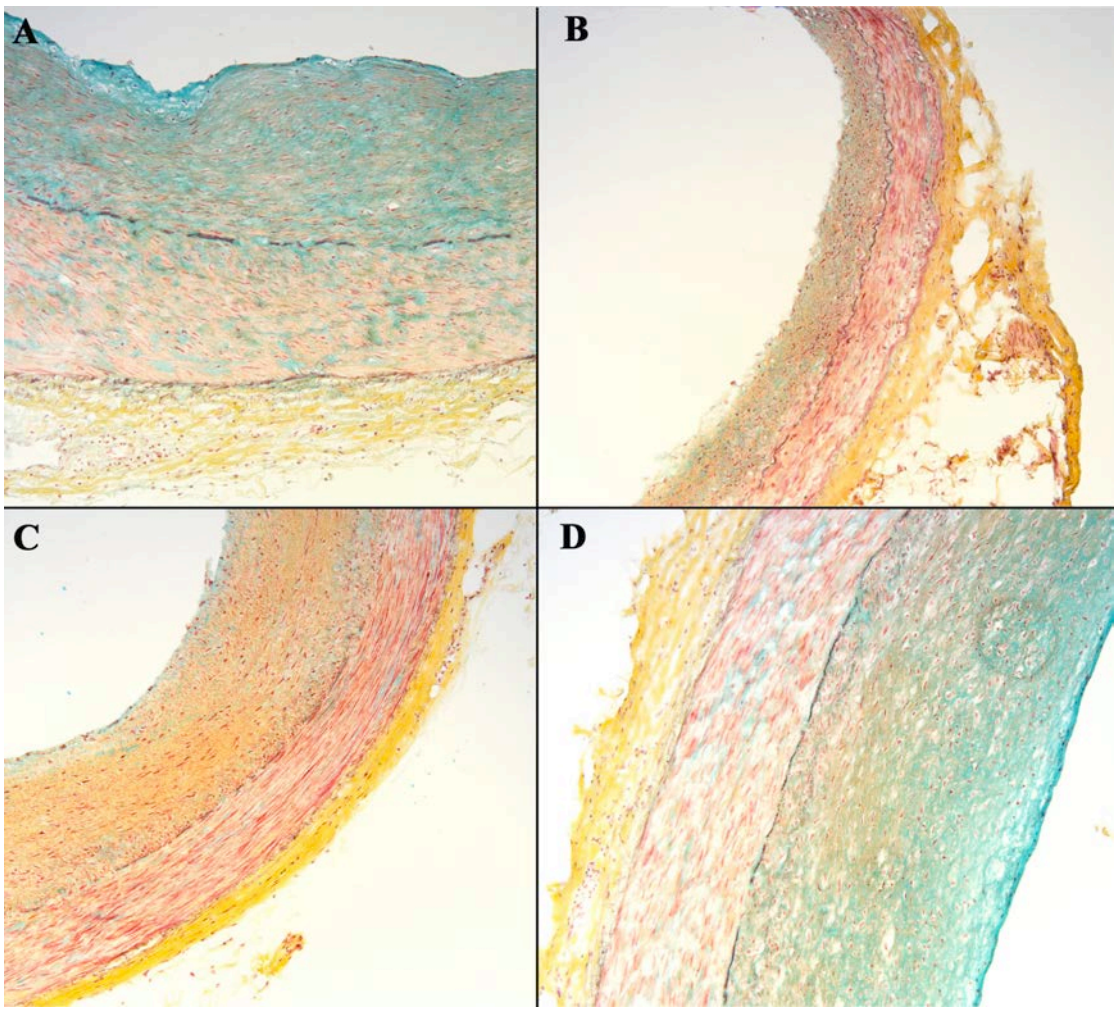

Figure 61 **Movat Pentachrome staining of the AD-HIES coronary arteries**

Right **(A),** left circumflex **(B)**, left anterior descending **(C)**, and left main at the bifurcation point **(D)** coronary arteries stained with a Movat Pentachrome stain. The left circumflex **(B)** and left anterior descending **(C)** coronary arteries demonstrated similar density of collagen into the neointima and adventitia, which appeared denser than the other coronary arteries. The right **(A)** and left main **(D)** coronary artery's collagen content was slightly less dense in the neointima, with more ground substance and mucin content, and much more looser in the adventitia. In both right (A) and LMbp **(D)** coronary arteries, there was a region with loser collagen content on the near lumen area. For the LMbp, it corresponded to the region with plaque in the adjacent segment of the same artery. Those results were correlated with the previous results with Masson staining and EVG staining, but as opposed to the Masson stain, the collagen content and ground substance or mucin can be differentiated. Blue: ground substance, mucin. Yellow: collagen, reticular fibers. Red: muscle, red blood cells. Bright red: fibrin. Pink: cytoplasm. Black: Nuclei, elastic fibers. 10X Magnification.

(Fig. 61A) and left main at the bifurcation point (Fig. 61D) coronary arteries presented a looser pattern of collagen fiber into the adventitia, with a less important collagen content in the neointima, visualized by the blue/greenish color of the neointimal layer. In fact, the very near lumen area of both coronary arteries seemed to present a total absence of collagen in some areas, with presence of only ground substance and mucin. For the left main coronary artery, it corresponded to the same area on the adjacent segment of the same coronary artery with plaque. It could be interesting to see if by cutting more cross-sections of the right coronary artery, we will also find a beginning of plaque formation. It also has to be mention that when dissected, the pathologist identified this segment as possibly presenting an aneurysm. In the AD-HIES left main coronary with plaque (Fig. 62), there was the same loss of staining in the necrotic core (Fig. 62A, B), which is, as mentioned earlier, characteristic of late core. There was also absence of SMC labeling in the near lumen neointima, in spite of the large size of the necrotic core, and an important thinning of the collagen in the neointimal area, with loss of collagen content in the shoulder region of the plaque. Instead, the collagen content was almost entirely replaced by ground substance and mucin (Fig. 62A, B). On the segment below the plaque (Fig. 62C), there was a thinning of the medial layer and an absence of the adventitial layer. The segment opposite to the plaque also presented a mixture of ground substance, mucin and collagen in the neointima, associated with a much looser density of collagen in both neointima and adventitia.

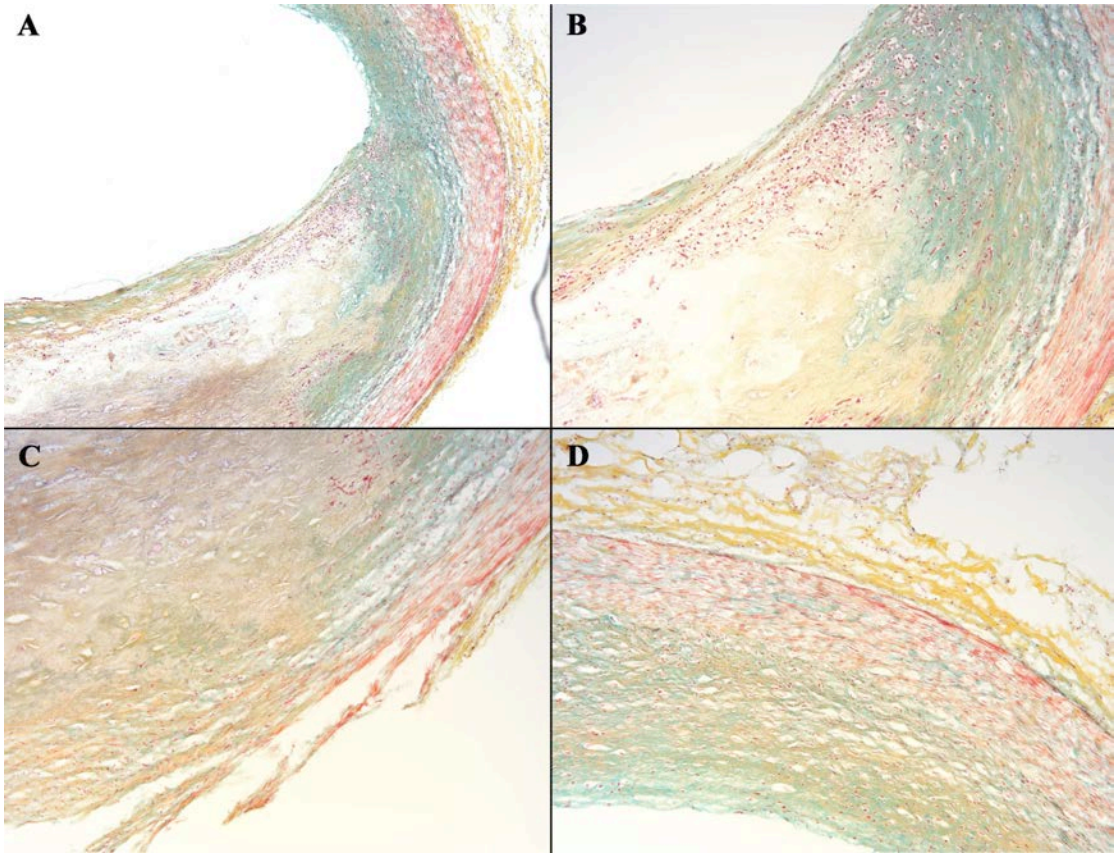

Figure 62 **Movat Pentachrome staining of the AD-HIES left main coronary artery at the plaque site**

Movat pentachrome staining in the left main coronary artery at the plaque site **(A, B, C, D)**. In the necrotic core, there was absence of staining, which is characteristic of a late core **(A, B),** and the collagen content in the fibrous cap was extremely thinned in some parts of the shoulder regions, and completely replaced by ground substance and mucin in other parts **(B)**. The segment opposite to the plaque showed collagen staining, but the fibers seemed to be looser in both neointima and adventitia **(D)**. There was also presence of ground substance and mucin in the neointima of the wall opposite the plaque. The wall below the plaque showed thinning of the medial layer, which almost entirely disappeared, and absence of the adventitial layer (**C).** Blue: ground substance, mucin. Yellow: collagen, reticular fibers. Red: muscle, red blood cells. Bright red: fibrin. Pink: cytoplasm. Black: Nuclei, elastic fibers. **(A)** 5X Magnification. **(B, C, D)** 10X Magnification.

5.3.10 Results Summary

The comparison between CAD plaques (Chapter 3) and AD-HIES plaques can lead to better understanding of the plaque formation process (Table 4). Generally, when compared to CAD cross-sections with plaques, AD-HIES cross-sections with plaque possessed many common characteristics shared with vulnerable plaques. First, in the AD-HIES sections with plaque, there was no important stenosis, with a lumen diameter not significantly different from the normal adjacent vessel, but a total vessel diameter much larger (positive remodeling). Second, $\alpha v\beta 3$ expression was present, but at a lesser degree than in plaques with important stenosis. Third, α-actin labeling showed very few SMCs in the neointima, consistent with the absence of fibrous cap formation. Fourth, MMP-9 was overexpressed in the near lumen area. Fifth, there was an important infiltration of macrophages in the neointima. Importantly, instead of being concentrated into the shoulder areas as usually seen in atherosclerotic plaques, macrophages were localized along the entire near lumen length above the plaque. Sixth, there were very few CD40+ cells, consistent with the absence of stenosis. Seventh, the collagen content was very sparse in the necrotic core area, and near lumen area. Finally, the IEL and EEL in the plaque area had almost completely disappeared. It also has to be mentioned that AD-HIES cross-sections without plaque possessed two major differences with CAD cross-sections without plaque. First, they showed an unusual high number of macrophages in the adventitial layer. Second, the pattern of their elastic fibers (IEL and EEL) contained many discontinuities, sometime associated with complete absence of elastic fiber in parts of the cross-sections.

TABLE 4 Left Main Coronary Artery Measurements at the plaque site

Morphological Characteristics and Immunohistological Labeling	CAD			AD-HIES	
	Cross section w/o plaque	Cross section with plaque (vulnerable)	Cross section with plaque (stable)	Cross section w/o plaque	Cross section with plaque
Lumen diameter	=	= or $(^{-}/_{+})<$	-	=	=
Vessel diameter	=	+	+ or -	=	+++
Stenosis	-	-/+	++	-	-
αvβ3	-	+	++	-	+
α-actin	-/+	-/+	++	-/+	-/+
MMP-9	+	+++	++	+	+++ Near lumen
CD-68	-/+	++	-/+	++ Adventitia	+++ Near Lumen Diffused
CD-40	-	-/+	+++	-	-/+
Collagen	++	+	++	++	-/+
Elastic Fiber	++	-/+	+	-/+	-

Table 4 **Morphological and Immunohistological comparison between CAD coronary artery cross-sections and AD-HIES cross-section**

Morphological and immunohistological markers of CAD cross-sections without plaque, with vulnerable plaque, and with stable plaque, compared to AD-HIES cross-sections without plaque, and with plaque. Note that the column qualifying CAD with vulnerable plaque has been deducted from literature, since no vulnerable plaque where obtained for staining. All the others column represented a summary of the findings in chapter 3 and chapter 4.

5.4 DISCUSSION

The present immunohistological study revealed an atherosclerotic plaque at the bifurcation point of the left main (LMbp) coronary artery, a rare feature in AD-HIES patient. This atherosclerotic plaque is consistent with compensatory positive remodeling and histologically presented advanced atherosclerosis and vulnerability. We reported four major molecular differences inside the coronary wall tissue of the segments without plaque, versus the coronary wall with plaque (Fig. 63). First, the localization of the macrophages, which were found mostly confined to the adventitia in the AD-HIES wall without plaque, with the exception of the plaque area presenting important intimal macrophage infiltration on the near lumen area. Secondly, the presence of matrix metalloproteinase 9 (MMP-9) mainly located in the adventitia, with again the exception of the plaque, which showed an important overexpression of MMP-9 in the near lumen area. Thirdly, the paucity or low level of CD40 expression in all samples, with a greater density of CD40+ cells in the segment with plaque, although far less important than seen in CAD samples with stenosis. Finally, the paucity of αvb3 in the AD-HIES samples without plaque, associated with a low level of expression in the segment with the plaque, which correlated with the expression of vasa vasorum (vv) in plaque with low-grade stenosis and positive remodeling[126, 127]. We also observed a crucial morphological difference in the AD-HIES plaque: the presence of compensatory enlargement and positive remodeling without significant lumen narrowing, despite the 60% cross-sectional stenosis, and a remodeling index of 1.63, as previously described by Glagov[17]. Effectively, according to Glagov, after 40% cross-sectional stenosis, the balance between

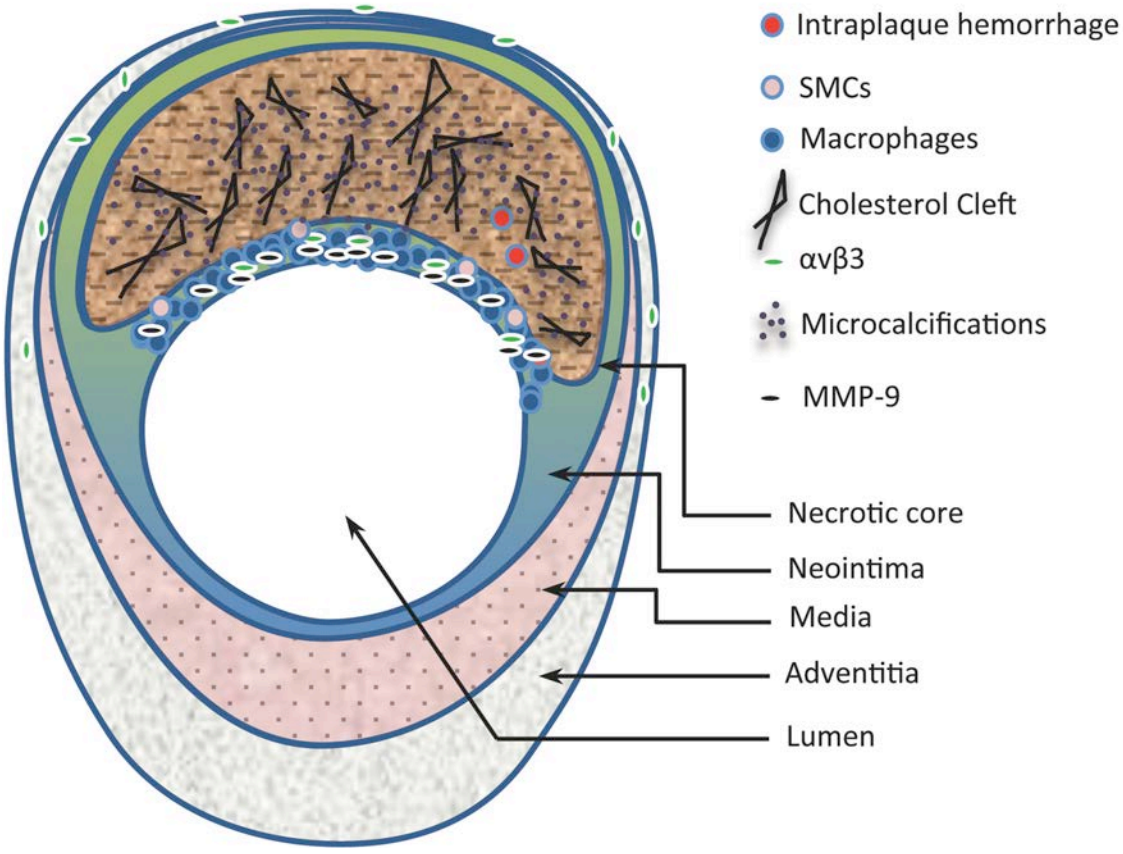

Figure 63 **Schematic representation of the AD-HIES plaque at the bifurcation site of the left main coronary artery**

The AD-HIES plaque possessed many common characteristics shared with vulnerable plaques. First the vessel was in positive remodeling phase. The necrotic core was very important and contained cholesterol clefts, microcalcifications and small intraplaque hemorrhages. The fibrous cap thickness was evaluated under 45µm, which is a criterion for vulnerability. There was a low density of αvβ3 expression, which is usually seen in minimally stenotic plaques. The plaque also featured some characteristics of an atherosclerotic aneurysm. Indeed, there was a heavy macrophages infiltration on the whole length of the near lumen with associated MMP-9 overexpression. Moreover, there were very few SMCs into the neointima. The media and adventitia below the plaque were almost absent, and there was a lost of collagen into the necrotic core. Finally, there was a beginning of adventitial thickening in the wall opposite the plaque, which could be indicating a remodeling process in the plaque free segment as opposed as on the plaque segment.

positive remodeling and lumen preservation should quickly switch toward negative remodeling and lumen stenosis, as the plaque enlarges. The healing/stenosis process seemed to be prevented in the AD-HIES plaque. Our findings suggest that the AD-HIES patient presented undetectable non-stenotic low-grade atherosclerosis that caused weakness of the vessel wall, impaired healing, dilatation and ultimately aneurysm. We hypothesized that AD-HIES disease, with STAT3 mutation, is characterized by a defect in Interleukin-6 (IL-6) signaling via STAT3. Therefore, when there is lipid infiltration and beginning of atherosclerosis, an improper healing of the developing plaque (default in negative remodeling and stenosis), and an exacerbated positive remodeling will lead to dilatation of the vessel wall, and ultimately formation of an aneurysm.

Effectively, although the atherosclerotic plaque could not be formally classified as an aneurysm, because the dilatation of the vessel at the plaque site was only 1.3 times the diameter of the adjacent normal segment, it could be postulated that the plaque will further develop into an aneurysm. This hypothesis was supported by the vessel wall composition, which presented many features of an atherosclerotic aneurysm, including compensatory positive remodeling, medial thinning and destruction, speckled microcalcifications, MMP-9 overexpression in the near lumen area, lipid and foam cell deposition, cholesterol clefts, inflammatory reaction in the adventitia, intraplaque hemorrhages, mild neovascularization, and absence of neointimal formation (smooth muscle cells and collagen forming the cap). It was also supported by the absence of luminal stenosis, despite the large necrotic core size (66%), and the important compensatory enlargement of the vessel. As mentioned before, Glagov clearly

demonstrated that after a cross-sectional percentage of stenosis of 40%, the lumen markedly decrease in close relation to the percentage of stenosis[17]. We did not observe this phenomenon in the AD-HIES plaque. Indeed, after more than 60% cross-sectional stenosis, the lumen was still almost entirely preserved, which, in conjunction with previous imaging studies, point out toward the formation of aneurysm[101] (Fig. 64).

One important feature of aneurysms is the presence of medial necrosis[68]. When there is

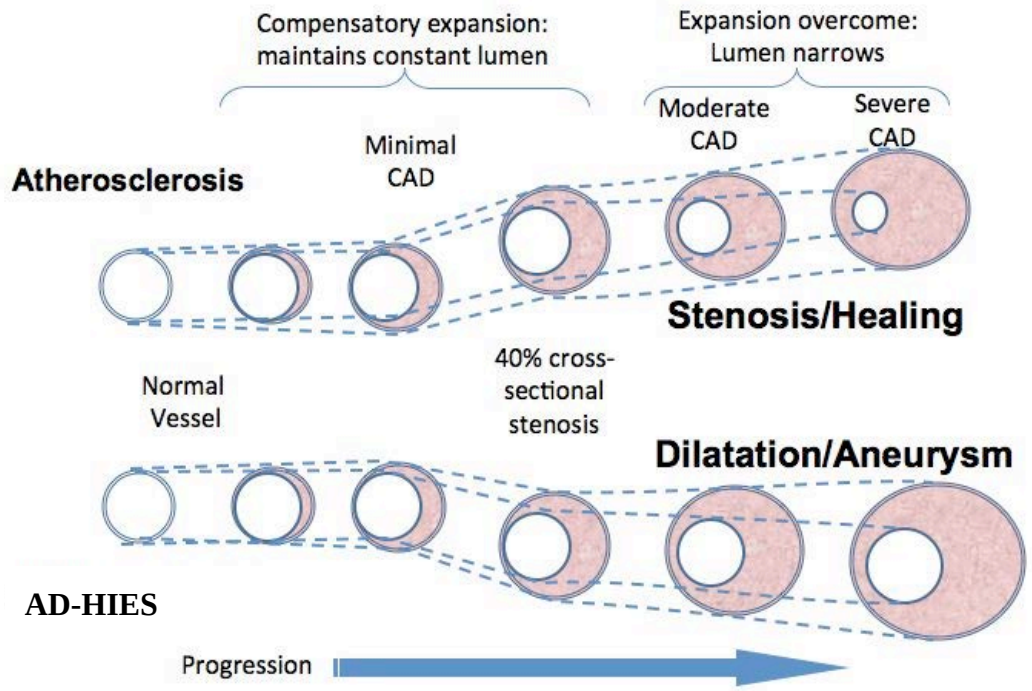

Figure 64 **Theory of aneurysm formation in AD-HIES**

In Glagov scenario **(upper panel)**, after 40% cross-sectional stenosis, the phenomenon of compensatory enlargement of the vessel wall is overcome and lumen narrows in relation to the percentage of stenosis. In the AD-HIES case **(lower panel)**, this stenosis/healing process is inhibited, which ultimately lead to dilatation and aneurysm.

an injury or diminution of blood flow in a normal vessel, apoptotic VSMCs were shown to promote proliferation, migration, and matrix synthesis in adjacent VSMCs[67]. This process promotes vessel remodeling, medial repair, and neointima formation (healing) via a STAT3 dependent pathway, as demonstrated by previous study[161, 162]. We can postulate that mutation in STAT3 can lead to impaired vessel repair, formation of edema and eventually aneurysm. Effectively, if there is endothelial damages without appropriate proliferation and migration of the SMCs, no neointimal formation and matrix deposit, associated with apoptosis of the media, the vessel wall will gradually weaken, eventually leading to aneurysm formation. Moreover, VSMCs death has been reported to play a central role in plaque rupture, with an associated augmentation in symptomatic plaques compared to stable plaques[66]. In the AD-HIES plaque, there was an important medial atrophy below the plaque, at the point of no longer being able to differentiate between neointima, media and adventitia. There was also absence of neointimal formation, despite the important growing intimal mass represented by the necrotic core. Unlike atherosclerotic samples, there were few SMCs at the lumen surface, which would have been expected in a plaque with an important necrotic core size. In accordance to this theory, a previous study on Watanabe rabbit model susceptible to myocardial infarction (MIWHHL) have linked the invasion of atheromatous plaques into tunica media to coronary outward remodeling [96]. They also showed that in those areas, collagen fibers and the internal elastic lamina had partly disappeared and apoptotic smooth muscle cells were observed.

MMPs-9 are also key players in the process of atherosclerosis and aneurysm formation, because of their importance in matrix remodeling and their effect on SMCs migration[154, 163]. Studies showed that MMP-9 expression was associated with increased proteolysis of the matrix in the arterial wall and can be a susceptibility factor for the development of aneurysms in patients with coronary atherosclerosis. Indeed, by degrading collagen and elastin, MMP-9 allows vessels wall dilation and outward expansion, as well as destabilization and loss of vessel integrity. Also, it had been shown that the loss of collagen in the plaque's cap reduce tensile strength, while the absence of collagen from the lipid core promotes transfer of hydrodynamic stress to the cap during the cardiac cycle. Those two important factors will further promote plaque rupture[164]. MMP-9 expression has been show to be dependent of ERK signaling pathway and NFκB, which can explain the overexpression in AD-HIES disease, despite the mutation in STAT3[165, 166]. In the vessel wall of the AD-HIES plaque, MMP-9 are overexpressed inside the neointimal region, close to the lumen, which is associated with matrix degradation and thinning of the fibrous cap, vulnerable plaques and aneurysm formation[167].

Although Il-6 is very well known as a pro-inflammatory cytokine, a recent study linked the expression of IL-6 to the attenuation of the proinflammatory response[168]. They showed that expression of IL-6 induced by macrophage lipid loading induced ABCA1 expression, and that ABCA1 promote cholesterol efflux from macrophages to apoA1. This cellular recycling of free cholesterol reduces foam cell formation and apoptotic body responsible of intraplaque inflammation. They also show that this atheroprotective effect was abolished by inhibition of the Jak-2/STAT3 signaling pathway. The corresponding

STAT3 mutation in Job's patient could be responsible for the accumulation of cytotoxic-free cholesterol and impaired cholesterol efflux. Notably, in the AD-HIES plaque, there was a heavy infiltration of macrophages in the neointima and necrotic core shoulder (40 CD68 + cells by high power field) as seen in vulnerable plaques. Despite the fact that AD-HIES patient seems to develop less severe CAD, the plaque seen on our case possesses an unusually large lipid core (66% of the neointimal area) without associated stenosis, which would be in accord with this theory.

Beside macrophages, T cells and B cells also play a role in atherosclerosis and aneurysm formation[169]. CD40 expression on lymphocyte T, B cells, macrophages and SMCs, had been involved in restenosis and VEGF induce angiogenesis[170]. Since there is a default in lymphocytes T maturation in AD-HIES patients, that could explain both the lower incidence of plaque with stenosis in those patients, and the lower expression of $\alpha v\beta 3$ despite the large necrotic core area and the presence of inflammation. Effectively, when there is arterial injury, CD40 is involved in neointima thickening. Naïve T cell differentiation into Th17 (lymphocyte T maturation) depends principally upon the cytokines profile present during the process, and IL-6 via STAT3 is essential for Th17 differentiation[171]. Since STAT3 mutation is associated with Th17 deficiency, we can postulate that this could be the reason that AD-HIES patients presented a more vulnerable type of plaque, and developped less stenotic atherosclerosis than the regular population.

Neovascularization is another important topic in atherosclerosis and aneurysm formation. Whereas ischemia had been associated with both arteriogenesis and angiogenesis

processes, hypoxia and plaque inflammation had been linked principally to angiogenesis[172]. As opposed to arteriogenesis that presents fully-grown capillaries to bring oxygen to stenotic plaques, immature vessels characterize angiogenesis. Those vessels can come from the adventitia and/or endothelial cells that have been activated by inflammation, and there is often absence of SMCs[11]. Activated endothelial cells expressed VEGF, which in turn can potently induce vascular permeability and can cause edema in ischemic tissues[173]. Ox-LDLs are also involved in the upregulation of VEGF expression in both epithelial cells and macrophages[174]. Leaky endothelium is associated with lipids infiltration, intraplaque hemorrhages and plaque vulnerability[11, 173]. Interestingly, even though there was a paucity of αvb3 expression in the AD-HIES case, there was a low level of αvb3+ cells inside the adventitia and near lumen neointima of the plaque. This could be link to the presence of small hemorrhages seen into the plaque, as well as the important size of the lipid core. We can also postulate that because of the presence of ox-LDLs, activated endothelial cells and macrophages will express VEGF, which in turn will cause vascular permeability, intraplaque hemorrhage and edema. Without appropriate repair response from the vessel wall, this could lead to aneurysm formation. Interestingly, αvb3 and neovascularization has been involved in the progression of advanced atherosclerosis[175]. In the AD-HIES coronary artery with plaque, although there is an important necrotic core size with macrophage infiltration in the neointima, there were very little CD40+ cells (lymphocytes T), which can support this theory.

Adventitial thickening had also been related to remodeling[15]. There is evidence supporting the fact that greater adventitial thickening on the wall below the plaque favor inward growth, negative remodeling, stenosis and plaque healing. Moreover, negative remodeling is characterized by medial and adventitial thinning on the wall opposite the plaque. In the other hand, vasa vasorum on the wall opposite to plaque formation associated with adventitial thinning on the wall below the plaque favor outward growth, positive remodeling, plaque destabilization and aneurysm. The plaque in the AD-HIES coronary artery presented a thickening of the adventitia on the wall opposite to the plaque, associated with a thinned adventitia and media layers on the wall below the plaque. Interestingly, αvb3 expression seemed to be localized on the adventitial layer below the shoulder region of the plaque and on the adventitia below the plaque. This was a surprising result, because we would have expected the thickness of the adventitia to correlate with the αvb3 expression. This could although be explained by the fact that αvb3 expression is AD-HIES is related to inflammation. Indeed, αvb3 expression was concentrated on the epithelial surface and adventitial area, the same area where we found most of the macrophages. Moreover, absence of luminal stenosis was reflected by low level of αvb3 expression, as usually seen in plaques with signs of vulnerability (type IV). Also, it comforted the fact that AD-HIES abnormalities in IL-6/Gp130/Jak2-mediated STAT3 transactivation on target genes causes absence of lymphocyte T maturation, and that cross-talk between lymphocytes T and macrophages is important for plaque healing and stenosis.

In atherosclerosis and aneurysm formation, the SMC content, as well as the density and pattern of fibers and substances present inside the coronary walls (elastic fibers, collagen, ground substance, mucin), will greatly influence the biomechanical characteristics of the vessel wall[160]. Effectively, it had been shown that loss of elastin and collagen is associated with outward remodeling and can favor plaque vulnerability and aneurysms[164]. As seen with the special staining (EVG, Masson, and Movat) in the AD-HIES case, the very thinned external elastic lamina and discontinuous nature or total absence in certain areas of the internal elastic lamina, together with the large cross-sectional vessel areas despite the zero pressure state, could all support the clinical imaging findings of coronary wall dilation, ectasia and aneurysms. The fact that the segment of the coronary with plaque presented an important thinning of the medial layer, a lack of adventitial thickening, a late core with few SMCs in the near lumen area, and an important degradation of the collagen at the shoulder and neointimal areas also point out toward the formation of an aneurysm. Despite the fact that atherosclerotic plaque accumulation as a cause of aneurysm in AD-HIES might seem contradictory to the fact that they presented a paucity of severe coronary disease (seen by stenosis in imaging), we can postulate that the lack of compliance in their arteries favor the development of aneurysms. For example, diabetes patients had been showing a higher susceptibility to atherosclerosis than the regular population[176]. Some studies have shown that arteries from diabetes population are much less compliant. We can extrapolate this finding to AD-HIES disease and postulate that the fact that they had less compliant coronary arteries (seen by a diminution of elasticity) makes them more susceptible to develop aneurysm in the context of atherosclerosis presence. Consequently, in the presence of a

right storm scenario, atherosclerotic plaque without appropriate healing will result in ectasia and aneurysm formation.

The main limitation of this study is that it was limited to a report case. Although we based our conclusion on other AD-HIES patients that had been image by MRI and CT, the pathological examination has been done on only one person. Moreover, the cross-sectional nature of the study should be taken in consideration when evaluating positive remodeling. Therefore, outward and inward remodeling should be considered as relative value, rather than absolute value. Nevertheless, difference in vessel areas between a site of interest and an adjacent reference site as been an arbitrary and widely used measure for remodeling in cross-sectional studies[177]. Also, we are well aware that atherosclerosis and aneurysm are multifactorial processes involving many key determinants and multiple regulatory pathways that can tips the balance in favor of one or another. Accordingly, we are limited by the number of immunological markers used. For example, MMP-9 antibody used in this study can detect both activated and non-activated forms, so the presence of overexpression doesn't necessarily means that there is more MMP-9 activity. Also, many inhibitor of MMPs, mainly tissue inhibitor of matrix metalloproteinase (TIMPs), are present in the coronary wall and can influence the degree of activity of MMPs, so results should be interpreted carefully. The same can be applied for α-actin (SMCs), CD-40 (APCs), αvβ3 (angiogenesis), CD-68 (macrophages). Those molecules and processes have been reported to have both beneficial and detrimental effects on atherosclerotic and aneurysm formation, so again, more studies with more cases and other markers could help clarified the role of each one. Also, it is important to take into account

the risk factors and presence of other clinical manifestation in the evaluation of the patient. It is conceivable that another patient will present a different etiology, depending on the presence or absence of other pathological conditions.

In this chapter, we reported the case of an AD-HIES autopsy revealing an uncommon atherosclerotic plaque on the LM coronary artery at the bifurcation point. Despite the cross-sectional nature of the study and the fact that we are limited to a report case, we attempted to correlate the morphological and immunohistological features of the plaque with the development of aneurysm, as previously reported before in imaging study of AD-HIES patients[100, 101]. We postulated that despite the paucity of severe coronary disease in AD-HIES disease, advanced atherosclerosis process without proper healing mechanism (negative remodeling and stenosis), ultimately leads to aneurysm formation. Further imaging and histoimmunological studies will allow us to confirm this hypothesis.

GENERAL DISCUSSION

The first goal of this study was to evaluate a new αvβ3 ITOP, previously developed for targeting angiogenesis in cancer, for the detection of atherosclerotic plaques. In the theory of damage to the endothelium, it was postulated that epithelial cells are activated and express adhesion molecules that will recruit blood monocytes that will engulf lipids and ultimately become foam cells and create a necrotic core. The first type of lesions considered to be advanced and to have the possibility to become overt is the type IV lesions. Therefore, it becomes critical to develop imaging techniques allowing detection of this type of vulnerable plaques. In the WHHL study, human study and AD-HIES study, the αvβ3 ITOP seemed to detect plaques with medial disorganization and sign of inflammation, a characteristic of type IV plaques. Moreover, in addition of the adventitial labeling, there was a neointimal labeling that can be associated to endothelial activation. Taken together, those observations headed toward the potential of this αvβ3 ITOP to detect the first type of advanced plaques, the type IV lesions. In accord with this theory, the AD-HIES case presenting a plaque with positive remodeling and minimal stenosis (type IV) has been successfully labeled with the probe. The signal was found in the adventitia and near lumen area, which can be related to angiogenesis formation and endothelial activation. In the context of clinical imaging, it can represent a potential target for the detection of vulnerable plaques, as long as the detection method is sensitive enough and does not interfere with plaque stability. Combined with an imaging modality that can detect stenosis, we can discriminate between plaques that are considered to be healed or more stable, and plaques that present a more vulnerable type (Table 5).

Table 5 Timeline of atherosclerotic plaque detection						
Atherosclerotic plaque type	**I**	**II**	**III**	**IV**	**V**	**VI**
αvβ3 expression	-	-	-	+	+/-	+++
Lumen narrowing	-	-	-	+/-	+	++
Plaque detection	**-** Not detectable			**+/-** Early Plaque (Advanced atherosclerosis)	**+** Late plaque	

Another goal of this study was to understand atherosclerosis formation in the context of other diseases. For this purpose, an AD-HIES disease model was used to look at specific markers of atherosclerosis. Since AD-HIES patient had been shown to present unexpected high level of coronary artery dilatations and aneurysms, markers of those processes have been evaluated. Over the recent years, it had been largely debated if atherosclerosis and aneurysms were developing concurrently, or if one causes the other. Most imaging study concluded that the two mechanisms were likely to be developing in parallel, although studies were unable to convincingly refute the involvement of atherosclerosis in aneurysm formation. In the AD-HIES case, the hypothesis that the atherosclerotic plaque directly caused aneurysm formation seems to be the more plausible

(Fig. 65). Effectively, in a study published in Nature Medicine in 2004, it was shown that STAT3 inhibition by dominant negative mutation or antisense produced an augmentation of the proinflammatory cytokines (TNF-α, RANTES, IL-6), and inverse effects were observed with STAT3 activation (inhibition of RANTES and IL-6 expression)[178]. As seen previously, IL-6 activation via JAK/STAT3 cascade is involved in migration, proliferation (cell survival), remodeling and angiogenesis, ultimately leading to healing. In the other hand, IL-6 activation via ERK/MAPK cascade lead to MMP-9 expression, which is involved in compensatory enlargement (positive remodeling). Consequently, STAT3 mutation will lead to detrimental effects on plaque stabilization via two important mechanisms. First, they will be constant feeding of IL-6 cytokine, because STAT3 mutation upregulates IL-6 production. Second, STAT3 mutation will prevent the IL-6 response via Jak/STAT3 cascade. In conjunction, those two mechanisms will favor aneurysm formation. It can also be mention that the defect in lymphocyte T maturation (Th17 defect) caused by STAT3 mutation can further prevent proper plaque healing and exacerbate aneurysm formation, as cross-talk between macrophages and lymphocytes is important for neointima formation and stenosis processes.

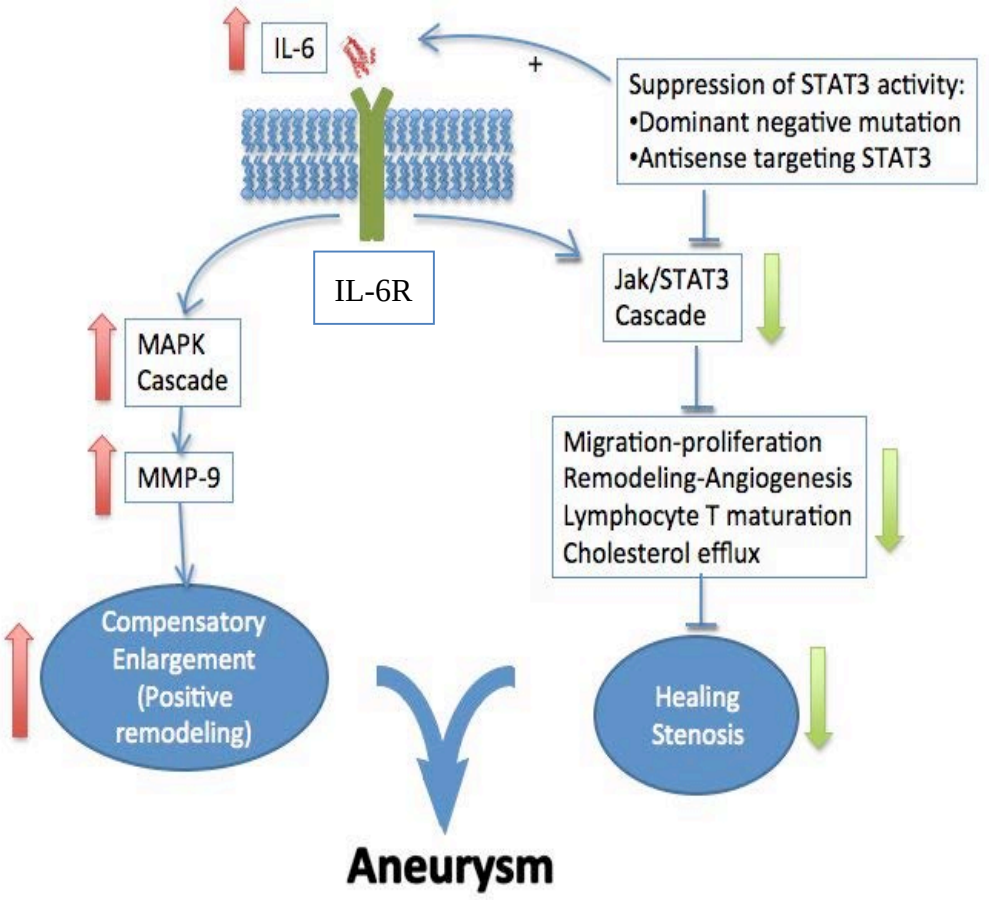

Figure 65 **Proposition of signaling pathways leading to aneurysm formation in AD-HIES disease**

STAT3 inhibition, by dominant negative mutation or antisense, lead to a pro-inflammatory state (IL-6 production). IL-6, via MAPK cascade, upregulates MMP-9 expression and favor compensatory arterial enlargement (positive remodeling). In the other hand, STAT3 mutation block IL-6 effect via JAK/STAT, which causes less migration, proliferation (cell survival), negative remodeling and angiogenesis. The consequences are detrimental to the process of healing. STAT3 mutation also prevents lymphocyte T maturation, which has been involved in stenosis formation. Taken together, the activation of the MAPK cascade and the inhibition of the Jak/STAT3 cascade, altogether with the proinflammatory state (IL-6 production) will ultimately favor aneurysm formation.

Finally, AD-HIES disease is also an interesting model for the development and study of the inflammatory process, because it is classify as an immunodeficiency disease. Effectively, those patients have recurrent bacterial infections and they have difficulty to clear them. It is therefore surprising to see a more vulnerable type of plaque in the AD-HIES disease model, as advanced atherosclerosis is often linked to an exacerbated inflammatory process. In the other hand, as mention before, it had been shown that mutation in STAT3 produced a more inflammatory state (RANTES, IL-6, TNF-α), as opposed to STAT3 activation that seemed to block Il-6 and RANTES expression[178]. This paradoxical situation is also present in HIV patient. Effectively, although HIV patients are immunocompromised, they are predisposed to atherosclerosis. It is unclear if this is due to the disease itself or to the medication taken. We can draw a parallel between these two diseases. Effectively, inflammatory processes, although recognized as being central in atherosclerosis formation, are also an important part of the healing mechanism. Therefore, anti-inflammatory therapy for the treatment of atherosclerotic disease can also lead to complications like aneurysm formation, in the presence of other conditions. It is also to be noted that both AD-HIES disease and HIV patients develop a lymphocyte T deficiency, either by absence of maturation or direct viral destruction. CD40 and CD40L, playing an important part in the cross-talk between macrophages and lymphocytes T, had been largely linked to restenosis and neointimal formation[156, 179, 180]. This pathway is considered to be of major importance in the development of atherosclerosis progression and complications, and strategies to inhibit it are under investigation. AD-HIES and HIV model can challenge this prevailing concept and showed that CD40 signaling can also provide a more beneficial effect, by allowing neointimal formation and luminal stenosis,

both involved into the plaque healing process. Effectively, macrophages releasing MMPs are an important process for clearing the path for SMCs migration. In presence of lymphocytes T, they can play their role and allow SMCs to begin the process of plaque healing. In the other way, in absence of lymphocyte T, their detrimental effect on ECM degradation is not counterbalance by SMCs proliferation, migration and matrix deposition. This could lead to diminution of vessel wall integrity and can cause plaque rupture. Rather than being involved in plaque rupture, lymphocyte T and IL-6 cascade, which are usually thought to be pro-inflammatory and detrimental to plaque stability, could be a major determinant in plaque healing. Consequently, presence of innate immunity, but defect in adaptive immunity could lead to absence of atherosclerosis healing and plaque rupture. Rather than being an exacerbated inflammatory process, plaque rupture will be the result of an inflammatory process that somewhere fails to be completed, because of the absence of key players, especially adaptive immunity. Indeed, many diseases causing low lymphocyte T count have been linked to atherosclerosis. For example, infections (viral or bacterial), HIV, tuberculosis, neurological and autoimmune diseases, and drugs can all lead to low level of circulating lymphocytes T. It is interesting to note that all of those diseases or conditions have also been linked to atherosclerosis. The same parallel can be deducted from atherosclerosis and aging. After all, there is no doubt that atherosclerosis is and aging disease, and aging is also responsible to lessen efficiency of immune system response. Although atherosclerosis is a multifaceted disease, the numeral relationships between immune defects, especially low lymphocyte T count, can hardly be seen as a pure coincidence. This can bring the intricate idea that reestablishing the crucial cross-talk between inflammatory cells can lead to plaque

stabilization. This also leads us to question the way we approach cardiovascular diseases. It becomes clear that genetic (as in the AD-HIES case) and the concomitant presence of other pathologies (HIV, asthma, infection, allergies, diabetes) can affect the atherosclerotic process and tips the balance toward plaque rupture and MI and stroke. In this regard, drugs and treatment administered to patients (particularly statins, NSAIDs, steroids) should take those other criteria into considerations. Consequently, in the future, it seems important to redirect the global medicine approach toward a more personalized medicine and an individual assessment of the patient.

CONCLUSION AND LIMITATION

In this study, we reported the efficiency of a new αvβ3 ITOP to specifically label atherosclerotic plaques both *in vitro* and *in vivo* on a Watanabe rabbit model. We also showed that the αvβ3 ITOP was efficiently labeling human atherosclerotic plaque *in vitro*. In both animal model and human, the intensity of the αvβ3 ITOP labeling seemed to be correlated with the degree of adventitial thickening. This was an important finding, since adventitial thickening had been previously reported in plaque neovascularization, a process that was also related to plaque vulnerability. Human and animal samples also revealed a relationship between the αvβ3 signal and some markers of vulnerability, as inflammatory infiltration, intraplaque hemorrhages, medial necrosis and calcifications. More extensive studies on the correlation between the intensity of the αvβ3 ITOP signal and the plaque morphology will be necessary. Moreover, in human samples, there was an association between the αvβ3 signal and the degree of stenosis. Effectively, angiogenesis and neovascularization are involved in both ischemia and hypoxia mechanisms. It seems intuitive that stenotic plaques will necessitate more angiogenesis to compensate for the lack of oxygen into the neointima. In this study, we showed that plaque with high stenosis demonstrated important αvβ3 ITOP labeling, and early plaque with minimal stenosis seemed to demonstrate a less intense αvβ3 ITOP signal. A better understanding of the ITOP probe in the context of plaque morphology and composition could lead to not only detection of advanced plaques, but also detection of plaques that have the potency to rupture.

One important limitation of this study is the absence of probe characterization. Although the probe had been tested on cancer model previously, there were no data on specificity of labeling on cell lines. This is an important step, as it allows demonstration of the specificity of the probe for a certain target, αvβ3 in our case, compare to other types of integrins, as αvβ5 for example. For example, there are different cell lines, as M21, MCF7, A375 or U251, that are expressing either avb3, avb5, both or neither of them, that can be use to evaluate the specificity of our compound.

Another limitation is the cross-sectional nature of the study. Effectively, both *in vitro* and *in vivo* experiments have been done on either cross-sectional sections of aortas, or cross-sectional sections of coronary arteries. This limit the conclusions that could be draw, because there is no information on the entire arterial or coronary tree. For further probe characterization and morphological analysis, probe imaging on the entire aortic tissue *ex vivo*, or *in vivo* imaging with another imaging agent, will be necessary. PET agents, for example, could be used.

The present study focused on pathology and immunohistology data. We evaluated the efficiency of the probe by immunofluorescence, as well as characterized the morphology and molecular markers of the samples by histological staining, immunofluorescence and immunochemistry. In order to confirm the results, it would be interesting to look at other methods of analysis. For examples, we could use Western Blot to confirm the presence of αvβ3 in the aortic tissue of the Watanabe rabbit with plaque. For MMP expression, we could use zymography, which not only shows the overexpression of MMPs, but also the presence of active molecule by showing enzymatic activity. The use of in situ PCR on slide would be interesting to verify the overexpression of αvβ3 in human samples.

Electromobility shift essay (EMSA) could also have confirmed in the AD-HIES case the diminution of STAT3 activity. Even though the pathological data and immunological studies demonstrated the efficiency of our αvβ3 ITOP probe to label atherosclerotic plaques, confirmation of the results with other techniques is always beneficial.

FUTURE PERSPECTIVES

Clinical Applicability

As mentioned before, the actual techniques for the detection of atherosclerosis are mostly based on plaque with stenosis. Unfortunately, it had been shown that the majority of ruptured plaques causing cardiovascular events are plaques in positive remodeling phase, with minimal degree of stenosis. Thus, it becomes very important to be able to detect plaque not only at an earlier stage, but also be able to assess the plaque composition and potency to rupture. Because of its physicochemical properties, especially high affinity (IC_{50} of 3nM *in vitro*) and great selectivity (IC50 > 100μM *in vitro*), the αvβ3 ITOP has great potential to detect plaques with signs of vulnerability. Moreover, it has 20X times higher binding affinity for αvβ3 compared to the commercially available cyclic peptide c[RGDfv], and the *in vivo* results on tumor bearing mice showed efficient and specific labeling. Recently, the probe had also been labeled with ^{68}Ga and linked with NODAGA, and tested on human cancer with very promising results. The probe didn't show any toxicity and efficiently detect cancer in human. In this first human study in a breast cancer patient, the study reported 25 integrin αvβ3 positive lesions detected by the probe

(THERANOST cRGD™), versus 12 by ^{18}F FDG. They also pointed out many advantages over ^{18}F and ^{64}Cu labeled RGD peptides, like the availability of ^{68}Ga, the convenient radiolabelling, the high stability and the good imaging properties. This could translate into an interesting probe to detect atherosclerotic plaques with neovascularization process or vulnerability markers. More importantly, we showed that this αvβ3 ITOP could detect *in vitro* the first type of advanced plaques (type IV) in an AD-HIES model. This plaque was characterized by positive remodeling and showed important signs of vulnerability. If the detection method for the ITOP is sensitive enough, the potential for clinical translation and applicability is promising.

The ITOP is currently being modified by a group of chemist at the NIH (Dr. Martin Briechber), who are working on different possibilities for imaging modality. As mention, it had been labeled with ^{68}Ga and successfully used in human for cancer detection. Since toxicity study in human had been done, it could be easier to translate it into nuclear imaging of atherosclerosis. It is also being labeled with near infrared fluorescence (NIRF), which possesses better sensitivity and less background than green fluorescence (FITC). Unfortunately, because coronary arteries are localized deeper in the body, it will necessitate the use of catheters. Still, with the recent development in new and more efficient catheters, detection of vulnerable plaques with this ITOP becomes possible.

On the other hand, one important point has to be mention: the αvβ3 ITOP developed is an antagonist of the αvβ3 receptor. The possibility of inhibiting the receptor and it effects on angiogenesis has to be kept in mind when using it as a molecular marker for imaging. Effectively, as mention before, even though neovascularization has been linked to detrimental effects as plaque vulnerability and instability, beneficial effects on plaque

healing and stenosis had also been demonstrated. Further investigations will be needed to insure enough sensitivity for efficient detection of atherosclerotic plaques, without producing any adverse effect on plaque stability. Nevertheless, chemical modifications and changes in design can be use to improve safety, if it becomes a concern. It can also be noted that the αvβ3 ITOP could be better suitable as a molecular tool for the analysis of atherosclerosis, as it seemed to response with more sensitivity to the αvβ3 receptor than the commercially available antibody. Nevertheless, its use in cancer detection and treatment remains appropriate.

Future Investigation on Pathology and Plaque Morphology

The field of atherosclerosis and plaque characterization involves a variety of specialties, and necessitates an important degree of general knowledge in a variety of field. Indeed, mathematical models, biological characterization, pathological observation, and imaging modalities, all come together to help elucidate the complex phenomenon involved in plaque vulnerability, plaque destabilization, and their clinical outcomes. During the past few years, important emphasis had been made on the understanding and characterization of the vulnerable plaques. Continuing this fundamental work is very important, as it can lead to early detection of atherosclerosis, and prevent the apparition of the clinical sequelae. Importantly, future investigations on plaques characterized as “vulnerable” will allow the development and perfecting of imaging techniques, and put the emphasis on the molecules with the most impact on plaque vulnerability. For example, understanding signaling pathways involved in vascular remodeling, particularly positive remodeling, will be a major advancement, since it is often seen in plaque rupture, and it is extremely

difficult to observe by the actual imaging modalities. Also the association between immunodeficiency and plaque formation would be an interesting field to look at, as in the AD-HIES case, atherosclerosis seems to be linked to aneurysm formation. A link between immunodeficiency and atherosclerosis can also be observed in HIV patient, who had been reported to be susceptible to atherosclerosis. This suggests an important role of the adaptive immunity in atherosclerotic plaque healing. Another important player, as seen in this study, will be plaque neovascularization and its impact on plaque vulnerability. It is all the more important since advancement in imaging technique as MRI and CT, with the help of contrast agent, now allow us to better visualized the adventitia layer of the coronary artery. If we can better understand the association between neovascularization and vulnerability, we can develop imaging technique to assess plaque instability. It is also important to understand the different mechanisms of plaque vascularization, depending of the cytokine profile and growth factors involved, as it can tip the balance in favor of plaque stabilization or in an opposite way toward instability. This fundamental work to understand the basic molecular processes associated with atherosclerosis progression and plaque vulnerability is crucial, as it can provide molecular targets to develop and perfect all the different imaging modalities.

Clinical Work in Atherosclerosis Field

In this study, we emphasized the importance of working closely with clinicians to better understand and detect vulnerable plaques. In fact, imaging modalities combined with pathological data can lead to important advances in the detection of atherosclerotic plaques. Animal model can be very helpful to help elucidating important mechanism of

plaque ruptures/healing (positive remodeling, intraplaque hemorrhage, inflammation, etc.), but they are also limiting, in a sense that there is no perfect animal model that completely mimic human atherosclerotic processes, each one presenting its own strengths and weaknesses. Indeed, no animal model can recreate the phenomenal complexity of human atherosclerotic processes. Ultimately, we need to test our hypothesis on human and in a clinical setting, so we can validate the finding of animal studies. Also, human samples from autopsies from different populations and genetic background are extremely useful to help understanding atherosclerosis. Indeed, it is the evaluation and characterization of atherosclerosis in patients with other pathologies, as seen in AD-HIES and HIV diseases, that will allow us to progress with the ultimate goal of detecting atherosclerotic plaques before the clinical outcomes. Moreover, cell based studies on cells extracted from different patients are becoming a very efficient tool to investigate atherosclerotic diseases. It allows better understanding of the cytokine profile for different type of cells in a more clinical setting than with cell culture, because cells are extracted directly from human tissues or blood. In this regard, combining autopsy samples or blood analysis, research data and clinical reports will constitute a powerful tool for future investigation and discovery.

Other Probe Design (ox-LDL)

The focus of this thesis was the characterization of a new optical imaging probe targeting $\alpha v\beta 3$ receptors, in diverse atherosclerotic models (animals, humans, STAT3 genetic disease). As documented in the chapter about the biomarkers of instability, there are other molecular targets that we can use to develop probes. MMPs are one example of

molecules playing an important role in plaque destabilization and vulnerability. There are already an important number of publications showing successful use of MMP probes in the detection of atherosclerosis, particularly MMP activatable probes. Macrophages are also of interest for the development of probes, because they definitively play a central role in the development of atherosclerosis, and being natural phagocytes, they are easily labeled. Most importantly, there is a growing interest into oxidized LDLs, as potent markers of atherosclerotic disease. Indeed, since LDL oxidation appears to be one of the first steps of plaque accumulation and also the one causing most of the vascular damages, we can postulate that ox-LDL will be an interesting target to look at. On the other hand, structural component of the vascular wall can also be use as imaging probe. For example, elastic fibers forming the internal and external elastic lamina in coronary arteries are crucial for tissue integrity and the degradation of those fibers can lead to a diminution of arteries' elasticity, positive remodeling and plaque ruptures. Accordingly, imaging elastic fibers as well as plaque lipids can be a good method to predict possible rupture. These molecular targets are usually strongly correlated with plaque instability, but there is also a multitude of other possible players that need to be evaluated for developing probes, as well as many probe designs (monomer, polymer, nanoparticle, antibody, etc.…).

In order to overcome the challenge of detecting atherosclerosis before the clinical outcome of heart attack and stroke, it becomes essential that basic research scientists and physicians collaborate closely together to develop a better understanding of plaque vulnerability and apply it to perfect the actual imaging techniques. Effectively, with the major contribution of clinicians and their access to patients with different pathologies, basic research will allow to identify important targets in plaque development and rupture

that can be further incorporated into imaging techniques. Indeed, the studies of patients with different genetic background can greatly help elucidating the mechanism of atherosclerosis and plaque ruptures. Therefore, it is fundamental that we continue to strengthen the collaboration between researchers and clinicians, and that we develop more bench-to-bedside projects.

REFERENCES

[1] Lopez AD, Murray CC. The global burden of disease, 1990-2020. Nat Med. 1998 Nov;4(11):1241-3.

[2] Roger VL, Go AS, Lloyd-Jones DM, Benjamin EJ, Berry JD, Borden WB, et al. Heart disease and stroke statistics--2012 update: a report from the American Heart Association. Circulation. 2012 Jan 3;125(1):e2-e220.

[3] Mauriello A, Sangiorgi GM, Virmani R, Trimarchi S, Holmes DR, Jr., Kolodgie FD, et al. A pathobiologic link between risk factors profile and morphological markers of carotid instability. Atherosclerosis. 2010 Feb;208(2):572-80.

[4] Libby P. Inflammation in atherosclerosis. Nature. 2002 Dec 19-26;420(6917):868-74.

[5] Libby P. Current concepts of the pathogenesis of the acute coronary syndromes. Circulation. 2001 Jul 17;104(3):365-72.

[6] Libby P. Inflammation in atherosclerosis. Arteriosclerosis, thrombosis, and vascular biology. 2012 Sep;32(9):2045-51.

[7] Glagov S, Vito R, Giddens DP, Zarins CK. Micro-architecture and composition of artery walls: relationship to location, diameter and the distribution of mechanical stress. J Hypertens Suppl. 1992 Aug;10(6):S101-4.

[8] Subbotin VM. Analysis of arterial intimal hyperplasia: review and hypothesis. Theoretical biology & medical modelling. 2007;4:41.

[9] Libby P. Atherosclerosis: disease biology affecting the coronary vasculature. Am J Cardiol. 2006 Dec 18;98(12A):3Q-9Q.

[10] Fuster V, Moreno PR, Fayad ZA, Corti R, Badimon JJ. Atherothrombosis and high-risk plaque: part I: evolving concepts. J Am Coll Cardiol. 2005 Sep 20;46(6):937-54.

[11] Virmani R, Kolodgie FD, Burke AP, Finn AV, Gold HK, Tulenko TN, et al. Atherosclerotic plaque progression and vulnerability to rupture: angiogenesis as a source of intraplaque hemorrhage. Arteriosclerosis, thrombosis, and vascular biology. 2005 Oct;25(10):2054-61.

[12] Burke AP, Kolodgie FD, Farb A, Weber D, Virmani R. Morphological predictors of arterial remodeling in coronary atherosclerosis. Circulation. 2002 Jan 22;105(3):297-303.

[13] Ohayon J, Finet G, Gharib AM, Herzka DA, Tracqui P, Heroux J, et al. Necrotic core thickness and positive arterial remodeling index: emergent biomechanical factors for evaluating the risk of plaque rupture. American journal of physiology. 2008 Aug;295(2):H717-27.

[14] Kroner ES, van Velzen JE, Boogers MJ, Siebelink HM, Schalij MJ, Kroft LJ, et al. Positive remodeling on coronary computed tomography as a marker for plaque vulnerability on virtual histology intravascular ultrasound. Am J Cardiol. 2011 Jun 15;107(12):1725-9.

[15] Varnava AM, Mills PG, Davies MJ. Relationship between coronary artery remodeling and plaque vulnerability. Circulation. 2002 Feb 26;105(8):939-43.

[16] Hong YJ, Jeong MH, Choi YH, Ko JS, Lee MG, Kang WY, et al. Positive remodeling is associated with more plaque vulnerability and higher frequency of plaque prolapse accompanied with post-procedural cardiac enzyme elevation compared with intermediate/negative remodeling in patients with acute myocardial infarction. J Cardiol. 2009 Apr;53(2):278-87.
[17] Glagov S, Weisenberg E, Zarins CK, Stankunavicius R, Kolettis GJ. Compensatory enlargement of human atherosclerotic coronary arteries. N Engl J Med. 1987 May 28;316(22):1371-5.
[18] Finn AV, Nakano M, Narula J, Kolodgie FD, Virmani R. Concept of vulnerable/unstable plaque. Arteriosclerosis, thrombosis, and vascular biology. 2010 Jul;30(7):1282-92.
[19] Stary HC, Chandler AB, Dinsmore RE, Fuster V, Glagov S, Insull W, Jr., et al. A definition of advanced types of atherosclerotic lesions and a histological classification of atherosclerosis. A report from the Committee on Vascular Lesions of the Council on Arteriosclerosis, American Heart Association. Circulation. 1995 Sep 1;92(5):1355-74.
[20] Stary HC, Chandler AB, Dinsmore RE, Fuster V, Glagov S, Insull W, Jr., et al. A definition of advanced types of atherosclerotic lesions and a histological classification of atherosclerosis. A report from the Committee on Vascular Lesions of the Council on Arteriosclerosis, American Heart Association. Arteriosclerosis, thrombosis, and vascular biology. 1995 Sep;15(9):1512-31.
[21] Li X, Kramer MC, van der Loos CM, Koch KT, de Boer OJ, Henriques JP, et al. A pattern of disperse plaque microcalcifications identifies a subset of plaques with high inflammatory burden in patients with acute myocardial infarction. Atherosclerosis. 2011 Sep;218(1):83-9.
[22] Libby P, Theroux P. Pathophysiology of coronary artery disease. Circulation. 2005 Jun 28;111(25):3481-8.
[23] Naghavi M, Libby P, Falk E, Casscells SW, Litovsky S, Rumberger J, et al. From vulnerable plaque to vulnerable patient: a call for new definitions and risk assessment strategies: Part I. Circulation. 2003 Oct 7;108(14):1664-72.
[24] Stary HC, Blankenhorn DH, Chandler AB, Glagov S, Insull W, Jr., Richardson M, et al. A definition of the intima of human arteries and of its atherosclerosis-prone regions. A report from the Committee on Vascular Lesions of the Council on Arteriosclerosis, American Heart Association. Arterioscler Thromb. 1992 Jan;12(1):120-34.
[25] Stary HC, Blankenhorn DH, Chandler AB, Glagov S, Insull W, Jr., Richardson M, et al. A definition of the intima of human arteries and of its atherosclerosis-prone regions. A report from the Committee on Vascular Lesions of the Council on Arteriosclerosis, American Heart Association. Circulation. 1992 Jan;85(1):391-405.
[26] Stary HC, Chandler AB, Glagov S, Guyton JR, Insull W, Jr., Rosenfeld ME, et al. A definition of initial, fatty streak, and intermediate lesions of atherosclerosis. A report from the Committee on Vascular Lesions of the Council on Arteriosclerosis, American Heart Association. Circulation. 1994 May;89(5):2462-78.
[27] Stary HC, Chandler AB, Glagov S, Guyton JR, Insull W, Jr., Rosenfeld ME, et al. A definition of initial, fatty streak, and intermediate lesions of atherosclerosis.

A report from the Committee on Vascular Lesions of the Council on Arteriosclerosis, American Heart Association. Arterioscler Thromb. 1994 May;14(5):840-56.
[28] Leuschner F, Nahrendorf M. Molecular imaging of coronary atherosclerosis and myocardial infarction: considerations for the bench and perspectives for the clinic. Circulation research. 2011 Mar 4;108(5):593-606.
[29] Zhang Y, Wang H. Integrin signalling and function in immune cells. Immunology. 2012 Apr;135(4):268-75.
[30] Labat-Robert J. Cell-Matrix interactions, the role of fibronectin and integrins. A survey. Pathologie-biologie. 2012 Feb;60(1):15-9.
[31] Malinin NL, Pluskota E, Byzova TV. Integrin signaling in vascular function. Current opinion in hematology. 2012 May;19(3):206-11.
[32] Weerasinghe D, McHugh KP, Ross FP, Brown EJ, Gisler RH, Imhof BA. A role for the alphavbeta3 integrin in the transmigration of monocytes. The Journal of cell biology. 1998 Jul 27;142(2):595-607.
[33] Moraes J, Assreuy J, Canetti C, Barja-Fidalgo C. Leukotriene B4 mediates vascular smooth muscle cell migration through alphavbeta3 integrin transactivation. Atherosclerosis. 2010 Oct;212(2):406-13.
[34] Brooks PC, Clark RA, Cheresh DA. Requirement of vascular integrin alpha v beta 3 for angiogenesis. Science (New York, NY. 1994 Apr 22;264(5158):569-71.
[35] Huang J, Roth R, Heuser JE, Sadler JE. Integrin alpha(v)beta(3) on human endothelial cells binds von Willebrand factor strings under fluid shear stress. Blood. 2009 Feb 12;113(7):1589-97.
[36] Xiong JP, Stehle T, Diefenbach B, Zhang R, Dunker R, Scott DL, et al. Crystal structure of the extracellular segment of integrin alpha Vbeta3. Science (New York, NY. 2001 Oct 12;294(5541):339-45.
[37] Xiong JP, Mahalingham B, Alonso JL, Borrelli LA, Rui X, Anand S, et al. Crystal structure of the complete integrin alphaVbeta3 ectodomain plus an alpha/beta transmembrane fragment. The Journal of cell biology. 2009 Aug 24;186(4):589-600.
[38] Kim C, Ye F, Hu X, Ginsberg MH. Talin activates integrins by altering the topology of the beta transmembrane domain. The Journal of cell biology. 2012 May 28;197(5):605-11.
[39] Shimaoka M, Takagi J, Springer TA. Conformational regulation of integrin structure and function. Annual review of biophysics and biomolecular structure. 2002;31:485-516.
[40] Chen N, Leu SJ, Todorovic V, Lam SC, Lau LF. Identification of a novel integrin alphavbeta3 binding site in CCN1 (CYR61) critical for pro-angiogenic activities in vascular endothelial cells. The Journal of biological chemistry. 2004 Oct 15;279(42):44166-76.
[41] Hoshiga M, Alpers CE, Smith LL, Giachelli CM, Schwartz SM. Alpha-v beta-3 integrin expression in normal and atherosclerotic artery. Circulation research. 1995 Dec;77(6):1129-35.
[42] Srivatsa SS, Fitzpatrick LA, Tsao PW, Reilly TM, Holmes DR, Jr., Schwartz RS, et al. Selective alpha v beta 3 integrin blockade potently limits neointimal hyperplasia and lumen stenosis following deep coronary arterial stent injury:

evidence for the functional importance of integrin alpha v beta 3 and osteopontin expression during neointima formation. Cardiovasc Res. 1997 Dec;36(3):408-28.
[43] Bendeck MP, Irvin C, Reidy M, Smith L, Mulholland D, Horton M, et al. Smooth muscle cell matrix metalloproteinase production is stimulated via alpha(v)beta(3) integrin. Arteriosclerosis, thrombosis, and vascular biology. 2000 Jun;20(6):1467-72.
[44] Yung YC, Chae J, Buehler MJ, Hunter CP, Mooney DJ. Cyclic tensile strain triggers a sequence of autocrine and paracrine signaling to regulate angiogenic sprouting in human vascular cells. Proceedings of the National Academy of Sciences of the United States of America. 2009 Sep 8;106(36):15279-84.
[45] Asano Y, Ihn H, Yamane K, Jinnin M, Mimura Y, Tamaki K. Increased expression of integrin alpha(v)beta3 contributes to the establishment of autocrine TGF-beta signaling in scleroderma fibroblasts. J Immunol. 2005 Dec 1;175(11):7708-18.
[46] Antonov AS, Kolodgie FD, Munn DH, Gerrity RG. Regulation of macrophage foam cell formation by alphaVbeta3 integrin: potential role in human atherosclerosis. Am J Pathol. 2004 Jul;165(1):247-58.
[47] Cheng J, Zhang J, Merched A, Zhang L, Zhang P, Truong L, et al. Mechanical stretch inhibits oxidized low density lipoprotein-induced apoptosis in vascular smooth muscle cells by up-regulating integrin alphavbeta3 and stablization of PINCH-1. The Journal of biological chemistry. 2007 Nov 23;282(47):34268-75.
[48] Storgard CM, Stupack DG, Jonczyk A, Goodman SL, Fox RI, Cheresh DA. Decreased angiogenesis and arthritic disease in rabbits treated with an alphavbeta3 antagonist. J Clin Invest. 1999 Jan;103(1):47-54.
[49] Winter PM, Neubauer AM, Caruthers SD, Harris TD, Robertson JD, Williams TA, et al. Endothelial alpha(v)beta3 integrin-targeted fumagillin nanoparticles inhibit angiogenesis in atherosclerosis. Arteriosclerosis, thrombosis, and vascular biology. 2006 Sep;26(9):2103-9.
[50] Xie J, Shen Z, Li KC, Danthi N. Tumor angiogenic endothelial cell targeting by a novel integrin-targeted nanoparticle. Int J Nanomedicine. 2007;2(3):479-85.
[51] Slevin M, Krupinski J, Badimon L. Controlling the angiogenic switch in developing atherosclerotic plaques: possible targets for therapeutic intervention. Journal of angiogenesis research. 2009;1:4.
[52] Siefert SA, Sarkar R. Matrix metalloproteinases in vascular physiology and disease. Vascular. 2012 Aug 15.
[53] Li H, Xu H, Sun B. Lipopolysaccharide regulates MMP-9 expression through TLR4/NF-kappaB signaling in human arterial smooth muscle cells. Molecular medicine reports. 2012 Oct;6(4):774-8.
[54] Swarnakar S, Mishra A, Chaudhuri SR. The gelatinases and their inhibitors: the structure-activity relationships. Exs. 2012;103:57-82.
[55] Radhika A, Sudhakaran PR. Upregulation of macrophage-specific functions by oxidized LDL: lysosomal degradation-dependent and -independent pathways. Molecular and cellular biochemistry. 2012 Sep 30.
[56] Xu S, Shriver AS, Jagadeesha DK, Chamseddine AH, Szocs K, Weintraub NL, et al. Increased expression of Nox1 in neointimal smooth muscle cells promotes

activation of matrix metalloproteinase-9. Journal of vascular research. 2012;49(3):242-8.
[57] Paolillo R, Iovene MR, Romano Carratelli C, Rizzo A. Induction of VEGF and MMP-9 expression by toll-like receptor 2/4 in human endothelial cells infected with Chlamydia pneumoniae. International journal of immunopathology and pharmacology. 2012 Apr-Jun;25(2):377-86.
[58] Lemaitre V, O'Byrne TK, Borczuk AC, Okada Y, Tall AR, D'Armiento J. ApoE knockout mice expressing human matrix metalloproteinase-1 in macrophages have less advanced atherosclerosis. The Journal of clinical investigation. 2001 May;107(10):1227-34.
[59] Gough PJ, Gomez IG, Wille PT, Raines EW. Macrophage expression of active MMP-9 induces acute plaque disruption in apoE-deficient mice. The Journal of clinical investigation. 2006 Jan;116(1):59-69.
[60] Newby AC. Dual role of matrix metalloproteinases (matrixins) in intimal thickening and atherosclerotic plaque rupture. Physiological reviews. 2005 Jan;85(1):1-31.
[61] Ross R. Atherosclerosis--an inflammatory disease. N Engl J Med. 1999 Jan 14;340(2):115-26.
[62] Murray PJ, Wynn TA. Protective and pathogenic functions of macrophage subsets. Nat Rev Immunol. 2011 Nov;11(11):723-37.
[63] Fernandez-Hernando C, Jozsef L, Jenkins D, Di Lorenzo A, Sessa WC. Absence of Akt1 reduces vascular smooth muscle cell migration and survival and induces features of plaque vulnerability and cardiac dysfunction during atherosclerosis. Arteriosclerosis, thrombosis, and vascular biology. 2009 Dec;29(12):2033-40.
[64] Clarke MC, Littlewood TD, Figg N, Maguire JJ, Davenport AP, Goddard M, et al. Chronic apoptosis of vascular smooth muscle cells accelerates atherosclerosis and promotes calcification and medial degeneration. Circulation research. 2008 Jun 20;102(12):1529-38.
[65] Ewence AE, Bootman M, Roderick HL, Skepper JN, McCarthy G, Epple M, et al. Calcium phosphate crystals induce cell death in human vascular smooth muscle cells: a potential mechanism in atherosclerotic plaque destabilization. Circulation research. 2008 Aug 29;103(5):e28-34.
[66] Bennett M, Yu H, Clarke M. Signalling from dead cells drives inflammation and vessel remodelling. Vascul Pharmacol. 2012 May-Jun;56(5-6):187-92.
[67] Yu H, Clarke MC, Figg N, Littlewood TD, Bennett MR. Smooth muscle cell apoptosis promotes vessel remodeling and repair via activation of cell migration, proliferation, and collagen synthesis. Arteriosclerosis, thrombosis, and vascular biology. 2011 Nov;31(11):2402-9.
[68] Diaz-Zamudio M, Bacilio-Perez U, Herrera-Zarza MC, Meave-Gonzalez A, Alexanderson-Rosas E, Zambrana-Balta GF, et al. Coronary artery aneurysms and ectasia: role of coronary CT angiography. Radiographics. 2009 Nov;29(7):1939-54.
[69] Teitelbaum SL. Osteoporosis and integrins. The Journal of clinical endocrinology and metabolism. 2005 Apr;90(4):2466-8.
[70] Winter PM, Caruthers SD, Allen JS, Cai K, Williams TA, Lanza GM, et al. Molecular imaging of angiogenic therapy in peripheral vascular disease with

alphanubeta3-integrin-targeted nanoparticles. Magn Reson Med. 2010 Aug;64(2):369-76.
[71] Salehi-Had H, Roh MI, Giani A, Hisatomi T, Nakao S, Kim IK, et al. Utilizing targeted gene therapy with nanoparticles binding alpha v beta 3 for imaging and treating choroidal neovascularization. PloS one. 2011;6(4):e18864.
[72] Bishop GG, McPherson JA, Sanders JM, Hesselbacher SE, Feldman MJ, McNamara CA, et al. Selective alpha(v)beta(3)-receptor blockade reduces macrophage infiltration and restenosis after balloon angioplasty in the atherosclerotic rabbit. Circulation. 2001 Apr 10;103(14):1906-11.
[73] Quinn MJ, Byzova TV, Qin J, Topol EJ, Plow EF. Integrin alphaIIbbeta3 and its antagonism. Arteriosclerosis, thrombosis, and vascular biology. 2003 Jun 1;23(6):945-52.
[74] Brooks PC, Montgomery AM, Rosenfeld M, Reisfeld RA, Hu T, Klier G, et al. Integrin alpha v beta 3 antagonists promote tumor regression by inducing apoptosis of angiogenic blood vessels. Cell. 1994 Dec 30;79(7):1157-64.
[75] Ribatti D, Levi-Schaffer F, Kovanen PT. Inflammatory angiogenesis in atherogenesis--a double-edged sword. Annals of medicine. 2008;40(8):606-21.
[76] Scatena M, Almeida M, Chaisson ML, Fausto N, Nicosia RF, Giachelli CM. NF-kappaB mediates alphavbeta3 integrin-induced endothelial cell survival. The Journal of cell biology. 1998 May 18;141(4):1083-93.
[77] Winter PM, Morawski AM, Caruthers SD, Fuhrhop RW, Zhang H, Williams TA, et al. Molecular imaging of angiogenesis in early-stage atherosclerosis with alpha(v)beta3-integrin-targeted nanoparticles. Circulation. 2003 Nov 4;108(18):2270-4.
[78] Blankenberg S, Barbaux S, Tiret L. Adhesion molecules and atherosclerosis. Atherosclerosis. 2003 Oct;170(2):191-203.
[79] Doyle B, Caplice N. Plaque neovascularization and antiangiogenic therapy for atherosclerosis. J Am Coll Cardiol. 2007 May 29;49(21):2073-80.
[80] Waldeck J, Hager F, Holtke C, Lanckohr C, von Wallbrunn A, Torsello G, et al. Fluorescence Reflectance Imaging of Macrophage-Rich Atherosclerotic Plaques Using an {alpha}v{beta}3 Integrin-Targeted Fluorochrome. J Nucl Med. 2008 Oct 16.
[81] Sherif HM, Saraste A, Nekolla SG, Weidl E, Reder S, Tapfer A, et al. Molecular imaging of early alphavbeta3 integrin expression predicts long-term left-ventricle remodeling after myocardial infarction in rats. J Nucl Med. 2012 Feb;53(2):318-23.
[82] Zhang Y, Yang Y, Cai W. Multimodality Imaging of Integrin alpha(v)beta(3) Expression. Theranostics. 2011;1:135-48.
[83] Lanzardo S, Conti L, Brioschi C, Bartolomeo MP, Arosio D, Belvisi L, et al. A new optical imaging probe targeting alphaVbeta3 integrin in glioblastoma xenografts. Contrast media & molecular imaging. 2011 Nov-Dec;6(6):449-58.
[84] Liu S, Liu H, Ren G, Kimura RH, Cochran JR, Cheng Z. PET Imaging of Integrin Positive Tumors Using F Labeled Knottin Peptides. Theranostics. 2011;1:403-12.
[85] Beer AJ, Schwaiger M. PET imaging of alphavbeta3 expression in cancer patients. Methods in molecular biology (Clifton, NJ. 2011;680:183-200.

[86] Doss M, Kolb HC, Zhang JJ, Belanger MJ, Stubbs JB, Stabin MG, et al. Biodistribution and radiation dosimetry of the integrin marker 18F-RGD-K5 determined from whole-body PET/CT in monkeys and humans. J Nucl Med. 2012 May;53(5):787-95.
[87] Zhu Z, Miao W, Li Q, Dai H, Ma Q, Wang F, et al. 99mTc-3PRGD2 for integrin receptor imaging of lung cancer: a multicenter study. J Nucl Med. 2012 May;53(5):716-22.
[88] Boles KS, Schmieder AH, Koch AW, Carano RA, Wu Y, Caruthers SD, et al. MR angiogenesis imaging with Robo4- vs. alphaVbeta3-targeted nanoparticles in a B16/F10 mouse melanoma model. Faseb J. 2010 Nov;24(11):4262-70.
[89] Lee H, Akers W, Bhushan K, Bloch S, Sudlow G, Tang R, et al. Near-infrared pH-activatable fluorescent probes for imaging primary and metastatic breast tumors. Bioconjugate chemistry. 2011 Apr 20;22(4):777-84.
[90] Jang BS, Lim E, Hee Park S, Shin IS, Danthi SN, Hwang IS, et al. Radiolabeled high affinity peptidomimetic antagonist selectively targets alpha(v)beta(3) receptor-positive tumor in mice. Nuclear medicine and biology. 2007 May;34(4):363-70.
[91] Kim YS, Nwe K, Milenic DE, Brechbiel MW, Satz S, Baidoo KE. Synthesis and characterization of alpha(v)beta(3)-targeting peptidomimetic chelate conjugates for PET and SPECT imaging. Bioorganic & medicinal chemistry letters. 2012 Sep 1;22(17):5517-22.
[92] Burnett CA, Xie J, Quijano J, Shen Z, Hunter F, Bur M, et al. Synthesis, in vitro, and in vivo characterization of an integrin alpha(v)beta(3)-targeted molecular probe for optical imaging of tumor. Bioorg Med Chem. 2005 Jun 1;13(11):3763-71.
[93] Duggan ME, Duong LT, Fisher JE, Hamill TG, Hoffman WF, Huff JR, et al. Nonpeptide alpha(v)beta(3) antagonists. 1. Transformation of a potent, integrin-selective alpha(IIb)beta(3) antagonist into a potent alpha(v)beta(3) antagonist. J Med Chem. 2000 Oct 5;43(20):3736-45.
[94] Russell JC, Proctor SD. Small animal models of cardiovascular disease: tools for the study of the roles of metabolic syndrome, dyslipidemia, and atherosclerosis. Cardiovasc Pathol. 2006 Nov-Dec;15(6):318-30.
[95] Shiomi M, Ito T. The Watanabe heritable hyperlipidemic (WHHL) rabbit, its characteristics and history of development: a tribute to the late Dr. Yoshio Watanabe. Atherosclerosis. 2009 Nov;207(1):1-7.
[96] Shiomi M, Yamada S, Matsukawa A, Itabe H, Ito T. Invasion of atheromatous plaques into tunica media causes coronary outward remodeling in WHHLMI rabbits. Atherosclerosis. 2008 Jun;198(2):287-93.
[97] Holland SM, DeLeo FR, Elloumi HZ, Hsu AP, Uzel G, Brodsky N, et al. STAT3 mutations in the hyper-IgE syndrome. N Engl J Med. 2007 Oct 18;357(16):1608-19.
[98] Minegishi Y, Saito M, Tsuchiya S, Tsuge I, Takada H, Hara T, et al. Dominant-negative mutations in the DNA-binding domain of STAT3 cause hyper-IgE syndrome. Nature. 2007 Aug 30;448(7157):1058-62.
[99] Sowerwine KJ, Holland SM, Freeman AF. Hyper-IgE syndrome update. Ann N Y Acad Sci. 2012 Feb;1250:25-32.

[100] Freeman AF, Avila EM, Shaw PA, Davis J, Hsu AP, Welch P, et al. Coronary artery abnormalities in Hyper-IgE syndrome. J Clin Immunol. 2011 Jun;31(3):338-45.
[101] Chandesris MO, Azarine A, Ong KT, Taleb S, Boutouyrie P, Mousseaux E, et al. Frequent and widespread vascular abnormalities in human signal transducer and activator of transcription 3 deficiency. Circ Cardiovasc Genet. 2012 Feb 1;5(1):25-34.
[102] Nichols L, Lagana S, Parwani A. Coronary artery aneurysm: a review and hypothesis regarding etiology. Arch Pathol Lab Med. 2008 May;132(5):823-8.
[103] Dobrin PB, Baker WH, Gley WC. Elastolytic and collagenolytic studies of arteries. Implications for the mechanical properties of aneurysms. Arch Surg. 1984 Apr;119(4):405-9.
[104] Tilson MD. Status of research on abdominal aortic aneurysm disease. J Vasc Surg. 1989;9:367-9.
[105] Zatina MA, Zarins CK, Gewertz BL, Glagov S. Role of medial lamellar architecture in the pathogenesis of aortic aneurysms. J Vasc Surg. 1984 May;1(3):442-8.
[106] Bomberger RA, Zarins CK, Glagov S. Medial injury and hyperlipidemia in development of aneurysms or atherosclerotic plaques. Surg Forum. 1980;31:338-40.
[107] Johnsen SH, Forsdahl SH, Singh K, Jacobsen BK. Atherosclerosis in abdominal aortic aneurysms: a causal event or a process running in parallel? The Tromso study. Arteriosclerosis, thrombosis, and vascular biology. 2010 Jun;30(6):1263-8.
[108] Granger DN, Vowinkel T, Petnehazy T. Modulation of the inflammatory response in cardiovascular disease. Hypertension. 2004 May;43(5):924-31.
[109] Lassila R. Inflammation in atheroma: implications for plaque rupture and platelet-collagen interaction. Eur Heart J. 1993 Dec;14 Suppl K:94-7.
[110] Schroeder AP, Falk E. Vulnerable and dangerous coronary plaques. Atherosclerosis. 1995 Dec;118 Suppl:S141-9.
[111] Paulhe F, Racaud-Sultan C, Ragab A, Albiges-Rizo C, Chap H, Iberg N, et al. Differential regulation of phosphoinositide metabolism by alphaVbeta3 and alphaVbeta5 integrins upon smooth muscle cell migration. The Journal of biological chemistry. 2001 Nov 9;276(45):41832-40.
[112] Moreno PR, Purushothaman KR, Zias E, Sanz J, Fuster V. Neovascularization in human atherosclerosis. Curr Mol Med. 2006 Aug;6(5):457-77.
[113] Moreno PR, Purushothaman KR, Fuster V, O'Connor WN. Intimomedial interface damage and adventitial inflammation is increased beneath disrupted atherosclerosis in the aorta: implications for plaque vulnerability. Circulation. 2002 May 28;105(21):2504-11.
[114] Wilson SH, Herrmann J, Lerman LO, Holmes DR, Jr., Napoli C, Ritman EL, et al. Simvastatin preserves the structure of coronary adventitial vasa vasorum in experimental hypercholesterolemia independent of lipid lowering. Circulation. 2002 Jan 29;105(4):415-8.
[115] Sirol M, Fuster V, Fayad ZA. Plaque imaging and characterization using magnetic resonance imaging: towards molecular assessment. Curr Mol Med. 2006 Aug;6(5):541-8.

[116] Sinha R, Kim GJ, Nie S, Shin DM. Nanotechnology in cancer therapeutics: bioconjugated nanoparticles for drug delivery. Mol Cancer Ther. 2006 Aug;5(8):1909-17.
[117] McCarthy JR, Kelly KA, Sun EY, Weissleder R. Targeted delivery of multifunctional magnetic nanoparticles. Nanomed. 2007 Apr;2(2):153-67.
[118] Jaffer FA, Nahrendorf M, Sosnovik D, Kelly KA, Aikawa E, Weissleder R. Cellular imaging of inflammation in atherosclerosis using magnetofluorescent nanomaterials. Mol Imaging. 2006 Apr-Jun;5(2):85-92.
[119] Heroux J, Gharib AM, Danthi NS, Cecchini S, Ohayon J, Pettigrew RI. High-affinity alphavbeta3 integrin targeted optical probe as a new imaging biomarker for early atherosclerosis: initial studies in Watanabe rabbits. Mol Imaging Biol. 2010 Jan-Feb;12(1):2-8.
[120] Hilfiker A, Hilfiker-Kleiner D, Fuchs M, Kaminski K, Lichtenberg A, Rothkotter HJ, et al. Expression of CYR61, an angiogenic immediate early gene, in arteriosclerosis and its regulation by angiotensin II. Circulation. 2002 Jul 9;106(2):254-60.
[121] Moreno PR, Purushothaman M, Purushothaman KR. Plaque neovascularization: defense mechanisms, betrayal, or a war in progress. Ann N Y Acad Sci. 2012 Apr;1254:7-17.
[122] Nicholls SJ, Tuzcu EM, Wolski K, Sipahi I, Schoenhagen P, Crowe T, et al. Coronary artery calcification and changes in atheroma burden in response to established medical therapies. Journal of the American College of Cardiology. 2007 Jan 16;49(2):263-70.
[123] Shiomi M, Ito T, Yamada S, Kawashima S, Fan J. Correlation of vulnerable coronary plaques to sudden cardiac events. Lessons from a myocardial infarction-prone animal model (the WHHLMI rabbit). Journal of atherosclerosis and thrombosis. 2004;11(4):184-9.
[124] Sun H, Unoki H, Wang X, Liang J, Ichikawa T, Arai Y, et al. Lipoprotein(a) enhances advanced atherosclerosis and vascular calcification in WHHL transgenic rabbits expressing human apolipoprotein(a). The Journal of biological chemistry. 2002 Dec 6;277(49):47486-92.
[125] Little WC, Applegate RJ. Role of plaque size and degree of stenosis in acute myocardial infarction. Cardiol Clin. 1996 May;14(2):221-8.
[126] Kwon HM, Sangiorgi G, Ritman EL, Lerman A, McKenna C, Virmani R, et al. Adventitial vasa vasorum in balloon-injured coronary arteries: visualization and quantitation by a microscopic three-dimensional computed tomography technique. Journal of the American College of Cardiology. 1998 Dec;32(7):2072-9.
[127] Mulligan-Kehoe MJ. The vasa vasorum in diseased and nondiseased arteries. Am J Physiol Heart Circ Physiol. 2010 Feb;298(2):H295-305.
[128] Choi D, Hwang KC, Lee KY, Kim YH. Ischemic heart diseases: current treatments and future. J Control Release. 2009 Dec 16;140(3):194-202.
[129] Scholz D, Schaper W. Preconditioning of arteriogenesis. Cardiovasc Res. 2005 Feb 1;65(2):513-23.
[130] Herrmann J, Lerman A. Atherosclerosis in the back yard. Journal of the American College of Cardiology. 2007 May 29;49(21):2102-4.

[131] Simons M. Angiogenesis: where do we stand now? Circulation. 2005 Mar 29;111(12):1556-66.
[132] Moreno PR, Purushothaman KR, Sirol M, Levy AP, Fuster V. Neovascularization in human atherosclerosis. Circulation. 2006 May 9;113(18):2245-52.
[133] Kilarski WW, Jura N, Gerwins P. An ex vivo model for functional studies of myofibroblasts. Lab Invest. 2005 May;85(5):643-54.
[134] Osinsky S, Bubnovskaya L, Ganusevich I, Kovelskaya A, Gumenyuk L, Olijnichenko G, et al. Hypoxia, tumour-associated macrophages, microvessel density, VEGF and matrix metalloproteinases in human gastric cancer: interaction and impact on survival. Clin Transl Oncol. 2011 Feb;13(2):133-8.
[135] Gao L, Chen Q, Zhou X, Fan L. The role of hypoxia-inducible factor 1 in atherosclerosis. J Clin Pathol. 2012 May 8.
[136] Hulten LM, Levin M. The role of hypoxia in atherosclerosis. Curr Opin Lipidol. 2009 Oct;20(5):409-14.
[137] Sluimer JC, Daemen MJ. Novel concepts in atherogenesis: angiogenesis and hypoxia in atherosclerosis. J Pathol. 2009 May;218(1):7-29.
[138] Manduteanu I, Simionescu M. Inflammation in atherosclerosis: a cause or a result of vascular disorders? J Cell Mol Med. 2012 Feb 20.
[139] Hansson GK, Libby P, Schonbeck U, Yan ZQ. Innate and adaptive immunity in the pathogenesis of atherosclerosis. Circulation research. 2002 Aug 23;91(4):281-91.
[140] Campbell KA, Lipinski MJ, Doran AC, Skaflen MD, Fuster V, McNamara CA. Lymphocytes and the adventitial immune response in atherosclerosis. Circulation research. 2012 Mar 16;110(6):889-900.
[141] Hristov M, Gumbel D, Lutgens E, Zernecke A, Weber C. Soluble CD40 ligand impairs the function of peripheral blood angiogenic outgrowth cells and increases neointimal formation after arterial injury. Circulation. 2010 Jan 19;121(2):315-24.
[142] Lindholt JS, Shi GP. Chronic inflammation, immune response, and infection in abdominal aortic aneurysms. Eur J Vasc Endovasc Surg. 2006 May;31(5):453-63.
[143] Monaco C, Andreakos E, Kiriakidis S, Feldmann M, Paleolog E. T-cell-mediated signalling in immune, inflammatory and angiogenic processes: the cascade of events leading to inflammatory diseases. Curr Drug Targets Inflamm Allergy. 2004 Mar;3(1):35-42.
[144] Buchner K, Henn V, Grafe M, de Boer OJ, Becker AE, Kroczek RA. CD40 ligand is selectively expressed on CD4+ T cells and platelets: implications for CD40-CD40L signalling in atherosclerosis. J Pathol. 2003 Oct;201(2):288-95.
[145] Khurana R, Zhuang Z, Bhardwaj S, Murakami M, De Muinck E, Yla-Herttuala S, et al. Angiogenesis-dependent and independent phases of intimal hyperplasia. Circulation. 2004 Oct 19;110(16):2436-43.
[146] Tieu BC, Ju X, Lee C, Sun H, Lejeune W, Recinos A, 3rd, et al. Aortic adventitial fibroblasts participate in angiotensin-induced vascular wall inflammation and remodeling. Journal of vascular research. 2011;48(3):261-72.
[147] Galis ZS, Muszynski M, Sukhova GK, Simon-Morrissey E, Libby P. Enhanced expression of vascular matrix metalloproteinases induced in vitro by

cytokines and in regions of human atherosclerotic lesions. Ann N Y Acad Sci. 1995 Jan 17;748:501-7.
[148] Kalyani R, Thej MJ, Prabhakar K, Kiran J. Accelerated atherosclerosis in a human immunodeficiency virus infected patient not on highly active anti-retroviral therapy: An autopsy case report. J Cardiovasc Dis Res. 2011 Oct;2(4):241-3.
[149] Guaraldi G, Zona S, Orlando G, Carli F, Ligabue G, Fiocchi F, et al. Human immunodeficiency virus infection is associated with accelerated atherosclerosis. J Antimicrob Chemother. 2011 Aug;66(8):1857-60.
[150] Kaneko H, Anzai T, Takahashi T, Kohno T, Shimoda M, Sasaki A, et al. Role of vascular endothelial growth factor-A in development of abdominal aortic aneurysm. Cardiovasc Res. 2011 Jul 15;91(2):358-67.
[151] Owens GK, Kumar MS, Wamhoff BR. Molecular regulation of vascular smooth muscle cell differentiation in development and disease. Physiological reviews. 2004 Jul;84(3):767-801.
[152] Gomez D, Owens GK. Smooth muscle cell phenotypic switching in atherosclerosis. Cardiovasc Res. 2012 Jul 15;95(2):156-64.
[153] Hirschberg K, Tarcea V, Pali S, Barnucz E, Gwanmesia PN, Korkmaz S, et al. Cinaciguat prevents neointima formation after arterial injury by decreasing vascular smooth muscle cell migration and proliferation. Int J Cardiol. 2012 Feb 20.
[154] Chandrasekar B, Mummidi S, Mahimainathan L, Patel DN, Bailey SR, Imam SZ, et al. Interleukin-18-induced human coronary artery smooth muscle cell migration is dependent on NF-kappaB- and AP-1-mediated matrix metalloproteinase-9 expression and is inhibited by atorvastatin. The Journal of biological chemistry. 2006 Jun 2;281(22):15099-109.
[155] Ingersoll MA, Platt AM, Potteaux S, Randolph GJ. Monocyte trafficking in acute and chronic inflammation. Trends Immunol. 2011 Oct;32(10):470-7.
[156] Song Z, Jin R, Yu S, Nanda A, Granger DN, Li G. Crucial role of CD40 signaling in vascular wall cells in neointimal formation and vascular remodeling after vascular interventions. Arteriosclerosis, thrombosis, and vascular biology. 2012 Jan;32(1):50-64.
[157] Hakkinen T, Karkola K, Yla-Herttuala S. Macrophages, smooth muscle cells, endothelial cells, and T-cells express CD40 and CD40L in fatty streaks and more advanced human atherosclerotic lesions. Colocalization with epitopes of oxidized low-density lipoprotein, scavenger receptor, and CD16 (Fc gammaRIII). Virchows Arch. 2000 Oct;437(4):396-405.
[158] Sukhova GK, Wang B, Libby P, Pan JH, Zhang Y, Grubb A, et al. Cystatin C deficiency increases elastic lamina degradation and aortic dilatation in apolipoprotein E-null mice. Circulation research. 2005 Feb 18;96(3):368-75.
[159] Metaxa E, Tremmel M, Natarajan SK, Xiang J, Paluch RA, Mandelbaum M, et al. Characterization of critical hemodynamics contributing to aneurysmal remodeling at the basilar terminus in a rabbit model. Stroke. 2010 Aug;41(8):1774-82.
[160] Cheng JK, Wagenseil JE. Extracellular matrix and the mechanics of large artery development. Biomech Model Mechanobiol. 2012 May 15.
[161] Shibata R, Kai H, Seki Y, Kato S, Wada Y, Hanakawa Y, et al. Inhibition of STAT3 prevents neointima formation by inhibiting proliferation and promoting

apoptosis of neointimal smooth muscle cells. Hum Gene Ther. 2003 May 1;14(7):601-10.
[162] Daniel JM, Dutzmann J, Bielenberg W, Widmer-Teske R, Gunduz D, Hamm CW, et al. Inhibition of STAT3 signaling prevents vascular smooth muscle cell proliferation and neointima formation. Basic research in cardiology. 2012;107(3):261.
[163] Johnson C, Galis ZS. Matrix metalloproteinase-2 and -9 differentially regulate smooth muscle cell migration and cell-mediated collagen organization. Arteriosclerosis, thrombosis, and vascular biology. 2004 Jan;24(1):54-60.
[164] Yla-Herttuala S, Bentzon JF, Daemen M, Falk E, Garcia-Garcia HM, Herrmann J, et al. Stabilisation of atherosclerotic plaques. Position paper of the European Society of Cardiology (ESC) Working Group on atherosclerosis and vascular biology. Thrombosis and haemostasis. 2011 Jul;106(1):1-19.
[165] Kim JY, Kim WJ, Kim H, Suk K, Lee WH. The Stimulation of CD147 Induces MMP-9 Expression through ERK and NF-kappaB in Macrophages: Implication for Atherosclerosis. Immune Netw. 2009 Jun;9(3):90-7.
[166] Mahajan N, Dhawan V. Inhibition of C-reactive protein induced expression of matrix metalloproteinases by atorvastatin in THP-1 cells. Molecular and cellular biochemistry. 2010 May;338(1-2):77-86.
[167] Mastoraki ST, Toumpoulis IK, Anagnostopoulos CE, Tiniakos D, Papalois A, Chamogeorgakis TP, et al. Treatment with simvastatin inhibits the formation of abdominal aortic aneurysms in rabbits. Ann Vasc Surg. 2012 Feb;26(2):250-8.
[168] Frisdal E, Lesnik P, Olivier M, Robillard P, Chapman MJ, Huby T, et al. Interleukin-6 protects human macrophages from cellular cholesterol accumulation and attenuates the proinflammatory response. The Journal of biological chemistry. 2011 Sep 2;286(35):30926-36.
[169] Uchida HA, Kristo F, Rateri DL, Lu H, Charnigo R, Cassis LA, et al. Total lymphocyte deficiency attenuates AngII-induced atherosclerosis in males but not abdominal aortic aneurysms in apoE deficient mice. Atherosclerosis. 2010 Aug;211(2):399-403.
[170] Chakrabarti S, Rizvi M, Morin K, Garg R, Freedman JE. The role of CD40L and VEGF in the modulation of angiogenesis and inflammation. Vascul Pharmacol. 2010 Sep-Oct;53(3-4):130-7.
[171] Ziegler SF, Buckner JH. FOXP3 and the regulation of Treg/Th17 differentiation. Microbes Infect. 2009 Apr;11(5):594-8.
[172] Chen CH, Walterscheid JP. Plaque angiogenesis versus compensatory arteriogenesis in atherosclerosis. Circulation research. 2006 Oct 13;99(8):787-9.
[173] Cao Y. Therapeutic angiogenesis for ischemic disorders: what is missing for clinical benefits? Discov Med. 2010 Mar;9(46):179-84.
[174] Bochkov VN, Philippova M, Oskolkova O, Kadl A, Furnkranz A, Karabeg E, et al. Oxidized phospholipids stimulate angiogenesis via autocrine mechanisms, implicating a novel role for lipid oxidation in the evolution of atherosclerotic lesions. Circulation research. 2006 Oct 13;99(8):900-8.
[175] Moulton KS, Vakili K, Zurakowski D, Soliman M, Butterfield C, Sylvin E, et al. Inhibition of plaque neovascularization reduces macrophage accumulation and

progression of advanced atherosclerosis. Proceedings of the National Academy of Sciences of the United States of America. 2003 Apr 15;100(8):4736-41.
[176] Bloomgarden ZT. Cardiovascular disease in diabetes. Diabetes Care. 2010 Apr;33(4):e49-54.
[177] Pasterkamp G, Schoneveld AH, Hijnen DJ, de Kleijn DP, Teepen H, van der Wal AC, et al. Atherosclerotic arterial remodeling and the localization of macrophages and matrix metalloproteases 1, 2 and 9 in the human coronary artery. Atherosclerosis. 2000 Jun;150(2):245-53.
[178] Wang T, Niu G, Kortylewski M, Burdelya L, Shain K, Zhang S, et al. Regulation of the innate and adaptive immune responses by Stat-3 signaling in tumor cells. Nature medicine. 2004 Jan;10(1):48-54.
[179] Song Z, Jin R, Yu S, Rivet JJ, Smyth SS, Nanda A, et al. CD40 is essential in the upregulation of TRAF proteins and NF-kappaB-dependent proinflammatory gene expression after arterial injury. PloS one. 2011;6(8):e23239.
[180] Donners MM, Beckers L, Lievens D, Munnix I, Heemskerk J, Janssen BJ, et al. The CD40-TRAF6 axis is the key regulator of the CD40/CD40L system in neointima formation and arterial remodeling. Blood. 2008 May 1;111(9):4596-604.

ANNEX I

Rabbit Protocol

NATIONAL INSTITUTES OF HEALTH
ANIMAL STUDY PROPOSAL

(See NIH Manual 3040-2)

Leave Blank
PROPOSAL #K037-NIBIB-10

APPROVAL DATE 10/6/2010

EXPIRATION DATE 10/6/2013

A. ADMINISTRATIVE DATA:

Institute or Center NIDDK Principal Investigator Ahmed M. Gharib, Ph.D. Building/Room 10/CRC/3-5340 E-Mail agharib@mail.nih.gov Tel 301-451-8982 FAX 301-480-3166

Emergency Treatment and Animal Care instructions shall be provided on the attached form at the end of this document.

Division, Laboratory, or Branch National Institute of Biomedical Imaging and Bioengineering

Project Title αvß3-targeted Imaging of Early Atherosclerosis in Watanabe Heritable Hyperlipidemia (WHHL) Rabbits with a New Integrin Antagonist

Initial Submission [X] Renewal [ ] or Modification [ ] of Proposal Number

List the names of all individuals authorized to conduct procedures involving animals under this proposal and identify key personnel (i.e., Co- investigator(s)): A brief summary of the training and/or experience for procedures each individual will be expected to perform in this ASP must be documented and available to the ACUC. The name(s) of the supervisor, mentor, or trainer who will provide assurance each individual is/has achieved proficiency in those procedures shall be included in that documentation.

Ahmed M. Gharib, Ph.D., Principal Investigator, 301-451-8982, PI refresher course 12/17/2009 Julie Heroux, Contract Technician, 301-451-9092, user refresher course 4/27/2009 Mary B. Angstadt, Technician (CC), 301-594-0050, user refresher course 7/9/2008 Zu-Xi Yu, Ph.D., Visiting Fellow, (NHLBI), 301-496-5035, user refresher course 7/31/2007

B. ANIMAL REQUIREMENTS:

Species Rabbits Age/Weight/Size 10-25 months/ 3-5 Kg Sex Male & Female
Stock or Strain New Zealand White (NZW); Watanabe (WHHL) **Source(s)** Brown Family Enterprises, LLC., dba Gemini Research of Alabama, Harlan **Holding Locations(s)** Bldg 14F **Animal Procedure Location(s)** Bldg 10/B1D315 (MIF), Bldg 10/B1D221 (Procedure Room), Bldg 10/B1D200-202 (Imaging Facility)

Estimated Number of Animals:

Year 1	Year 2	Year 3	TOTAL
32	14	14	60

C. TRANSPORTATION:

Transportation of animals must conform to all NIH and Facility guidelines/policies. If animals will be transported between facilities, describe the methods and containment to be utilized. If animals will be transported within the Clinical Center, also include the route and elevator(s) to be utilized.

On arrival, rabbits will be housed in Building 14F and transportation will be carried out by a qualified individual using approved transport boxes in accordance with applicable regulations. On the day of experiment, rabbits will be delivered to the B1 loading dock of Building 10 and carried out to the procedure room or imaging location room B1D200-202 and B1D315 (MIF). When

transporting the rabbits in Bldg 10, animals will be transported in NIH approved filtered cardboard carriers, following NIH Guidelines, via stairwells or elevators 8, 9, 16, 21, 28 or 38.

D. **STUDY OBJECTIVES:** Provide no more than a 300 word summary of the objectives of this work. Why is this work important/interesting? How might this work benefit humans and/or animals? This should be
written so that a non-scientist can easily understand it. Please eliminate or minimize abbreviations, technical terms, and jargon. Where they are necessary, they should be defined.

Aim:
The goal of this study is to evaluate the potential of a new molecular marker (αvß3 integrin antagonist) in the detection of the vulnerable atherosclerotic plaque by fluorescence, magnetic resonance imaging (MRI) and dual modality imaging.

Rationale of the study:
Previous studies have shown the great potential of targeting αvß3 integrin for the development of contrast agent that enhance the detection of the plaque and can also be used for the delivery of therapeutic drugs[1-2]. From these results, we investigated the possibility of targeting αvß3, *in vitro*, on rabbit aortas, with a new fluorescent labeled (FITC) integrin antagonist developed in a collaborating laboratory[3]. This study clearly demonstrated a specific signal enhancement into the vasculature of the disease animal model (Watanabe Heritable Hyperlipidemic rabbit) compare to the control animal model (New Zealand White rabbit).

The present study has three objectives:

1) To assess *ex vivo*, by histological techniques, the possibility of specifically label the early atherosclerotic plaque with fluorescence (FITC) labeled αvß3 integrin antagonist.
2) To evaluate *in vivo*, by MRI, the possibility of specifically label the early atherosclerotic plaque with the same αvß3 integrin antagonist labeled with gadolinium and then compare the results with other known MRI contrast agents (Gadofluorine, Feridex, Gadolinium, etc.).
3) To investigate the feasibility of combining both MRI and Fluorescence imaging modality in a MRI guided fluorescence imaging system that could be further used for the delivery of drugs specifically in the atherosclerotic lesion.

E. RATIONALE FOR ANIMAL USE: 1) Explain your rationale for animal use. 2) Justify the appropriateness of the species selected. 3) Justify the number of animals to be used. **(Use additional sheets if necessary.)**

1) We would like to use animals for our study because only animal models can

reflect the complexity of the atherosclerosis disease. Since the study is about optimizing the imaging technique for the detection of atherosclerotic plaque, neither cellular models or computational models can reproduce the *in vivo* environment necessary for the evaluation of these imaging techniques. Moreover, because the contrast agent that will be used in this study (αvß3 integrin antagonist) has already been studied with *in vitro* experiments and proved to target the plaque, we would like to test it in an *in vivo* experiment.

2) We choose rabbits because of the availability of a genetic model that mimics the atherosclerosis disease (Watanabe Heritable Hyperlipidemic rabbit) and the practical size of the animal. Mice are also available with genetic disease background (ApoE knockout mice for example), but the smaller size of mice's vessels renders them difficult for catheter utilization and imaging technique and complicates the analysis of the imaging data. Pigs are also used for atherosclerosis studies, but the housing and maintenance are costly. For all these reasons, we think that Watanabe Heritable Hyperlipidemic rabbits (WHHL) and control New Zealand White rabbits (NZW) will be the most suitable model for imaging (MRI, Fluorescence) the target (αvß3 integrin receptor) with an adequate resolution.

3) We would like to study the effect of a contrast agent (integrin antagonist) on the visualization of early atherosclerotic plaque by different imaging techniques and then, compare this agent with other known contrast agents. To reach this goal, we include 18 rabbits for the optimization of the imaging technique: testing of imaging sequences, baseline testing with integrin contrast agent, baseline testing with other contrast agents (Gadofluorine-M, Feridex, etc.), imaging timeline, etc.

For the study, we would like to use 6 Watanabe rabbits for each of the 3 experimental conditions (fluorescence, MRI and dual imaging), in order to meet the requirements for journal publication. Also, we would like to use 2 normal NZW rabbits for each experimental technique (Fluorescence, MRI and dual imaging), to measure the efficiency of the contrast agent (no signal in the control animals without atherosclerotic plaque). Our rabbits requirements are based on two similar MRI studies that have shown greater signal enhancement in the rabbits injected with avß3 targeted particles[1-2].

In summary, for the first year, we would like to use a total of 32 rabbits for optimization of the experimental conditions and the fluorescence labeling study. If the results of these studies are promising, we would like to continue the imaging study with 14 rabbits during the second year (MRI) and 14 rabbits during the third year (dual imaging) for evaluating the potential of the new target molecule (avß3 integrin antagonist) on the plaque visualization (See Table 1).

Please note that if at any point during the study, objectives have been accomplished, we may not need to use all rabbits that have been requested. Also, if during the study some preliminary results point out toward the failure of the project, we may stop the project immediately without using the remaining rabbits.

Table 1 Number of Rabbits Required

	Rabbits	*Watanabe rabbits injected with targeted particle*	*Watanabe rabbits injected with non-targeted particle*	*NZW rabbits*
Types of Imaging				
Optimization		12	0	6
Fluorescence	*Histology*	6	6	2
MRI	*In vivo*	6	6	2
MRI + Fluorescence	*In vivo*	6	6	2

Total Number WHHL Rabbits: 48
Total Number NZW Rabbits: 12
Total Number of Rabbits: 60

References:

1-Winter PM, Morawski AM, Caruthers SD, et al. Molecular imaging of angiogenesis in early- stage atherosclerosis with avß3-integrin-targeted nanoparticles. Circulation. 2003;108:2270-2274.

2-Winter PM, Neubauer AM, Caruthers SD, et al. Endothelial avß3-integrin-targeted fumagillin nanoparticles inhibit angiogenesis in atherosclerosis. Arterioscler Thromb Vasc Biol. 2006;26:2103-2109.

F. DESCRIPTION OF EXPERIMENTAL DESIGN AND ANIMAL PROCEDURES: Briefly explain the experimental design and specify all animal procedures. This description should allow the ACUC to understand the experimental course of an animal from its entry into the experiment to the endpoint of the study. Specifically address the following: (Use additional sheets if necessary.)

S **Injections or Inoculations** (substances, e.g., infectious agents, adjuvants, etc.; dose, sites, volume, route, and schedules)
S **Blood Withdrawals** (volume, frequency, withdrawal sites, and methodology)
S **Minor surgical procedures** (that do not invade a body cavity)
S **Non-Survival Surgical Procedures** (Provide details of major survival surgical procedures in Section G.)
S **Radiation** (dosage and schedule)
S **Methods of Restraint** (e.g., restraint chairs, collars, vests, harnesses, slings, etc.)
S **Animal Identification Methods** (e.g., ear tags, tattoos, collar, cage card, etc.)
S **Other Procedures** (e.g., survival studies, tail biopsies, etc.)
S **Potentially Painful or Distressful Effects**, if any, the animals are expected to experience (e.g., pain or distress, ascites production, etc.) For Column E studies provide: 1) a description of the procedure(s) producing pain and/or distress; 2) scientific justification why pain and/or distress can not be relieved.
S **Experimental Endpoint Criteria** (i.e., tumor size, percentage body weight gain or loss, inability to eat or drink, behavioral abnormalities, clinical symptomatology, or signs of toxicity) must be specified when the administration of tumor cells, biologics, infectious agents, radiation or toxic chemicals are expected to cause significant symptomatology or are potentially lethal. List the criteria to be used to determine when euthanasia is to be performed. Death as an endpoint must always be scientifically justified.

Injections of Inoculations

Fluorescence procedures:

For the *ex vivo* fluorescence imaging, the rabbit will be brought to the 10/B1D221 procedure room and injected with 0.3mmol/Kg of body weight of fluorescence-labeled (FITC) αvβ3 integrin antagonist into the ear vein. The rabbit will then be anesthetized 2 hours later and immediately euthanized by the methods described in the section I and J. The rabbits will be dissected to excise portions of the coronary arteries and aorta for histological analysis using confocal fluorescence microscopy.

MRI procedures:

Rabbits will be delivered to the NMR center in rabbit transport box and kept in the box until anesthetized. For the experiments in which contrast agent should be administered in advance, they will be given IV into the rabbits auricular vein according to the table below, at the end of the section, for doses and timeline.
For these experiments, a baseline scan could be done just before the contrast agent injection. Anesthesia will be induced using a ketamine 25-50mg/kg (usually 30mg/kg) and xylazine 5mg/kg mixture. This will be administered subcutaneously (SC) or intramuscularly (IM) using a 25 gauge needle in the biceps femoris muscle of either hindleg. The eyes will be lubricated with sterile opthalmic petroleum ointment applied to the corneas. For anesthesia maintenance, the rabbit will be intubated with 1-3% isoflurane, with a mix of oxygen and medical air.

MR safe conductive leads will be placed for the detection of ECG. Optimum positioning and composition of ECG leads is to be determined. A pressure transducer for respiratory detection will be placed on the abdomen. A fiber optic temperature probe (Model 1025 Monitoring & Gating System , SA Instrument Inc, NY) will be placed beneath the abdomen or a standard MR compatible rectal temperature probe can also be used. Lightly-adhesive tape may be used as

needed to stabilize the position of the body. The body of the rabbit will be supported on a platform and in order to maintain body temperature, a circulating warm water pad or a warm air blower at the magnet bore will be used. The respiration waveform and rate and ECG will be read on a computer monitoring/gating system. Respiration and temperature are monitored throughout the experiment for surveillance and maintenance of anesthesia.

MRI studies of the aorta in the area of the aortic root and arch and/or thoracic and abdominal aorta will be performed on a 3T MR scanner (B1D200-202). A combination of black-blood, Gated Proton Density T1- and T2- weighted spin echo or gradient echo imaging of the chest will be performed as indicated, but not limited to these sequences. The imaging period will be approximatively 2 to 3 hours. The animal is monitored continuously on the MRI monitor screen and any animal movement will become apparent on the images. At the end of the scan (except for the baseline scan), the rabbit will be immediately euthanized and dissected (the rabbit will never be woke up), to examine the tissues by histological and microscopical techniques.

Catheterization procedure and Dual imaging:

Rabbits will be brought to the NMR center and anesthetized and imaged according to the previously described procedure in the MRI section. The femoral artery will be punctured percutaneously (small incision) while the rabbit (already anesthetized) is still outside the MR scanner. If a suitable access to the femoral artery cannot be achieved percutaneously, we may use a cut down procedure and vessel exposure as an alternative technique for the cannula placement.

Heparin (100 IU/kg body weight) will then be administered as an intravascular bolus. A canula will be used to access the femoral arteries. A catheter used for active MR imaging will then be advanced through the canula to reach the aorta. Standard guidewires may also be used when necessary.
Catheterization will be performed during free breathing. Cardiac triggering may be used to obtain time-difference images. The intravascular devices will be visualized by active catheter technologies which make the catheter tip show up extremely bright in an image, or by the lack of signal present.

For the catheterization, gadolinium (Gd) contrast material could be injected to confirm engagement and right positioning into the target region. Real-time images and the procedure time for each target region will be recorded. Real-time images will be utilized to confirm the tip position of the tracking devices on selected still-frame images. The catheter sheath will be coupled to a fluorescence imaging fiber optic apparatus which emits laser light at different colors. This apparatus permits the detection of fluorescence-labeled contrast agents and uses an computer located outside the MR scanner. At the end of the scan, the

anesthetized rabbit will be euthanized and dissected, to examine the tissues by histological and microscopical techniques.

List of contrast agents that can be used for IV injection into the auricular vein:

Gadolinium	0.1mmol/kg	20min before MRI
Gadofluorine-M	50µmol/kg	24hrs before MRI
Feridex	15µmol/kg	10min before MRI
Resovist	0.45mmol	24hrs before MRI

Blood Withdrawals

One or two mL of blood sample would be obtained via the auricular artery using a 23 gauge butterfly catheter. This blood sample will be used for cholesterol, lipoprotein, and proteomic analysis. This will be done once, just before the scan and after the anesthesia to minimize pain.

Animal Identification Methods

The rabbits will be tattooed on either of the ears and then placed in cage identified by card.

Resultant Effects, if any, the animals are expected to experience

We do not expect any adverse effects with the contrast agents and with the Watanabe rabbits at this age.

Experimental Endpoint Criteria

At the end of the scan, the animals will be euthanized in order to dissect and excise portions of the coronary arteries and the aorta and further analyze tissues by histology.

G. MAJOR SURVIVAL SURGERY - If proposed, complete the following: NoneX

1. Identify and describe the surgical procedure(s) to be performed. Include the aseptic methods to be utilized. (Use additional sheets if necessary):

2. Who will perform surgery and what are their qualifications and/or experience?

3. Where will surgery be performed, Building and Room

4. Describe post-operative care required, including consideration of the use of post-operative analgesics, and identify the responsible individual:

5. Has major survival surgery been performed on any animal prior to being placed on this study? Y/N If yes, please explain:

6. Will more than one major survival surgery be performed on an animal while on this study? Y/N If yes, please justify:

H. RECORDING PAIN OR DISTRESS CATEGORY - ***The ACUC is responsible for applying U.S. Government Principle IV. contained in Appendix 3: Proper use of animals, including the avoidance or minimization of discomfort, distress, and pain when consistent with sound scientific practices, is imperative. Unless the contrary is established, investigators should consider that procedures that cause pain or distress in human beings may cause pain or distress in other animals.*** Check the appropriate category(ies)and indicate the approximate number of animals in each. Sum(s) should equal total from Section B.

IF ANIMALS ARE INDICATED IN COLUMN E, A SCIENTIFIC JUSTIFICATION IS REQUIRED TO EXPLAIN WHY THE USE OF ANESTHETICS, ANALGESICS, SEDATIVES OR TRANQUILIZERS DURING AND/OR FOLLOWING PAINFUL OR DISTRESSFUL PROCEDURES IS CONTRAINDICATED. FOR USDA REGULATED SPECIES, PLEASE COMPLETE THE EXPLANATION FOR COLUMN E LISTINGS FORM AT THE END OF THIS DOCUMENT. THIS FORM WILL ACCOMPANY THE NIH ANNUAL REPORT TO THE USDA. FOR ALL OTHER SPECIES, THE JUSTIFICATION FOR SUCH STUDIES MUST BE PROVIDED IN SECTION F. NOTE: THIS COLUMN E FORM, AND ANY ATTACHMENTS, e.g., THE ASP, ARE SUBJECT TO THE FREEDOM OF INFORMATION ACT.

NUMBER OF ANIMALS USED EACH YEAR

	Year 1	Year 2	Year 3
[ ] **USDA Column C** - Minimal, Transient, or No Pain or Distress			
[X] **USDA Column D** - Pain or Distress Relieved By Appropriate Measures	32	14	14
[ ] **USDA Column E** - Unrelieved Pain or Distress			

Describe your consideration of alternatives to procedures listed for Column D and E that may cause more than momentary or slight pain or distress to the animals, and your determination that alternatives were not available. [Note: Principal investigators must certify in paragraph N.5. that no valid alternative was identified to any described procedures which may cause more than momentary pain or distress, whether it is relieved or not.] Delineate the methods and sources used in the search below. **Database references must include databases (2 or more) searched, the date of the search, period covered, and keywords used:**

Database: ILAR; search date: 6/9/2010; period covered: 1964-Present; Keywords: restraint, MRI, rabbit;
No results found for rabbit

Database: Pubmed; search date: 6/9/2010; period covered: 1966-Present; Keywords: restraint, MRI, rabbit; found only one paper in Magnetic Resonance in Medicine journal (Magn Reson Med. 2000 Sep;44(3):474-8).
The title is fMRI of visual system activation in the conscious rabbit. They said that the rabbit is ideal for these experiments (conscious MRI) because of its natural tolerance for restraint. They acquired high spatial and temporal resolution

magnetic resonance images during long periods of restraint with conscious rabbits (no anesthesia). We will anesthetize rabbits for the MRI which should result in less stress and pain.

I. ANESTHESIA, ANALGESIA, TRANQUILIZATION - For animals indicated in Section H, Column D, specify the anesthetics, analgesics, sedatives or tranquilizers that are to be used. Include the name of the agent(s), the dosage, route and schedule of administration. None____

Anesthesia will be induced using a ketamine 25-50mg/kg (usually 30mg/kg) and xylazine 5mg/kg mixture. This will be administrated subcutaneously (SC) or intramuscularly (IM) using a 25 gauge needle in the biceps femoris muscle of either hindleg. For anesthesia maintenance, the rabbit will be intubated with 1-3% isoflurane, with a mix of oxygen and medical air. Isoflurane will be used in an area approved by the Division of Health and Safety (DOHS)

J. METHOD OF EUTHANASIA OR DISPOSITION OF ANIMALS AT END OF STUDY: Indicate the proposed method, and if a chemical agent is used, specify the dosage and route of administration. If the method(s) of euthanasia include those not recommended by the AVMA Panel Report on Euthanasia, provide justification why such methods must be used. Indicate the method of carcass disposal if not as MPW. None ____

Pentobarbital IV at a dose of 85 to 150 mg/kg or injection of KCl (potassium chloride) IV at a dose of 1-2meq/Kg when animal is under isoflurane anesthesia. The carcass will then be disposed off in MPW box lined with two trash bags.

K. HAZARDOUS AGENTS: Use of hazardous agents requires the approval of an IC safety specialist. Registration Documents for the use of recombinant DNA or potential human pathogens may be attached at the discretion of the ACUC. None ____

YES [X] NO [ ] List Agents and Registration Document Number (If Applicable)

1. Radionuclides _____
2. Biological Agent _____
3. Hazardous Chemical or Drugs isoflurane
4. Recombinant DNA _____

Study conducted at Animal Biosafety Level: ABL-1

Describe the practices and procedures required for the safe handling and disposal of contaminated animals and material associated with this study. Use of volatile anesthetics requires a description of scavenging methods used. Also describe methods for removal of radioactive waste and, if applicable, the monitoring of radioactivity.

Gas anesthetics (e.g. isoflurane) will be scavenged using an approved anesthetic gas scavenging system, e.g., in-house vacuum, down-draft table, chemical fume hood, or ducted biosafety cabinet.

Carcasses will be disposed of in a double-bagged Medical Pathological Waste (MPW) box, as described previously in Section J.

Additional safety considerations:

L. BIOLOGICAL MATERIAL/ANIMAL PRODUCTS FOR USE IN ANIMALS

(e.g., cell lines, antiserum, etc.): None X

1. Specify Material_____

2. Source_____ Material Sterile or Attenuated _____Yes _____No

3 If derived from rodents, has the material been MAP/RAP/HAP/PCR tested?__Yes (Attach copy of results) No_____

4. I certify that the MAP/RAP/HAP/PCR tested materials to be used have not been passed through rodent species outside of the animal facility in question and/or the material is derived from the original MAP tested sample. To the best of my knowledge the material remains uncontaminated with rodent pathogens.

_____ **Initials of Principal Investigator**

M. SPECIAL CONCERNS OR REQUIREMENTS OF THE STUDY -

List any special housing, equipment, animal care (i.e., special caging, water, feed, or waste disposal, etc.). Include justification for exemption from participation in the environmental enrichment plan for nonhuman primates or exercise for dogs. None ____

The Watanabe Heritable Hyperlipidemic (WHHL) rabbits will be obtained from a NIH non- approved vendor (Brown Family Enterprises, LLC dba Gemini Research of Alabama) and housed in Building 14F. The Health Report from the vendor should be obtained by the animal program coordinator.

N. PRINCIPAL INVESTIGATOR CERTIFICATIONS:

1. I certify that I have attended an approved NIH investigator training course.
   Year of Course Attendance: 2005 Year(s) of Refresher Training: 2008; 2009

2. I certify that I have determined that the research proposed herein is not unnecessarily duplicative of previously reported research.

3. I certify that all individuals working on this proposal who have animal contact are participating in the NIH Animal Exposure Program (or equivalent, as applicable, for contract personnel).

4. I certify that the individuals listed in Section A are authorized to conduct procedures involving animals under this proposal, have attended the course "Using Animals in Intramural Research: Guidelines for Animal Users" will complete refresher training as required, and received training in the biology, handling, and care of this species; aseptic surgical methods and techniques (if necessary); the concept, availability, and use of research or testing methods that limit the use of animals or minimize distress; the proper use of anesthetics, analgesics, and tranquilizers (if necessary); procedures for reporting animal welfare concerns. I further certify that I am responsible for the professional conduct of all personnel listed in Section A.

5. **FOR ALL COLUMN D AND COLUMN E PROPOSALS (see section H):** I certify that I have reviewed the pertinent scientific literature and the sources and/or databases (2 or more) **as noted in section H,** and have found no valid alternative to any procedures described herein which may cause more than momentary pain or distress, whether it is relieved or not.

6. I will obtain approval from the ACUC before initiating any significant changes in this study (See PM 3040-2, F.4.d.).

Principal Investigator: Signature_____ _____Date_____

O. CONCURRENCES: PROPOSAL NUMBER _____ (LEAVE BLANK)

Laboratory/Branch Chief: certification of review and approval on the basis of scientific merit. Scientific Director's signature required for proposals submitted by a Laboratory or Branch Chief
Name Ira W. Levin, Ph.D. Signature_____Date_____

Safety Representative: certification of review and concurrence (Required of all studies utilizing hazardous agents)

Name Diana Stadler Signature_____Date_____

Facility Manager: certification of resource capability in the indicated facility to support the proposed study

Facility 14F Name Dave Dorsey Signature_____Date_____

COMMENTS:

Facility Veterinarian: certification of review

Name JoanneSmith,D.V.M. Signature_____ _____Date_____

Attending Veterinarian: certification of Review

Name Mark St. Claire, D.V.M. Signature _____Date__

P. FINAL APPROVAL:

Certification of review and approval by the NIDDK Animal Care and Use Committee Chairperson

Chairperson Samuel W. Cushman, Ph.D. Signature_____Date_____

INSTRUCTIONS FOR EMERGENCY ANIMAL TREATMENT AND CARE

Principal Investigator: _____Ahmed Gharib___Date form completed:7/7/2010
Protocol Number:_____ASP K037___
Office Phone: _____301-451-8982__
Home Phone:_____301-951-9537___

Protocol Title: __ αvß3-targeted imaging of early atherosclerosis in Watanabe Heritable Hyperlipidemia (WHHL) rabbits with a new integrin antagonist_____
Use a separate form if ***care is different*** for each species
Species: _____ Watanabe rabbit _____**Species**: _____
Species: _____ New Zealand White rabbit ___**Species**: _____

Animal Housing Location: Bldg __14F_____
Use separate form if care differs by location
Bldg _____
Bldg _____

List of Procedures:
(surgery, tumor implant, catheter**)_** Auricular blood drawn, Contrast agent injection**__**
Primary Point of Contact (P.O.C.) in Case of Emergency: Ahmed Gharib
Work Tel: _301-451-8982_ **Home Tel**: _301-951-9537___ **Pager or Cell** #: 10212076
Alternate Point of Contact in Case of Emergency: Julie Heroux
Work Tel: _301-451-9092_ **Home Tel**: _240-751-4451____**Pager or Cell** #:
Potential or Expected Complications: _____ N/A _____
Circumstances Requiring Contact: _____ Dead Animal _____

Treatment (indicate appropriate response):
Treatment determined by **veterinarian**: [X] Yes [ ] No
If **NO**, specify **restrictions** as follows: _____
Specific treatment as follows: _____N/A_____
What **drugs** are **contraindicated**? _____N/A_____

Criteria for **Euthanasia** (indicate appropriate response)
At Vet discretion if poor condition, severe pain or distress: [X] Yes [ ] No
If NO, specify treatments **or** restrictions:
_____

Notify P.O.C. *[X] Yes [ ] No
Requested **euthanasia agent** and **route of administration**: _____N/A_____
Specific **criteria** for **euthanasia**: ____N/A_____

If Euthanasia is performed or animals are found dead:

a. Contact P.O.C.	[X] Yes	[ ] No
b. Refrigerate carcass	[ ] Yes	[X] No
c. Dispose of carcass	[X] Yes	[ ] No

d. Submit to DVR for necropsy [ ] Yes [X] No
CAN number to use for submission: _____8327125_____

Additional Comments:

_____

Principal Investigator:

_____

Signature

Date

_____

_____

*** The veterinarian will take the appropriate action in an emergency if no response from the PI/POC is received within 30 minutes after an attempt at notification is made.**

ANNEX II

Book Chapter
(Introduction to Molecular Biology)

2

Introduction to Molecular Biology

JULIE HEROUX and AHMED M. GHARIB

National Heart, Lung, and Blood Institute (NHLBI), National Institutes of Health (NIH), Bethesda, Maryland, U.S.A.

INTRODUCTION

Within the past few years, the field of molecular biology has emerged as a powerful tool in medical and clinical research and also opened many exciting possibilities for the understanding, treatment, and imaging of a variety of diseases. Since the discovery of deoxyribonucleic acid (DNA) structure half a century ago (1), enormous advances in this field have been made. The progress led to the sequencing of the whole human genome, but the number of genes contained in the human genome is still fluctuated and under evaluation. The first human chromosome to be completely sequenced was chromosome 22 in the year 1999 (2). In 2000, the completion of a "working draft" of the entire human genome closed an important chapter in the field of genetics but opened huge avenues in medical research (3). Finally, the year 2003 marked not only the 50th anniversary of the discovery of the double-strand DNA helix but also the final step and completion of the human genome sequence (4).

From there, research groups and pharmaceutical companies have been trying to study and identify potential targets among many families of genes that could be involved in diseases such as atherosclerosis, diabetes, and cancer. Moreover, scientific efforts have been made to elucidate the molecular mechanisms inside the cells that lead to these pathological conditions. As a result of this effort, many genes or proteins have been characterized and evaluated for a potentially differential expression in the context of specific diseases. Furthermore, a constantly growing number of new disciplines have emerged including functional genomics, proteomics, metabolimics, or pharmacogenomics, each one related to the study of a specific area in biology.

One of the areas that have become increasingly important among the field of molecular biology is molecular imaging. This discipline combines expertise in several domains, which include molecular biology, physics, chemistry, biomedical engineering, and pathology, to obtain precious information about the development of a specific disease and to allow imaging of various pathological conditions. Therefore, it is important for a molecular imager to understand the basics of molecular biology in order to exploit this growing and evolving new field. Thus, the purpose of this chapter is to introduce these basic concepts.

MOLECULAR STRUCTURE

DNA Structure

Discovery

In 1865, Gregor Mendel, an Austrian monk, was the first to publish a theory about genetic rules that govern inheritance (5). By conducting crossbreeding experiments on pea plants, he was able to propose a generalized set of

rules, now known under the name of Mendel's law of heredity or Mendelian inheritance. He postulated that the transmission of hereditary characteristics from parent organisms to their progeny are governed by discrete units that are transmitted from generation to generation, even if some of these units are not expressed as visually observable trait in every generation. These units were the first report of the discovery of what we now call genes. He also postulated that for each characteristic, an organism inherit two alleles, one from each parent. Unfortunately, the results of Mendel's work were initially very controversial and neglected by the scientific community until the "re-discover" of the theory in 1900, by three European scientists Hugo de Vries, Carl Correns, and Erich von Tschermak.

After the publication of Mendel's law of inheritance, it took nearly a century to finally elucidate the double helix structure of DNA, as first described by Watson and Crick (6). The proposed double helix structure of DNA was based on X-ray crystallography studies. In 1962, Francis Crick, Maurice Wilkins, and James Watson were awarded the Nobel Prize in Medicine and Physiology for this pioneering discovery. Their findings described how DNA is arranged into genes that are contained within the chromosomes, which is the primary genetic material. Additional findings described mitosis and meiosis processes, where cell division by mitosis maintains the parental chromosome number while cell division by meiosis reduces the parental chromosome number.

Structure

DNA is a long polymer of simple structural units called nucleotides with a backbone made of sugars (2-deoxyribose) and phosphate groups joined by ester bonds. Attached to the sugar is one of the four types of molecules called bases. The four bases present in DNA are classified into two differents subtypes: purine and pyrimidine. The purine class includes adenine (A) and guanine (G), while the pyrimidine class is represented by cytosine (C) and thymine (T) (Fig. 1). Nucleotides are linked together by phosphodiester bonds to form polynucleotides. Usually, in living organisms, DNA exists not as a single-strand molecule, but rather as a pair of strands that entwine like a vine to form a double helix. In this double helix, the two stands of DNA are in an antiparallel arrangement, whereby the direction of the nucleotides in one strand is opposite to the direction of the nucleotides in the other strand. The ends of a single DNA strand are referred to as the 5′ (five prime) and 3′ (three prime) ends. The segment constituting the backbone of the DNA (sugars and phosphate groups) holds the chain together while the bases (adenine, cytosine, guanine, and thymine) are responsible for the interactions with the other strand of the double helix (Fig. 2). These

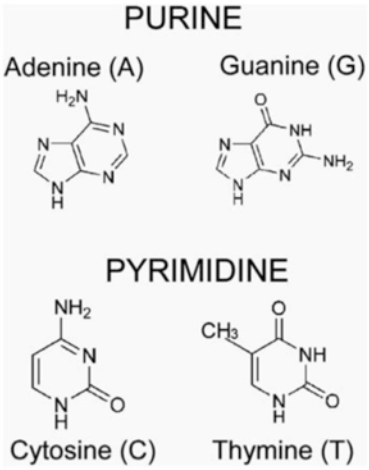

Figure 1 The four bases present in DNA. Adenine (A) and guanine (G) are purine class bases while cytosine (C) and thymine (T) are pyrimidine class bases.

interactions are achieved through hydrogen bonds and are responsible for stabilizing the double helix. Each base on one strand forms a link with just one specific base on the other strand by the process of complementary base pairing (Fig. 3). For the base pairing, purines form hydrogen bonds with pyrimidines, where A bonds only to T and C bonds only to G. These two types of base pairs form different numbers of hydrogen bonds: AT pair forms two bonds, while CG pair forms three bonds and is therefore stronger. Other forces like hydrophobic interactions can also hold the double-strand helix together.

Chromatin and Chromosome

In eukaryotes, the nucleus contains long double-stranded DNA molecules tightly packed and bounded to chromosomal proteins to form chromatin. Chemically, chromatin consists primarily of DNA associated with proteins and a small amount of RNA. The proteins inside the chromatin structure belong to two different classes: (*i*) basic proteins (positively charged at neutral pH) called histones and (*ii*) acidic proteins (negatively charged at neutral pH) called nonhistone chromosomal proteins. Nonhistone proteins are very heterogeneous and are involved in the regulation of expression of specific genes. Histone proteins play a major role in the structural integrity and the packaging of the DNA. Histones belong to five different groups: H1, H2a, H2b, H3, and H4. Histones and DNA are associated in a complex structure that forms small ellipsoidal beads (11 nm diameter and 6 nm high) called nucleosomes, which constitute the basic structural subunits of chromatin

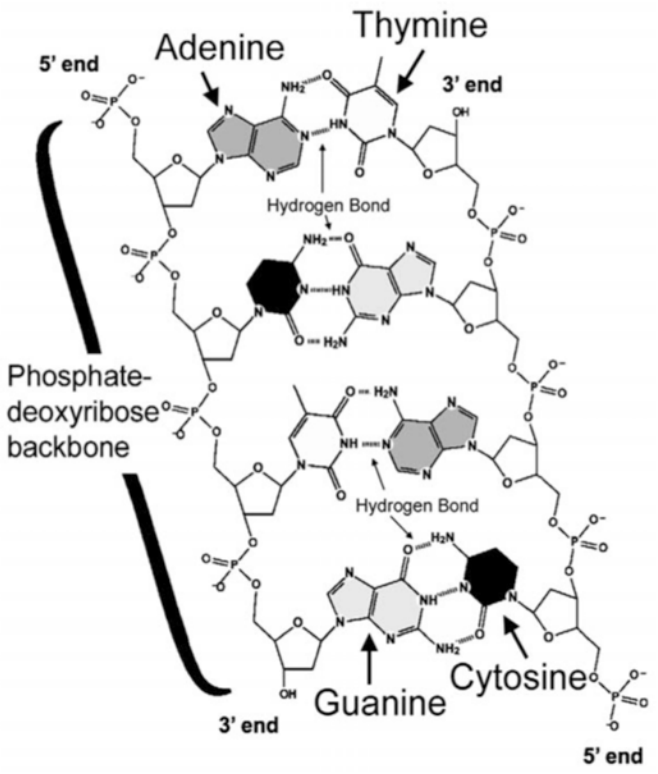

Figure 2 Chemical structure of DNA with its two asymmetric ends 5′ and 3′. The backbone segment of the DNA (sugars and phosphate groups) holds the chain together and the bases (adenine, cytosine, guanine, and thymine) interact with the other strand of the double helix. Hydrogen bonds stabilize the double helix.

(Fig. 4). The nucleosome core is 146-nucleotides pairs in length and is wrapped around an octamer of histones (two molecules each of H2a, H2b, H3, and H4). The complete chromatin subunit comprises the nucleosome core, the linker DNA associated with one molecule of histone H1, and some nonhistone proteins. The different levels of chromatin compaction are clearly visible in cells. In non-dividing cells, there are two types of chromatin refered to as euchromatin and heterochromatin. A euchromatin is a relatively relaxed form of chromatin allowing for the transcription and expression of the genes in this segment of DNA. On the other hand, the DNA segment in a hetrochromatin is more tightly packed and therefore is inaccessible to transcription. The interconversion between the euchromatin and heterochromatin form is called chromatin remodeling. Chromatin undergoes various forms of structural remodeling, mainly by acetylation and methylation. Acetylation (protein modification) results in the loosening of chromatin and lends itself to replication and transcription. Methylation (DNA and protein modification) strongly holds DNA together and restricts access to various enzymes.

In the early stages of mitosis or meiosis, the chromatin strands become more and more condensed. The chromosome becomes visible as a pair of sister chromatids attached to each other at the centromere, forming the classic four arm structure. Eukaryotic chromosomal DNA is also characterized by another feature called telomere. Telomeres are highly repetitive specialized DNA sequences protecting the end of a linear chromosome from degradation and gradual shortening. Without telomeres, a cell will lose a small piece of one of its strands of DNA at each division, which can quickly result in a loss of vital genetic information. For this reason, it is believed that telomeres are implicated in the aging process.

RNA Structure

The RNA structure is very similar to the DNA structure, except that the sugar in the backbone is a ribose instead of

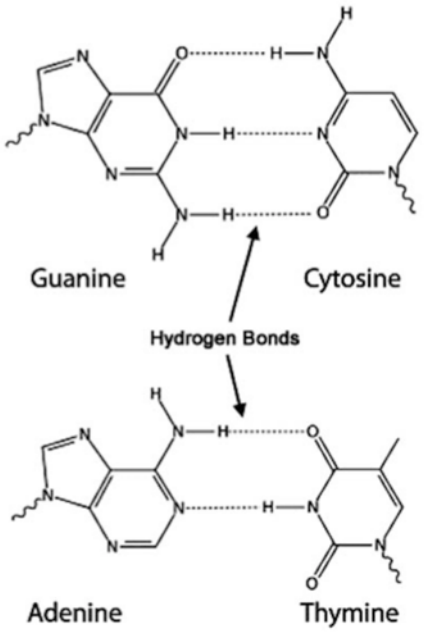

Figure 3 Complementary bases pairing in DNA. GC base pair forms three intermolecular hydrogen bonds, while AT base pair forms two intermolecular hydrogen bonds.

a 2-deoxyribose. Additionally, in RNA, a uracil (U) replaces the thymidine base. The other major difference between DNA and RNA is its secondary structure. While in living organisms DNA is rarely found in a single strand, the majority of RNA molecules are found in a single-strand form. Instead of forming a double-strand helix like DNA, RNA forms double-strand structure either with another DNA strand during the replication process or within itself by means of intramolecular hydrogen bonds. The types of RNA secondary structures define various types of RNA.

Types of RNA

Messenger RNA

Messenger ribonucleic acid (mRNA) is a molecule of RNA encoding a chemical "blueprint" for a protein product. mRNAs are intermediary molecules that carry genetic information from DNA in the cell nucleus to ribosomes in the cytoplasm for protein synthesis. After the translation process, the mRNA will be degraded. On average, between 10,000 and 20,000 different mRNA species can be observed in each cell at a given time. Despite this large number, mRNA composes only 3% to 5% of the total cytoplasmic RNA.

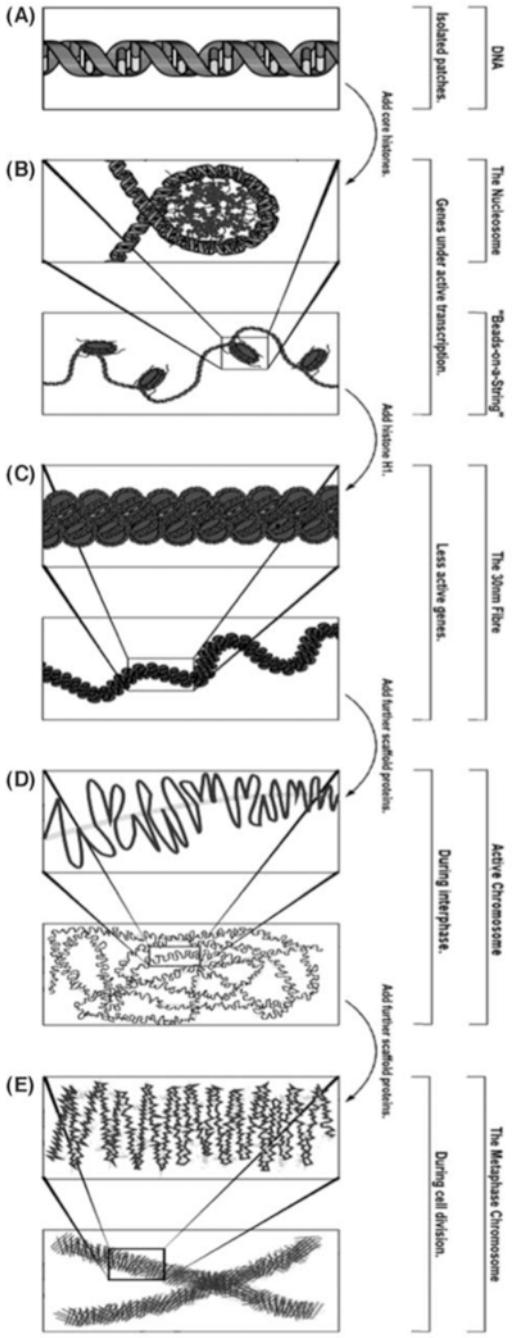

Figure 4 The major structures in DNA compaction: (**A**) DNA, (**B**) the nucleosome, (**C**) the 10 nm "beads-on-a-string" fiber, (**D**) the 30 nm fiber, and (**E**) the metaphase chromosome.

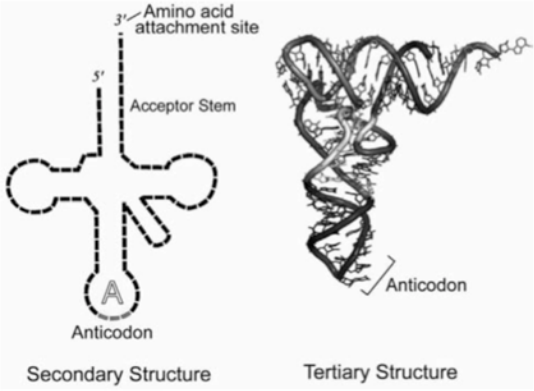

Figure 5 Secondary and tertiary structure of a transfer RNA (tRNA). The secondary structure is usually visualized as a cloverleaf structure, with an anticodon loop (A) that will base pair with the codon in the mRNA and an acceptor stem, which contains the 3′-hydroxyl attachment site for the amino acid. The tertiary structure is L-shaped and allows the tRNA to fit into the P and A sites of the ribosome.

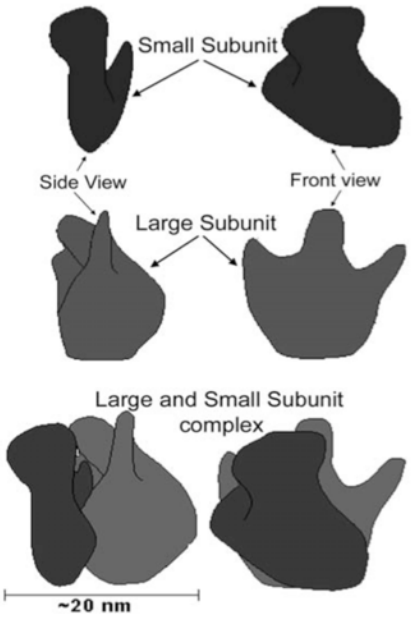

Figure 6 Ribosomes are small and dense structures that assemble proteins during the translation process. They are about 20 nm in diameter and are composed of 65% ribosomal RNA and 35% ribosomal proteins. Ribosomes consist of two subunits that fit together and work as one to translate the mRNA into a polypeptide chain during protein synthesis.

Transfer RNA

Transfer RNA (tRNA) is a small (73–93 nucleotides) RNA molecule folding into a cloverleaf-shaped structure as a result of intramolecular base pairing (Fig. 5). Each tRNA functions as an adaptor between a specific amino acid and its corresponding codon in mRNA. Basically, it delivers amino acids, one by one, to the growing polypeptide chain at the ribosomal site. In a typical eukaryotic cell, there are 32 different types of tRNA and each one carries one of the 20 amino acids existing in proteins at its 3′ end. It also contains a three bases region called anticodon, which can base pair to the corresponding three bases codon region on mRNA.

Ribosomal RNA

Ribosomal RNA (rRNA) is the structural component of the ribosome, which is the intricate cytoplasmic machine translating nucleotide sequence of mRNAs into amino acid sequence of polypeptides (Fig. 6). The ribosome can be viewed as protein manufacturing machinery in all living cells. The rRNAs interact with more than 50 different ribosomal proteins to produce the complex tridimensional structure of the ribosome. Eukaryotic ribosomes are very complex machinery and contain four rRNA molecules and about 80 different proteins. The four eukaryotic rRNAs are designated 5S (the S represents Svedberg units), 5.8S, 18S, and 28S rRNA and are approximately 120, 160, 1900, and 4800 nucleotides in length, respectively. The small subunit of the ribosome is constituted of the 18S rRNA along with about 30 different proteins, whereas the large subunit is composed of the 28S, 5.8S, and 5S rRNA along with some 45 different proteins. In prokaryotes, these subunits are different in size and numbered 23S, 16S, and 5S rRNA.

Small nuclear RNA and small nucleolar RNA

Small nuclear RNAs (snRNAs) are a class of small RNA molecules (ranging from 100 to 215 nucleotides) that are present in spliceosomes (described later in this chapter) and play a key role in the excision of noncoding sequences (introns) from the transcripts of nuclear genes. Unlike the other types of RNA, snRNAs never leave the nucleus of the cells. snRNAs are always associated with specific proteins and beside their role in RNA splicing, they are also involved in regulation of transcription factors and maintaining the telomeres.

Small nucleolar RNAs (snoRNA) are a large group of snRNAs located in the nucleus and the cajal bodies of eukaryotic cells. These are small RNA molecules that play an essential role in RNA biogenesis, particularly in ribosome formation by splicing the 45S rRNA precursor into 28S, 18S, and 5S molecules. snoRNAs also guide chemical modifications of nucleotides in rRNAs and other RNA genes.

MicroRNA, small temporal RNA, and small interfering RNA

MicroRNAs (miRNAs) are tiny RNA molecules that appear to regulate the expression of mRNA. miRNAs

and small temporal RNAs (stRNAs) are single-stranded noncoding RNA molecules of about 21 to 23 nucleotides in length that regulate gene expression. miRNA and stRNA molecules are partially complementary to one or more mRNA and function as silencers of gene expression.

Small interfering RNA (siRNA), sometimes known as short interfering RNA or silencing RNA, are a class of 20- to 25-nucleotide long, double-stranded RNA molecules. siRNA is involved in the RNA interference (RNAi) pathway where the siRNA interferes with the expression of a specific gene through a mRNA degradation pathway.

XIST RNA

Xist RNA is a spliced, polyadenylated, noncoding RNA that is expressed exclusively to deactivate one of the X chromosomes in females. The silencing is achieved by wide alteration in X chromosome chromatin structure, a conversion of active euchromatin into inactive heterochromatin.

Protein Structure

Proteins constitute 15% of the wet weight of cells and about 50% of its dry weight. Proteins are by far the most prevalent component of living organisms and are considered building blocks of the human body. They also play many roles vital to the survival of all cells.

Primary Structure

Proteins are composed of long sequences of monomers of amino acids linked together by a covalent bond and called polypeptides. There are 20 different amino acids (Table 1). Each amino acid contains at least one carboxyl group (COOH) and one α-amino group (NH_2), but differs from others by a side chain. This side chain can be anything from a hydrogen atom to a complex ring. These highly variable side groups provide the structural diversity of proteins. The side chains are classified into four types: (*i*) hydrophobic or nonpolar groups, (*ii*) hydrophilic or polar chains, (*iii*) acidic or negatively charged groups, and (*iv*) basic or positively charged chains. This chemical diversity among side groups is responsible for the phenomenal versatility of proteins.

Three-Dimensional Structure

Proteins have four different levels of organization namely the primary, secondary, tertiary, and quaternary structures (Fig. 7). The primary structure of a protein is its amino acids sequence. The secondary structure refers to the special interrelationships of the amino acids within a segment of the polypeptides. The most common forms of secondary structures, which were discovered by Linus Pauling and Robert Corey in 1940 (7), are α-helices and β-sheets. Whereas the secondary structure refers to the spatial organization of adjacent amino acids, the tertiary structure or conformation of a protein is defined by the overall folding of the complete polypeptide. Finally, the quaternary structure is the association between two or more polypeptides in a multimeric unit.

Table 1 The Name of the 20 Different Amino Acids, Their Abbreviations, and Side Chain Properties

Amino Acid	3-Letter	1-Letter	Side chain polarity	Side chain acidity or basicity
Alanine	Ala	A	nonpolar	neutral
Arginine	Arg	R	polar	basic (strongly)
Asparagine	Asn	N	polar	neutral
Aspartic acid	Asp	D	polar	acidic
Cysteine	Cys	C	polar	neutral
Glutamic acid	Glu	E	polar	acidic
Glutamine	Gln	Q	polar	neutral
Glycine	Gly	G	nonpolar	neutral
Histidine	His	H	polar	basic (weakly)
Isoleucine	Ile	I	nonpolar	Neutral
Leucine	Leu	L	nonpolar	Neutral
Lysine	Lys	K	polar	Basic
Methionine	Met	M	nonpolar	Neutral
Phenylalanine	Phe	F	nonpolar	Neutral
Proline	Pro	P	nonpolar	Neutral
Serine	Ser	S	polar	Neutral
Threonine	Thr	T	polar	Neutral
Tryptophan	Trp	W	nonpolar	Neutral
Tyrosine	Tyr	Y	Polar	Neutral
Valine	Val	V	Nonpolar	Neutral

MECHANISMS

Replication

DNA replication is the process of copying double-stranded DNA molecules and it takes place during the S phase of cell cycle for eukaryotes. This process is extremely important for all living organisms. The fidelity of DNA replication is astounding, with an average of only one mistake per billion nucleotides incorporated. With an estimated 40,000 genes and three billion base pairs, the human genome needs to be replicated every time before a cell divides: DNA replication must work very fast, but more importantly, with great precision. Proofreading and error-checking mechanisms ensure the accuracy of the whole process. In eukaryote, several hours are needed to complete the DNA replication process despite the synthesis rate of 30,000 nucleotides per minute. Due to the complexity of eukaryotic genome, DNA replication on a strand is started simultaneously at several origins.

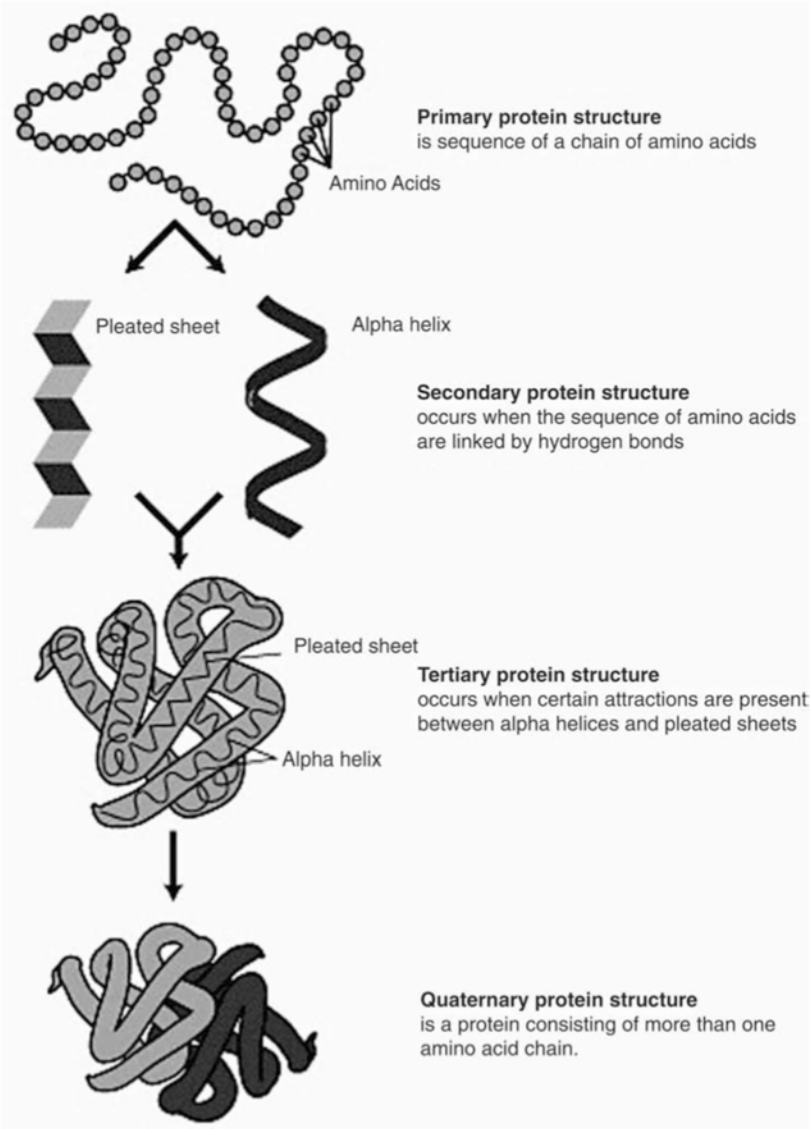

Figure 7 Different levels of protein conformation, from its primary structure to its quaternary structure.

Semiconservative Replication

At the end of the replication process, two DNA molecules identical to each other and identical to the parental molecule are produced. Since a single strand of the DNA helix holds the same genetic information in the complementary strand, both strands can serve as templates for replication. The template strand is preserved in its entirety and the new strand is assembled from nucleotides that are pairing with the base in the template. This process is called semiconservative replication because each of the individual parental DNA strands is preserved as part of the two newly formed DNA duplexes (Fig. 8).

Replication Process

Although knowledge of the structure of the replication machinery in eukaryotes is still limited due to its

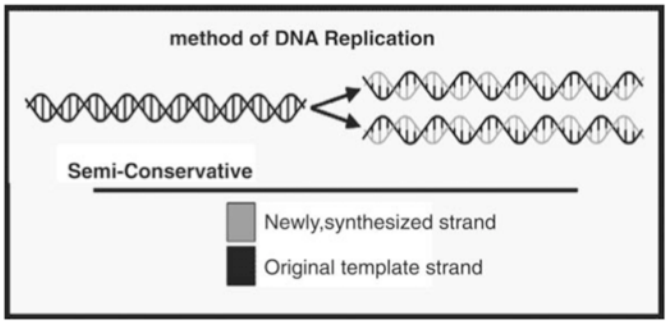

Figure 8 Semiconservative replication process. In this process, the template strand is preserved in its entirety and the new strand is assembled from nucleotides that are pairing with the base in the template.

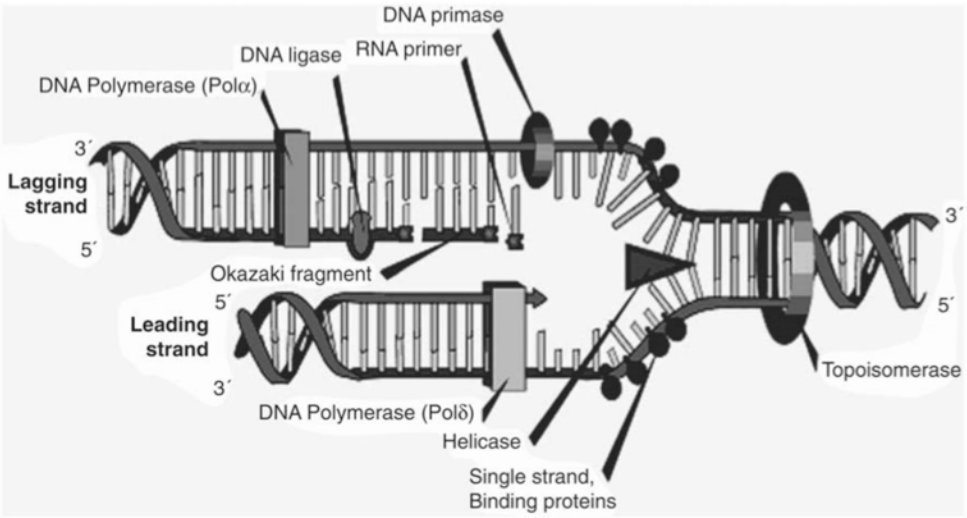

Figure 9 Schematic representation of a DNA replication fork with the key features of transcription process and its several enzymes.

complexity, there are many similarities with the simpler prokaryotes DNA replication process. In eukaryotic cells, DNA exists in the nucleus as a very compact and condensed structure. In order to begin the replication process, this structure must be opened up, so the DNA polymerase enzyme can copy the DNA template. The replication process takes place at a specific site called origin of replication, which is rich in AT content. The first step in DNA replication begins with the binding of the origin recognition complex (ORC) to the origin of replication. ORC complex is a hexamer of related proteins that function as a replication initiation factor that promotes the unwinding or denaturation of DNA. Following the binding of the ORC complex, other proteins (Cdc6/Cdc18 and Cdt1) will bind and coordinate the recruitment of the minichromosome maintenance function (MCM) complex to the origin of replication. The MCM complex is a hexamer and is thought to be the major DNA helicase in eukaryotic organisms. Once the binding of MCM occurs, a fully licensed pre-initiation replication complex (pre-RC) now exists. This process occurs during the G1 phase of the cell cycle and therefore, cannot initiate the replication. Replication only occurs during the S phase. Thus, separating the licensing and activation is a mechanism that ensures only one replication per origin in a cell cycle.

After the unwinding of the double helix, a new DNA strand is synthesized in the 5′ to 3′ direction for each parental strand by an enzyme called DNA polymerase. The synthesis of the new strand at the replication fork is bidirectional (Fig. 9), with two different DNA polymerases in function. One is for the leading strand and the other is for the lagging strand. In the leading strand, the

DNA polymerase catalyzes the formation of a phosphodiester bond between the 5′-phosphate on an incoming nucleotide and the free 3′-hydroxyl group on the growing polynucleotide. Thus, the growing DNA fragment is synthesized by complementary base pairing with the parental DNA template. By this mechanism, the DNA polymerase moves along the template and adds nucleotides in the 5′→3′ direction. This is true for the parental strand in 3′→5′ orientation, which is called leading strand. However, it works differently for the second strand with the 5′→3′ orientation, which is called lagging strand. The replication fork moves only in one direction and DNA replication goes only in the 5′→3′ direction, so how can this replication process be bidirectional? The paradox was solved by the discovery of Okazaki fragments (8). Instead of the continuous replication as in the leading strand, the lagging strand is produced in a discontinuous manner, which is accomplished by the synthesis of short DNA sections called Okazaki fragments. These fragments are produced from short RNA primers synthesized by an enzyme called RNA polymerase or primase. Thus, the free 3′-hydroxyl group of the RNA primer can be used by the DNA polymerase to extend the DNA. In eukaryotes, the lagging strand synthesis is carried out by the DNA polymerase α-primase complex and the primers are later removed by enzymes like ribonucleases and endonucleases. The gaps created by excised RNA are filled out by the DNA polymerase and then linked by DNA ligase to form a continuous strand of DNA.

Transcription

Transcription is the process by which a DNA template is copied to form an mRNA by a RNA polymerase. This results in the transfer of the genetic information from DNA to RNA. This is the first step in gene expression. The transcription mechanism is situated in the nucleus of the cell. The resultant mRNA will be processed and transported into the cytoplasm for the translation process. A segment of DNA that is transcribed to form one molecule of RNA is called transcription unit. In most mammalian cells, it is estimated that only 1% of the DNA sequence will be transcribed into functional mRNA. The transcription process can be divided into three important steps: (*i*) initiation of RNA chain, (*ii*) elongation of the chain, and (*iii*) termination of the transcription that results in the transcript release.

Initiation

Unlike prokaryote, eukaryotes require transcription factors to initiate transcription process. The transcription factors must bind the promoter region in DNA and form an appropriate initiation complex before the initiation of the transcription. In eukaryotic cells, three types of RNA polymerases (RNA polymerase I, II, and III) are involved in this process. The promoter region is constituted of specific nucleic acid sequence recognized by the polymerase. There are various types of promoters, such as the TATA box or the CATT box promoter regions, but all of them contain the specific sequence referred to as the starting site of transcription. In the vast majority of eukaryotic genes, the RNA polymerase II is responsible of the initiation of transcription. For the correct initiation of the transcription, the transcription factors must interact with the promoter region in a specific order. For example, in order to bind to the promoter region and initiate transcription efficiently, the DNA polymerase II (Fig. 10) requires transcription factors: TFIID, TFIIA, TFIIB, TFIIF, and TFIIE (**T**ranscription **F**actor for Polymerase **II**). After the arrival of the transcription factors, the polymerase II can bind to the promoter region and begin the transcription. Usually, the promoters for the genes transcribed by the RNA polymerases are situated upstream from the transcription start points, with some exceptions such as the genes transcribed by the RNA polymerase III.

For sustained transcription in eukaryotes, the promoter needs additional short regulatory sequences that are also located at varying distances from the starting point. Some of these elements are close to the core promoter and called proximal elements, while some others are situated several kilobases upstream or downstream and called enhancers or repressor sequences. The binding of these transcription factors to the DNA promoter regions causes local unwinding of the double helix, like in DNA replication, which allows the transcription to start.

Elongation

The elongation process is accomplished by base-pairing mechanism as is DNA replication. However, unlike in replication, there is only one transcript and the base pair are RNA-DNA instead of DNA-DNA. While in replication, either DNA strand can serve as a template, in transcription, the polymerase proceeds only along a strand in 3′ to 5′ direction. In other words, the synthesis of the mRNA is 5′→3′ directed on the 3′→5′ oriented template DNA strand. Thus, the mRNA molecule produced is complementary to the DNA template (3′→5′ or antisense) strand and identical to the DNA nontemplate (5′→3′ or sense) strand. For the complementary base-pairing process, the same rules are applied, but the AT coupling in DNA-DNA duplex is replaced by an AU coupling in RNA-DNA duplex. The elongation of the RNA chain is catalyzed by the RNA polymerase enzyme, which produces covalent link between each ribonucleoside

Figure 10 Schematic representation of the transcription bubble. The elongation of the RNA chain is catalyzed by the RNA polymerase on the template strand (3′ to 5′) of the DNA.

triphosphate. RNA polymerase contains both unwinding and rewinding activities, so the process forms a structure called transcription bubble that moves along the DNA during the transcription process (Fig. 10).

Termination

In prokaryotes, the transcription termination mechanisms are very well defined. There are two processes leading to the termination of the transcription. One is Rho independent and the other Rho dependent. In the Rho-independent type, RNA transcription stops when the newly synthesized RNA molecule forms a hairpin loop and sequence of many Us, which makes it detach from the DNA template. In the Rho-dependent process, a protein called "Rho" destabilizes the RNA-template DNA complex allowing for the release of the mRNA. Unlike prokaryotes, the termination process in eukaryotes is poorly understood. It involved the endonucleolytic cleavage of the RNA transcript rather than the termination of the transcription. This cleavage event that produces the 3′ end of the transcript usually occurs downstream a conserved consensus sequence AAUAAA, which is located near the end of the transcript unit.

Posttranscriptional Modifications

After the transcription process, the population of primary transcripts in the nucleus is called heterogeneous nuclear RNA (hnRNA). This population of RNA molecules is highly varied in sizes. Likewise, the primary transcript product is called pre-mRNA, because it will undergo three major modifications prior to its transport to the cytoplasm for translation. These modifications include 5′ capping, 3′ polyadenylation, and splicing.

Capping

The first processing step for the mRNA is the 5′ capping. This process referred to the addition of a 7-methylguanosine cap at the 5′ end of the primary transcript. This residue is linked to the initial nucleoside of the transcript by a 5′–5′ phosphate linkage. This 5′ cap addition stabilizes the mRNA as it undergoes translation and plays a role in the initiation of translation.

Polyadenylation

The addition of poly (A) tails at the 3′ end of the transcript is called polyadenylation. This process takes place in the nucleus of the cell after transcription. After the

polyadenylation signal has been transcribed, an endonuclease complex cleaves the mRNA chain and 50 to 250 adenosine residues are added to the free 3′ end at the cleavage site by the poly (A) polymerase. The polyadenylation process initially depends on the existence of the AAUAAA sequence for the first 10 nucleotides, but then is simply dependent on the preexisting poly (A) tail for the remaining 50 to 250 nucleotides. The poly (A) tails of eukaryotic mRNAs enhance their stability and facilitates their transport from the nucleus to the cytoplasm.

RNA splicing

RNA splicing is the process by which introns (the regions of RNA that do not code for proteins) are removed from the pre-mRNA and the remaining exons (regions that carry the code needed for protein synthesis) are connected to reform a single continuous RNA molecule. In 1989, Tom Cech won the Nobel Prize for his works on the mechanism of RNA splicing (9), prize that he shared with Sidney Altman for his work on RNA. Although the splicing occurs after the complete pre-mRNA synthesis and end-capping, some primary transcripts with many exons can be spliced during transcription. The splicing process needs to be very accurate, because an error in only one nucleotide (removal or addition) can cause a complete shift in the open reading frame of the code. This shift will, therefore, result in a new sequence of codons that will end in a completely different amino acid sequence or possibly insert a stop codon for the termination of the synthesis of the peptide. This kind of error in the splicing process accounts for about 15% of the genetic disease. The machine responsible for the RNA splicing is called spliceosome and is composed of a large enzymatic complex, which includes 145 different proteins (snRNPs or small nuclear ribonucleoproteins) and several snRNAs. This complex recognizes specific splice sites in the introns of pre-mRNA sequences. A pre-mRNA can be spliced in many different ways, thus producing different mature mRNAs that encode for different protein sequences. This process is called alternative splicing and it allows the production of a large amount of proteins from a limited amount of DNA.

An intron in the pre-mRNA molecule often begins with nucleotides GU and finishes with AG, which is preceded by a pyrimidine-rich sequence called polypyrimidine tract. The splicing reaction occurs in two steps, (Fig. 11) in a region called branchpoint sequence, which is situated 10 to 40 nucleotides upstream of the polypyrimidine tract. The first step is the attack of the G residue in the 5′ splicing site by the 2′-hydroxyl of the A residue in branchpoint. It results in the formation of a lariat and a free exon. In the second step, the 3′ end G residue of the intron is cleaved, which brings the two exons together and release the intron in a lariat form. This process generates a mature mRNA molecule that can further be exported into the cytosol for the translation process.

Translation

Translation refers to the process by which the genetic information stored in an mRNA is translated into the amino acid sequence (protein), according to the

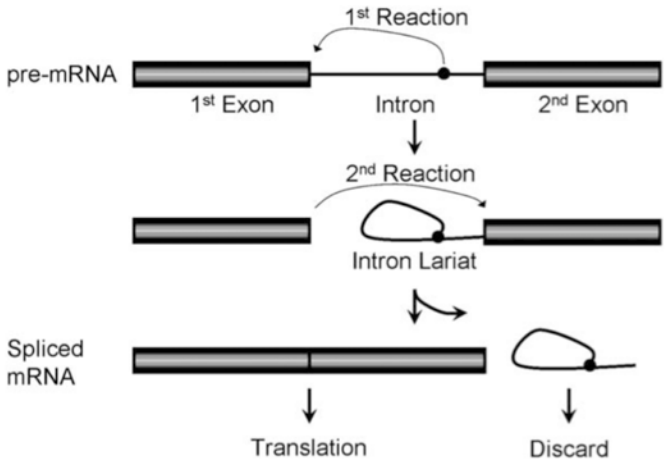

Figure 11 Diagram illustrating the two-step biochemistry of splicing. The first step is the formation of a lariat and free exon and the second one is the cleavage of the 3′ end of the intron, which brings the two exons together and release the intron in a lariat form. The resultant mature mRNA can be transported in the cytosol for translation.

specification of the genetic code. Unlike transcription, which takes place in the nucleus of the cell, the translation process is effectuated in the cytosol. This process is extremely complex, requiring numerous macromolecules including over 50 polypeptides, at least 20 amino acid–activating enzymes, from 40 to 60 tRNA molecules and a large number of soluble proteins involved in the polypeptide chain initiation, elongation, and termination. With this enormous complexity, it is not surprising that the process is highly regulated and guided by a combination of rules, called genetic code.

Genetic Code

The first elucidation of a codon was done by Marshall Nirenberg and Heinrich J. Matthaei in 1961 at the National Institutes of Health (10). The genetic code contains a total of 64 different codons derived from four different nucleotides bases: 61 codons specify amino acids while 3 others specify a STOP signal. The rules of the genetic code (Table 2) can be grouped into seven important properties, which are as follows:

1. The genetic code is composed of nucleotides triplets, in other words, an amino acid in the peptide is specified by three nucleotides in the mRNA called codon.
2. The genetic code is nonoverlapping, with each nucleotide in the mRNA belonging to just one codon except in rare exceptions.
3. The genetic code is coma free, which means that during the translation, the codons are read consecutively without any forms of punctuation.
4. The genetic code is degenerate, with more than one codon specifying one amino acid (61 codons for 20 amino acids).
5. The genetic code is ordered, which means that codons for similar amino acids or multiple codons for the same amino acids are closely related, usually with a difference of only one nucleotide.
6. The genetic code contains start and stop codons.
7. The genetic code is nearly universal and all the codons have the same meaning in all living organisms, with minor exception.

This combination of rules is applies for the transfer of information from an mRNA into amino acids sequence of a protein and translation can be divided in three processes: initiation, elongation, and termination.

Initiation

In eukaryotes, the initiation of the transcription begins with the binding of a protein called cap-binding protein (CBP) to the 7-methylguanosine cap at the 5′ end of the mRNA, followed by the binding of other initiation factors and the recruitment of the 40S subunit of the ribosome. The ribosome scans the mRNA in the 5′ to 3′ direction until it encounters the first methionine starting codon (AUG).

Table 2 Genetic Code Showing the 64 Codons and the Amino Acid Specified for Each Codon

		2nd base			
		U	**C**	**A**	**G**
1st base	**U**	UUU (Phe/F)Phenylalanine	UCU (Ser/S)Serine	UAU (Tyr/Y)Tyrosine	UGU (Cys/C)Cysteine
		UUC (Phe/F)Phenylalanine	UCC (Ser/S)Serine	UAC (Tyr/Y)Tyrosine	UGC (Cys/C)Cysteine
		UUA (Leu/L)Leucine	UCA (Ser/S)Serine	UAA Ochre (*stop*)	UGA Opal (*stop*)
		UUG (Leu/L)Leucine	UCG (Ser/S)Serine	UAG Amber (*stop*)	UGG (Trp/W)Tryptophan
	C	CUU (Leu/L)Leucine	CCU (Pro/P)Proline	CAU (His/H)Histidine	CGU (Arg/R)Arginine
		CUC (Leu/L)Leucine	CCC (Pro/P)Proline	CAC (His/H)Histidine	CGC (Arg/R)Arginine
		CUA (Leu/L)Leucine	CCA (Pro/P)Proline	CAA (Gln/Q)Glutamine	CGA (Arg/R)Arginine
		CUG (Leu/L)Leucine	CCG (Pro/P)Proline	CAG (Gln/Q)Glutamine	CGG (Arg/R)Arginine
	A	AUU (Ile/I)Isoleucine	ACU (Thr/T)Threonine	AAU (Asn/N)Asparagine	AGU (Ser/S)Serine
		AUC (Ile/I)Isoleucine	ACC (Thr/T)Threonine	AAC (Asn/N)Asparagine	AGC (Ser/S)Serine
		AUA (Ile/I)Isoleucine	ACA (Thr/T)Threonine	AAA (Lys/K)Lysine	AGA (Arg/R)Arginine
		AUG (Met/M)Methionine, (*start*)[a]	ACG (Thr/T)Threonine	AAG (Lys/K)Lysine	AGG (Arg/R)Arginine
	G	GUU (Val/V)Valine	GCU (Ala/A)Alanine	GAU (Asp/D)Aspartic acid	GGU (Gly/G)Glycine
		GUC (Val/V)Valine	GCC (Ala/A)Alanine	GAC (Asp/D)Aspartic acid	GGC (Gly/G)Glycine
		GUA (Val/V)Valine	GCA (Ala/A)Alanine	GAA (Glu/E)Glutamic acid	GGA (Gly/G)Glycine
		GUG (Val/V)Valine	GCG (Ala/A)Alanine	GAG (Glu/E)Glutamic acid	GGG (Gly/G)Glycine

Triplet nucleotide sequence or codon refers to the sequence in mRNA, not DNA. The direction is 5′ to 3′.
[a]The codon AUG both codes for methionine and serves as an initiation site; the first AUG in an mRNA's coding region is where translation into protein begins.

The 40S subunit contains two tRNA-binding sites in its cleft, called P site for peptidyl tRNA site and A site for aminoacyl tRNA site. When the ribosome arrives to the starting codon, an initiator tRNA charged with a methionine binds to the ribosomal complex. The Met-charged initiator tRNA is brought to the P site of the small ribosomal subunit by eukaryotic Initiation Factor 2 (eIF2). The hydroxylation of a GTP then signals the dissociation of several factors from the small ribosomal subunit, which results in the association of the large subunit (or the 60S subunit) to the transcription complex. The complete ribosome (80S) is now formed. The Met-charged initiator tRNA is the only tRNA to first bind the P site, as all the others tRNA have to enter the A site first. Even if many proteins start with the amino acid methionine, in some cases it is cleaved after by a protease.

Elongation

Once the initiation complex is complete, the elongation process begins (Fig. 12), which is carried out by a set of elongation factors. The addition of each new amino acid within the growing polypeptide occurs in three steps: (*i*) the binding of an aminoacyl-tRNA into the A site of the ribosome, (*ii*) the formation of a new peptide bond, and (*iii*) the translocation of the ribosome to the next three nucleotides (next codon) along the mRNA chain. In the first step, the specificity of the tRNA binding is provided by the mRNA codon located on the A site. In other words, the anticodon on the incoming tRNA must pair with the mRNA codon present in the A site. The binding of the tRNA into the ribosome complex requires GTP hydrolysis. After both P site and A site are occupied, the two proximal amino acids are joined together to form a peptide bond by the catalytic activity of an enzyme called peptidyl transferase. This enzymatic activity is situated on the ribosome and no energy is expended at this stage. During this step, the ribosome uses the energy from GTP hydrolysis to move three nucleotides toward the 3′ end of the mRNA. As the ribosome moves, the peptidyl-tRNA present in the A site is translocated in the P site with the aid of translocase enzyme and GTP, while the uncharged tRNA in the P site is translocated to the E site. The A site is now unoccupied and ready for the next tRNA molecule complementary to the mRNA codon. These three steps will be repeated in a cyclic manner during the whole elongation process until the termination happens.

Termination

The polypeptide chain elongation process undergoes termination when the ribosome comes across a stop codon in the A site, for which there is no tRNA. There are three different stop codons: UAA, UAG, and UGA. In eukaryotes, each of these three codons can be recognized by a releasing factor called eukaryotic release factor (eRF). The release factor induces a nucleophilic attack of the C-terminus of the nascent peptide by water. This process releases the polypeptide from the tRNA, triggering the translocation of the tRNA from the A site to the P site,

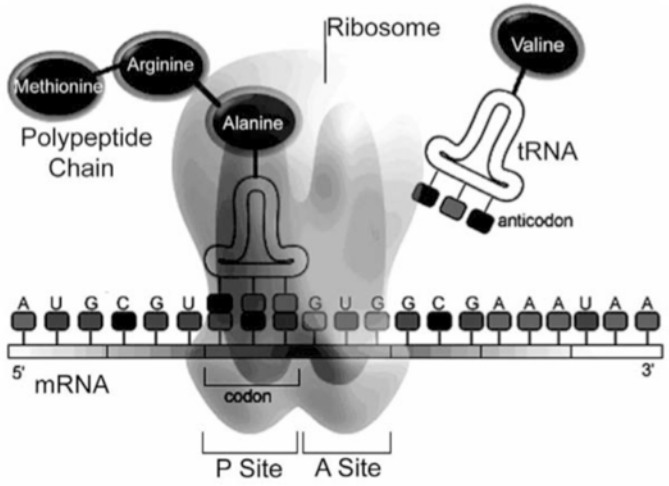

Figure 12 Elongation step in translation process. Each aminoacyl-tRNA, except the first one, first enters into the A site of the ribosome. The amino acids in the A site is then connected to the polypeptide chain in the P site with a peptide bond. As the ribosome moves along the mRNA in the 5′→3′ direction, the now uncharged tRNA is translocated into the P site and the next aminoacyl-tRNA enters the A site. Thus, the ribosome and tRNA molecules translate the genetic code contained in the mRNA into an amino acid sequence, to produce a protein.

the dissociation of the small and large subunit of the ribosome and the release of the mRNA. Ribosomal subunits are now ready for the next round of protein synthesis, while the mRNA can be either retranslated or degraded. All mRNAs are eventually degraded when the synthesis of a protein in no longer required.

Posttranslational Modifications

In mammalian cells, there are different compartments called organelles, which include the rough endoplasmic reticulum (ER), the smooth endoplasmic reticulum, the Golgi apparatus, the lysosomes, and the peroxisomes. In these cells, most proteins destined for secretion are targeted to the ER by a signal sequence at the amino end of the peptide, called signal peptide. This sequence is recognized by a signal recognition particle (SRP), which binds to the signal peptide. The protein-SRP complex can therefore bind to the SRP receptor on the target ER membrane. Proteins destined for other compartment are initially directed into the ER and will then follow the secretory pathway with similar signal peptides. This process is posttranslational and the proteins are packaged into vesicles as they move between the lumen of different organelles. After its synthesis, a protein can undergo some other posttranslational modifications while in these compartments. Basically, a protein is a simple chain of a combination of 20 different amino acids, but the posttranslational modifications of these amino acids can extend the range of functions of this protein. A large variety of posttranslational modifications exists for proteins, including addition of functional groups by the processes of biotinylation, glycosylation and/or phosphorylation. Other forms of posttranslational modifications include the addition of other peptides, changes in the chemical nature such as deamidation, or structural changes such as addition of disulfide bridges. All these modifications will allow the production of the vast complexity of different protein types, from enzymes that catalyze fundamental reactions to antibodies participating in the immune response.

SUMMARY

The field of molecular biology is extremely vast, involving numerous processes and biological molecules. The impressive machinery by which a progenitor cell can transmit its genetic information to daughter cells, or by which it can synthesize the various macromolecules necessary for its survival, is precisely and accurately regulated. However, all this complexity could be resumed by a general theory called the central dogma of molecular biology. According to this central dogma, genetic information is stored in DNA and flows from DNA to DNA during the transmission from generation to generation, or from DNA to protein during its phenotypic expression in an organism. The transfer of genetic information from DNA to proteins is a two-step process, beginning with the transcription of the DNA in an mRNA (DNA-RNA transfer) and finishing by the translation of this mRNA into a protein (RNA-protein transfer). The central dogma also states that unlike the transcription that can be sometimes reversible, the translation process that transfer genetic information from RNA to protein, is irreversible. This central dogma of molecular biology is largely responsible for the ability of a cell to maintain its order in a chaotic environment. Understanding the processes involved in the central dogma is important for studying both hereditary and nonhereditary diseases. Additionally, grasping the concepts of these biological processes is crucial for the application of the different molecular biology methods discussed in the next chapter.

REFERENCES

1. The double helix-50 years. Nature 2003; 421(suppl):396–401.
2. Dunham I, Shimizu N, Roe BA, et al. The DNA sequence of human chromosome 22. Nature 1999; 402(6761):489–495.
3. Venter JC, Adams MD, Myers EW, et al. The sequence of the human genome. Science 2001; 291(5507):1304–1351.
4. White House Press Release.
5. Mendel JG. Versuche über Plflanzenhybriden Verhandlungen des naturforschenden Vereines in Brünn, Bd. IV für das Jahr, 1865. Abhandlungen 1866; 3–47.
6. Watson JD, Crick F. Molecular structure of nucleic acids; a structure for deoxyribose nucleic acid. Nature 1953; 171(4356):737–738.
7. Pauling L, Corey RB, Branson HR. The structure of proteins; two hydrogen-bonded helical configurations of the polypeptide chain. Proc Natl Acad Sci U S A 1951; 37(4): 205–211.
8. Okazaki R, Okazaki T, Sakabe K, et al. Mechanism of DNA chain growth. I. Possible discontinuity and unusual secondary structure of newly synthesized chains. Proc Natl Acad Sci U S A 1968; 59(2):598–605.
9. Zaug AJ, Cech TR. In vitro splicing of the ribosomal RNA precursor in nuclei of Tetrahymena. Cell 1980; 19(2):331–338.
10. Martin RG, Matthaei JH, Jones OW, et al. Ribonucleotide composition of the genetic code. Biochem Biophys Res Commun 1962; 6:410–414.

ANNEX III

Book Chapter
(Methods in Molecular Biology)

3

Methods in Molecular Biology

JULIE HEROUX and AHMED M. GHARIB

National Heart, Lung and Blood Institute (NHLBI), National Institutes of Health (NIH), Maryland, U.S.A.

INTRODUCTION

There is a vast diversity of methods in molecular biology. These range from the simple techniques used for DNA or RNA extraction, to the more complex methods utilized for the production of transgenic animals. All of these techniques constitute very valuable tools essential for understanding the pathogenesis of various diseases and for the development of new treatments. Moreover, understanding these techniques is important for the development of image-guided therapeutic methods and molecular imaging. Here, we will emphasize and revisit the basic principles behind various molecular biology protocols, which should allow multidisciplinary imaging specialists to better understand the techniques. With this in mind, the description of these methods will be presented not so much as a technique, but more as an approach focusing on the molecular level of biological events.

BASIC CLONING TECHNIQUES

The mammalian genome contains about 3×10^9 nucleotides pairs, with a single gene averaging 3000 nucleotide pairs (many are larger). Thus, isolation of a single gene is a meticulous process requiring rigorous methods that will be discussed in this chapter. Most techniques used for analyzing genes require significant amount of the gene sequence in a relatively pure form. The development of recombinant DNA and gene cloning technologies has allowed for the isolation, the replication and the study of chromosomes by different techniques, such as nucleic acid sequencing, electron microscopy, and other analytical techniques. There are two essential steps in the gene cloning procedure: (*i*) incorporation of the gene into a small self-replicating chromosome called cloning vector and (*ii*) amplification of the structure by its replication in an appropriate host. The first step involves the in vitro production of recombinant DNA by fusing one or more DNA fragments (gene) of interest with the vector. The second step is gene cloning, where the recombinant vectors transfect an appropriate host cell line and replicate, thereby producing many copies of the cloned gene.

Restriction Endonucleases

Due to the immense size of genomic DNA, any gene or DNA fragment of interest first needs to be cleaved out or separated into smaller more manageable fragments before it can be cloned or sequenced. This is achieved using a special group of bacterial enzymes called restriction endonucleases. Thus, one of the most powerful tools for molecular biologists, in conjunction with polymerase chain reaction (PCR), was the discovery of these

Table 1 Some Important Restriction Endonucleases from Different Organisms Showing the Preferential Cleaving Site for Each Enzyme and the Resultant DNA Fragment with Blunt or Cohesive Ends

Enzyme	Source	Recognition sequence	Cut
*Eco*RI	*Escherichia coli*	5′GAATTC	5′—G AATTC—3′
		3′CTTAAG	3′—CTTAA G—5′
*Bam*HI	*Bacillus amyloliquefaciens*	5′GGATCC	5′—G GATCC—3′
		3′CCTAGG	3′—CCTAG G—5′
*Hin*dIII	*Hemophilus influenzae*	5′AAGCTT	5′—A AGCTT—3′
		3′TTCGAA	3′—TTCGA A—5′
*Not*I	*Nocardia otitidis*	5′GCGGCCGC	5′—GC GGCCGC—3′
		3′CGCCGGCG	3′—CGCCGG CG—5′
*Hin*fI	*Hemophilus influenzae*	5′GANTC	5′—G ANTC—3′
		3′CTNAG	3′—CTNA G—5′
*Sma*I[a]	*Serratia marcescens*	5′CCCGGG	5′—CCC GGG—3′
		3′GGGCCC	3′—GGG CCC—5′
*Hae*III[a]	*Hemophilus aegyptius*	5′GGCC	5′—GG CC—3′
		3′CCGG	3′—CC GG—5′′
*Alu*I[a]	*Arthrobacter luteus*	5′AGCT	5′—AG CT—3′
		3′TCGA	3′—TC GA—5′
*Eco*RV[a]	*Escherichia coli*	5′GATATC	5′—GAT ATC—3′
		3′CTATAG	3′—CTA TAG—5′
*Kpn*I[3]	*Klebsiella pneumoniae*	5′GGTACC	5′—GGTAC C—3′
		3′CCATGG	3′—C CATGG—5′
*Sac*I[3]	*Streptomyces achromogenes*	5′GAGCTC	5′—GAGCT C—3′
		3′CTCGAG	3′—C TCGAG—5′
*Sal*I[3]	*Streptomyces albue*	5′GTCGAC	5′—G TCGAC—3′
		3′CAGCTG	3′—CAGCT G—5′
*Sca*I[3]	*Streptomyces caespitosus*	5′AGTACT	5′—AGT ACT—3′
		3′TCATGA	3′—TCA TGA—5′
*Sph*I[3]	*Streptomyces phaeochromogenes*	5′GCATGC	5′—G CATGC—3′
		3′CGTACG	3′—CGTAC G—5′
*Xba*I[3]	*Xanthomonas badrii*	5′TCTAGA	5′—T CTAGA—3′
		3′AGATCT	3′—AGATC T—5′

[a]Blunt ends.

restriction enzymes. In 1970, Hamilton Smith (1) and Daniel Nathan (2) first discovered the existence of this type of enzyme and later, in 1978, won the Nobel Prize in Physiology and Medicine for their work. Now, more then 200 different endonucleases isolated from different organisms are commercially available. The name given to each enzyme reflects its origin with the first letter for the genus, next two letters for the species, and a letter for strain specificity if applicable (*Eco*RI: *Escherichia coli*, strain RY13, was first discovered in this strain). The biological function of these restriction endonucleases is to protect the host against invasion by foreign DNA. Unlike the other types of endonucleases that cut randomly into a DNA sequence, restriction endonuleases cleave into very specific nucleotide sequences, which are called restriction sites and the resulting double-stranded DNA fragment is hence called restriction fragment. Usually, restriction endonucleases recognize DNA sequences that are four to eight nucleotides long and called palindromes. Palindromes are nucleotides pair sequence (in a double-stranded DNA segment) that can be read the same from 5′ to 3′ for each strand as seen in this example:

5′-GGATCC-3′
3′-CCTAGG-5′

Some enzymes cut directly in the middle of the sequence, generating "blunt ends," while others cleave both strands at different points, generating staggered ends called cohesives or "sticky" ends (Table 1). The off-staggered cleavage produces segments of DNA with complementary single-stranded ends that can be joined together again by DNA ligase. This enzyme catalyses formation of 3′ → 5′ phosphodiester bond between the 3′-hydroxyl end of one restriction fragment strand and the 5′-phosphate end of another during the time that the cohesive ends are transiently base paired. These cohesive or sticky ends are very useful for "cutting and pasting" DNA from different origin to create recombinant molecule with the aid of a DNA ligase. Therefore, a hybrid combination of two fragments is called recombinant DNA molecule.

Vectors and Plasmids

In 1972, Cohen et al. developed a recombinant DNA technology that allowed DNA from one organism to be cloned into a carrier DNA molecule and be replicated and expressed in a new host (3). This technique, called molecular cloning, has revolutionized the field of molecular biology. DNA molecule used to carry a foreign DNA fragment into a bacterial or eukaryotic host organism is called cloning vector. There are several different types of vectors. The simplest and most commonly used DNA vector is derived from viral chromosomes and called plasmid. Plasmids are extrachromosomal, doubled-stranded circular molecules of DNA present in microorganisms, especially bacteria. They range from about 1 kilobase (kb) to over 200 kb in size, with an average 15 kb, and replicate autonomously. Other types of cloning vectors include cosmids, bacteriophages, bacterial artificial chromosomes (BACs), and yeast artificial chromosomes (YACs).

A cloning vector has three essential components (Fig. 1): (*i*) an origin of replication; (*ii*) a dominant selectable marker gene, usually conferring drug resistance to the host cell; and (*iii*) at least one unique restriction endonuclease cleavage site, which is present only once in the vector. Usually, a cloning vector contains unique cleavage site for several different restriction enzymes. This cluster of unique restriction sites is called polylinker or multiple cloning sites (MCS). In addition to these features, a vector may contain a promoter inserted in front of the polylinker site. This promoter drives the expression of the DNA fragment inserted into the polylinker site. The insertion of a DNA fragment into a cloning vector is carried out by treating both vehicle and foreign DNA with the same restriction enzyme, then ligating the fragments with a DNA ligase.

Transformation and Transfection

Transformation is the genetic alteration of a cell resulting from the uptake and expression of foreign genetic material (DNA). Transformation of eukaryotic cell is usually called transfection.

Transformation

In nature, transformation does not occur in every species of bacteria. Instead, it takes place only in the species possessing proteins and enzymatic machinery necessary to bind free DNA molecules and transport them into the cytoplasm. Only cells that secrete a competence factor, competent cells, are considered able to serve as recipient cells in transformation. This natural capability of taking up DNA is called natural competence. However, there are mechanisms that can force passive incorporation of a plasmid into an artificially permeabilized cell; this is called artificial competence. For example, cell wall permeability to DNA can be induced by chilling cells in the presence of divalent cations such as Ca^{2+} or heating them. Electroporation is another way to make holes in bacterial (and other) cells, by briefly shocking them with an electric field of 10 to 20 kV/cm. If the plasmid is present when the shock is applied, it can enter the cell through these holes and natural membrane repair mechanisms will then close these holes.

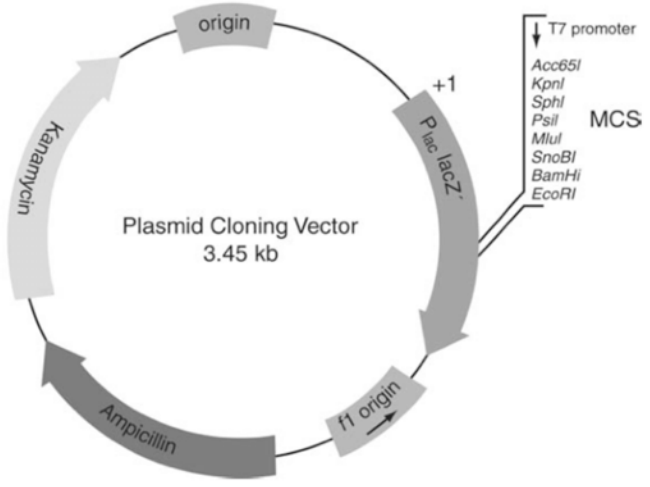

Figure 1 Schematic representation of a typical plasmid with (*i*) an origin of replication, (*ii*) a selectable marker gene conferring ampicillin and kanamycin drug resistance, and (*iii*) a multiple cloning site (MCS). Additionally, features are also presents, like a T7 promoter for the expression of the inserted gene.

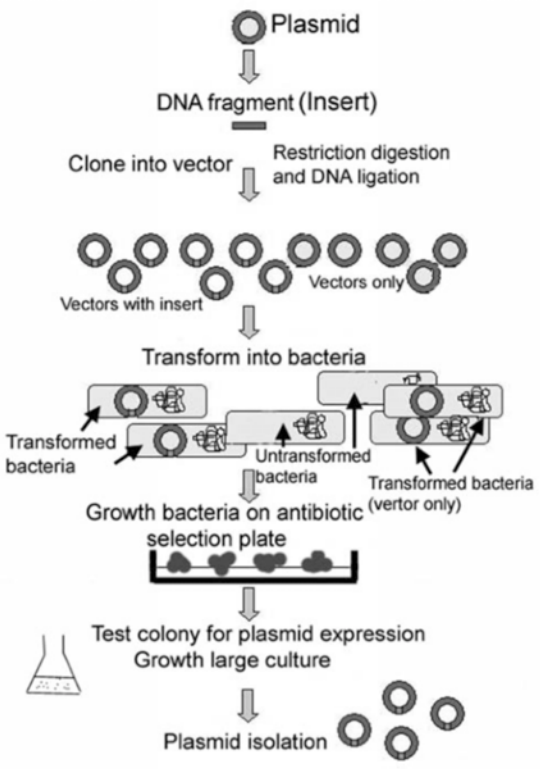

Figure 2 An overview of DNA cloning in bacteria, using a plasmid vector. The target insert is first cloned into a vector, and the construction is then used to transform bacteria. Bacteria with incorporated vectors are selected by growing them on antibiotic plate and finally, plasmid are purified from large culture preparation.

Only one type of recombinant plasmid can transform a single bacterial cell. In other words, multiple different types of vector molecules cannot replicate in a single bacteria. This provides a powerful tool for isolating a clone of interest (Fig. 2).

Transfection

Like transformation process, transfection typically involves opening transient pores or holes in the cell plasma membrane, to allow the uptake of material. There are various methods of introducing foreign DNA into a eukaryote cell. They fall into three categories, namely, (*i*) biochemical methods using calcium phosphate, DEAE, dextran, and several cationic liposome-based transfection agents; *(ii)* physical methods including electroporation and direct injection; and (*iii*) transduction mediated by viruses. In the liposome-based transfection technique, lipid-based agents (Lipofectamine 2000, Superfect, FuGEN6, Poly-l-lysine) form complexes with DNA. The resultant lipid-coated DNA is taken into the cell using nonreceptor-mediated endocytosis.

Transfection efficiency is variable and can be affected by the cell line, DNA quality, and the nature of transfection, whether stable or transient. In transient transfection, the transfected DNA is not integrated into the host chromosomal DNA, and foreign DNA is lost at the later stage when the cells undergo mitosis. If the transfected gene integrates into the genome of the cell, a stable transfection occurs. To accomplish this, another gene has to be cotransfected into the cell, which gives the cell a selection advantage, such as drug resistance.

Complementary DNA

A large percentage of DNA sequence in eukaryotes is not expressed. Thus, expressed sequences can be identified more easily by working with complimentary DNA (cDNA). Additionally, cDNA sequences are smaller in size and can be cloned more efficiently into a variety of vectors. The first step of cDNA synthesis depends on an enzyme called RNA-dependent DNA polymerase or reverse transcriptase (Fig. 3). Reverse transcription exploits a characteristic of mature mRNAs known as the 3′-polyadenylated region, commonly called the poly (A) tail, as a common binding site for poly (T) DNA primers. These primers will anneal to the 3′ end of every mRNA in the solution, allowing 5′ to 3′ synthesis of cDNA by the reverse transcriptase enzyme. Gene-specific primers or random hexamer primers can also be used to generate the cDNA. The mRNA is subsequently removed by treatment with RNase H. The second strand of the cDNA is usually synthesized by a combined action of both DNA polymerase 1 and T4 DNA polymerase, which used the RNA fragments as amorces. DNA polymerase I is used since the 5′ → 3′ exonuclease activity is needed to remove RNA in front of the enzyme. DNA polymerase I also removes the RNA primer from the 5′ lagging strand and fills in the recessed 3′ end. T4 DNA ligase then joins the various fragments together into a continuous strand of DNA. The final products are cDNA molecules with blunt ends, which can be further ligated to linkers containing restriction sites using T4 DNA ligase. The cDNA molecules are ultimately cleaved at the restriction site of the linker and ligated into a compatible vector for the formation of a cDNA library. The ligation mixture is transformed into a bacterial or phage host. A cDNA library can be used for different purposes. There is a broad diversity of cDNA libraries that are available commercially. As cDNA sequences differ in each library, comparison between libraries constructed from cells derived from different organisms can provide useful information.

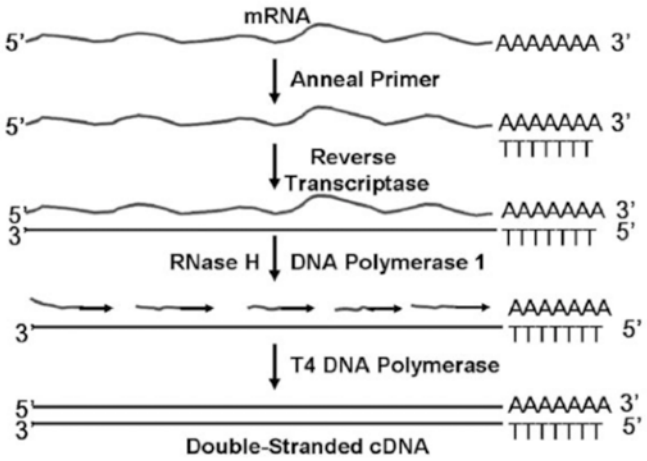

Figure 3 Schematic description of the principal steps of double-stranded cDNA synthesis from an mRNA template. *Source*: From Pandit SD, Li KC. Acad Radiol 2004; 11(suppl 1):S42–S53.

DNA, RNA, AND PROTEIN ANALYSIS

Gel Electrophoresis

Electrophoresis was discovered by Reuss, in 1809, and is defined by the motion of dispersed particles relative to a fluid under the influence of an electric field that is space uniform (4). Gel electrophoresis is the process by which biological macromolecules such as DNA, RNA, or proteins are separated on the basis of their electrophoretic mobility, into a gel, from the cathode (negatively charge) toward the anode (positively charge) of an electrical current. DNA and RNA molecules have a relatively constant negative charge per unit mass, so they migrate naturally toward the anode on the basis of their size and conformation. However, for the separation of proteins, an anionic detergent sodium dodecyl sulfate (SDS) is used, which applies a negative charge to each protein in proportion to its size. By this process, and because size is closely proportional to the mass, proteins (similarly to nucleic acid) migrate according to their molecular weight toward the anode. The gel refers to the matrix used for containing and separating the target molecules, and is a cross-linked polymer with different composition and porosity. The composition of the gel used depends on the target molecules. For example, acrylamide is preferred for proteins and small DNA or RNA, while agarose is generally used for large (greater than a few hundred bases) DNA and RNA. The matrix created by the polymerization of the gel creates molecular sieves, retarding the passage of large molecules more than small molecules. After the migration, different techniques of staining can be used to visualize the separated bands. The most common stains are Coomassie Brilliant Blue or silver stain for proteins and ethidium bromide or ^{32}P radioactive isotope for DNA and RNA. There are other methods of band visualization, including photograph under ultraviolet light for fluorescent molecules or autoradiogram for molecules with radioactive atoms.

Gel electrophoresis is usually used for analytical purposes, but may also be used as a preparative technique for partial purification of molecules prior to the application of other methods, such as cloning, PCR, mass spectrometry, or DNA sequencing.

DNA Analysis by Southern Blot Hybridization

This technique was developed by the British biologist Edwin Southern (5) in 1975. The method utilizes a radioactive or chemiluminescent probe to visualize genes and others DNA fragments that have been previously separated by electrophoresis (Fig. 4). First, restriction endonucleases are used to cleave high–molecular weight DNA into smaller fragments. After the digestion, these fragments are separated by agarose gel electrophoresis and then transferred onto a nitrocellulose or nylon membrane. The DNA is denatured either prior to or during the transfer using alkaline solution to produce single-stranded DNA. After the complete transfer, the DNA is immobilized on the membrane by high temperature drying or ultraviolet irradiation. This process creates an exact replicate of the gel on the nylon or nitrocellulose membrane. The membrane is now ready to be hybridized or annealed with a DNA or RNA probe containing the sequence of interest. This hybridization is based on the complementary

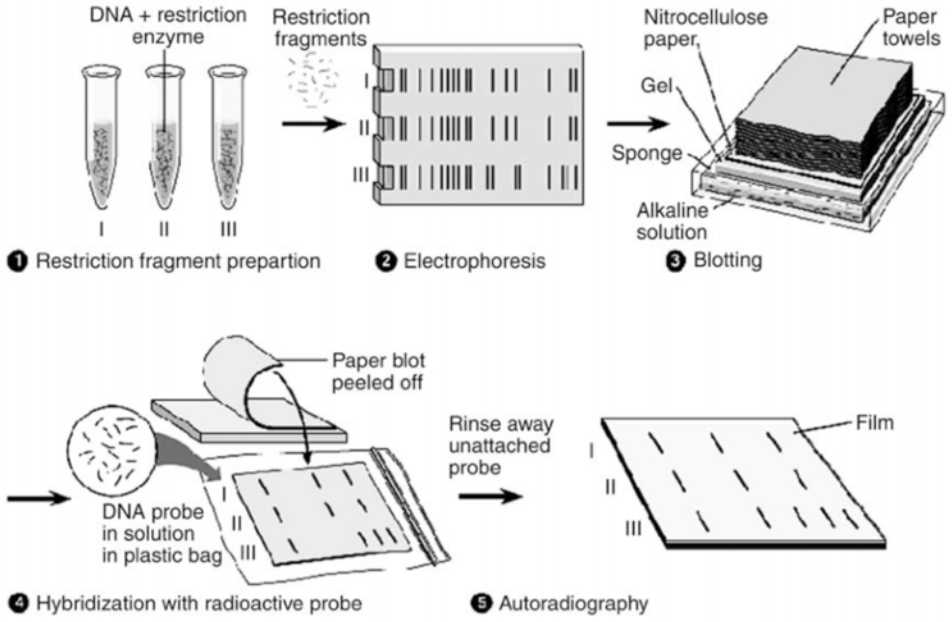

Figure 4 Schematic representation of a Southern blot analysis, showing DNA preparation (enzymatic digestion), electrophoresis, Southern blot transfer, and revelation by autoradiography. *Source*: From Charles Mallery, Department of Biology, University of Miami, Coral Gables, Florida, U.S.A. (last updated November 11, 2001).

nucleotide sequences between the probe and the DNA molecule on the membrane. Radioactive or chemiluminescent probes are visualized with autoradiography or color development of the membrane, respectively.

RNA Analysis by Northern Blot Hybridization

RNA, like DNA, can be similarly transferred from agarose gels to nitrocellulose or nylon membranes for hybridization studies. The procedure is very similar to the Southern blot hybridization and is called Northern blot. However, in Northern blot technique, care should be taken to prevent RNases contamination, because RNA is extremely sensitive to degradation. Also, formaldehyde should be applied to keep RNA molecules denatured during electrophoresis, because of the presence of secondary structure inside RNA molecules.

Protein Analysis by Westhern Blot

Western blot as opposed to Southern and Northern blots involves the transfer of proteins from polyacrylamide gels, instead of agarose gels, to nitrocellulose membranes. Unlike the capillary action of the Southern or Northern blot technique, Western blot requires an electrical current for moving the proteins from the gel to the surface of the membrane. Another major difference between these techniques is the use of antibodies instead of probes for the detection of the protein of interest. These antibodies are designed to bind specifically and exclusively to the protein or a fragment of the protein of interest. There are various methods used for the identification of a specific protein with antibodies, including radioactive isotopes, fluorescent, colorimetric, or chemiluminescent detection. In all of these techniques, the antibody is labeled by conjugation with a reporting molecule. The detection can be achieved either in a one-step or a two-step process. Depending on the detection method, sensitivity is extremely variable. The so-called "enhanced chemiluminescent" (ECL) detection is considered to be among the most sensitive detection methods for blotting analysis.

GENES AND CHROMOSOMES ANALYSIS

Polymerase Chain Reaction

PCR technologies are fundamental to many other molecular biology techniques. By amplification of a selected DNA sequence, PCR allows other techniques to be performed, even when a very small amount of DNA is available. PCR reactions such as in DNA fingerprinting,

are largely used in forensic cases and paternity testing. They also provide shortcuts for many cloning and sequencing applications. Another major application is in diagnosis of inherited human diseases, especially in prenatal diagnosis, where only limited amount of DNA is available. It may also be used as an amplification step for the genetic analysis of various nonhereditary neoplasms.

PCR was invented by Kary Mullis (6), who won the 1993 Nobel Prize for this work. Basically, PCR allows in vitro cloning of a given sequence, with only a small amount of DNA (few molecules) and without the need of living cells. However, to apply this technique, the nucleotide sequence of a short segment on each side of the region of interest needs to be known.

The PCR proceeds in three steps, which are repeated multiple times (Fig. 5). The first step is the heat denaturation (94°C) of the DNA to be amplified. The second step is the annealing of the complimentary stands of the target

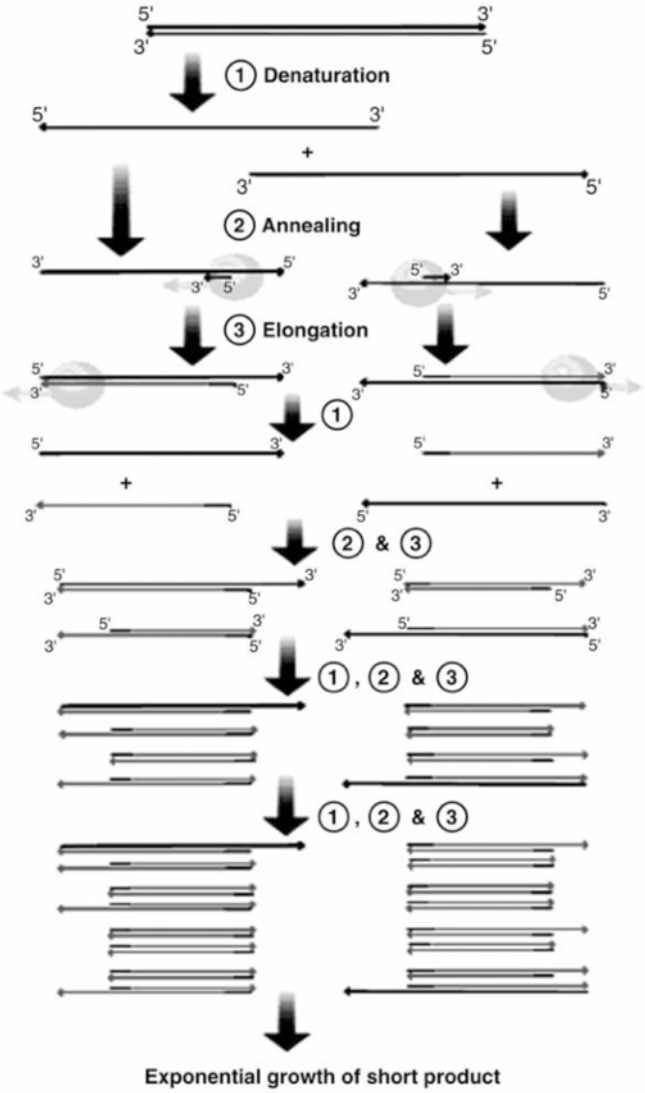

Figure 5 Schematic drawing of the polymerase chain reaction (PCR) cycle with its three important steps: (1) denaturing at 96°C, (2) annealing at 68°C, and (3) elongation at 72°C (P = polymerase). After, the completion of the first cycle, the two resulting DNA strands make up the template DNA for the next cycle, thus doubling the amount of DNA duplicated for each new cycle.

using two short sequences of single-stranded DNA called primers. Annealing temperature is usually between 50°C and 60°C, but varies according to the primers. In the third extension step, an enzyme called Taq DNA polymerase covalently extends the primers at the 3′-hydroxyl end, using target DNA as a template for the incorporation of nucleotides. This process creates a DNA strand complementary to the strand of the primers annealed. This denaturation, annealing, and extension cycle is repeated many times (usually 30–40), which leads to the exponential amplification of the targeted DNA product. Normally, a few kilobases products can be amplified, but some PCR reagents (Elongase tag) can amplify up to 40-kb products.

Reverse Transcription-Polymerase Chain Reaction

Reverse transcription-polymerase chain reaction (RT-PCR) is the process by which an RNA strand is first reverse transcribed into a cDNA, followed by amplification of the resulting DNA using PCR. The first step is the same as the one in cDNA synthesis whereby the target mRNA is extended by a reverse transcriptase with the use of oligo-dT primer, random hexamer primer, or gene-specific primer. The generated cDNA is then amplified by PCR using gene-specific primers. This method is very sensitive for the amplification of low copy number RNA molecules. It is widely used in diagnosis of genetic diseases or as a measure of the gene expression levels by real-time PCR.

Real-Time PCR

Real-time PCR, also called quantitative real-time PCR, is based on the same principle used in PCR, but it allows quantification of the target product after each round of amplification. In other words, instead of the qualitative nature of the PCR, the real-time PCR technique is quantitative. In this technique, commercially available fluorescence detecting thermocyclers are used to amplify specific nucleic acid sequences while simultaneously following the concentration of the products. There are two common methods of RT-PCR product quantification. One utilizes fluorescent dyes, such as SYBR green (asymmetrical cyanine dye), that intercalate with double-strand DNA. Another uses modified DNA oligonucleotide probes that fluoresce when hybridized with a complementary DNA as in Taqman technique (Fig. 6). This method involves the use of an oligonucleotide reporter probe where the fluorophore is quenched by another molecule. When the probe anneals to the complementary target inside the amplified DNA fragment, the probe is still quenched. However, during PCR reaction, the probe is degraded by the 5′ → 3′ Taq polymerase activity and the reporter is then unquenched resulting in emission of fluorescence. The major advantages of real-time PCR are its high sensitivity and the ability to process many samples simultaneously.

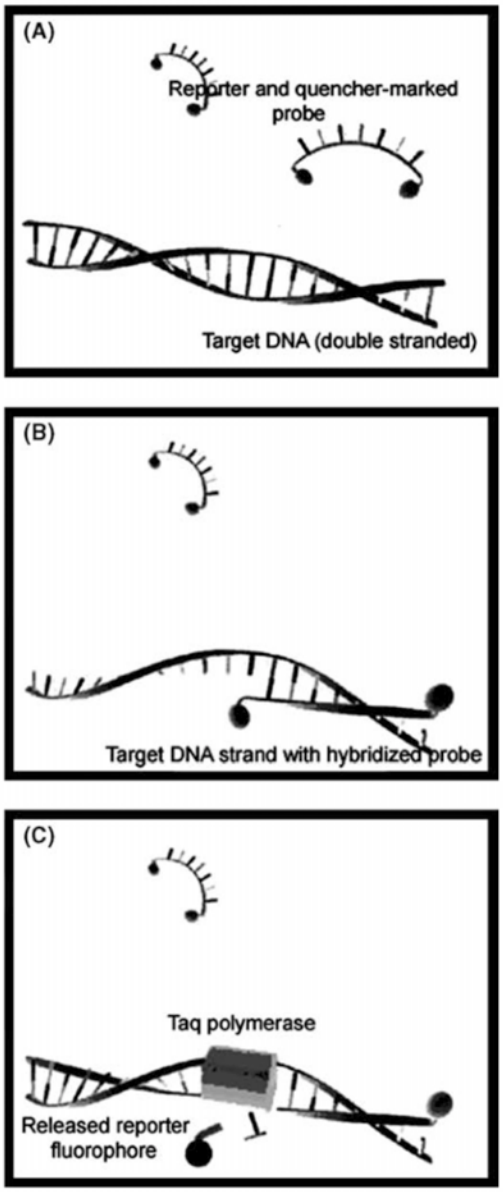

Figure 6 Principle of Taqman technique: (**A**) In intact probes, reporter fluorescence in quenched. (**B**) Probes and the complementary DNA strand are hybridized while reporter fluorescence is still quenched. (**C**) During the PCR, the probe is degraded by the Taq polymerase and the fluorescent reporter is released.

DNA Sequencing

The term DNA sequencing encompasses biochemical methods for determining the order of the nucleotide bases in a DNA oligonucleotide. Modern sequencing is derived from the chain-termination method developed by Sanger and coworkers (7) in 1977. From 1976 to 1977, Allan Maxam and Walter Gilbert (8) developed a DNA sequencing method based on chemical modification of DNA, which rapidly becomes more popular, since purified DNA could be used directly, while the initial Sanger method required production of single-stranded DNA. However, with the development and improvement of chain-termination method in combination with the technical complexity (hazardous chemicals, difficulties with scale-up) of Maxam-Gilbert sequencing, the Sanger method has regained popularity. The key feature of this method is the incorporation of dideoxynucleotides triphosphates (ddNTPs) as DNA chain terminators. Briefly, the technique requires a single-stranded DNA template, a DNA primer, a DNA polymerase, labeled nucleotides, and modified nucleotides lacking the 3′-hydroxyl group necessary for the formation of a phosphodiester bond between two nucleotides. The DNA template is divided into four separate sequencing reactions, each one containing only one of the four dideoxynucleotides (ddATP, ddGTP, ddCTP, or ddTTP). Thus, incorporation of these nucleotides into the nascent DNA strand terminates the elongation process and creates fragments of different length. The dideoxynucleotides are added at lower concentration than the standard deoxynucleotides to allow strand elongation sufficient for sequence analysis. The DNA fragments are then denatured and separated by gel electrophoresis, creating a ladder of DNA fragments, each one differing in length by one single base. DNA bands can be subsequently visualized by autoradiography or ultraviolet light allowing the sequence to be read (Fig. 7).

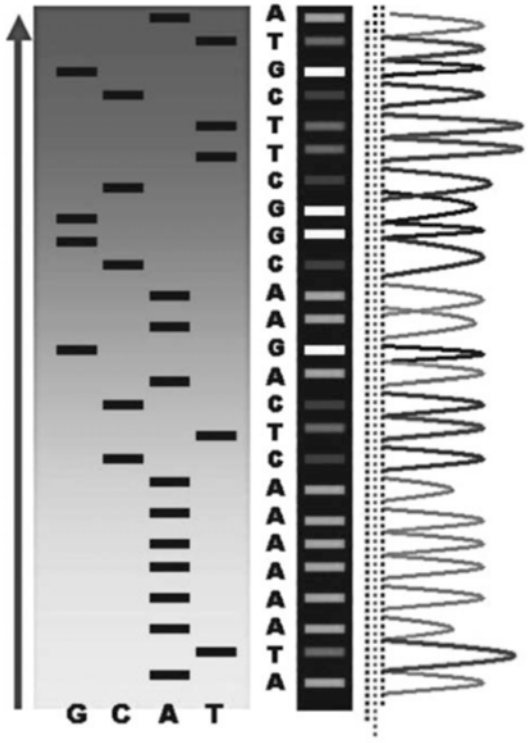

Figure 7 Sequence ladder results from Sanger sequencing by radioactive sequencing compared with fluorescent peaks.

DNA Microarrays

Microarrays are often used for expression profiling studies, where the expression of thousands of genes can be monitored simultaneously using DNA to DNA hybridization and fluorophores detection. The level of gene expression is based on the amount of mRNA translated by the cells, which is usually correlated to the level of protein production. In fact, DNA microarray is a collection of microscopic DNA spots called probes (cDNA, oligonucleotides, or small fragment of PCR products corresponding to mRNAs), arrayed on a solid surface by covalent attachment to chemically suitable matrices. cDNA from two samples to be compared (e.g., diseased vs. healthy tissue) can be affixed onto two different matrices or a single matrix, but in the latter case, samples should be labeled with two different fluorophores (Fig. 8). This technique is used in various applications, including forensic science, assessment of genetic susceptibility to disease (single nucleotide polymorphism microarray), or identification of DNA-based drug candidates.

Microarray techniques are always coupled with statistical analysis and bioinformatics. To be able to decipher the enormous amount of information in a single microarray (Fig. 9), many software and normalization techniques are necessary. Even with these advanced analysis techniques, DNA microarrays pose a large number of statistical problems, because of the biological complexity of gene expression. Thus, experimental designs are of critical importance if statistically and biologically valid conclusions are to be drawn from the data.

With the great advances in sequencing techniques and the existence of technical variations of chain-termination sequencing, the goal of sequencing the complete human genome was achieved. Modern sequencers now use multiple capillary electrophoresis and sequencing techniques

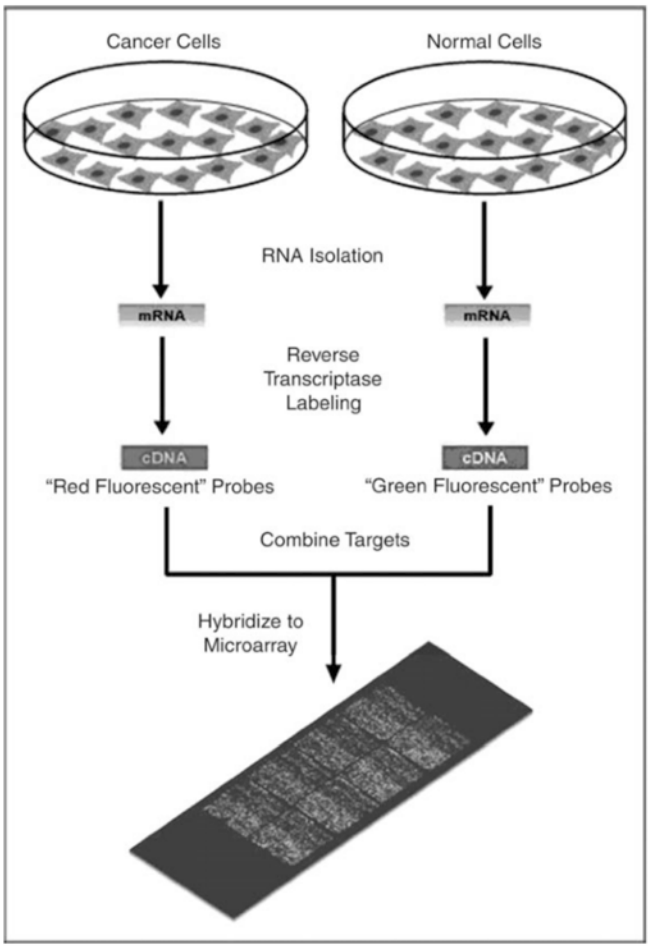

Figure 8 Diagram of typical dual-color microarray experiment, typically hybridized with cDNA from two samples to be compared (diseased tissue vs. healthy tissue) that are labeled with two different fluorophores.

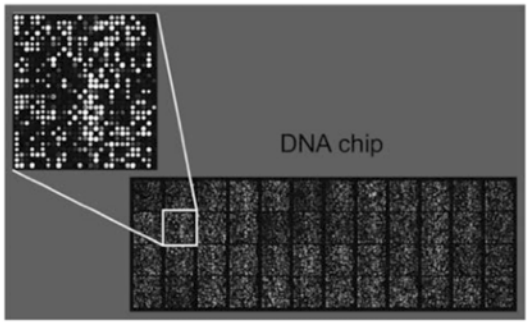

Figure 9 Example of an approximately 40,000 probe spotted oligo microarray with enlarged inset to show detail and complexity of the analysis.

that are applied in a variety of fields such as diagnostic and forensic research.

SUMMARY

Since the late 1950s and early 1960s, molecular biologists have learned to characterize, isolate, and manipulate the molecular components of cells and organisms. These components include DNA, RNA, and proteins, which are all related and interconnected. The modern molecular techniques have proved to be extremely useful in a vast diversity of fields, such as biological process characterization, forensic analysis and treatment, and characterization of disease. These techniques are increasingly being incorporated in many molecular imaging laboratories. They are not only important for the understanding of

disease processes, but also for developing imaging probes that are visualized by imaging devices, such as magnetic resonance and positron emission tomography scanners. Therefore, understanding such methods is vital for the progress of the field of molecular imaging.

REFERENCES

1. Orkin SH, Alter BP, Altay C, et al. Application of endonuclease mapping to the analysis and prenatal diagnosis of thalassemias caused by globin-gene deletion. N Engl J Med 1978; 299(4):166–172.
2. Kelly TJ Jr., Smith HO. A restriction enzyme from Hemophilus influenzae. II. J Mol Biol 1970; 51(2):393–409.
3. Cohen SN, Chang AC, Boyer HW, et al. Construction of biologically functional bacterial plasmids in vitro. 1973. Biotechnology 1992; 24188–192.
4. Reuss FF. Mem Soc Imperiale Naturalistes de Moscow 1809; 2:327.
5. Southern EM. Long range periodicities in mouse satellite DNA. J Mol Biol 1975; 94(1):51–69.
6. Mullis K, Faloona F, Scharf S, et al. Specific enzymatic amplification of DNA in vitro: the polymerase chain reaction. 1986. Biotechnology 1992; 2417–27.
7. Sanger F, Nicklen S, Coulson AR. DNA sequencing with chain-terminating inhibitors. Proc Natl Acad Sci U S A 1977; 74(12):5463–5467.
8. Maxam AM, Gilbert W. A new method for sequencing DNA. Proc Natl Acad Sci U S A 1977; 74(2):560–564.

ANNEX IV

Paper

MOLECULAR IMAGING AND BIOLOGY

© Academy of Molecular Imaging, 2009
Published Online: 7 November 2009

Mol Imaging Biol (2010) 12:2–8
DOI: 10.1007/s11307-009-0242-z

BRIEF ARTICLE

High-Affinity αvβ3 Integrin Targeted Optical Probe as a New Imaging Biomarker for Early Atherosclerosis: Initial Studies in Watanabe Rabbits

Julie Heroux,[1,5] Ahmed M. Gharib,[1] Narasimhan S. Danthi,[2] Sylvain Cecchini,[3] Jacques Ohayon,[1,4] Roderic I. Pettigrew,[1,5]

[1]*Laboratory of Integrative Cardiovascular Imaging Science, National Institute of Diabetes Digestive and Kidney Diseases, Bethesda, MD, 20892, USA*
[2]*Laboratory of Diagnostic Radiology Research, Clinical Center, Bethesda, MD, 20892, USA*
[3]*Laboratory of Biochemical Genetics, National Heart Lung and Blood Institute, Bethesda, MD, 20892, USA*
[4]*Laboratoire TIMC IMAG, Faculté de Médecine de Grenoble, La Tronche Cedex, 38706, France*
[5]*NIH/NIDDK, 10 Center Drive, Bldg. 10, Room 3-5340, MSC 1263, Bethesda, MD, 20892, USA*

Abstract

Purpose: A newly developed synthetic αvβ3 integrin targeted optical probe (ITOP) has been demonstrated to target cancer cells, *in vivo*. Compared to the commercially available cyclic peptide c[RGDfv], this optical probe has at least 20 times better binding affinity for the αvβ3 receptor. The present *in vitro* study was designed to investigate the possibility of detecting early atherosclerotic plaque by using this ITOP.

Procedures: Experiments were performed on five Watanabe heritable hyperlipidemic rabbits and two New Zealand White rabbits for control. Our ITOP was used for detecting the presence of αvβ3 receptors *in vitro*.

Results: Segments of plaque accumulation from two distinct regions of ascending and descending aortas were labeled in Watanabe rabbits. The signal was found principally in the adventitia and proximal intima of the aortic vessel, corresponding directly to the expression of integrin αvβ3 as determined by antibody assay. Moreover, there was a close association between the level of labeling with the αvβ3 targeted probe and the thickness of the adventitia.

Conclusions: This high-affinity ITOP identifies the site and extent of αvβ3 expression and correlates with adventitial thickness. Recent evidence associates αvβ3 expression with the inflammatory process in early vulnerable plaque, making this compound a promising potential biomarker for early atherosclerotic disease.

Key words: Aorta, Atherosclerosis, αvβ3 integrin, Immunohistofluorescence, Molecular imaging, Targeted optical probe, Watanabe heritable hyperlipidemic rabbits

Source of support: Intramural NIH funding

Electronic supplementary material The online version of this article (doi:10.1007/s11307-009-0242-z) contains supplementary material, which is available to authorized users.

Correspondence to: Julie Heroux; herouxj@niddk.nih.gov, Roderic I. Pettigrew; *e-mail:* rpettigrew@nih.gov

Abbreviations FITC, Fluorescein isothiocyanate; NZW, New Zealand White; WHHL, Watanabe heritable hyperlipidemic; ECM, Extracellular matrix; IC_{50}, Inhibitory concentration; ITOP, Integrin targeted optical probe; OCT, Optimal cutting temperature; H&E, Hematoxylin and eosin; NI, Neointima; M, Media; Ad, Adventitia; DAPI, 4′,6-Diamidino-2phenylindole

Introduction

Despite all the recent technological and medical advances, cardiovascular disease remains the leading cause of death in the Western World and needs to be detected at an earlier stage [1]. With the understanding of atherosclerosis as an inflammatory disease [2, 3], there is a growing interest in the detection of components of the inflammatory process as early biomarkers of this disease. One potential promising molecular target for the detection of atherosclerotic plaque is the αvβ3 receptor [4, 5], which is a widely recognized target for the development of molecular probes in pathological conditions [6, 7]. In addition, human atherosclerosis lesions show extensive expression of αvβ3 [8], which plays a role in thrombus formation [9], cell migration [10], neovascularization [7, 11], as well as many other processes. Although αvβ3 is expressed on a variety of cells, its expression seems to be predominant in smooth muscle cells and endothelial cells [8, 12]. Macrophages also express αvβ3 during foam cells formation [13]. Most interesting is the fact that αvβ3 expression seems to be an early event in plaque formation [5, 14] and is also correlated with plaque instability [4, 15]. Additionally, previous studies have shown the great potential of targeting αvβ3 integrin for the development of contrast agents that enhance the detection of plaque [16, 17] and for the delivery of therapeutic drugs [18].

Recently, an integrin targeted optical probe (ITOP) was synthesized and has been shown to efficiently target the αvβ3 receptor with high affinity in an *in vivo* mouse model of cancer [19]. The probe is a small non-peptidic carbamate integrin antagonist (RGD mimic), which is fluorescently labeled and targets the αvβ3 integrin. Compared to nanoparticles having sizes of hundreds of nanometers (nm), this probe is much smaller (<1 nm), which should translate into better clearance from blood and better diffusion into the targeted tissue. *In vitro*, this labeled compound has very high affinity for αvβ3 (IC_{50} of 3 nM) and greater selectivity towards αvβ3 compared to αIIbβIIIa, αvβ5, and αvβ6 (IC50>100 μM) [19]. This ITOP has at least 20 times higher binding affinity for αvβ3 compared to the commercially available cyclic peptide c [RGDfv] labeled with fluorescein isothiocyanate (FITC; personal communication, Narasimhan Danthi). When intravenously injected in tumor bearing mice, the ITOP persisted in the tumor for more than 4 h, while it disappeared from most of the other tissues within an hour, demonstrating that its biodistribution is conducive for use in imaging. Based on these animal experiments [19], we have not seen immunogenic reactions associated with our ITOP. As a first step, in this *in vitro* study, we have explored the utility of this ITOP to probe the molecular processes involved in atherosclerotic plaque formation, in a Watanabe rabbit model.

Materials and Methods

Integrin αvβ3 Targeted Optical Probe Synthesis

The αvβ3 ITOP 4-[2-(3,4,5,6-tetrahydropyrimidin-2ylamino)ethyl-oxy] benzoyl-2-(*S*)-[*N*-(3-amino-neopenta-1-carbamyl)]-aminoethylsulfonylamino-β-alanine fluorescein thiourea (Fig. 5, suppl. data) was synthesized as previously described. Briefly, ITOP was developed from a potent fibrinogen receptor antagonist (3-amino-2(*S*)-arylsulfonylaminopropionic acid derivative) [20] with further structural modifications, followed by conjugation to FITC. The conjugation of the fluorophore to the integrin antagonist did not alter the binding affinity or selectivity to integrin αvβ3. This compound represents the first example of a non-peptidic integrin αvβ3 targeted optical probe. In the binding assays as well as in the cell adhesion inhibition assays this compound showed very high binding affinity (3nM) and selectivity to αvβ3 compared to αIIbβIIIa, αvβ5, and αvβ6 [19].

Experimental Design

All experiments were performed on specimens taken from 3- to 12-month-old Watanabe heritable hyperlipidemic (WHHL) rabbits, two females and three males (n=5), fed a standard rabbit chow diet. The animals were purchased from Brown Family Enterprises (Gemini Research of Alabama, Odenville, Alabama, USA). Control aortic tissues without atherosclerosis were taken from New Zealand White (NZW) rabbits (n=2) and purchased from Zyagen (San Diego, CA, USA). Prior to any experiments, rabbits were anesthetized with a ketamine (30 mg/kg) and xylazine (5 mg/kg) cocktail administered subcutaneously and then euthanized by intravenous pentobarbital (100 mg/kg) injection while still under anesthesia. The aortic arch was excised and cut into different sections prior to be quick frozen in optimal cutting temperature (OCT) media for histological and immunohistological experiments. All experiments were performed in accordance with protocols approved by the Animal Care and Use Committee of the National Heart Lung and Blood Institute.

Histology

OCT blocks from frozen aortic tissue were cut into 7–8-μm sections with a cryostat and mounted onto slides. Routine hematoxylin and eosin (H&E) straining was performed on the frozen sections. An antibody against human αvβ3, anti-human integrin αvβ3, clone LM609 (Chemicon International, Temecula, CA, USA), was used to confirm the presence of the integrin and as a reference for the localization of any experimental fluorescence signal. This antibody was used in conjunction with an anti-mouse horseradish peroxidase detection kit, according to the specifications of the company (Chemicon International). Expression of αvβ3 integrin in the aortic wall was assessed by immunohistofluorescence with the new ITOP. Sections were thawed

for 15 min at room temperature, fixed for 10 min with cold acetone, washed in phosphate buffer solution, and then incubated with the targeted fluorescent probe for 1 h. After the incubation period, the slides were washed again, mounted with VECTASHIELD mounting medium containing DAPI (Vector Laboratories, Burlingame, CA, USA) and a coverslip was applied. For signal specificity experiments, slides were incubated with the unlabeled ITOP prior to the washing and mounting steps. Images of staining or fluorescence signal were acquired under a microscope (Nikon E1000 with a Nikon DXM-1200 color camera) using a visible or ultraviolet light source, respectively.

Results

Plaque Labeling

Histological staining (H&E) of WHHL rabbit aortic tissue demonstrated intimal thickening, which was absent in the control. Examination of the aortic tissue incubated for 1 h with the ITOP showed a strong fluorescent signal (Fig. 1a). Aortic tissue that has been incubated with non-labeled ITOP showed a loss of signal (Fig. 6, suppl. data). Signal enhancement was predominately localized in the adventitia and the neointima, though there was also some fluorescence in the media. In contrast, the specific fluorescent signal of the integrin targeted probe was absent in the control NZW rabbits (Fig. 1b). There was some autofluorescence in the aortic tissue, but it was negligible.

Signal Correlation with an Anti-αvβ3 Antibody

A transverse image of the ascending aorta of the WHHL rabbit shows that the intimal thickening (neointima) of the tissue is a component of the atherosclerotic plaque (Fig. 2). Upon comparison, the immunohistological labeling of αvβ3 (Fig. 2, right panels) and the fluorescence signal of the ITOP (Fig. 2, left panels) appear co-localized to the same regions. Higher magnification (×100) of the neointimal region (Fig. 2c, d) demonstrated corresponding strong fluorescence and immunohistological signals near the interface of the lumen and intima. The fluorescent and immunohistological labeling are mostly localized in the adventitia and proximal intima of the ascending aorta; a similar distribution was shown in the descending aorta sections (Fig. 1).

Adventitia Labeling

Higher magnification images of the adventitial sections demonstrated co-localization between the ITOP signal and the DAPI (4′,6-diamidino-2phenylindole) labeling of cell nuclei, suggesting that the signal from the fluorescent molecule is found close to the nucleus of the cell (Fig. 3). Adventitial co-localization results also showed neovessel-like structures, located around regions delineated by cells labeled with fluorescent ITOP.

Labeling and Adventitia Thickness

Comparison between fluorescent staining with the αvβ3 targeted probe (Fig. 4, upper panel) and histological staining (Fig. 4, bottom panel) of the corresponding descending aorta section demonstrates a qualitative correlation between fluorescent signal intensity and adventitial thickness. Thus, a mild signal was present in plaques with a small adventitia thickness (Fig. 4a, b, d, e), while a strong signal appeared on plaque with marked adventitia thickness (Fig. 4c, f). There is also some inverse correlation between the intensity of fluorescence labeling and the organization level of the plaque. Staining was very intense (Fig. 4c) when the media was disorganized (Fig. 4f) and less intense (Fig. 4a, b) when the media was well delineated (Fig. 4d, e).

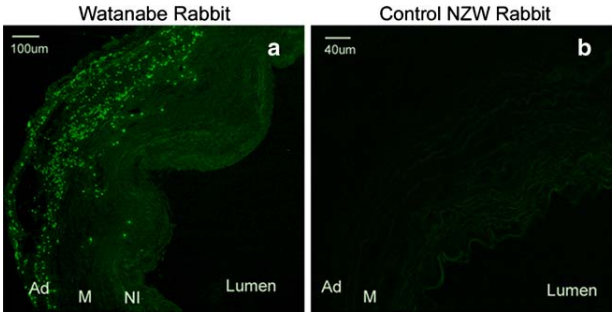

Fig. 1. Fluorescence microscopy of Watanabe rabbit descending aorta sections (transverse cut) from tissue incubated with FITC-αvβ3 targeted probe. **a** Image (×40 magnification) of slide exposed to FITC-αvβ3 targeted probe (2.8 μM) for 1 h. **b** Background fluorescence of the same region in slide from control NZW rabbit exposed to the fluorescent ITOP with the same conditions (×100 magnification). Results indicate specific plaque labeling with the fluorescent targeted probe with a very small amount of autofluorescence background from tissues. *FITC* fluorescein isothiocyanate, *Ad* adventitia, *M* media, *NI* neointima.

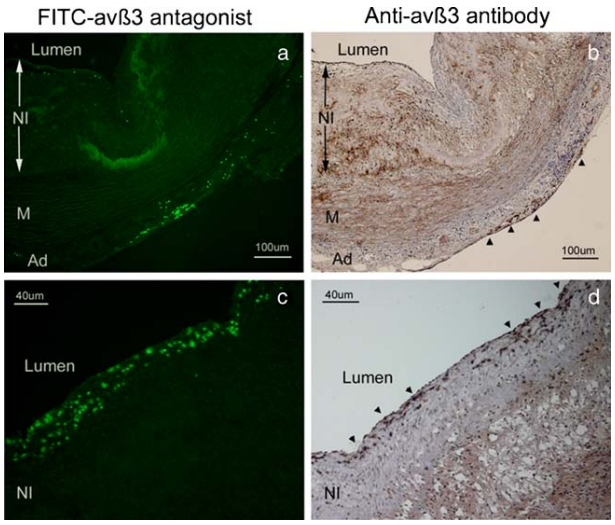

Fig. 2. Co-localization study of αvβ3 expression on Watanabe rabbit ascending aorta sections labeled with fluorescence (**a**, **c**) or immunohistochemistry (**b**, **d**). The *upper panels* display the whole aortic wall (×40 magnifications), while the *bottom panels* are focused on the neointimal region (×100 magnifications). Both the fluorescence signal (**a**, **c**) and the immunohistological labeling (**b**, **d**) are co-localized predominantly in the adventitia and proximal neointima. *Arrowheads* illustrate immunohistological staining. *FITC* fluorescein isothiocyanate, *Ad* adventitia, *M* media, *NI* neointima.

Discussion

Integrin expression, particularly αvβ3, in atherosclerotic plaque is a critical component of the inflammatory process that can drive the plaque toward a more unstable state [21, 22] leading to plaque rupture [23–25]. Many processes taking place during the initiation and progression of inflammatory vascular lesions require αvβ3 expression, including foam cell formation [13], smooth muscle cell migration [26], and thrombus formation [9].

In this study, we describe the use of a novel synthetic high affinity and high specificity αvβ3 integrin targeted

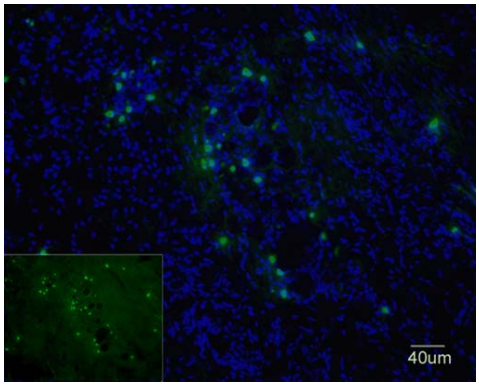

Fig. 3. Fluorescence microscopy of localization of the αvβ3 targeted-probe labeling inside the adventitia. This image (×400 magnifications) shows a composite image of the ITOP staining and DAPI staining (nucleus of cells) of the same aortic region. *Smaller inset image* represents the targeted-probe labeling alone. The targeted-probe signal appears to be localized on the surface of the cells, near the nucleus. There is presence of some structures similar to early neovessels that are labeled with fluorescence. *FITC* fluorescein isothiocyanate, *DAPI* 4′,6-diamidino-2phenylindole.

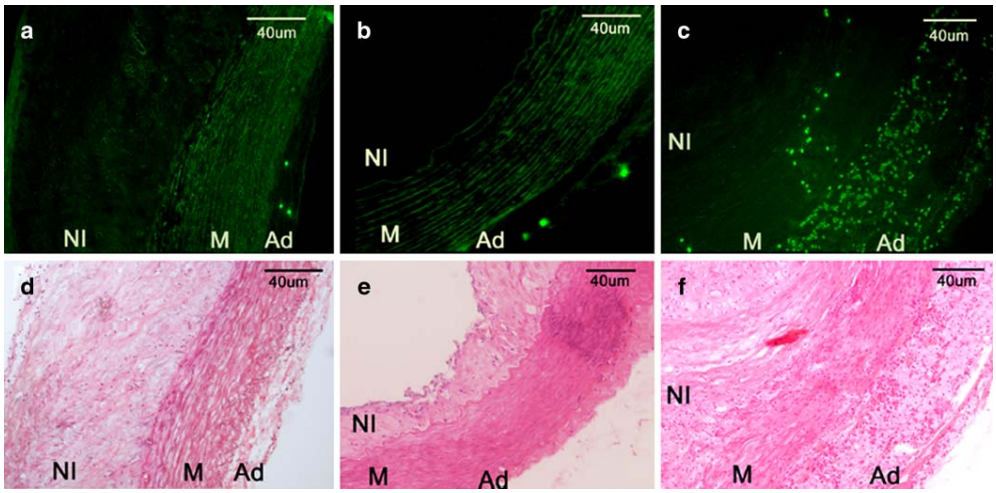

Fig. 4. Intensity of fluorescence staining in Watanabe rabbit descending aorta sections (**a**, **b**, **c**) correlated with adventitia thickness and plaque histology (**d**, **e**, **f**). In images (×100 magnifications) of aorta sections with relatively small adventitia (mild thickening; **d**, **e**), the level of staining and the intensity of the αvβ3 targeted-probe signal is relatively mild (**a**, **b**). In a similar direct correlation, for the aorta sections with large adventitia (marked thickening; **f**), the signal from the αvβ3 targeted probe is marked (**c**). There was also an apparent inverse correlation between the intensity of labeling and the organization within the plaque. Staining is very intense when the media appears disrupted (**c**) and less intense when the media is well delineated (**a**, **b**). *FITC* fluorescein isothiocyanate, *Ad* adventitia, *M* media, *NI* neointima.

optical probe and confirmed the *in vitro* specific labeling of rabbit atherosclerotic plaques (Figs. 1 and 2). We also show that the ITOP signal is localized near the nucleus of the cell (Fig. 3), which indicates that fluorescence is correlated to cells (αvβ3 receptors are membrane-bound) instead of unspecific ECM labeling. One interesting observation in the present work is that the fluorescent signal of the integrin targeted optical probe seems to extend from the adventitia toward the media of the aortic wall (Fig. 1a). The presence of fluorescent signal in the media is correlated with strong labeling and expansion of the adventitial layer (Figs. 1a and 3). This finding might be associated with the development of the angiogenic processes that first begins within the adventitia (vasa vasorum expansion) and then extends to the media of the vessel wall [27]. Nevertheless, further studies must be carried out to clarify the relationship between our compound and the natural history of angiogenesis in atheroma. Most importantly, there is a strong correlation between the labeling of atherosclerotic plaque with the integrin targeted probe and the thickness of the adventitia (Fig. 4). Thus, adventitial thickness is characterized by a strong and widely distributed signal enhancement with the probe, which may signal a more advanced inflammatory state. Moreover, stronger αvβ3 labeling is situated where the media is less organized, which is another sign of the presence of inflammation.

In agreement with other studies [5, 8, 16], we also found that the most significant accumulation of the αvβ3 receptor was in the adventitia of the aortic wall, a privileged site for the formation of neovessels. We also observed a characteristic expansion of the adventitia, a process which has been extensively described by others studies [5, 16, 28, 29]. This expansion allows angiogenesis and will further attract more inflammatory cells and lipids into the plaque, contributing to plaque growth, instability, and rupture.

In addition to the adventitial localization of the signal, we also observed fluorescence within the neointima of plaques, close to the lumen. Previous studies have shown that activated or proliferative endothelial cells express high levels of αvβ3 [7, 11]. This integrin is critical for the survival signal of these cells and is also recognized to influence adhesion and migration pathways [12]. Hence, it is not surprising to observe evidence of αvβ3 within the intima.

With the broad development of nanoparticles in disease detection [30, 31], we can extrapolate the use of this new αvβ3 integrin targeted probe for imaging atherosclerosis in combination with a variety of high-resolution molecular imaging techniques [32, 33]. The synthetic nature of this molecule makes it attractive for the development of various nanoparticle structures incorporating this molecule to target the plaque. For example, this ITOP was efficiently used in a combined imaging/treatment system for targeted drug

delivery and imaging of cancer angiogenesis [34]. For coronary atherosclerotic plaque assessment, we are working on labeling this ITOP with near-infrared molecules as part of a dual imaging system, which may allow MRI-guided catheter to detect fluorescent probes. This can lead to the delivery of treatments into specific unstable area of the plaque.

Relative to peptide-based molecules, this synthetic probe provides easier production and purification. Moreover, its affinity as a labeled probe for the αvβ3 receptor is higher than the commercially available labeled cyclic peptide c [RGDfv]. This should translate into a smaller injected dose for the plaque detection and also a better sensitivity. In addition, our ITOP is specific to αvβ3, whereas linear and cyclic RGD peptide specificity is broader (αvβ3, αIIbβ3a, αvβ5).

The physiochemical characteristics of this probe are also important. As opposed to antibodies, this small synthetic molecule (<1 nm) has less potential to induce an immune response and has important advantages related to the blood clearance and its diffusion into the targeted atherosclerotic tissue. Moreover, unlike antibodies, the probe is very suitable for further derivatives or structure modifications. However, future *in vivo* studies will be necessary to evaluate the labeling efficiency and kinetic uptake properties of this new optical probe.

Conclusions

This *in vitro* work demonstrates that a new high-affinity ITOP identifies the presence of αvβ3 expression associated with early atherosclerotic plaque development in the aortas of Watanabe rabbits. The studies further suggest that the αvβ3 expression identified by this probe corresponds to the degree of adventitial thickening. As such, this new probe holds promise for meeting the challenge of detecting early atherosclerotic lesions and identifying vulnerable plaque.

Acknowledgments. The authors would like to thank Dr. Zu Xi Yu (Pathology Core Facility, NHLBI, NIH) for kindly assisting us with the pathology components of the studies and Mary Angstadt for her help with animal care. Jacques Ohayon was supported by grants from the ANR 2006-2009, ATHEBIOMECH, France.

References

1. Lopez AD, Murray CC (1998) The global burden of disease, 1990–2020. Nat Med 4(11):1241–1243
2. Ross R (1999) Atherosclerosis–an inflammatory disease. N Engl J Med 340(2):115–126
3. Libby P (2002) Inflammation in atherosclerosis. Nature 420(6917): 868–874
4. Virmani R, Kolodgie FD, Burke AP *et al* (2005) Atherosclerotic plaque progression and vulnerability to rupture: angiogenesis as a source of intraplaque hemorrhage. Arterioscler Thromb Vasc Biol 25 (10):2054–2061
5. Winter PM, Morawski AM, Caruthers SD *et al* (2003) Molecular imaging of angiogenesis in early-stage atherosclerosis with alpha(v) beta3-integrin-targeted nanoparticles. Circulation 108(18):2270–2274
6. Storgard CM, Stupack DG, Jonczyk A, Goodman SL, Fox RI, Cheresh DA (1999) Decreased angiogenesis and arthritic disease in rabbits treated with an alphavbeta3 antagonist. J Clin Invest 103(1):47–54
7. Brooks PC, Clark RA, Cheresh DA (1994) Requirement of vascular integrin alpha v beta 3 for angiogenesis. Science 264(5158):569–571
8. Hoshiga M, Alpers CE, Smith LL, Giachelli CM, Schwartz SM (1995) Alpha-v beta-3 integrin expression in normal and atherosclerotic artery. Circ Res 77(6):1129–1135
9. Quinn MJ, Byzova TV, Qin J, Topol EJ, Plow EF (2003) Integrin alphaIIbbeta3 and its antagonism. Arterioscler Thromb Vasc Biol 23 (6):945–952
10. Weerasinghe D, McHugh KP, Ross FP, Brown EJ, Gisler RH, Imhof BA (1998) A role for the alphavbeta3 integrin in the transmigration of monocytes. J Cell Biol 142(2):595–607
11. Brooks PC, Montgomery AM, Rosenfeld M *et al* (1994) Integrin alpha v beta 3 antagonists promote tumor regression by inducing apoptosis of angiogenic blood vessels. Cell 79(7):1157–1164
12. Scatena M, Almeida M, Chaisson ML, Fausto N, Nicosia RF, Giachelli CM (1998) NF-kappaB mediates alphavbeta3 integrin-induced endothelial cell survival. J Cell Biol 141(4):1083–1093
13. Antonov AS, Kolodgie FD, Munn DH, Gerrity RG (2004) Regulation of macrophage foam cell formation by alphaVbeta3 integrin: potential role in human atherosclerosis. Am J Pathol 165(1):247–258
14. Blankenberg S, Barbaux S, Tiret L (2003) Adhesion molecules and atherosclerosis. Atherosclerosis 170(2):191–203
15. Doyle B, Caplice N (2007) Plaque neovascularization and antiangiogenic therapy for atherosclerosis. J Am Coll Cardiol 49(21):2073–2080
16. Winter PM, Neubauer AM, Caruthers SD *et al* (2006) Endothelial alpha (v) beta3 integrin-targeted fumagillin nanoparticles inhibit angiogenesis in atherosclerosis. Arterioscler Thromb Vasc Biol 26(9):2103–2109
17. Waldeck J, Hager F, Holtke C *et al* (2008) Flucscorescence reflectance imaging of macrophage-rich atherosclerotic plaques using an {alpha}v {beta}3 integrin-targeted fluorochrome. J Nucl Med 49:1845–1851
18. Bishop GG, McPherson JA, Sanders JM *et al* (2001) Selective alpha(v) beta(3)-receptor blockade reduces macrophage infiltration and restenosis after balloon angioplasty in the atherosclerotic rabbit. Circulation 103(14):1906–1911
19. Burnett CA, Xie J, Quijano J *et al* (2005) Synthesis, *in vitro*, and *in vivo* characterization of an integrin alpha(v) beta(3)-targeted molecular probe for optical imaging of tumor. Bioorg Med Chem 13(11):3763–3771
20. Duggan ME, Duong LT, Fisher JE *et al* (2000) Nonpeptide alpha(v)beta (3) antagonists. 1. Transformation of a potent, integrin-selective alpha (IIb)beta(3) antagonist into a potent alpha(v)beta(3) antagonist. J Med Chem 43(20):3736–3745
21. Granger DN, Vowinkel T, Petnehazy T (2004) Modulation of the inflammatory response in cardiovascular disease. Hypertension 43 (5):924–931
22. Libby P (2006) Atherosclerosis: disease biology affecting the coronary vasculature. Am J Cardiol 98(12A):3Q–9Q
23. Fuster V, Moreno PR, Fayad ZA, Corti R, Badimon JJ (2005) Atherothrombosis and high-risk plaque: part I: evolving concepts. J Am Coll Cardiol 46(6):937–954
24. Lassila R (1993) Inflammation in atheroma: implications for plaque rupture and platelet-collagen interaction. Eur Heart J 14(Suppl K): 94–97
25. Schroeder AP, Falk E (1995) Vulnerable and dangerous coronary plaques. Atherosclerosis 118(Suppl):S141–S149
26. Paulhe F, Racaud-Sultan C, Ragab A *et al* (2001) Differential regulation of phosphoinositide metabolism by alphaVbeta3 and alphaVbeta5 integrins upon smooth muscle cell migration. J Biol Chem 276 (45):41832–41840
27. Moreno PR, Purushothaman KR, Zias E, Sanz J, Fuster V (2006) Neovascularization in human atherosclerosis. Curr Mol Med 6(5):457–477
28. Moreno PR, Purushothaman KR, Fuster V, O'Connor WN (2002) Intimomedial interface damage and adventitial inflammation is increased beneath disrupted atherosclerosis in the aorta: implications for plaque vulnerability. Circulation 105(21):2504–2511
29. Wilson SH, Herrmann J, Lerman LO *et al* (2002) Simvastatin preserves the structure of coronary adventitial vasa vasorum in experimental hypercholesterolemia independent of lipid lowering. Circulation 105 (4):415–418
30. Sirol M, Fuster V, Fayad ZA (2006) Plaque imaging and characterization using magnetic resonance imaging: towards molecular assessment. Curr Mol Med 6(5):541–548

31. Sinha R, Kim GJ, Nie S, Shin DM (2006) Nanotechnology in cancer therapeutics: bioconjugated nanoparticles for drug delivery. Mol Cancer Ther 5(8):1909–1917
32. McCarthy JR, Kelly KA, Sun EY, Weissleder R (2007) Targeted delivery of multifunctional magnetic nanoparticles. Nanomed 2(2):153–167
33. Jaffer FA, Nahrendorf M, Sosnovik D, Kelly KA, Aikawa E, Weissleder R (2006) Cellular imaging of inflammation in atherosclerosis using magnetofluorescent nanomaterials. Mol Imaging 5(2):85–92
34. Xie J, Shen Z, Li KC, Danthi N (2007) Tumor angiogenic endothelial cell targeting by a novel integrin-targeted nanoparticle. Int J Nanomedicine 2(3):479–485

ABSTRACT

Purpose The detection of early atherosclerosis, before the development of its later sequelae of myocardial infarction, angina or stroke, constitutes an important challenge in current diagnostic medicine. Despite all the recent technological advances, cardiovascular disease remains the leading cause of death in the Western World and needs to be detected at an earlier stage to allow for more timely therapeutic intervention. This study is focusing on the detection of atherosclerosis or more specifically plaque vulnerability with the help of molecular imaging and pathological observation. Effectively, to predict plaque rupture, molecular imaging has emerged as a powerful diagnostic tool, consequent to the development of a growing number of new probes with affinity for key molecular targets. As a result, such selective molecules with high affinity for overexpressed targets in plaque formation, as αvβ3 integrin, should hold promises as probes for imaging atherosclerosis. With the help of molecular imaging combined with pathological observations, we can better comprehend, predict, and detect plaque vulnerability and rupture.

Objectives The overall objective of this study was to evaluate different molecular tools to predict the vulnerability of the atheromatous plaque. The major objective of the research was to investigate the possibility of detecting atherosclerotic plaques by using a newly developed synthetic αvβ3 integrin targeted optical probe (ITOP) showing particularly high affinity and specificity for αvβ3 receptors. We also investigate the relationship between this probe and pathological observation of atherosclerotic plaques from WHHL animal model and different human samples.

Procedures and Results For this study, experiments were performed on 12 Watanabe heritable hyperlipidemic (WHHL) rabbits and 1 New Zealand White (NZW) rabbit for control. First, our ITOP labeled with fluorescein isothiocyanate was used for detecting the presence of αvβ3 receptors *in vitro* and *ex vivo* on a Watanabe rabbit model. Fluorescence microscopy demonstrated a strong labeling of atherosclerotic plaques, which was absent in tissue from normal NZW rabbits. Segments of plaque accumulation from two distinct regions of ascending and descending aortas were labeled in each rabbits. The signal was found principally in the adventitia and proximal intima of the aortic vessel, corresponding directly to the expression of integrin αvβ3 as determined by antibody assay. Moreover, there was a close association between the level of labeling with the αvβ3 targeted probe and the thickness of the adventitia. Secondly, the ITOP was evaluated on human atherosclerotic samples, and was found to efficiently labeled atherosclerotic plaques. Moreover, we observed the same tendency as in the Watanabe rabbit: the ITOP intensity correlated with the degree of adventitial thickening. Finally, we tested the ITOP on AD-HIES coronary arteries, and have been able to detect a plaque corresponding to the first type of advanced atherosclerosis (type IV). We also found a relationship between plaque morphology and predisposition to aneurysms in AD-HIES.

Conclusions αvβ3 expression is related to inflammatory and stenotic processes. Our ITOP can efficiently label *in vitro* the first type of advanced atherosclerotic plaques. In combination with noninvasive imaging techniques that evaluates stenosis, it has great potential for the detection of vulnerable plaques.

RESUMÉ

But La détection précoce de l'athérosclérose, avant le développement de ses séquelles pathologiques, comme l'infarctus du myocarde, l'angine ou l'accident cérébraux-vasculaire (ACV), représente un important défi au niveau de la médecine diagnostique actuelle. En dépit de toutes les récentes avances technologiques, les maladies cardiovasculaires demeurent la principale cause de décès dans les pays occidentaux et la détection à un stage plus précoce s'avère nécessaire pour permettre une intervention thérapeutique adéquate. Notre étude se concentre sur la détection de l'athérosclérose ou plus spécifiquement la vulnérabilité de la plaque, grâce à l'imagerie moléculaire et l'observation pathologique. Effectivement, pour prédire la rupture de la plaque, l'imagerie moléculaire a émergé comme outil diagnostique puissant suite au développement croissant de nouvelles sondes ayant de l'affinité pour les molécules cibles du processus d'athérosclérose. Comme résultantes, ces molécules sélectives possédant une forte affinité pour des cibles surexprimées durant le processus de formation de la plaque, comme l'$\alpha v\beta 3$ par exemple, devrait représentées des sondes prometteuses pour la détection de l'athérosclérose. Avec l'aide de l'imagerie moléculaire combinée à l'observation pathologique, nous pourrons mieux comprendre et prédire la vulnérabilité et rupture de la plaque.

Objectif L'objectif global de notre étude était d'évaluer et de prédire la vulnérabilité de la plaque d'athérome à l'aide de différents marqueurs moléculaires. Le principal objectif de notre recherche était d'évaluer la possibilité de détecter précocement la plaque en utilisant une ITOP (integrin targeted optical probe). Cette sonde synthétique

nouvellement développée et ciblant l'intégrine αvβ3 avait déjà démontré une affinité et spécificité particulièrement élevée pour le récepteur de l'αvβ3 dans le cancer. Nous avons également exploré la relation entre cette sonde et l'observation pathologique des plaques d'athéromes sur le modèle animale WHHL et sur des plaques humaines provenant de différents patients.

Procédure et Résultats Pour cette étude, les expériences ont été réalisées sur un total de 12 lapins Watanabe hyperlipidémiques de souche WHHL (Watanabe heritable hyperlipidemic) et 1 lapin contrôle NZW (New Zealand White). Premièrement, notre ITOP, marquée avec la fluorescéine isothiocyanate (FITC), a été utilisée pour détecter *in vitro* et *ex vivo* la présence du récepteur de l'αvβ3. La microscopie à fluorescence a révélé un important marquage de la plaque d'athérome, lequel était absent dans les tissus provenant des lapins contrôles NZW. Le marquage a été détecté au niveau de segments de plaques provenant de deux régions distinctes de l'aorte ascendante et descendante dans chaque lapin. Le signal a été détecté principalement au niveau de l'adventitia et de l'intima proximale des vaisseaux aortiques, correspondant directement à l'expression de l'intégrine αvβ3, déterminée par essai immunochimique avec un anticorps contre l'αvβ3. De plus, une forte association s'est révélée entre le niveau de marquage de la sonde ciblant l'αvβ3 et l'épaisseur de l'adventitia. Deuxièmement, nous avons évalué notre sonde sur des échantillons humains affectés par l'athérosclérose et comparé les résultats avec l'évaluation morphologique de la plaque. Nous avons remarqué la même tendance que chez le lapin, soi un marquage plus important lorsque l'adventitia s'épaissi. Finalement, nous avons testé la sonde sur des artères coronaires provenant d'une autopsie d'un patient affecté par le AD-HIES et comparé les résultats avec l'évaluation

morphologique de leurs artères coronaires. Nous avons trouvé un lien entre la morphologie de la plaque et la prévalence d'anévrysmes coronaires chez ces patients.

Conclusion L'expression de l'αvβ3 est reliée à la foi aux processus inflammatoires et à la sténose. Notre ITOP à marqué efficacement *in vitro* le premier type de plaque d'athérome classé comme avancé (type IV) et pouvant produire des manifestations cliniques. En combinaison avec l'imagerie noninvasive détectant la sténose, il pourrait s'avéré utile dans la détection de la plaque vulnérable.